

**EVALUATION OF SLURRY POND RECLAMATION AT
THE MAE MOH MINE BY PREFABRICATED VERTICAL
DRAINS WITH PRELOADING TECHNIQUE**



Huy Dong Ngo

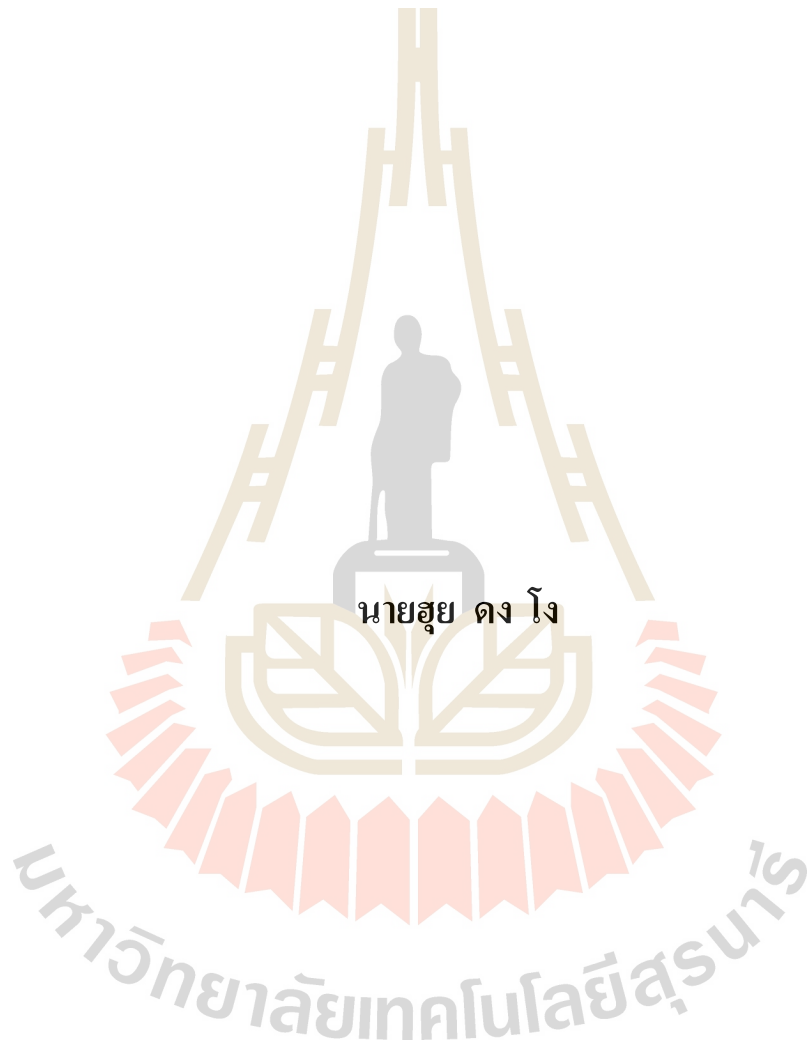
**A Thesis Submitted in Partial Fulfillment of the Requirements for the
Degree of Doctor of Philosophy in Civil, Transportation**

and Geo-resources Engineering

Suranaree University of Technology

Academic Year 2019

การประเมินการฟื้นฟูโปโคลนในเมืองแม่เมาะด้วยแผ่นระบายน้ำ
แนวตั้งสังเคราะห์ร่วมกับเทคนิคการถมน้ำหนักก่อน



นายสุย ดง โง

วิทยานิพนธ์นี้เป็นส่วนหนึ่งของการศึกษาตามหลักสูตรปริญญาวิศวกรรมศาสตรดุษฎีบัณฑิต

สาขาวิชาวิศวกรรมโยธา ขนส่ง และทรัพยากรธรณี

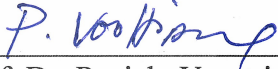
มหาวิทยาลัยเทคโนโลยีสุรนารี

ปีการศึกษา 2562

**EVALUATION OF SLURRY POND RECLAMATION AT THE
MAE MOH MINE BY PREFABRICATED VERTICAL DRAINS
WITH PRELOADING TECHNIQUE**

Suranaree University of Technology has approved this thesis submitted in partial fulfillment of the requirements for the Degree of Doctor of Philosophy.

Thesis Examining Committee



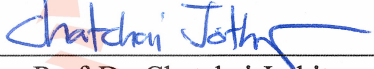
(Prof. Dr. Panich Vootripruex)

Chairperson



(Prof. Dr. Suksun Horpibulsuk)

Member (Thesis Advisor)



(Assoc. Prof. Dr. Chatchai Jothityangkoon)

Member



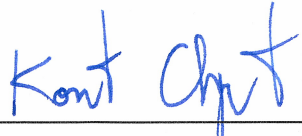
(Assoc. Prof. Dr. Avirut Chinkulkijniwat)

Member

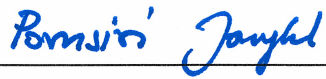


(Dr. Apichat Suddepong)

Member



(Assoc. Prof. Flt. Lt. Dr. Kontorn Chamniprasart)



(Assoc. Prof. Dr. Pornsiri Jongkol)

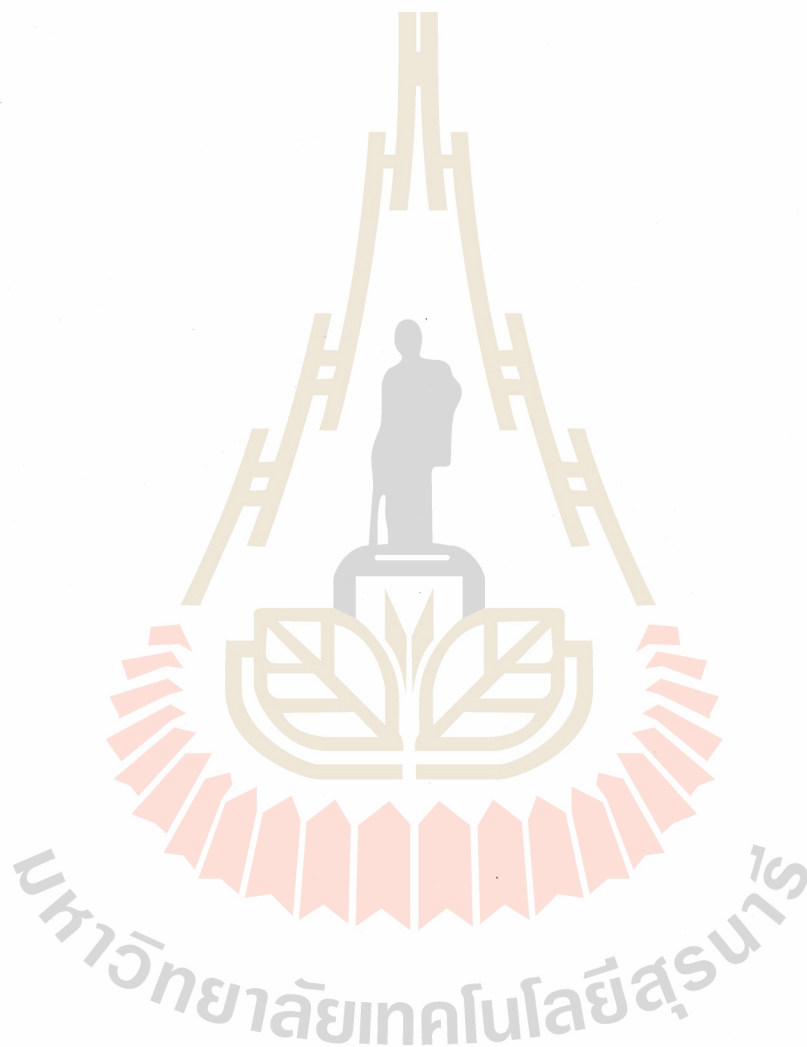
Vice Rector for Academic Affairs
and Internationalization

Dean of Institute of Engineering

สุข ดง โง : การประเมินการฟื้นฟูบ่อโคลนในเหมืองแม่เมาะด้วยแผ่นระบายน้ำ แนวตั้ง
สังเคราะห์ร่วมกับเทคนิคการถมน้ำหน้าก่อน (EVALUATION OF SLURRY POND
RECLAMATION AT THE MAE MOH MINE BY PREFABRICATED VERTICAL
DRAINS WITH PRELOADING TECHNIQUE) อาจารย์ที่ปรึกษา : ศาสตราจารย์
ดร.สุขสันต์ หอพิบูลสุข, 171 หน้า.

การถมคืนพื้นที่บ่อโคลนที่เป็นชั้นดินอ่อนมากในเหมืองแม่เมาะ จังหวัดลำปาง เป็นงานที่
ท้าทายสำหรับวิศวกรธรณีเทคนิค งานวิจัยนี้ศึกษาพฤติกรรมการอัดตัวของดินโคลนอ่อน
มากปรับปรุงด้วยเทคนิคการให้น้ำหน้าบรทุกก่อนร่วมกับแผ่นระบายน้ำแนวตั้ง การศึกษาแบ่ง
ออกเป็น 3 ส่วน ได้แก่ คุณสมบัติการอัดตัวของดินโคลนอ่อนมาก ประสิทธิภาพของแผ่นระบาย
น้ำแนวตั้งต่อการอัดตัวของดินโคลนอ่อนมากในแบบจำลองย่อส่วนและการวิเคราะห์เชิง
ตัวเลข และพฤติกรรมการอัดตัวของดินโคลนอ่อนมากปรับปรุงด้วยแผ่นระบายน้ำแนวตั้งใน
แปลงทดสอบ กระบวนการตกตะกอนของดินโคลนในเหมืองแม่เมาะแบ่งออกเป็น 2 ช่วงที่มี
ลักษณะเฉพาะที่แตกต่างกัน ได้แก่ ช่วงการรวมกลุ่มของอนุภาคและช่วงการตกตะกอน ดินโคลน
สามารถแบ่งได้เป็นดินที่เกิดการตกตะกอนสูงและดินที่เกิดการตกตะกอนต่ำโดยการใช้ค่าความชื้น
วิกฤต กราฟการอัดตัวของดินโคลนสามารถทำนายได้ด้วยสมการทั่วไปสำหรับการอัดตัว
คายน้ำร่วมกับค่าทั่วไปของอัตราส่วนโพรงที่ได้เสนอในงานวิจัยนี้ เส้นสถานะเนื้อแท้ของดินที่เกิด
การตกตะกอนสูงถูกเสนอเพื่อจำแนกสถานะของหน่วยแรงของดินและทำนายการทรุดตัวของดิน
โคลนอ่อนมากซึ่งมีความสำคัญต่องานถมบ่อโคลนของเหมืองแม่เมาะ ผลทดสอบการอัดตัวของน้ำ
ของดินโคลนปรับปรุงด้วยแผ่นระบายน้ำแนวตั้งในแบบจำลองย่อส่วนและในแปลงทดสอบใน
สนาม ชี้ให้เห็นว่า การทรุดตัวอย่างมากในระหว่างการล่าช้าของการลดลงของความดันน้ำส่วนเกิน
เป็นพฤติกรรมเฉพาะที่พบในดินโคลนอ่อนมาก กำลังต้านทานแรงเฉือนของดินโคลนอ่อนมาก
สามารถประมาณได้ด้วยความสัมพันธ์ประสิทธิผลบนพื้นฐานของสมการของ SHANSEP ซึ่ง
ความสัมพันธ์ประสิทธิผลหาได้จากวิธีของ Asaoka ในทางปฏิบัติ แบบจำลอง Plane strain
สำหรับการวิเคราะห์ด้วยวิธีไฟไนต์เอลิเมนต์แบบ 2 มิติ ที่เสนอโดย Chai et al. และ Indraratna and
Redana ถูกแนะนำสำหรับทำนายการทรุดตัวเนื่องจากการอัดตัวของดินโคลนอ่อนมากใน
เหมืองแม่เมาะปรับปรุงด้วยแผ่นระบายน้ำแนวตั้ง การเพิ่มขึ้นของกำลังต้านทานแรงเฉือนเมื่อ
สิ้นสุดการให้น้ำหน้าบรทุกแต่ละขั้นของการถมดินแสดงให้เห็นถึงประสิทธิภาพของแผ่นระบาย
น้ำแนวตั้งต่อการปรับปรุงดินโคลนอ่อนมากในเหมืองแม่เมาะ ผลลัพธ์ของงานวิจัยนี้นำมาซึ่งวิธี

ออกแบบการถมบ่อโคลนในเหมืองแม่เมาะที่มีประสิทธิภาพด้วยเทคนิคการให้น้ำหนักบรรทุกก่อน
ร่วมกับแผ่นระบายน้ำแนวดิ่งในพื้นที่ Sump1 C1



สาขาวิชา วิศวกรรมโยธา

ปีการศึกษา 2562

ลายมือชื่อนักศึกษา

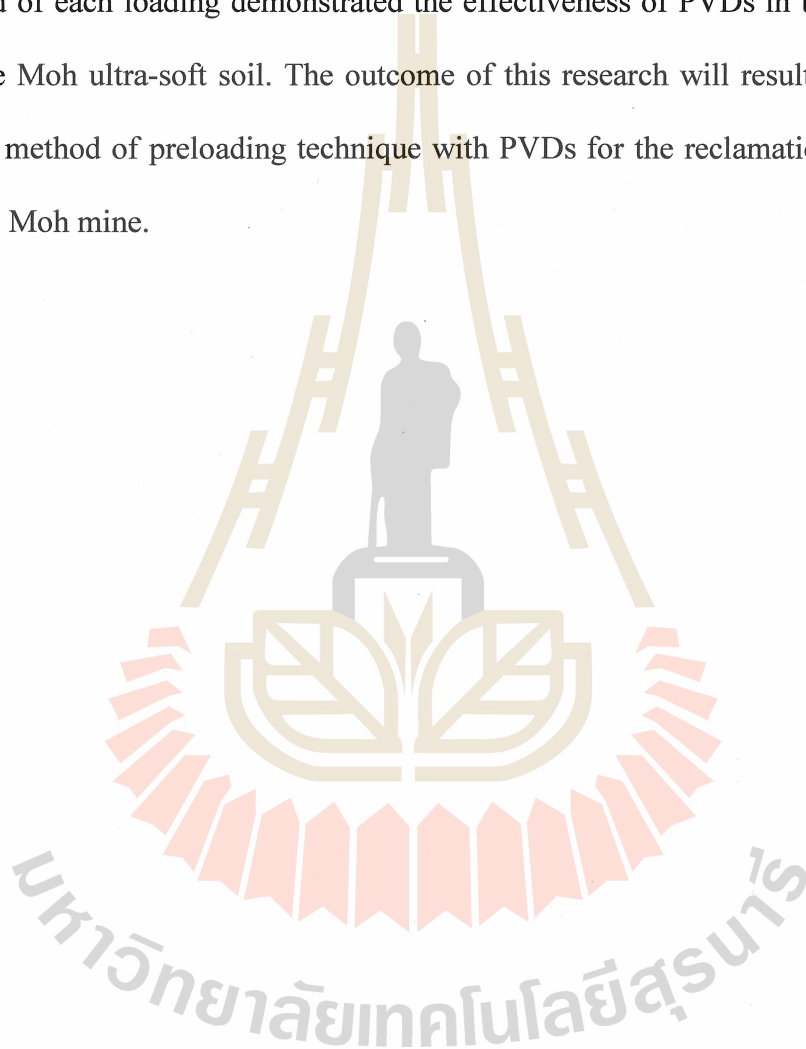
ลายมือชื่ออาจารย์ที่ปรึกษา

HUY DONG NGO : EVALUATION OF SLURRY POND
RECLAMATION AT THE MAE MOH MINE BY PREFABRICATED
VERTICAL DRAINS WITH PRELOADING TECHNIQUE. THESIS
ADVISOR : PROF. SUKSUN HORPIBULSUK, Ph.D., 171 PP.

RECLAMATION/ULTRA-SOFT SOIL/MAE MOH MINE/PREFABRICATED
VERTICAL DRAIN

This thesis studies the performance of prefabricated vertical drains (PVDs) on the improvement of ultra-soft soil in Mae Moh mine, Lampang, Thailand. The consolidation behavior of the ultra-soft soil improved with PVDs was investigated in this research. The investigation consisted of 3 parts: the compressibility characteristics of ultra-soft soil, the effectiveness of PVDs in the consolidation settlement of ultra-soft soil in model grounds and numerical simulation, and the consolidation behavior of ultra-soft soil improved with PVDs in a field trial. Sedimentation process of Mae Moh slurry was divided into two distinct different stages: flocculation and settling. The slurry was divided into large and small sedimentation slurry separated using critical water content (w_{cr}) as the reference. The consolidation curve could be predicted by a proposed generalized consolidation equation using generalized void ratio. The intrinsic state line for large sedimentation soil was proposed for examining the stress state and predicting the consolidation curve of the ultra-soft soil, which is significant for reclamation project of Mae Moh mine. Based on the large-scale model and the field trial results, a large settlement with delay of excess pore water pressure dissipation is a distinct behavior of Mae Moh ultra-soft soil. The undrained shear strength (S_u) can be approximated by the vertical

effective stress (σ'_v) based on SHANSEP equation where the σ'_v was determined from Asaoka's observation method. In practice, the plane strain models proposed by Chai et al. and Indraratna and Redana's were suggested to predict the consolidation settlement of the Mae Moh ultra-soft soil improved with PVD. The increase of S_u at the end of each loading demonstrated the effectiveness of PVDs in the improvement of Mae Moh ultra-soft soil. The outcome of this research will result in the effective design method of preloading technique with PVDs for the reclamation of Sump1 C1 in Mae Moh mine.



School of Civil Engineering

Academic Year 2019

Student's Signature 

Advisor's Signature 

ACKNOWLEDGMENTS

First and Foremost, I wish to extend my sincere gratitude to my advisor Prof. Dr. Suksun Horpibulsuk for his supervision, encouragement and support, all of which have been given to me with his endless kindness, throughout my Ph.D. study at Suranaree University of Technology. Without his guidance and persistence assistance, this thesis would not have been possible.

Besides, I would like to express my deepest appreciation to my thesis committee: Prof. Dr. Panich Voottipruex, Assoc. Prof. Dr. Avirut Chinkulkijniwat, Assoc. Prof. Dr. Chatchai Jothityangkoon, and Dr. Apichat Suddepong, for their encouragement, insightful comments, and constructive suggestion.

I would like to acknowledge the valuable support from Mr. Artit Udomchai, Dr. Menglim Hoy, Mr. Wisanukhorn Samingthong, Mr. Somsak Sookawapee, Mr. Apinun Buritatum, Mr. Chakkrit Yeanyong, and other staff in the Center of Excellence in Innovation for Sustainable Infrastructure Development, Suranaree University of Technology and Mr. Prajueb Doncommul and Mr. Apipat Chaiwan, Mae Moh mine, EGAT during laboratory testing and field construction at the Mae Moh mine, Thailand.

In addition, a profound gratitude is expressed to Prof. Dr. Arul Arulrajah of Department of Civil and Construction Engineering at Swinburne University of Technology, Australia for his reviews, and suggestions of my research, which are very helpful for developing excellent manuscripts published in the leading international journals.

I wish to acknowledge the financial support from Suranaree University of Technology under SUT Scholarships for Graduate International Students (Vithedbundit) during my Ph.D. study. This work was financially supported by Suranaree University of Technology, Electricity Generating Authority of Thailand grant no 61-G201000-11-IO.SS03G3008344. I also wish to thank all the staff and faculty members as well as friends at the School of Civil Engineering, Suranaree University of Technology for the academic, administrative and technical support during my Ph.D. study.

Last but not least, I would like to thank my family for their love, understanding, and supporting me spiritually throughout my Ph.D. study and my life.

Huy Dong Ngo

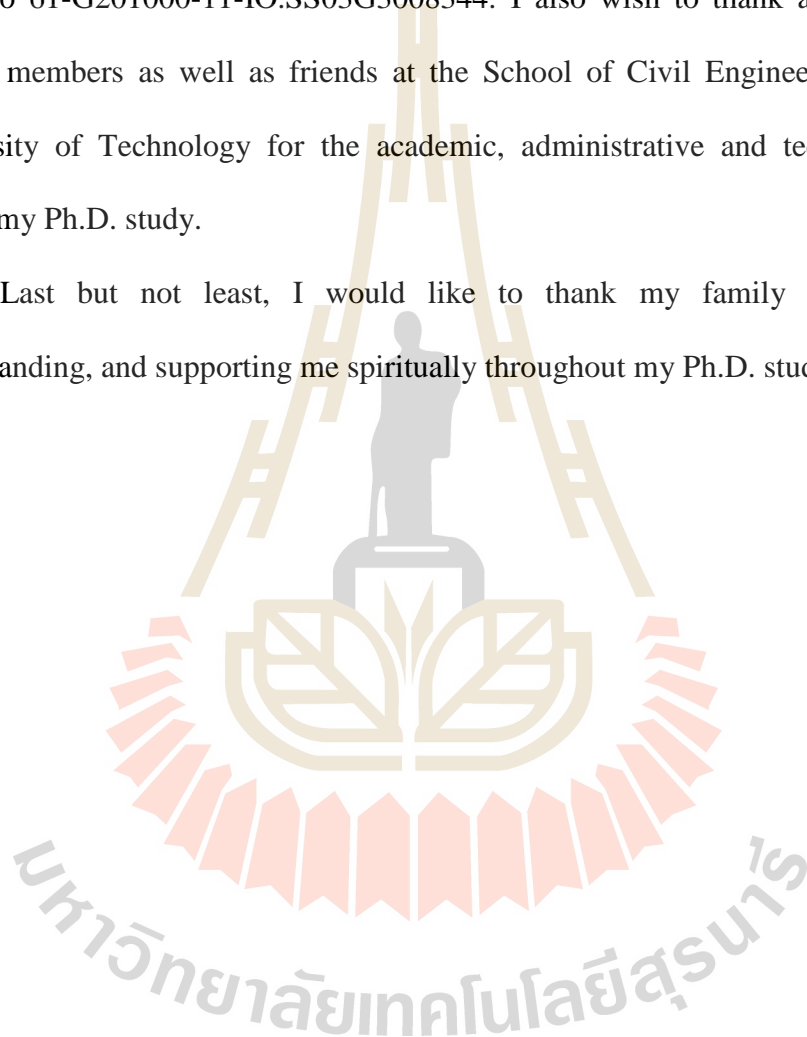


TABLE OF CONTENTS

	Page
ABSTRACT (THAI)	I
ABSTRACT (ENGLISH).....	III
ACKNOWLEDGEMENTS.....	V
TABLE OF CONTENTS.....	VII
LIST OF TABLES	XII
LIST OF FIGURES	XIII
SYMBOLS AND ABBREVIATIONS	XVIII
CHAPTER	
I INTRODUCTION.....	1
1.1 Problem statement.....	1
1.2 Objective of study.....	4
1.3 Structure of dissertation.....	4
1.4 References	6
II LITURATURE REVIEW.....	9
2.1 Introduction.....	9
2.2 Introduction of Prefabricated Vertical Drains (PVDs)	9
2.3 Consolidation theory with PVD.....	10
2.4 Factor affecting on the performance of PVDs	12
2.4.1 Smear effect	12

TABLE OF CONTENTS (Continued)

	Page
2.4.2 Selection of PVDs.....	15
2.4.2.1 Selection of filter.....	15
2.4.2.2 Selection of discharge capacity.....	17
2.4.3 Deformation of PVDs under loading conditions	19
2.4.4 Hydraulic gradient	20
2.4.5 Clogging effect.....	21
2.5 The performance of PVDs improved ultra-soft soil	22
2.5.1 Laboratory investigation	22
2.5.2 Field performance	25
2.6 References	28
III COMPRESSIBILITY OF ULTRA-SOFT SOIL IN	
THE MAE MOH MINE, THAILAND	33
3.1 Introduction	33
3.2 Material and methods.....	37
3.2.1 Soil sample.....	37
3.2.2 Sedimentation test	39
3.2.3 Consolidation test.....	42
3.3 Result and discussion.....	43
3.3.1 Sedimentation of slurry	43
3.3.2 Consolidation behavior of sedimentation soil.....	47
3.3.2.1 Consolidation curve	47

TABLE OF CONTENTS (Continued)

	Page
3.3.2.2 Hydraulic conductivity.....	50
3.3.2.3 Estimation of consolidation curve of Mae Moh sedimentation soil.....	51
3.4 Assessment of stress state of ultra-soft soil	59
3.5 Conclusion	62
3.6 References.....	63
IV CONSOLIDATION BEHAVIOR OF ULTRA-SOFT SOIL IMPROVED WITH PREFABRICATED VERTICAL DRAIN AT THE MAE MOH MINE, THAILAND.....	68
4.1 Introduction.....	68
4.2 Large-scale consolidation test.....	70
4.2.1 Soil sample.....	70
4.2.2 Selection of PVD	71
4.2.3 Model test.....	73
4.2.4 Numerical simulation.....	76
4.3 Results and discussion	82
4.3.1 Model test results	82
4.3.1.1 Settlement results	82
4.3.1.2 Excess pore water pressure	86
4.3.1.3 Water content and undrained shear strength.....	92

TABLE OF CONTENTS (Continued)

	Page
5.5 Field test results and discussion	127
5.5.1 Settlement	127
5.5.2 Excess pore water pressure	129
5.5.3 Degree of consolidation	133
5.5.4 Undrained shear strength	135
5.6 Conclusion	138
5.7 References	139
VI CONCLUSION AND RECOMMENDATIO	
6.1 General Summary	143
6.1.1 Compressibility of Mae Moh ultra-soft soil without PVDs	143
6.1.2 Consolidation behavior of Mae Moh ultra-soft soil improved with PVDs via laboratory testing	144
6.1.3 Consolidation behavior of Mae Moh ultra-soft soil improved with PVDs via full-scale test	145
6.2 Recommendation for future work	146
APPENDIX	
APPENDIX A. LIST OF PUBLICATIONS	147
BIOGRAPHY	171

LIST OF TABLES

Table	Page
2.1	Diameter of smear zone studied by various researchers 13
3.1	The comparison between measured and calculated water content after testing..... 44
3.2	Values of equation parameter for Mae Moh Slurry soil. 53
3.3	The soil parameters of Kemen and Baimahu clay used for simulation. 57
4.1	Cases tested..... 71
4.2	PVDs characteristics..... 72
4.3	Soil parameters for modeling case 1..... 78
4.4	Soil parameters for predictions of undrained shear strength. 99
5.1	Properties of ultra-soft soil and clay stone..... 113
5.2	Characteristics of PVD. 114
5.3	Soil parameter properties for finite element analysis. 115
5.4	Minimum factor of safety during construction process. 116
5.5	Characteristics of geotextile..... 118

LIST OF FIGURES

Figure	Page
2.1 Structure of PVD.....	10
2.2 Permeability along the radial distance from the central drain (a) Horizontal and (b) Vertical (Indraratna & Redana, 1998)	15
2.3 Required discharge capacity as a function of PVD length and permeability of soil (Chu et al., 2004).....	18
2.4 q_w of PVDs under $i = 0.1$ versus percentage settlement % (Tran et al., 2010).....	20
2.5 Decrease in discharge capacity with hydraulic gradient (Bo et al. 2016)	21
2.6 Large diameter consolidation tank (Chu et al., 2006).....	23
2.7 Settlement versus time curve measured from the model test under 110 kPa	24
2.8 Pore pressure dissipation versus time curve measured under 110 kPa vertical pressure	24
2.9 The water content distribution: (a) along the elevation perpendicular to the PVDs and (b) along the elevation facing the drains	25
2.10 The measure settlement and excess pore water pressure in the field (Chu et al., 2006)	27

LIST OF FIGURES (Continued)

Table		Page
3.1	Typical cross-section of In-pit dump in the Mae Moh mine (dimension in meter)	34
3.2	Sampling site	38
3.3	Grain size distribution curve	39
3.4	8 cylinders containing slurry at different initial water contents	40
3.5	Illustration of changing interface location before and after sedimentation process	41
3.6	Interface location of 8 samples the end of test	45
3.7	Sedimentation curves at different initial water contents in logarithmic time scale	45
3.8	Water content versus with time (log scale) relationship	46
3.9	Consolidation curve of sediment soil at different sedimentation water contents	49
3.10	Bilogarithmic consolidation curves of sediment soil at different sedimentation water contents.....	49
3.11	Yield stress versus sedimentation water content	50
3.12	e - log(k) relationship of sediment soil at different sedimentation water contents	51
3.13	Prediction of consolidation curves of sediment soil using S-shaped equation.....	54

LIST OF FIGURES (Continued)

Table		Page
3.14	Relationship between parameters a and b versus e_s/e_L	55
3.15	Prediction of consolidation curves of Mae Moh sediment soil using generalized S- shaped equation.....	56
3.16	Prediction of consolidation curves of Keman and Baimaha sediment clay using generalized S-shaped equation.....	58
3.17	Intrinsic state line for large sedimentation soil	60
4.1	Large scale of consolidation tank (dimensions are in mm)	74
4.2	Geometry conditions using a) Axisymetry model; b) Plane strain model using Chai et al.'s method; c) Plane strain model using Lin et al.'s method and Indraratna and Redana's method.....	78
4.3	Measured settlement versus time curves of 3 cases under 3 loading stages.....	84
4.4	Ultimate settlements of each loading stage predicted by using Asaoka's observational method.....	85
4.5	Measured excess pore water pressure versus time relationships for case 1 ($W_i = 120\%$ and PVD 10cm)	88
4.6	Measured excess pore water pressure versus time relationships for case 2 ($W_i = 180\%$ and PVD 10 cm width)	89

LIST OF FIGURES (Continued)

Table	Page
4.7	Measured excess pore water pressure versus time relationships for case 3 ($W_i = 120\%$ and PVD 5 cm width)..... 90
4.8	Relationships between S/S_{ult} and u/u_o of Mae Moh ultra-soft dredged soil and soft Bangkok clay improved with PVD..... 91
4.9	Change of water contents at various distances from PVDs in 3 cases..... 94
4.10	Measured and predicted undrained shear strength (in kPa) during the consolidation process 94
4.11	Measured and predicted settlement versus time curves in case 1 97
4.12	Measured and predicted excess pore water pressures in case 1 97
5.1	Location of full-scale test site in the field..... 112
5.2	Geometry model..... 115
5.3	Stitching of the geotextile sheets: (a) Concept of sewing geotextile; (b) Sewing geotextile at the site; (c) Installing a connected geotextile in the pond; (d) Completion of connected geotextile installation the pond. 119
5.4	Construction procedure for platform 120
5.5	Completion of PVDs installation on 3 August 2019 122
5.6	Installation of Neodrain pipes on 30 September 2019: (a) Step 1: Installing neodrain pipes; (b) Step 2: Preparing geotextile to wrap the pipes; (c) Step 3: Wrapping the pipes by using geotextile; (d) Step 4: Connection the pipes with the tanks 123

LIST OF FIGURES (Continued)

Table	Page
5.7 Loading stage with time.....	125
5.8 Photos of trial pond after finishing construction of each loading stage: (a) Sand blanket; (b) Loading stage 1: 1.0 m clay stone; (c) Loading stage 2: 1.5 m clay stone; (d) Loading stage 3: 2.5 m clay stone.....	126
5.9 Plan and top views of full-scale test pond	126
5.10 Settlement versus time curves obtained from 3 settlement plates	128
5.11 Final settlements of each loading stage predicted by using Asaoka's observational method.	129
5.12 Measured excess pore water pressure versus time relationships	131
5.13 Relationship between S/S_f versus u/u_o of Mae Moh ultra-soft soil compared with soft Bangkok clay.....	133
5.14 Excess pore water pressure versus depth relationships at any time during sand blanket installation.....	134
5.15 Comparison of degrees of consolidation based on measured settlement (U_s %) and excess pore water pressure (U_e %) for Mae Moh ultra-soft soil and Bangkok soft clay.....	135
5.16 Settlement, excess pore water pressure and the undrained shear strength versus time relationships in loading stage 3.....	137
5.17 Undrained shear strength at different depths under different increased of vertical effective stresses (kPa)	138

SYMBOLS AND ABBREVIATIONS

PVD	=	Prefabricated Vertical Drains
EGAT	=	Electricity Generating Authority
PBD	=	Plastic board drain
PD	=	Packed drain
AOS	=	Apparaent opening size
D	=	Discharge factor
w_i	=	Initial water contents
w_f	=	Water content at the end of sedimentation test
w_s	=	Sedimentation water content
w_{cr}	=	Critical water content
w_t	=	Water content at time t
ISL	=	Intrinsic state line
°C	=	Degree Celsius
γ_{dmax}	=	dry unit weight
C_h	=	Horizontal coefficient of consolidation
u	=	Excess pore pressure
u_0	=	Initial excess pore pressure
u_t	=	Settlement at time t
t	=	Time
r	=	Radial distance

SYMBOLS AND ABBREVIATIONS (Continued)

r_e	=	Radius of equivalent soil cylinder
r_w	=	Equivalent radius of the drain
μ	=	PVDs spacing factor
l	=	Length of drainage path
q_w	=	Discharge capacity of PVDs
k_s	=	Hydraulic conductivity of smear zone
d_s	=	Diameter of smear zone
d_m	=	Equivalent diameter of the cross-section area of mandrel
O_{95}	=	Apparent opening size of filter
O^*_{95}	=	Actual filter of opening size
K	=	Reduction factors
i	=	Hydraulic gradient
Q	=	Discharge volume of water
h_0	=	Initial height of the slurry
e_0	=	Initial void ratio of the slurry
G_s	=	Specific gravity
m_v	=	Coefficient of volume change
e_L	=	Liquid limit ratio
e_s	=	Sedimentation void ratio
W_{cr}	=	Critical water content
FEM	=	Finite element method

SYMBOLS AND ABBREVIATIONS (Continued)

PPT	=	Pore pressure transducer
LVDTs	=	Linear Variable Displacement Transducers
λ^*	=	Modified compression index
λ^*	=	Modified swelling index
c'	=	Cohesion of soil
ϕ'	=	Friction angle
k_{ve}	=	Equivalent value of vertical hydraulic conductivity
k_v	=	Vertical hydraulic conductivity
k_s	=	Vertical hydraulic conductivity in smear zone
S_{ult}	=	Ultimate settlement
S_u	=	Undrained shear strength
M	=	Slope of critical state line
ϵ_c	=	Specific volume of soil at critical state line
λ	=	Slope of normal compression line

CHAPTER I

INTRODUCTION

1.1 Problem statement

The Mae Moh Mine is the largest open-pit lignite mine in Thailand, as well as in Southeast Asia, with a total mining area of approximately 37.5 km² and external dumping area of approximately 41.4 km². It is situated at the Mae Moh district, Lampang province in the north of Thailand, located 630 km away from Bangkok. The lignite material at the Mae Moh basin is the main raw feed material used to generate power at the Mae Moh power plants, operated by the Electricity Generating Authority of Thailand (EGAT). Approximately 16 million tons of coal are produced annually and transferred to the 10 units of the Mae Moh power plant in order to generate the total power supply of 2,400 Megawatt. The Mae Moh power plant can supply 50% of the electricity to the northern area, 30% to the central area, and 20% to the north-eastern area of Thailand.

Sump1 C1, a slurry pond with a total area of 80000 m² located in the north of the Mae Moh mine, is the main source for mining activities such as mineral processing and dust suppression. The discharge of surface water and groundwater flow has caused soil erosion along the mine slope, which has resulted in ultra-soft soil deposits located underwater in the slurry ponds over the years. The thickness of the ultra-soft soil in some ponds is even up to 40 m.

According to the mine planning and development of EGAT, this mine will be excavated to a depth of approximately 500 m from the original surface over the next four decades, resulting in this becoming the deepest open pit lignite mine in the world. The excavated soil from mining activities will be dumped in the Sump1 C1 for land reclamation. Therefore, Sump1 C1 will be subjected to a very high overburden material of approximately 300m within 2038. However, the soil in the ponds is in the ultra-soft state, with very low undrained shear strength and high water content of greater than liquid limit. In-pit dumping without mechanical property improvement of this ultra-soft soil is almost impossible. Due to very low undrained shear strength, the mud flood of the ultra-soft soil could occur immediately after the in-pit dump and causes detrimental effects on the mining activities. Therefore, it is imperative to improve the existing ultra-soft soil before commencing any construction activities in order to prevent any failure, which might causes detrimental effects on the mining activities.

In recent years, large – scale reclamation activities have been carried out by using several improvement techniques over the world (Almeida et al., 1993; Almeida et al., 2005; Choa et al., 2001; Hong & Shang, 1998; Morohoshi et al., 2010). A simple method called sand spreading technique was used to improve the soft soil conditions in Changi East reclamation project in Singapore (Bo et al., 2005; Choa, 1995; Choa et al., 2001). However, this treatment method takes long time to complete the construction, it allows sufficient time for the soft soil near the drainage boundary to develop the strength. The sand spreading technique also produces a very loose fill and hence a lower fill density.

A complicated method has been considered by using combined vertical drain as plastic board drain (PBD), small size fabric – packed drain (PD), sand – drain and large size partially fabric-packed sand drain for Tokyo International Airport Extension Project (Morohoshi et al., 2010). However, Morohoshi et al. (2010) reported that the sand drain was affected by low strength of surrounding soil and broken by deformation of soil during the sand drain installation. On the other hand, when the height of embankment fill is higher than critical height or lower than critical bearing capacity of soft soil layer, horizontal flow of soil caused the damage to sand drain.

A rapid improvement technique in large area reclamation work-low vacuum preloading method has been proposed by (Yusheng et al., 1999). After that, Li et al. (2002) developed the spatial vacuum drainage method. However, the drawback of these proposed methods is costly and requires long construction period. A suitable ground improvement method for the ultra-soft soil in the Mae Moh mine is the preloading technique with prefabricated vertical drains (PVDs). It is effective in term of economic and environmental perspectives as compared to other techniques, such as deep soil mixing and soil replacement (Bergado et al., 1990; Bergado et al., 2002; Chu et al., 2004; Hansbo, 1979). Even though preloading technique with PVDs have been used successfully in many land reclamation project in the world (Bergado et al., 1990; Bergado et al., 2002; Chu et al., 2004; Hansbo, 1979, 2005; R. Holtz, 1987; Holtz et al., 1991; Indraratna & Redana, 2000; Indraratna et al., 2005; A. L. Li & Rowe, 2001), the performance of PVD for the improvements of ultra-soft soil are still limited.

Therefore, this research is carried out to investigate the performance of PVD improving the ultra-soft soil in Mae Moh mine, Thailand. The research outputs will

confirm the effectiveness of using PVD for the improvement of ultra-soft soil in Mae Moh Mine, Thailand.

1.2 Objective of study

In order to use the PVDs for the improvement of Mae Moh ultra-soft soil, an evaluation in the laboratory and the field have to be fully conducted. The three main objectives of this research is of address as following outlines:

1. To investigate the compression behavior of Mae Moh ultra-soft soil without Prefabricated Vertical Drains
2. To study the consolidation behavior of Mae Moh ultra-soft soil improved with Prefabricated Vertical Drains using a series of large-scale model test and numerical analysis.
3. To investigate the performance of PVD improved Mae Moh ultra-soft soil using full-scale testing in the field.

1.3 Structure of dissertation

This thesis consists of six chapters, which are divided according to the following outlines:

- **Chapter I** is the introduction part that presents the problem statement and the objective of the study.
- **Chapter II** shows the literature review of the recent research papers involves the theory of consolidation with PVD, the performance of PVD in ultra-soft soil and the factors which affect the PVD performance on the consolidation of ultra-soft soil.

- **Chapter III** presents the study of compressibility characteristics of Mae Moh ultra-soft soil, which is composed of sedimentation and consolidation phases. A series of sedimentation tests were performed on the slurry under various initial water contents ranging from 116% to 437%. The consolidation behavior of the sedimentation soil at a wide range of effective stresses and water content was also investigated. Finally, a practical method for assessing the stress state of slurry and consolidation curve of sedimentation soil is proposed.

- **Chapter IV** presents the performance of PVD in the consolidation of Mae Moh ultra-soft soil via a series of large-scale model test. The effects of PVD dimension and water content of the ultra-soft soil on the settlement, excess pore pressure dissipation and undrained shear strength of PVD improved ground under various loading conditions were investigated. The large-scale consolidation test results were analyzed and compared with the simulation results by finite element method (FEM). Also, the suitable numerical method for predicting settlement at various consolidation time was recommended. The research outputs will facilitate the selection of design parameters and numerical method for the future design of dredged soil in Sump 1 C1 using preloading with PVD system.

- **Chapter V** presents the full scale test on PVDs improved ultra-soft soil at a trial slurry pond prior to the PVD construction in Sump1 C1. The successful construction with field measurement will be a lesson learned for a real construction project on the improvement of ultra-soft soil in Sump1 C1. The outcome of this field study will result in an effective design method for Sump1 C1 in Mae Moh mine and other similar slurry ponds.

- **Chapter VI** concludes the research work and provides the suggestion as well as recommendation for further research.

1.4 References

- Almeida, M., & Ferreira, C. (1993). **Field in situ and laboratory consolidation parameters of a very soft clay**. Paper presented at the Predictive Soil Mechanics, Proceedings of the Worth Memorial Symposium. Thomas Telford, London, UK.
- Almeida, M. S., Marques, M. E. S., & Spotti, A. P. (2005). **Two case histories of vertical drains in very soft clays**. Elsevier Geo-Engineering Book Series, 3, 145-157.
- Bergado, D., Singh, N., Sim, S., Panichayatum, B., Sampaco, C., & Balasubramaniam, A. (1990). **Improvement of soft Bangkok clay using vertical geotextile band drains compared with granular piles**. Geotextiles and Geomembranes, 9(3), 203-231.
- Bergado, D. T., Balasubramaniam, A., Fannin, R. J., & Holtz, R. D. (2002). **Prefabricated vertical drains (PVDs) in soft Bangkok clay: a case study of the new Bangkok International Airport project**. Canadian Geotechnical Journal, 39(2), 304-315.
- Bo, M. W., Choa, V., & Wong, K. S. (2005). **Reclamation and soil improvement on ultra-soft soil**. Proceedings of the Institution of Civil Engineers - Ground Improvement, 9(1), 23-31. doi:10.1680/grim.2005.9.1.23
- Choa, V. (1995). **Changi east reclamation project**. Paper presented at the Int'l Symposium on Compression and Consolidation of Clayey Soils.

- Choa, V., Bo, M., & Chu, J. (2001). **Soil improvement works for Changi East reclamation project**. Proceedings of the Institution of Civil Engineers-Ground Improvement, 5(4), 141-153.
- Chu, J., Bo, M., & Choa, V. (2004). **Practical considerations for using vertical drains in soil improvement projects**. Geotextiles and Geomembranes, 22(1-2), 101-117.
- Hansbo, S. (1979). **Consolidation of clay by band shaped prefabricated drains**. Ground Engineering, 12(5).
- Hansbo, S. (2005). **Experience of consolidation process from test areas with and without vertical drains**. In Elsevier Geo-Engineering Book Series (Vol. 3, pp. 3-49): Elsevier.
- Holtz, R. (1987). **Preloading with prefabricated vertical strip drains**. Geotextiles and Geomembranes, 6(1-3), 109-131.
- Holtz, R. D., Jamiolkowski, M., Lancellotta, R., & Pedroni, R. (1991). **Prefabricated vertical drains: design and performance**.
- Hong, H., & Shang, J. (1998). **Probabilistic analysis of consolidation with prefabricated vertical drains for soil improvement**. Canadian Geotechnical Journal, 35(4), 666-667.
- Indraratna, B., & Redana, I. (2000). **Numerical modeling of vertical drains with smear and well resistance installed in soft clay**. Canadian Geotechnical Journal, 37(1), 132-145.

- Indraratna, B., Rujikiatkamjorn, C., Balasubramaniam, A., & Wijeyakulasuriya, V. (2005). **Predictions and observations of soft clay foundations stabilized with geosynthetic drains and vacuum surcharge.** In Elsevier Geo-Engineering Book Series (Vol. 3, pp. 199-229): Elsevier.
- Li, A. L., & Rowe, R. K. (2001). **Combined effects of reinforcement and prefabricated vertical drains on embankment performance.** Canadian Geotechnical Journal, 38(6), 1266-1282.
- Li, L.-h., Wang, Q., Wang, N. x., Wang, J.-p., & Yi, X.-h. (2002). **Research on the feasibility of consolidating hydraulic fill in layers by the method of spatial vacuum drainage.** chinese journal of geotechnical engineering-chinese edition-, 24(4), 522-524.
- Morohoshi, K., Yoshinaga, K., Miyata, M., Sasaki, I., Saitoh, H., Tokoro, M., Ishikawa, M. (2010). **Design and long-term monitoring of Tokyo International Airport extension project constructed on super-soft ground.** Geotechnical and Geological Engineering, 28(3), 223-232.
- Yusheng, Q., Zhiyi, L., & Dazheng, C. (1999). **Study on the low-location vacuum pre-pressure reinforcement technique [J].** Geoscience, 4, 471-476.

CHAPTER II

LITERATURE REVIEW

2.1 Introduction

In this chapter, a brief introduction of prefabricated vertical drains (PVDs) and the consolidation theory with PVDs are presented in this chapter. The performance of PVD in ultra-soft soil in both laboratory testing and in the field and some factors which effect on the PVDs performance are discussed in detail. The primary focus is to critically analyze existing literature on the subject and understand whether it is applicable in the context of PVDs so that the importance of this study can be clearly articulated.

2.2 Introduction of Prefabricated Vertical Drains (PVDs)

The preloading technique with prefabricated vertical drains (PVDs) has been used widely for the improvement of soft soil in the world (Holtz 1987, Bergado et al., 1990, Almeida and Ferreira 1993, Bergado et al., 1993, Choa et al., 2001, Xiao 2001, Almeida and Marques 2003, Almeida et al, 2004, Chu et al., 2006). PVDs consists a synthetic geotextile jacket surrounding a plastic core, as shown in Fig. 2.1. A synthetic geotextile jacket is a physical barrier separating the core flow channels from the surrounding fine-grained soils and a filter to limit the passage of fine grained soil into the core area. A plastic core is support the filter fabric and to provide the longitudinal flow path along the drain length. The advantages of preloading technique with PVDs is as follows:

- Reduce the overall time, which is required to complete the primary consolidation under the loading conditions
- Reduce amount of surcharge required to achieve the desired amount of pre-compression in the given time.
- Reduce the water content of soil.
- Enhance the shear strength of the soil.

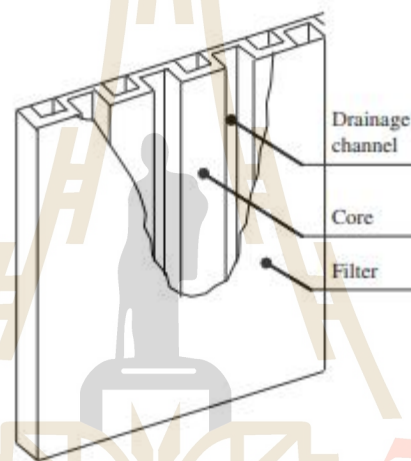


Figure 2.1: Structure of a PVD

2.3 Consolidation theory with PVDs

Barron (1948) proposed the solutions for both equal strain case and free strain case based on the simplifying assumptions of one dimensional consolidation theory (Terzaghi 1943). The conditions of Barron's theory is: (i) free vertical strain assuming that the vertical surface stress remains constant and the surface displacements are non-uniform during the consolidation process; (ii) equal vertical strain assuming that the vertical surface stress is non-uniform. The generalized three-dimensional equation of consolidation is proposed as follows:

$$\frac{\partial u}{\partial t} = C_v \left(\frac{\partial^2 u}{\partial z^2} \right) + C_h \left(\frac{\partial^2 u}{\partial r^2} + \frac{1}{r} \frac{\partial u}{\partial r} \right) \quad (2.1)$$

For the equal strains case, the equation is given as:

$$\frac{\partial u}{\partial t} = C_h \left[\left(\frac{\partial^2 u}{\partial r^2} \right) + \frac{1}{r} \left(\frac{\partial u}{\partial r} \right) \right] \quad (2.2)$$

in which u is the excess pore pressure at any point and at any time t ; r is the radial distance from the center of soil cylinder to the considered point; C_h is the horizontal coefficient of consolidation. For radial flow only, the solution of Barron (1948) under ideal conditions (no smear and no well resistance) is as follows:

$$U_h = 1 - \exp \left[\frac{8T_h}{F(n)} \right] \quad (2.3)$$

where:

$$T_h = \frac{C_h t}{4r_e^2} \quad (2.4)$$

$$F(n) = \left[\frac{n^2}{(1-n)} \right] \left[n(n) - \frac{3}{4} + \frac{1}{n^2} \right] \quad (2.5)$$

in which r_e is the radius of the equivalent soil cylinder, r_w is the equivalent radius of the drain, and n is the spacing ratio, which is taken as r_e/r_w .

Hansbo (1981) modified the Barron's equation for prefabricated drain applications. It dealt with simplifying assumption due to the physical dimensions, characteristics of prefabricated drains, and effect of installation. The modified general expression for average degree of consolidation is given as expressed as,

$$U_h = 1 - \exp\left[-\frac{8T_h}{\mu}\right] \quad (2.6)$$

The parameter μ represents the effect of PVDs spacing, the smear effect and well-resistance. It is given as,

$$\mu = \ln(n/s) + (k_h/k_s) \ln(s) - 0.75 + f z(2l-z) \frac{k_h}{q_w} \quad (2.7)$$

in which q_w is the discharge capacity of PVDs, l is length of drainage path, k_h and k_s are the hydraulic conductivity of undisturbed zone and smear zone, respectively.

2.4 Factors affecting on the performance of PVDs

2.4.1 Smear effect

In the field, the PVDs are installed by using a steel mandrel, which is penetrated into the soil layer with PVD inside it. The installation of PVDs cause a remolding of subsoil especially in the immediate vicinity of mandrel. The developed smear zone leads the increase in compressibility and the reduction in soil permeability adjacent to PVD. The smear zone with a reduction of permeability surrounded by the undisturbed zone was introduced by Hansbo (1979). The characteristics of smear

effect includes the diameter of the smear zone (d_s) and the permeability ratio (k_h/k_s) (Jamiolkowski et al., 1981, 1983, Hansbo 1987, Miura et al., 1998). The d_s value can be taken as follows (Jamiolkowski and Lancellotta 1981):

$$d_s = (2.5-3) \times d_m \quad (2.8)$$

where d_m is equivalent diameter of the cross-section area of mandrel. Based on the results of (Akagi 1979), the smear zone was evaluated by the simple expression:

$$d_s = 2 \times d_m \quad (2.9)$$

The d_s value proposed by various researchers is summarized in **Table 2.1**.

Table 2.1: Diameter of smear zone studied by various researchers

Reference	Diameter of Smear zone	Remark
Hansbo (1986)	$d_s = 2 \times d_m$	
Jamiolkowski and Lancellotta (1981)	$d_s = 2.5 \times d_m$	
Bergado et al. (1991)	$d_s = 2 \times d_m$	
Onnoue et al. (1991)	$d_s = 6-7 \times d_m$	
Chai and Miura (1999)	$d_s = 2-3 \times d_m$	<i>Saga Airport, Japan</i>
Sharma and Xiao (2000)	$d_s = 4 \times d_m$	<i>Kaoline clay</i>
Saowapakpiboon et al. (2010)	$d_s = 2 \times d_m$	<i>Bangkok clay</i>
Ghandeharioon et al.(2009)	$d_s = 3.1 \times d_m$	<i>Soft clay in Malaysia</i>
Rujikiatkamjorn et al.(2013)	$d_s = 3.7-5.5 \times d_m$	<i>Kaoline clay</i>
Indraratna et al. (2014)	$d_s = 6.3 \times d_m$	<i>Ballina clay Australia</i>
Sengul et al. (2017)	$d_s = 2.3-3.3 \times d_m$	<i>Kaoline clay</i>

Regarding the k_h / k_s value, Hansbo (1987) proposed that k_s can be taken as vertical hydraulic conductivity of undisturbed soil, k_v (Hansbo 1987). The value of k_h / k_s varied from 1 to 15, reported by (Jamiołkowski and Lancellotta 1981) or can be calculated as

$$\frac{k_h}{k_s} = \left(\frac{k_h}{k_s} \right)_l \times C_f \quad (2.10)$$

where subscript l is the value determined in the laboratory; C_f is permeability ratio between field and laboratory values, which can be considered as 1 in case of homogenous deposit, and is higher than 1 for stratified deposits.

Indraratna and Redana (1998) studied the effect of smear zone due to PVDs installation via a large-scale consolidation test. The d_s value was proposed as four times the diameter of central drain (mandrel). The k_h (inside the smear zone) was in the order of 60-91% of that of outer undisturbed zone, which is similar to Hansbo's recommendation while the k_v was almost remained constant even at the drain interface (**Fig. 2.2**) (Hansbo 1987).

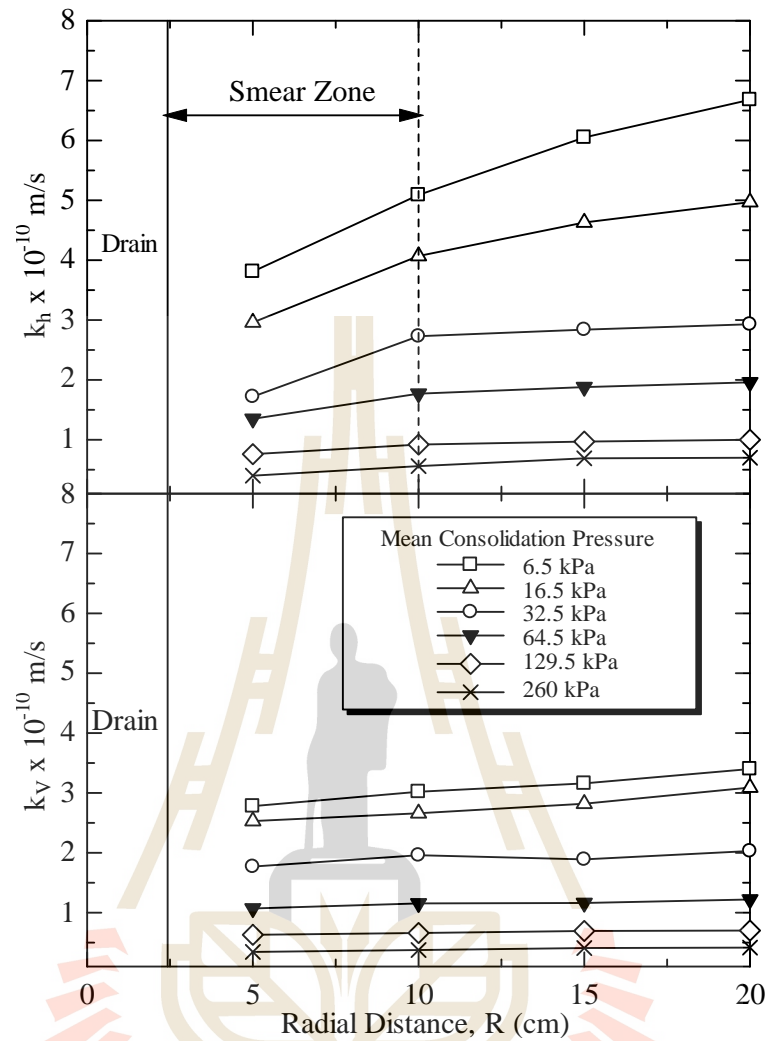


Figure 2.2: Permeability along the radial distance from the central drain (a) Horizontal and (b) Vertical (Indraratna and Redana 1998)

2.4.2 Selection of PVDs

2.4.2.1 Selection of filter

The selection of PVDs filter plays an important role in successful performance of PVD improved ultra-soft soil. The apparent opening size (O_{95}) is required to be small enough to prevent the fine grained soil entering into the filter and clogging the drainage channels leading to reduction of discharge capacity.

The criteria for AOS of the filter was suggested by Christopher and Fischer 1992, Luettich et al. 1992, Palmeria and Gardoni 2002, and Rowe and Li 2005. The requirement of O_{95} proposed by Carroll Jr (1983) is commonly used as follows:

$$\begin{cases} O_{95} \leq (2-3)D_{85} \\ O_{50} \leq (10-12)D_{50} \end{cases} \quad (2.11)$$

in which O_{50} is the size which is larger than 50% of the fabric pores, D_{85} and D_{50} refer to the sizes for 85% and 50% passing of soil particles by weight, respectively.

For Bangkok clay, Alfaro et al. (1994) suggested that the apparent opening size should be as:

$$\begin{cases} O_{95} \leq (2-3)D_{85} \\ O_{50} \leq (18-24)D_{50} \end{cases} \quad (2.12)$$

For Singapore marine clay, The O_{95} value has been suggested (Chu et al., 2004):

$$O_{95} \leq (4-7.5)D_{85} \quad (2.13)$$

However, the actual filter of opening size, O_{95}^* , is reduced under the vertical stress.

Therefore, Palmeira and Gardoni (2002) suggested that the effect of vertical stress should be taken into account, as follows:

$$O_{95}^* \leq O_{95} / K_{\dagger} K_{pc} \quad (2.14)$$

K_{\dagger} and K_{pc} are the reduction factors, which considers stress level and partial clogging on the geotextile pore constriction dimensions. The value of $K_{\dagger} K_{pc}$ varies from 1.9 - 4.4. On the other hand, the minimum permeability of the filter, k_f , is required to be higher than that of soil. According to consolidation test result by Bo (2008), the permeability of ultra-soft soil was less than 10^{-7} m/s. The k_f value of PVDs normally meets the requirements because most of the filter having the k_f value is higher than 10^{-4} m/s.

2.4.2.2 Selection of discharge capacity

Based on the back analysis data from three embankment projects, Mesri and Lo (1991) suggested that the discharge capacity of PVDs (q_w) can be taken as 5 times the discharge factor (D), which is defined as:

$$D = \frac{q_w}{(k_h \times l_m^2)} \quad (2.15)$$

where k_h is the horizontal permeability of soil, l_m is the maximum drainage length. The value of q_w has a wide range from 2 to 80 m³/year for most of clays. According to the **Eq. 11**, the higher value of k_h or l_m , the higher value of q_w . Xie (1987) proposed another conditions for required discharge capacity value based on numerical study, as follows:

$$\frac{f k_h l_m^2}{4q_w} < 0.1 \quad (2.16)$$

Then, the discharge capacity factor becomes:

$$D = \frac{q_w}{k_h l_m^2} \geq 7.85 \quad (2.17)$$

As a result, the q_w value after considering a factor of safety and all the influencing factors to be:

$$q_w \geq 7.85 F_s k_h l_m^2 \quad (2.18)$$

where F_s is the factor of safety which normally varies from 4 to 6. The relationship among these values for a factor of safety $F_s = 5$ is plotted in **Fig. 2.3** (Chu et al., 2004). **Fig. 2.3** shows that increase of l_m required higher the value of q_w .

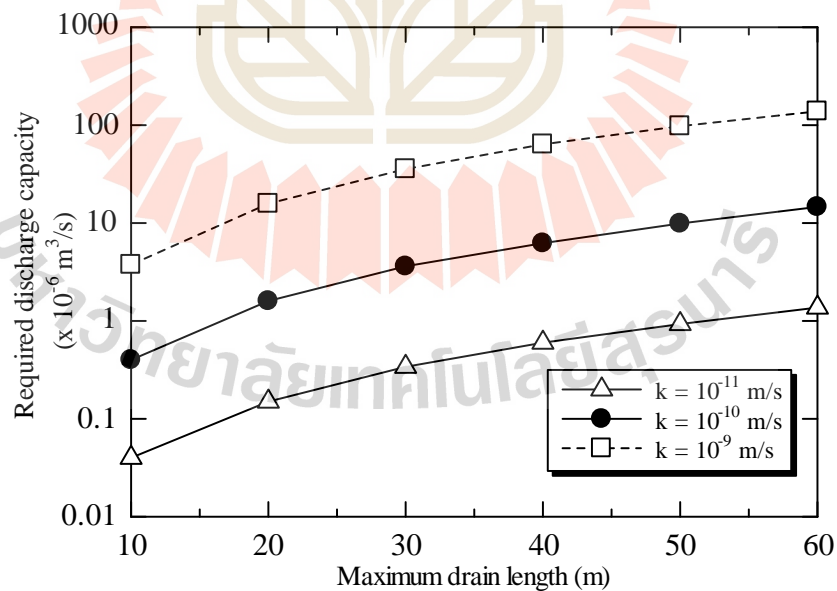


Figure 2.3 Required discharge capacity as a function of PVD length and permeability of soil (Chu et al., 2004)

2.4.3 Deformation of PVDs under loading conditions

Due to large deformation of ultra-soft soil, the deformation of PVDs by folding, crimping, bending, and buckling or kinking effect may reduce the discharge capacity significantly (Ali 1991, Aboshi et al., 2001, Chu et al., 2006). The q_w of various PVD types under a hydraulic gradient, $i = 1.0$ was studied by Lawrence and Koerner (1988). It is reported that the q_w reduced in a range of 9-72 % with a single 90° wedge. Chang et al. (1994) used an apparatus similar to a triaxial test device to measure the discharge capacity of PVDs with the induced shape of letters U or V under a maximum confining pressure of 294 kPa. It is reported that the q_w value at various i decreased by 20% to 92%. On the other hand, the q_w value was not affected at a vertical strain, v_a , of 15% (Sasaki 1981, Chai, Miura et al. 1997). A significantly the reduction of q_w value at $v_a > 15\%$ is reported by Ali (1991). Ali (1991) revealed that the q_w value at $v_a > 30\%$ and $i = 0.5$ reduced significantly, in the range of 47-99%. The q_w value varied with the stiffness of PVDs: the stiffer sleeve, the higher discharge capacity (Ali 1991). Chu et al. (2006) investigated the discharge capacity of a PVD improved ultra-soft soil under a vertical stress of 110 kPa. Chu et al. (2006) showed that the q_w reduced up to 84% at $v_a = 46\%$ during the consolidation process. Tran et al. (2010) developed a consolidation cell apparatus, which was a cylinder of 32 cm in diameter and 75 cm in high, to measure the q_w of such deformed PVDs under various i . Four different types of PVD were prepared with similar initial discharge capacities at approximately $1.2 \times 10^{-4} \text{ m}^3/\text{s}$. The q_w of PVD in all types reduced significantly up to 90 – 99% at vertical strain of 40%, except PVD type A (Figure 2.4).

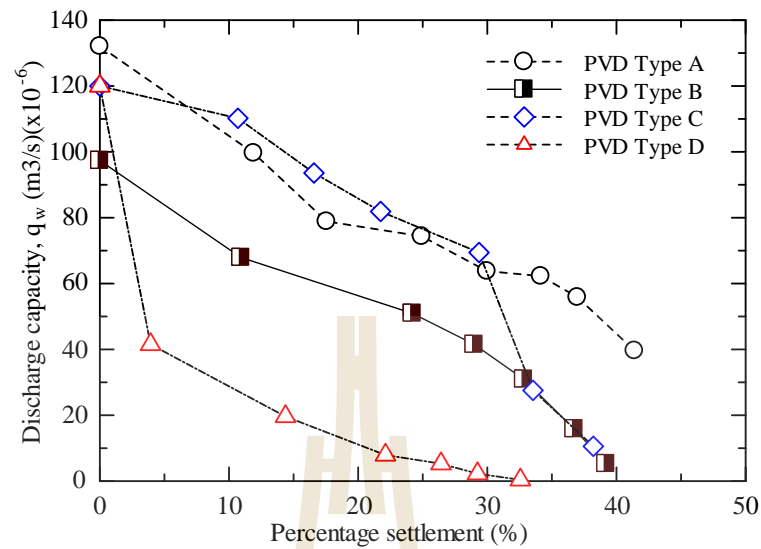


Figure 2.4: q_w of PVDs under $i = 0.1$ versus percentage settlement % (Tran et al., 2010)

2.4.4 Hydraulic gradient

The relationship between q_w and i was proposed by (Hansbo 1983):

$$q_w = \frac{Q}{i} \quad (2.19)$$

in which Q is the discharge volume of water along the PVD per unit time (m^3/s). Holtz et al. (1991) concluded that the q_w value was not affected by i . Whereas, several researchers showed that the i should be considered as a factor affecting on the q_w measurement. The q_w decreased significantly with the increase of i (Chai et al., 1997, Chu et al., 2004, Tran et al., 2010, Bo et al., 2016). Bo et al. (2016) indicated the variation of q_w with the i at different confining pressures for one type of PVD with dimension 100 mm x 100 mm, as shown in **Fig. 2.5**.

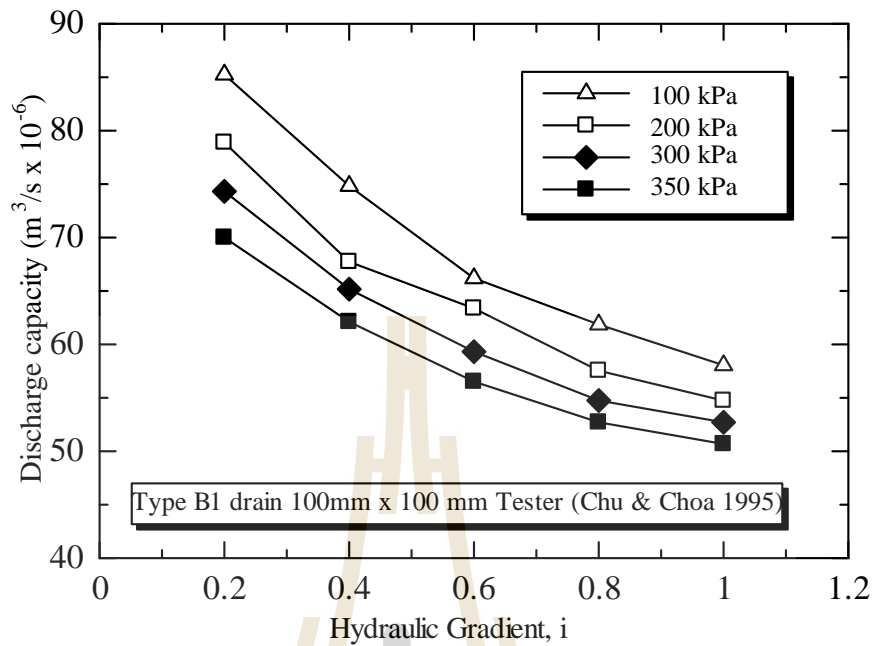


Figure 2.5 Decrease in discharge capacity with hydraulic gradients (Bo et al., 2016)

It can be seen that the decrease of q_w varies between 27.6 % and 32% with the increase of i from 0.2 to 1.0 at different values of vertical pressure. Tran et al. (2010) revealed that with the i varied from 0.1 to 1, the q_w decreases with the increase of i from 0.1 to 1 at v_a of 30%.

2.4.5 Clogging effect

During consolidation process, fine grained soil particles especially ultra-soft soil particles gradually infiltrate into the core of the PVD and consequently clog in the drainage channels leading to the reductions of q_w . Holtz et al. (1991) proposed that the effect of siltation could be neglected if the characteristic of filter was selected carefully and meet all the special criteria as requirements. Miura et al. (1998) conducted the discharge capacity test to investigate the factor influencing on q_w . The amount of water flow, Q (cm^3/sec) decreased approximately 94% during 130

days of testing. Then the hydraulic shocks (by firmly stepping on the inlet water flow hose) were used to check the clogging effect. It was found that some fine particles were pushed out of the drainage channel by pressure and deposited on the wall of the outlet. After shocking, the q_w increased rapidly over the next 30 days. It clearly proves that the part of clogging effect was removed by the hydraulic shocks.

2.5 The performance of PVDs improved ultra-soft soil

2.5.1 Laboratory investigation

Chu et al. (2006) conducted the laboratory testing by using large-scale consolidation apparatus with 0.495 m in diameter and 1 m in height to investigate the consolidation of ultra-soft soil improved by PVDs, as shown in **Fig. 2.6**. The soil was taken from a slurry pond in Changi-East Reclamation project, Singapore. The water content was 132%, which was higher approximately 2 times than the liquid limit of 73%. The undrained shear strength of the soil was extremely low, in the range of 0 to 10 kPa. PVDs having a dimensions of 100 x 5.3 mm was selected. The characteristic of PVD was selected carefully to meet the special requirement (AOS filter, required q_w , the permeability of filter). The results of settlements and the excess pore water pressure are presented in **Fig. 2.7** and **Fig. 2.8**.

The ultra-soft soil had large deformation during the test, the settlement until 100 days under the loading 110 kPa was approximately 335mm, which reached 46% of strains (**Fig. 2.7**). During the first 10 days of loading, there was no or little pore water pressure dissipating out of the soil eventhough the settlement was increased up to 20 % strain, (**Fig. 2.8**). Similar delay in consolidation of slurry was also observed by Tanaka (1997). Chu et al. (2006) stated that delay of excess pore

water pressure dissipation was the typical consolidation characteristic of ultra-soft soil, which deviates from natural soft clay. The test results showed that the water content of the soil reduced significantly after finishing the consolidation process, as shown in **Fig. 2.9**. The final water content values varied from 47% to 56% which were less than the initial water content of 132%. The lowest water content and void ratio were found to be near PVD and increased from the center of PVD to the edge of consolidation apparatus. The measured undrained shear strength had significantly changed from in-situ value of 1-10 kPa and 20 to 47 kPa after consolidation process. The decrease of water content and increase of undrained shear strength clearly showed that the effectiveness of using PVD for ultra-soft soil improvement.

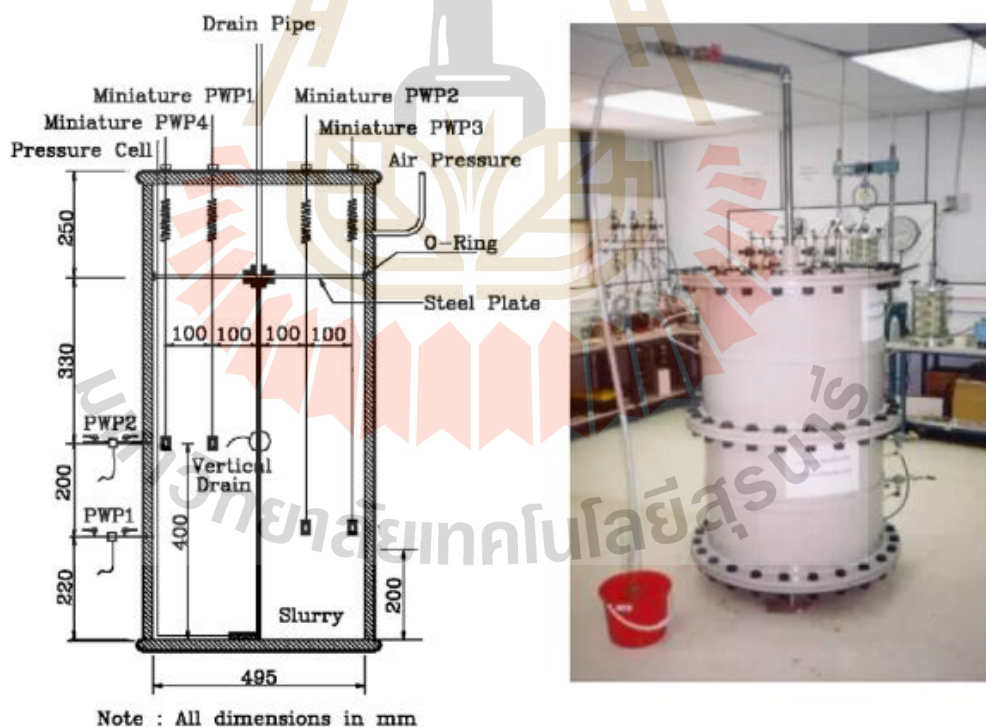


Figure 2.6: Large diameter consolidation tank (Chu et al., 2006)

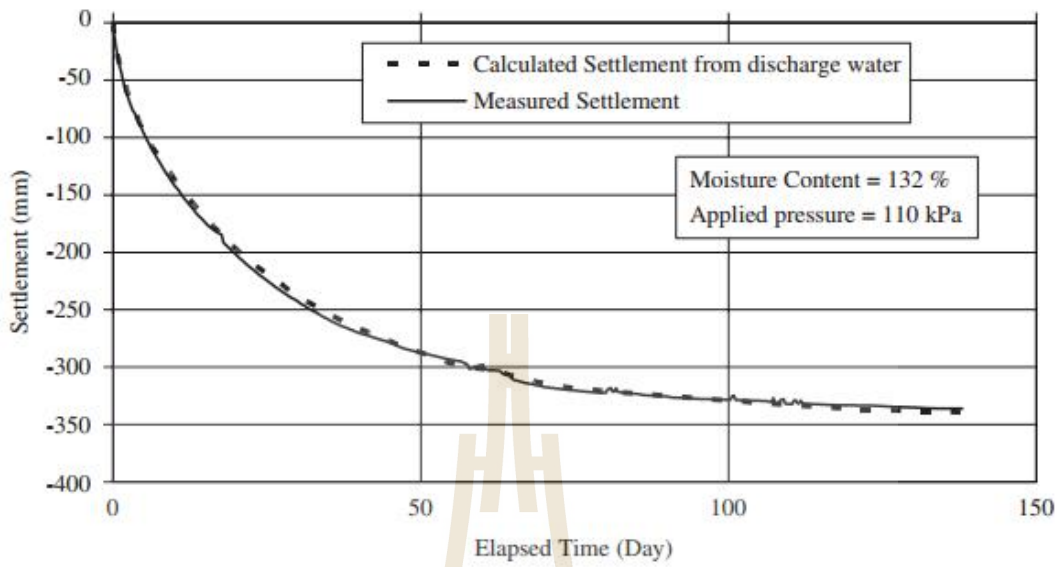


Figure 2.7: Settlement versus time curve measured from the large consolidation test under 110 kPa

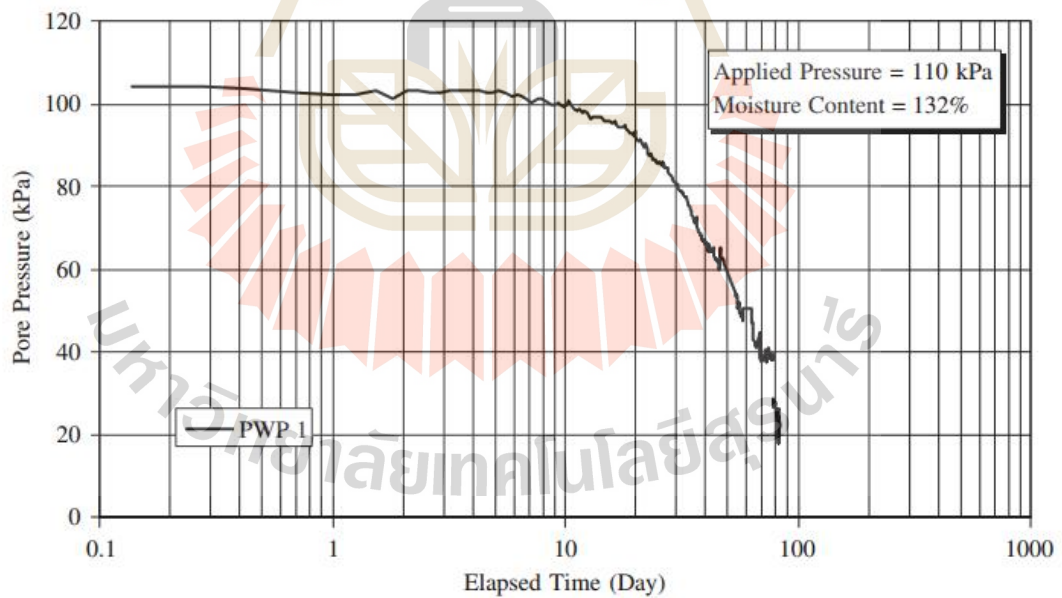


Figure 2.8: Pore pressure dissipation versus time curve under 110 kPa vertical pressure.

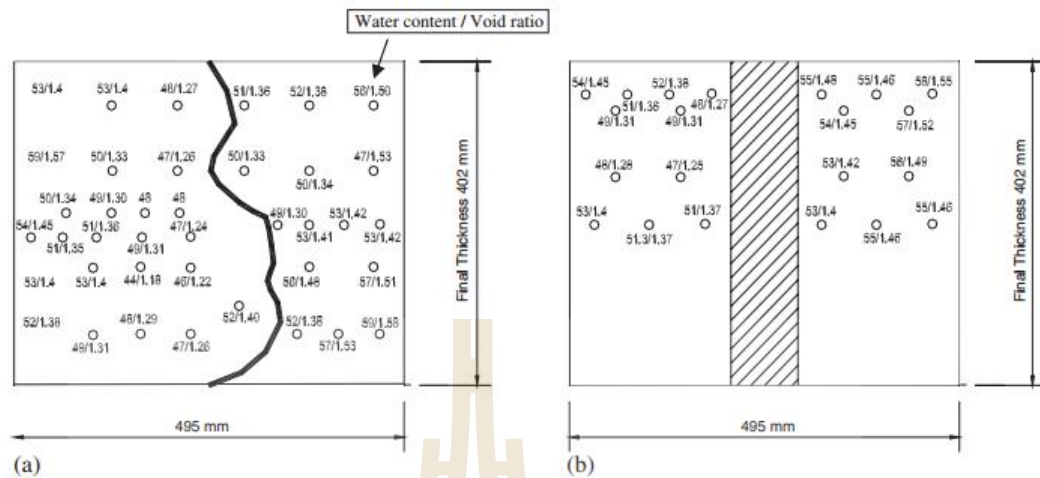


Figure 2.9 The water content distribution after testing: (a) along the elevation perpendicular to the PVDs and (b) along the elevation facing the PVDs.

2.5.2 Field performance

Besides the laboratory test, the field performance of PVD on the consolidation of ultra-soft soil was also studied (Bo et al. 2005, Chu et al. 2006, Arulrajah et al. 2009). The improvement of ultra-soft soil using PVDs in Singapore was reported by Chu et al. (2006). The total reclamation area of this project was approximately 180 ha in trapezoid shape. The thickness of ultra-soft soil deposits in this pond was up to 20m thick. The water content was higher than liquid limit with the range of 140 – 180 %. The shear strength of the soil was extremely low of 1-10 kPa. The special construction method is that the PVDs has been installed with two rounds during construction stage to minimize the folding effect of PVDs applied for ultra-soft clay. The extrusion of water occurred during PVD installation was observed (Chu et al., 2006). It indicated that the pore water pressure in the ground was still high after the first round of PVD installation. The benefit of two-stage PVD installations helped the water dissipate out of the soil faster and hence it reduced the consolidation

process. However, a failure was occurred in the first phase of spreading sand due to the non-uniform thickness of sand layer and hence differential settlements (Bo, Chu, Bo et al. 2006, 2008).

The measured settlement and excess pore water pressure in the field are plotted in **Fig 2.10**, respectively. The field measurements showed that the height of fill surcharge was reduced due to the settlement of the soil (Choa 1995, Chu et al., 2006). The slurry soil had settled approximately 2.7 m in 500 days. The delay of pore water pressure dissipation was observed in the field which was similar in the laboratory testing (Choa 1995, Choa et al., 2001, Chu et al., 2006, Bo 2008) (**Figure 10**). It can be seen that there were little reduction of pore water pressure measured by piezometer in the first 40 days after 2nd PVD installation. The undrained shear strength increased significantly after 14 month of surcharge showing the effectiveness of using PVDs for the improvement of ultra-soft soil in this project.



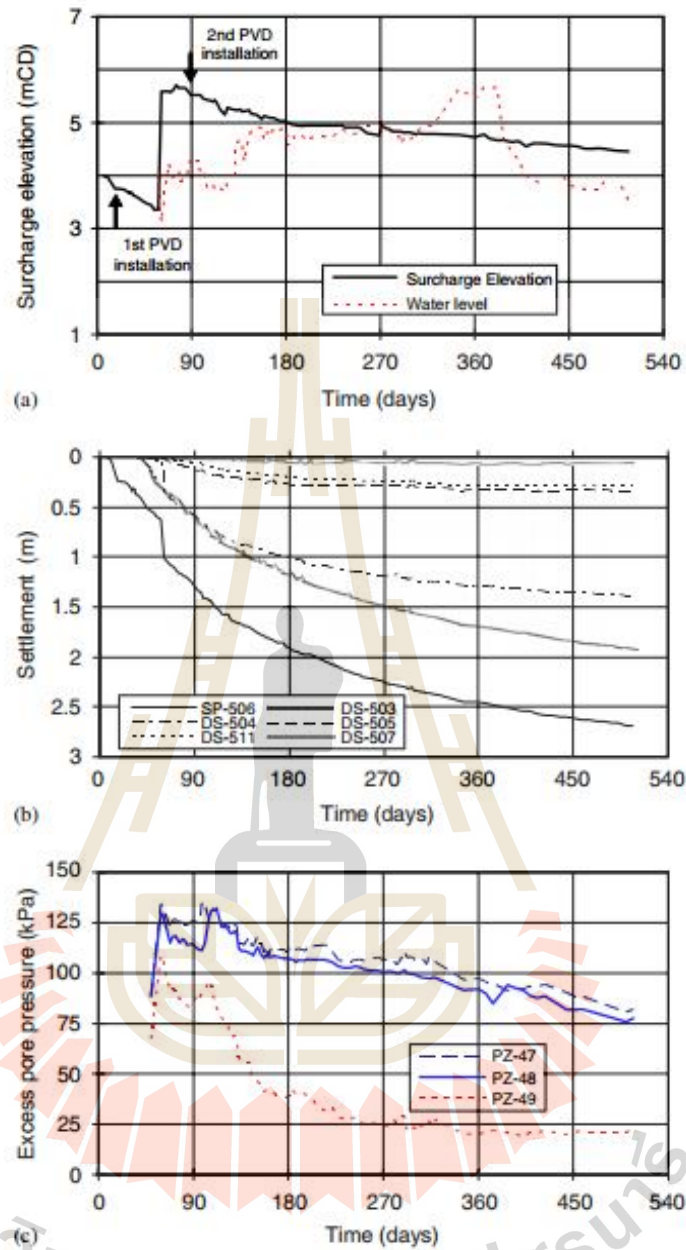


Figure 2.10 The measure settlement and excess pore water pressure in the field (Chu et al., 2006)

2.6 References

- Aboshi, H., et al. (2001). **Kinking deformation of PVD under consolidation settlement of surrounding clay.** *Soils and foundations* 41(5): 25-32.
- Akagi, T. (1979). **Consolidation caused by mandrel-driven sand drains.** Proceedings of the 6th Asian Regional Conference on Soil Mechanics and Foundation Engineering, Singapore, Southeast Asian Geotechnical Society, Bangkok.
- Alfaro, M., et al. (1994). **Improvement techniques of soft ground in subsiding and lowland environment,** CRC Press.
- Ali, F. H. (1991). **The flow behaviour of deformed prefabricated vertical drains.** *Geotextiles and Geomembranes* 10(3): 235-248.
- Almeida, M. and C. Ferreira (1993). **Field, in situ and laboratory consolidation parameters of a very soft clay.** Predictive Soil Mechanics: Proceedings of the Wroth Memorial Symposium Held at St. Catherine's College, Oxford, 27-29 July 1992, Thomas Telford.
- Almeida, M. and M. Marques (2003). **The behaviour of Sarapuí soft clay. Characterization and engineering properties of natural soils.** Edited by TS Tan, KK Phoon, DW Hight, and S. Leroueil. Swets & Zeitlinger, Lisse, the Netherlands: 477-504.
- Almeida, M., et al. (2004). **Consolidation of a very soft clay with vertical drains.** *Ground and Soil Improvement*, Thomas Telford Publishing: 29-39.
- Arulrajah, A., et al. (2009). **Instrumentation at Changi land reclamation project, Singapore.** *Proceedings of the Institution of Civil Engineers-Geotechnical Engineering* 162(1): 33-40.

- Barron, R. A. (1948). **Consolidation of fine-grained soils by drain wells.**
- Bergado, D., et al. (1993). **Improvement of soft Bangkok clay using vertical drains.** Geotextiles and Geomembranes 12(7): 615-663.
- Bergado, D., et al. (1990). **Improvement of soft Bangkok clay using vertical geotextile band drains compared with granular piles.** Geotextiles and Geomembranes 9(3): 203-231.
- Bergado, D. T., et al. (1991). **Smear effects of vertical drains on soft Bangkok clay.** Journal of Geotechnical Engineering 117(10): 1509-1530.
- Bo, M. (2008). **Compressibility of ultra-soft soil,** World Scientific Publishing Company.
- Bo, M., et al. (2005). **Reclamation and soil improvement on ultra-soft soil.** Proceedings of the Institution of Civil Engineers-Ground Improvement 9(1): 23-31.
- Bo, M. W., et al. (2016). **Laboratory measurements of factors affecting discharge capacity of prefabricated vertical drain materials.** Soils and foundations 56(1): 129-137.
- Carroll Jr, R. G. (1983). **Geotextile filter criteria.**
- Chai, J. C. and N. Miura (1999). **Investigation of factors affecting vertical drain behavior.** Journal of Geotechnical and Geoenvironmental Engineering 125(3): 216-226.
- Chai, J., et al. (1997). **Investigation on Some Factors Affecting Discharge Capacity of Prefabricated Vertical Drain.** 佐賀大学理工学部集報 26(1): 97-105.

- Chang, D., et al. (1994). **Laboratory study of vertical drains for a ground improvement project in Taipei.** Proceeding of the 5th International Conference on Geotextiles, Geomembranes and Related Products, Singapore.
- Choa, V. (1995). **Changi east reclamation project.** Int'l Symposium on Compression and Consolidation of Clayey Soils.
- Choa, V., et al. (2001). **Soil improvement works for Changi East reclamation project.** Proceedings of the Institution of Civil Engineers-Ground Improvement 5(4): 141-153.
- Chu, J., et al. (2004). **Practical considerations for using vertical drains in soil improvement projects.** Geotextiles and Geomembranes 22(1-2): 101-117.
- Chu, J., et al. (2006). **Improvement of ultra-soft soil using prefabricated vertical drains.** Geotextiles and Geomembranes 24(6): 339-348.
- Ghandeharioon, A., et al. (2009). **Analysis of soil disturbance associated with mandrel-driven prefabricated vertical drains using an elliptical cavity expansion theory.** International Journal of Geomechanics 10(2): 53-64.
- HANSBO, S. (1981). **Consolidation of fine-grained soils by prefabricated drains.** Proc. 10th ICSMFE, 1981 3: 677-682.
- Hansbo, S. (1983). **How to evaluate the properties of prefabricated drains.** Proceedings of the Eighth European Conference on Soil Mechanics and Foundation Engineering.
- Hansbo, S. (1986). **Preconsolidation of soft compressible subsoil by the use of prefabricated vertical drains.** Annales des travaux publics de Belgique.
- Hansbo, S. (1987). **Design aspects of vertical drains and lime column installations.** Southeast Asian geotechnical conference. 9.

- Holtz, R. (1987). **Preloading with prefabricated vertical strip drains**. Geotextiles and Geomembranes 6(1-3): 109-131.
- Holtz, R. D., et al. (1991). **Prefabricated vertical drains: design and performance**.
- Indraratna, B., et al. (2014). **Soil disturbance analysis due to vertical drain installation**.
- Indraratna, B. and I. Redana (1998). **Laboratory determination of smear zone due to vertical drain installation**. Journal of Geotechnical and Geoenvironmental Engineering 124(2): 180-184.
- Jamiolkowski, M. (1983). **Precompression and speeding up consolidation**. Proc. 8th Europe Conf. SMFE, AA Balkema.
- Jamiolkowski, M. and R. Lancellotta (1981). **Consolidation by vertical drains: uncertainties involved in prediction of settlement rates**. Proc., 10th Int. Conf. Soil Mechanical and Foundation Engineering, Balkema Rotterdam, The Netherlands.
- Lawrence, C. A. and R. M. Koerner (1988). **Flow behavior of kinked strip drains**. Symposium on Geosynthetics for Soil Improvement at the ASCE Convention.
- Mesri, G. and D. Lo (1991). **Field performance of prefabricated vertical drains**. Proceedings of the International Conference on Geotechnical Engineering for Coastal Development.
- Miura, N., et al. (1998). **Investigation on some factors affecting discharge capacity of prefabricated vertical drain**. Proceedings of the 6th International Conference on Geosynthetics, Atlanta, GA, USA.
- Onoue, A., et al. (1991). **Permeability of disturbed zone around vertical drains**. Geotechnical Engineering Congress—1991, ASCE.

- Palmeira, E. M. and M. G. Gardoni (2002). **Drainage and filtration properties of non-woven geotextiles under confinement using different experimental techniques**. *Geotextiles and Geomembranes* 20(2): 97-115.
- Rujikiatkamjorn, C., et al. (2013). **Conceptual model describing smear zone caused by mandrel action**. *Géotechnique* 63(16): 1377.
- Saowapakpiboon, J., et al. (2010). **Measured and predicted performance of prefabricated vertical drains (PVDs) with and without vacuum preloading**. *Geotextiles and Geomembranes* 28(1): 1-11.
- Sasaki, S. (1981). **Report of Experimental Test for the Prefabricated Drain Geodrain**. Tokyo Construction Co., Tokyo.
- Sengul, T., et al. (2017). **Laboratory determination of smear and transition zones due to prefabricated vertical drain installation**. *Marine Georesources & Geotechnology* 35(7): 895-904.
- Sharma, J. and D. Xiao (2000). **Characterization of a smear zone around vertical drains by large-scale laboratory tests**. *Canadian Geotechnical Journal* 37(6): 1265-1271.
- Tanaka, Y. (1997). **Non-uniformly consolidated ground around a vertical drain**. Proc. 30th Anniversary Symposium of Southeast Asian Geotechnical Society.
- Terzaghi, K. (1943). **Theory of consolidation**. *Theoretical Soil Mechanics*: 265-296.
- Tran-Nguyen, H., et al. (2010). **Effect of deformation of prefabricated vertical drains on discharge capacity**. *Geosynthetics International* 17(6): 431-442.
- Xiao, D. (2001). **Consolidation of soft clay using vertical drains**. Nanyang Technological University, School of Civil and Structural Engineering.
- Xie, K. (1987). **Consolidation theories and optimisation design for vertical drains**. Doctor of Philosophy Thesis, Hewing University, China.

CHAPTER III

COMPRESSIBILITY OF ULTRA-SOFT SOIL IN THE MAE MOH MINE, THAILAND

3.1 Introduction

The Mae Moh Mine is the largest open-pit lignite mine in Thailand, as well as in Southeast Asia, with a total mining area of approximately 37.5 km² and external dumping area of approximately 41.4 km². It is situated at the Mae Moh district, Lampang province in the north of Thailand, located 630 km away from Bangkok. The lignite material at the Mae Moh basin is the main raw feed material used to generate power at the Mae Moh power plants, operated by the Electricity Generating Authority of Thailand (EGAT). Approximately 16 million tons of coal are produced annually and transferred to the 10 units of the Mae Moh power plants in order to generate the total power supply of 2,400 Megawatt. Several water ponds were constructed as the main source for mining activities such as mineral processing and dust suppression. The discharge of surface water and groundwater flow has caused soil erosion along the mine slope, which has resulted in ultra-soft soil deposits located underwater in the slurry ponds over the years. The thickness of the ultra-soft soil in some ponds is even up to 40 m.

According to the mine planning and development of EGAT, this mine will be excavated to a depth of approximately 500 m from the original surface over the next four decades, resulting in this becoming the deepest open pit lignite mine in the world.

The excavated soil from mining activities will be dumped in the slurry ponds for land reclamation. **Fig. 3.1** shows a schematic of a slurry pond, which will be subjected to a very high overburden material of approximately 300m in the next 40 years. However, the soil in the ponds is in the ultra-soft state, with very low undrained shear strength and high water content of greater than liquid limit. In-pit dumping without mechanical property improvement of this ultra-soft soil is almost impossible. Due to very low undrained shear strength, the mud flood of the ultra-soft soil could occur immediately after the in-pit dump and causes detrimental effects on the mining activities.

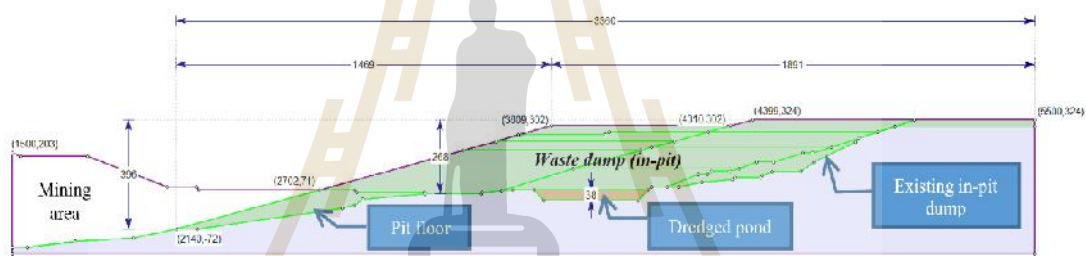


Figure 3.1. Typical cross-section of In-pit dump in the Mae Moh mine (dimension in meter)

A suitable ground improvement method for the ultra-soft soil in the Mae Moh mine is the preloading with vertical drains technique. It is effective in term of economic and environmental perspectives as compared to other techniques, such as deep soil mixing and soil replacement. The preloading can be performed using a 1-m thickness of clean sand as a drainage layer and the usage of abandoned clayey stone as a backfill material. A sufficient understanding of the mechanical behavior, especially compressibility and hydraulic conductivity of the ultra-soft soil is therefore required for calculating the settlement and rate of consolidation settlement (Chai et

al., 2004; Chai et al., 2018; Horpibulsuk et al., 2007; Horpibulsuk et al., 2011; Liu et al., 2013; Liu et al., 2018; Xu et al., 2019). The compressibility of the ultra-soft soil includes the sedimentation and consolidation stages. The ultra-soft soil under the sedimentation process is termed as a slurry while the ultra-soft soil after completion of sedimentation is termed as a sedimentation soil.

The sedimentation process is a special characteristic of slurry at high water content (Been & Sills, 1981; Blewett et al., 2001; Chen et al., 2019; Özer & Bromwell, 2012; Sills, 1998; Tan et al., 1990; Zhang et al., 2015). The evaluation of consecutive process from sedimentation to consolidation is a major challenge on the geological and geotechnical practical design of land-filling and disposal work. The void ratio of the sedimentation soil is a required parameter for the calculation of the consolidation settlement (Imai, 1980, 1981; Watabe & Saitoh, 2015). The first well-known theory of sedimentation was proposed by Kynch (1952) and was later modified by Fitch (1957, 1966, and 1979). The sedimentation of slurry has been studied by using a traditional method of slowly injecting slurry into a column or cylinder. Based on the observation of the sedimentation tests, three stages can be distinguished: flocculation, settling, and self-weight consolidation stages (Imai, 1980, 1981; Tan, 1995; Tan et al., 1990; Xu et al., 2012). Scotts et al. (1986) reported that the sedimentation and consolidation stages are different from each other. The sedimentation process includes the flocculation and settling stages. The self-weight consolidation occurs at the bottom of the settling column after the sedimentation process. During the sedimentation process, it is postulated that there is no effective stress in the slurry and the slurry acts as fluid (Xu et al., 2012). When soil particles come close to each other to develop the soil structure, the slurry turns into soil and the

effective stress can be determined. After the sedimentation process, the sedimentation soil has sufficient strength to carry an external load. The understanding of compression behavior of sedimentation soil in term of compressibility and hydraulic conductivity characteristics has played a key role in geological and geotechnical engineering practice for many decades (Chai et al., 2004; Desai, 2000; Horpibulsuk et al., 2007; Horpibulsuk et al., 2011; Wu et al., 2019; Xu et al., 2019). Forty-eight reconstituted clay samples at different water contents (ranging from 0.7 to 2.0 times their liquid limit) were tested using a modified oedometer test with a light loading cap (Hong et al., 2010). Most of these tests were applied at low effective stress of 0.5 kPa and gradually increased to reach high effective stress (1600 kPa). Based on the test results, it has been well documented that the completed virgin compression curve of reconstituted clay is represented by S-shape function (Horpibulsuk et al., 2016; Liu et al., 2013; Zeng et al., 2015). Horpibulsuk et al. (2016) proposed an S-shaped equation to predict the consolidation curve of reconstituted clays over the wide range of stresses and initial water contents.

Even though there are available research on sedimentation of slurries and consolidation behavior of sedimentation soils, they have been previously studied in isolation. As such, the role of water content on the overall compressibility characteristics of the ultra-soft soil is still uncertain. The compressibility characteristics of the ultra-soft soil are thus a challenge for geological and geotechnical designers in land reclamation projects.

The aim of this study is to assess the compressibility characteristics, which include sedimentation and consolidation at different initial water contents, w_i . A series of sedimentation tests were conducted which analyzed the change of soil

interface, void ratio, and water content over time. The consolidation behavior of the sedimentation soil at a wide range of effective stresses and water contents was also investigated. Finally, a practical method for assessing the stress state of slurry and consolidation curve of sedimentation soil is proposed, based on the complete S-shaped function (Horpibulsuk et al., 2016). The outcomes of this research will enable geological and geotechnical engineers to assess the compressibility of ultra-soft soils in land reclamation and ground improvement projects, such as in the Mae Moh slurry pond.

3.2 Materials and methods

3.2.1 Soil sample

The soil samples were taken from a slurry pond in a low lying area of the Mae Moh mine, Lampang province in Thailand. Disturbed samples were collected at a depth of approximately 1 m below soil surface of the pond with a backhoe and placed in a plastic tank. The studied site is shown in **Fig. 3.2**.



Figure 3.2 Sampling site.

The grain size distribution curve of the soil sample is shown in **Fig. 3.3**. The soil sample contained 41% clay and 58% silt with 1% sand. The liquid limit and the plastic limit were measured in accordance with Casagrande method (BS 1377 – Part 2: 4.3 and BS1377 – Part 2: 5.3), and were 57% and 26%, respectively. The specific gravity was 2.57. The soil had a very high in-situ water content of 98%, greater than 1.7 times the liquid limit. The in-situ strength was 1.5 kPa, which is considered to be extremely low. As this research mainly focuses on the compressibility and hydraulic conductivity characteristics of the ultra-soft soil, the chemical properties of the ultra-soft soil was not examined. The comparison of the physical and chemical properties between the ultra-soft soil and its parent rocks is however useful for soil science technology and is recommended for further research.

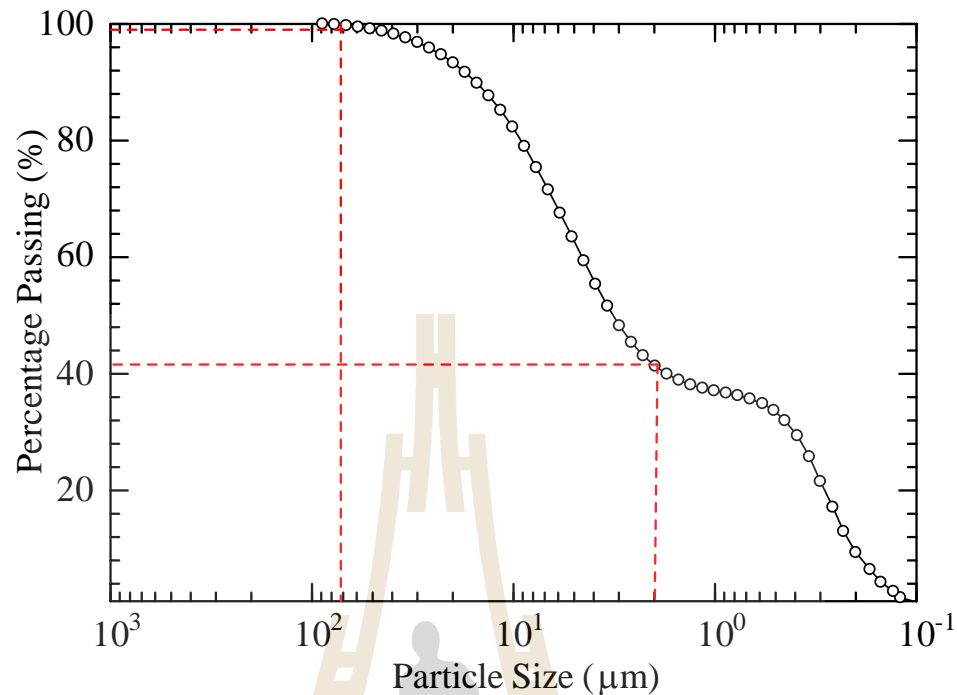


Figure 3.3 Grain size distribution curve.

3.2.2 Sedimentation test

To study the sedimentation behavior of slurry under various water contents, the water content of the samples was adjusted to be greater than that of the liquid limit. The slurry sample at the target w_i was thoroughly mixed using a mechanical mixer for 15 minutes and then slowly injected into a unified transparent glass cylinder, using a funnel with a small tube down to the bottom of the cylinder. The injection process was stopped upon reaching 36 cm height of the slurry (Imai, 1980, 1981; Tan, 1995; Tan et al., 1990; Xu et al., 2012). The cylinder was then covered with a plastic sheet to prevent water evaporation during testing and kept in the laboratory at a controlled temperature of $20 \pm 1^\circ$. Eight different initial water contents ($w_i = 116\%$, 137% , 193% , 219% , 230% , 325% , 400% , and 437%) were prepared as shown in **Fig. 3.4**. The w_i values were selected to cover the in-situ water

content and far higher than liquid limit of up to approximately 7.7 times so as to understand the role of w_i on the sedimentation behavior. During 42 days of the sedimentation process, the height of slurry was recorded at different times (minutes). A schematic diagram of the sedimentation process is shown in **Fig. 3.5**.

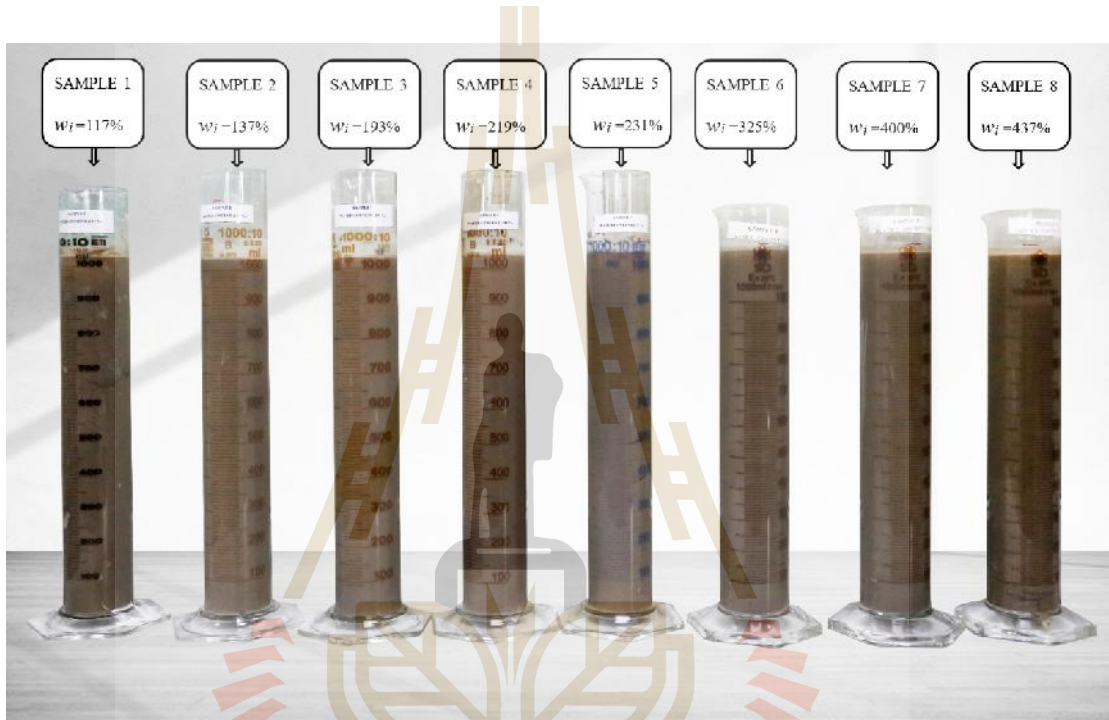


Figure 3.4. 8 cylinders containing slurry at different initial water contents.

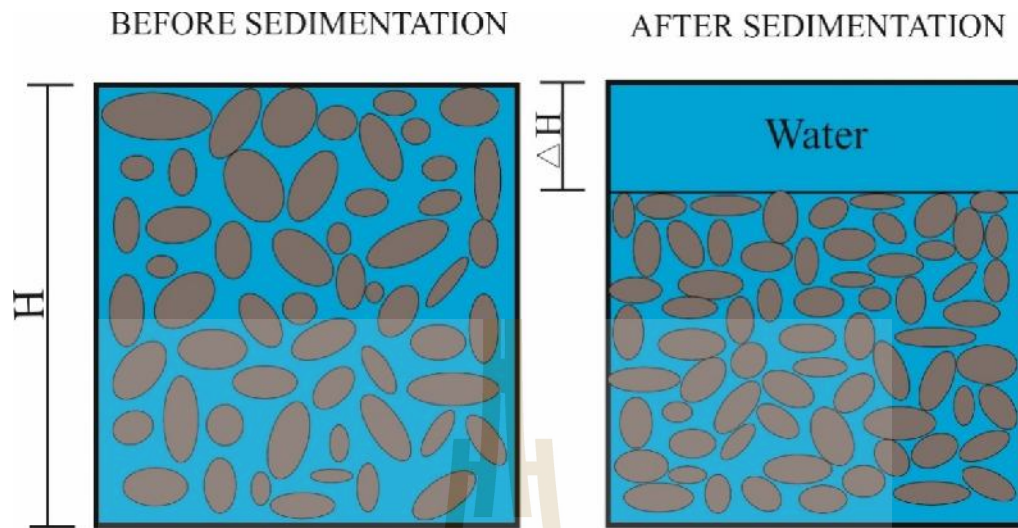


Figure 3.5. Illustration of changing interface location *before and after sedimentation* process.

According to the theory of soil mechanics (Terzaghi, 1951), a fully saturated soil consists of two phases: solid soil particles and pore water. Consequently, the water content of the sedimentation layer is the ratio of the mass of water to the mass of solid, except for the mass of water above the soil surface. The water content (w_t) of the slurry at time t can be calculated from the change of soil interface (the surface between slurry and water):

$$w_t = \left[e_o - \frac{\Delta h \times (1 + e_o)}{h_o} \right] \times \frac{S_r}{G_s} \quad (3.1)$$

where h_o and e_o are the initial height and initial void ratio of the slurry, respectively; Δh is the change of soil interface at time t using calibration scale in cylinder wall; G_s is specific gravity of the soil.

The calculated water contents were validated by comparing with the measured water content at the end of the test (w_f). After completion of the sedimentation test, the water above the soil mass was slowly taken out of each cylinder by using a small syringe. The soil mass was then oven-dried to determine the w_f of the slurry.

3.2.3 Consolidation test

The consolidation behavior of the sedimentation soil upon application of the additional load due to the effect of the sedimentation water content, w_s (water content at the end of sedimentation), as well as under the same loading sequence were studied. Six samples were prepared by mixing the slurry thoroughly with a quantity of distilled water to reach the target initial water contents. Once the target initial water contents were obtained, at 1.45, 1.79, 1.84, 1.97, 2.10, and 2.28 times the liquid limit, the slurry was carefully poured into the consolidation ring by controlling the mass of specimen, which was calculated by considering the slurry in fully saturated condition. A metal rod of 5 mm in diameter was used to remove air bubbles inside the oedometer ring (Hong et al., 2010; Zeng et al., 2015). The consolidation sample was 105 mm in diameter and 20 mm in nominal height. After preparing the sample in O-ring, the slurry was kept in the consolidation cell and covered by plastic sheet under room temperature for 42 days to ensure that the sedimentation process was completed. This rest period of 42 days was obtained from the sedimentation test. After that the samples were then subjected to both low and high loads. A very low effective vertical stress of 0.5 kPa was first applied and gradually increased with following vertical stresses of 1 kPa, 1.5 kPa, 2.5 kPa, 3.5 kPa, 5.5 kPa, 7.5 kPa, 9.5 kPa, 12.5 kPa, 25 kPa, 50 kPa, 100 kPa, 200 kPa, 500kPa, 1000 kPa, 2000kPa, 4000 kPa. The duration

of each loading step was fixed at 24 hours. For each loading increment, the hydraulic conductivity, k , was calculated by the following equation.

$$k = c_v m_v \gamma_w \quad (3.2)$$

where c_v is the coefficient of consolidation determined using the root time method proposed by Taylor (1942), m_v is the coefficient of volume change, and γ_w is the density of water.

3.3 Results and discussion

3.3.1 Sedimentation of slurry

Fig. 3.6 presents the change of interface location of the slurry samples at different initial water contents and their measured water contents (w_f) at the end of the test. The measured water contents were compared with the calculated ones using Eq. 1 at the end of the test as summarized in **Table 3.1**. The results indicated that the measured water contents are in excellent agreement with the calculated ones. On the other hand, the soil-fluid interface location decreases significantly after 42 days of sedimentation (comparing **Fig. 3.6** with **Fig. 3.4**). The sedimentation curves of the slurry at various w_i are shown in **Fig. 3.7**, which can be divided into two stages: flocculation and settling. The flocculation occurs at an early stage in which the soil particles were dispersed in the mixture and no interface between soil mass and water was observed in this stage. When the flocculation stage finishes, the settling begins whereby the flocs start to settle uniformly with a clearly observed interface change. During this stage, the interface location moves downward with a constant rate and the sedimentation curve shows a linear behavior in arithmetic time scale. After the

settling stage, the flocs in the slurry deposit onto bottom and voids are consolidated under self-weight in the self-weight consolidation stage (Scott et al., 1986).

Table 3.1: The comparison between measured and calculated water content after testing.

Cylinder No.	Initial water content, W_i (%)	Measured water content, $W_{f, \text{measured}}$ (%)	Calculated water content, $W_{f, \text{calculated}}$ (%)
1	117	110	111.02
2	137	125	124.75
3	193	165.7	165.78
4	219	161	159.67
5	231	160	161.70
6	325	161	162.49
7	400	167	166.03
8	437	158	160.15

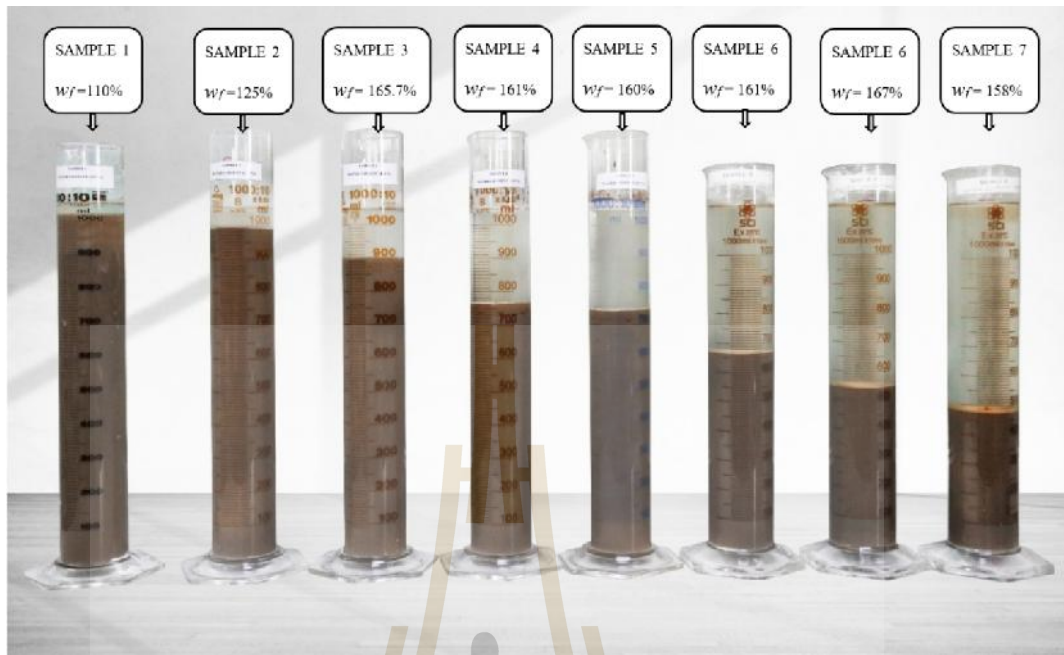


Figure 3.6. The interface location of 8 samples at the end of test.

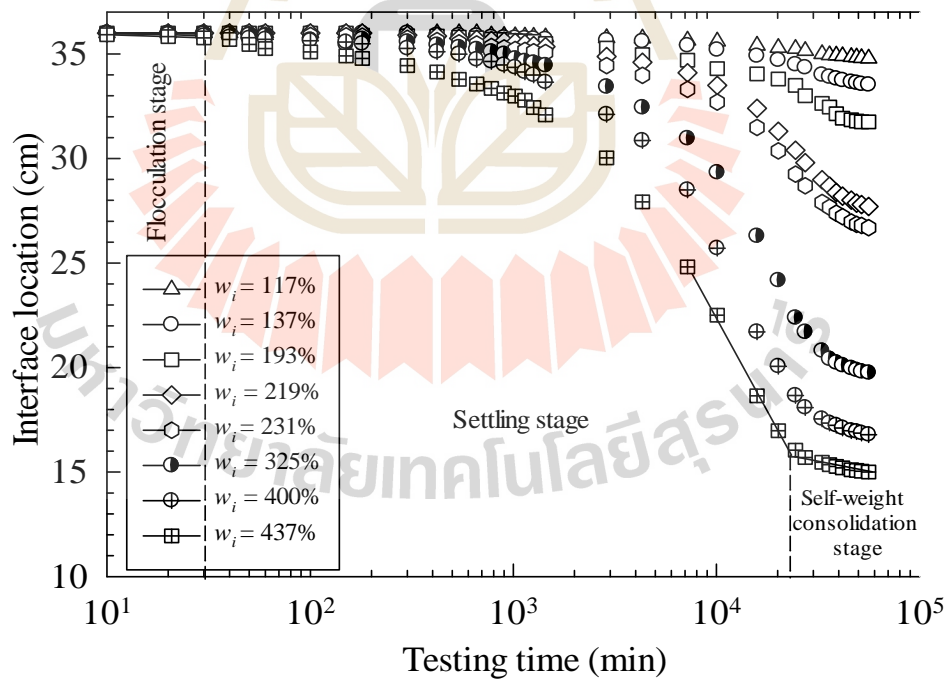


Figure 3.7. Sedimentation curves at different initial water contents in logarithmic time scale.

Similar to **Fig. 3.7**, the water content versus time was plotted and is presented in **Fig. 3.8**. The sedimentation water content, w_s , defined as the water content at the end of sedimentation, was determined from the interception of the two straight lines extended from settling and self-weight consolidation stages. The w_s can be considered as the transition point between the sedimentation process and the self-weight consolidation stage. It is worth noting that the w_s value was essentially the same, at 171% for the slurry with very high w_i while it deviates for slurry with low w_i . The constant w_s of the slurry at various w_i is defined herewith as critical water content, w_{cr} . The w_{cr} for the studied ultra-soft soil is therefore 171%. It is noted that w_{cr} was approximately 3 times liquid limit.

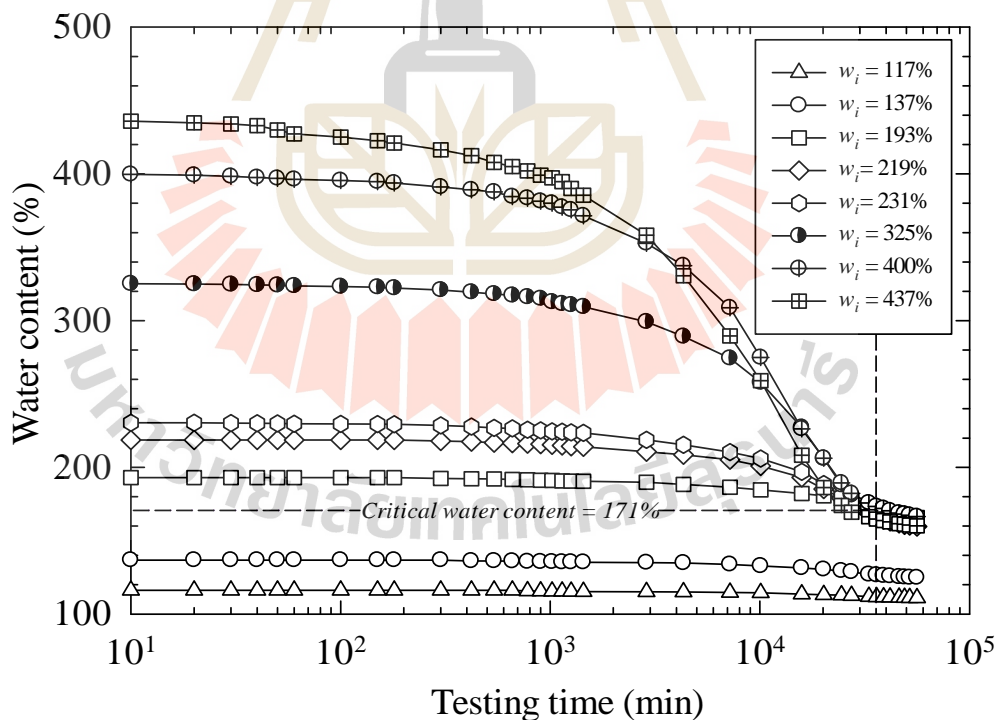


Figure 3.8 Water content versus with time (log scale) relationship.

Based on the sedimentation test result (**Fig. 3.8**), the slurry is divided into large and small sedimentation slurry separated using w_{cr} as the reference. The slurry with $w_i > w_{cr}$ is defined as large sedimentation slurry while the slurry with $w_i < w_{cr}$ is defined as small sedimentation slurry. Two stages (flocculation and settling) of the sedimentation process were clearly observed for the large sedimentation slurry. The soil particles are far apart from each other, hence the water content reduces significantly with high velocity in the settling stage. On the other hand, for the small sedimentation slurry, the change in water content with time during the first 1000 minutes is little and then the water content slightly decreases with time. This slight change in water content is consistent with change in soil interface in that very little compression takes place during the first 1000 minutes, and then the soil interface decreases with low velocity. As such, the w_s of small sedimentation slurry is dependent upon the w_i and practically its value can be assumed to be the w_i value.

3.3.2 Consolidation behavior of sedimentation soil

3.3.2.1 Consolidation curve

The w_s is assumed to be the same for high sedimentation slurry. As such, the consolidation curve of high sedimentation soil is unique, irrespective of w_i . On the other hand, the consolidation curve of small sedimentation soil varies and is dependent upon w_s , which will be examined in this section. The consolidation curves in term of void ratio versus effective vertical stress in a semi-logarithmic (e vs $\log \sigma'_v$) for six samples at different w_s are shown in **Fig. 3.9**. The consolidation behavior of sedimentation soil is an inverse S-shape curve, which is similar to previous studies reported by Hong et al. (2010) for Lianyungang, Baimahu clay and Liu et al. (2013) for Kemen clay. The transitional stress separating small and large

change in void ratio is defined as yield stress or suction pressure, which is similar to the pre-consolidation pressure for natural soils (Hong et al., 2010). Hong et al. (2010) explained that at pre-yield state, the load is carried by the suction pressure. At post-yield stage, the soil undergoes large compression strain due to the destructuring of soil structure.

The yield stress of the soil samples can be determined by the interception of two straight lines (pre-yield and post-yield state line) in bilogarithmic graph $\ln(1+e) - \log \sigma_v'$ as plotted in **Fig. 3.10** (Hong et al., 2010). These two straight lines are assumed for $\sigma_v' < 100$ kPa. The calculated yield stresses of six samples at different w_s are presented in **Fig. 3.11** and also compared with that of Lianyungang, Baimahu, and Kemen clays studied by Hong et al. (2010). It is evident that the yield stresses of all soils reduce with an increase of w_s . The reduction in yield stress is due to the fact that the higher w_s results in resistance to vertical consolidation pressure and the shear strength (Horpibulsuk et al., 2007; Horpibulsuk et al., 2011; Nagarai et al., 1998).

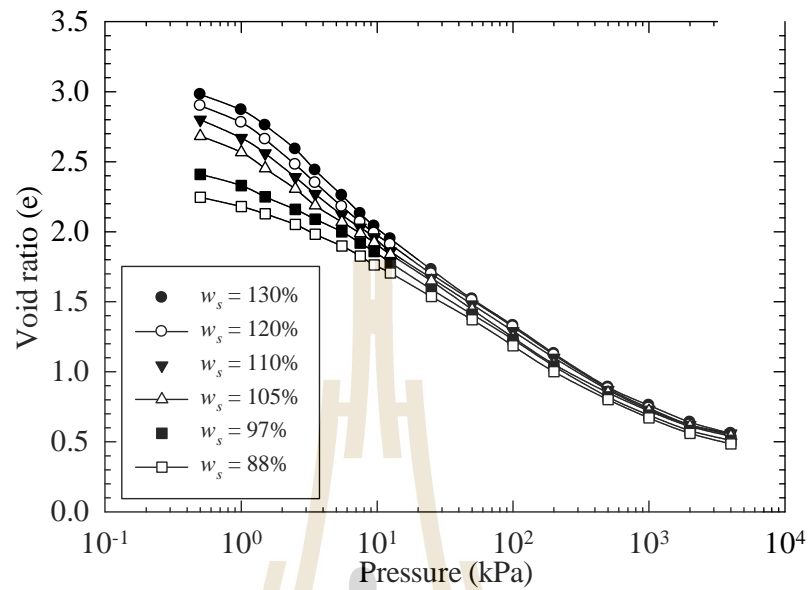


Figure 3.9 Consolidation curve of sediment soil at different sedimentation water contents.

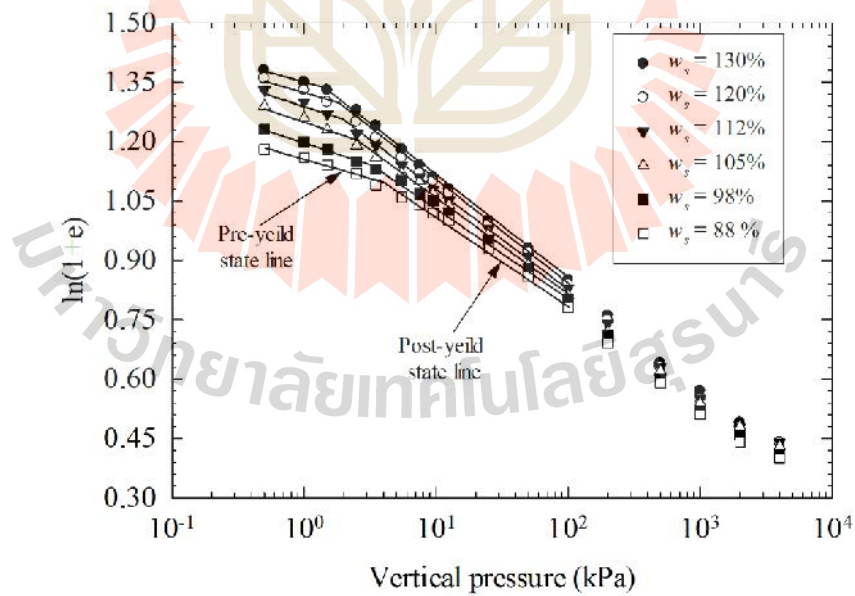


Figure 3.10 Bilogarithmic consolidation curves of sediment soil at different sedimentation water contents

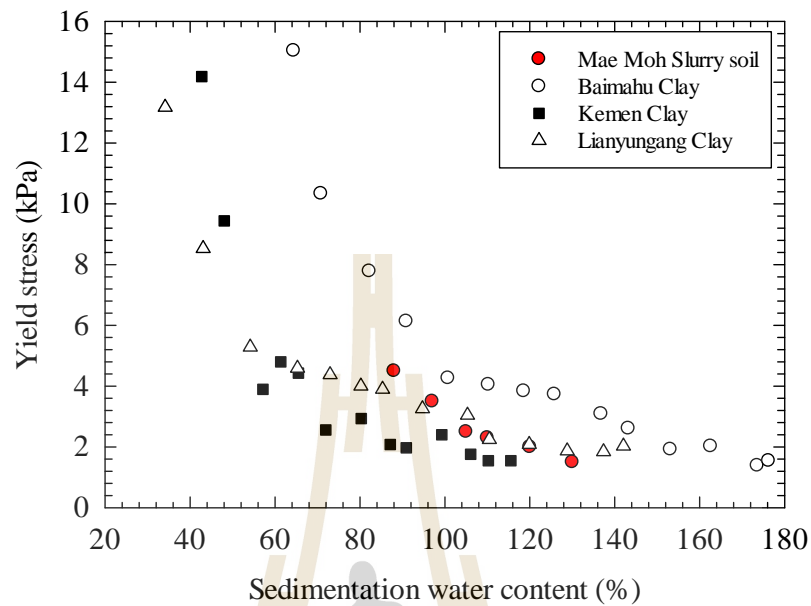


Figure 3.11 Yield stress versus sedimentation water content.

3.3.2.2 Hydraulic conductivity

Fig. 3.12 shows the relationship between the hydraulic conductivity and void ratio of sedimentation soil at various water contents. Even though the hydraulic conductivity of six samples at various v_v is different, the hydraulic conductivity is however the same at the same void ratio. The hydraulic conductivity significantly reduces with the reduction of void ratio. The non-linear relationship between specific volume and $\log k$ for the Mae Moh sedimentation soil samples can be represented by the following equation.

$$1+e = 141.84 \times k^{0.239} \quad (3.3)$$

where k is expressed in cm/s.

With Eq (3), the k value of Mae Moh sedimentation soil at any e can be approximated.

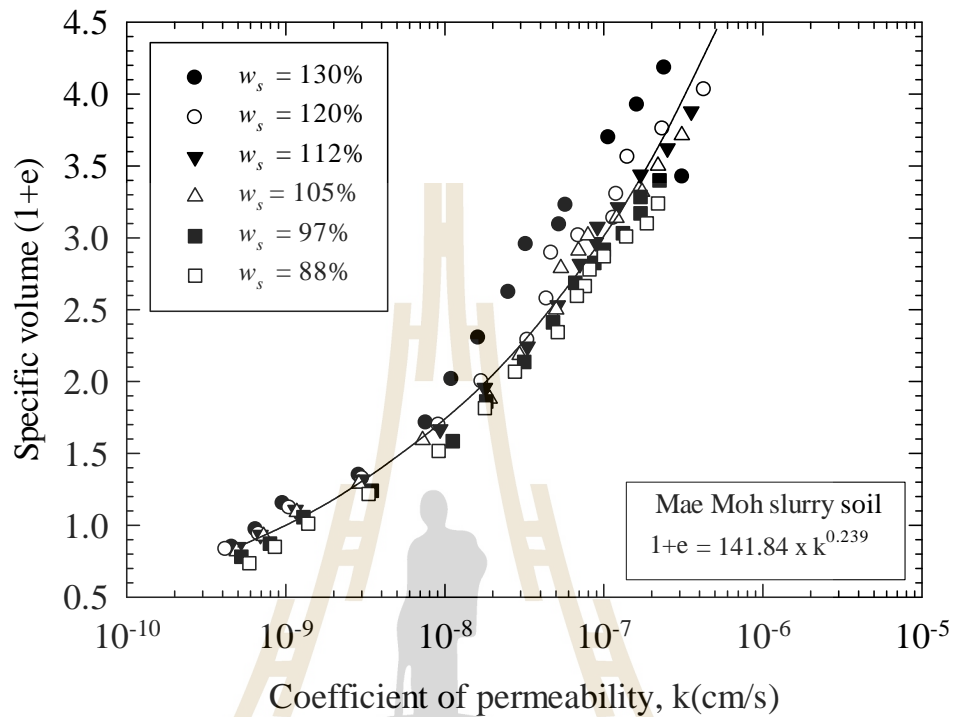


Figure 3.12 Specific volume-log (k) relationship of sediment soil at different sedimentation water contents.

3.3.2.3 Estimation of the consolidation curve of Mae Moh sedimentation soil.

Based on the collected compression data of 24 reconstituted clays, Horpibulsuk et al. (2016) proposed a robust S-shaped equation to predict the complete compression behavior of reconstituted clays with effective vertical stress σ'_v 0.01 kPa. The consolidation equation in term of void ratio and mean effective stress is given as (Horpibulsuk et al., 2016):

$$e = \left\{ \frac{a}{\exp\left(\frac{\tau'_v}{b}\right)^{0.5}} + \frac{0.31}{\tau'_v} \left[1 + \frac{10\tau'_v - 1}{\exp(0.0551\tau'_v)^{0.425}} \right] - 2.1 \right\} \times C_c^* + e_{100} \text{ for } \tau'_v \geq 0.01 \text{ kPa} \quad (3.4)$$

with $C_c^* = e_{100} - e_{1000}$

where e is the void ratio corresponding to a vertical effective stress τ'_v ; e_{100} and e_{1000} are the void ratio at $\tau'_v = 100$ kPa and 1000 kPa, respectively. Two parameters a and b are used to predict the compression behavior at a low range of stresses.

The applicability of the equation was illustrated by the excellent simulation of compression curves of various soils such as kaolin (Shipton & Coop, 2012), marine soil (Fukue & Mulligan, 2009), Weiner Tegel clay (Burland, 1990), and Huaian clay (Zeng et al., 2015). Therefore, Eq. (4) was adopted to predict the compression behavior of Mae Moh sedimentation soil. Two parameters a and b were obtained by a trial and error method. The trial and error process started from selecting the parameter a as a fixed value between 1 and 4 (recommended by Horpibulsuk et al., 2016), and then varies b value until fitting the experiment curve. The a and b values for Mae Moh sedimentation soil with w_s in a range of 88% to 130% are shown in **Table 3.2**. It is noted that the a value decreases with decreasing w_s . On the other hand, the b value increases with the decrease of w_s . The simulation results are comparable with the measured results as seen in **Fig. 3.13**

Table 3.2 Values of equation parameter for Mae Moh Slurry soil.

Water content of the soil	$e^*_{v,100}$	$e^*_{v,1000}$	a	b
W = 130 %	1.33	0.76	2.19	3.77
W = 120 %	1.32	0.74	1.87	4.07
W = 112 %	1.29	0.73	1.8	4.75
W = 105 %	1.24	0.72	1.7	5.07
W = 97 %	1.23	0.69	1.37	5.31
W = 88 %	1.19	0.67	1.17	5.62

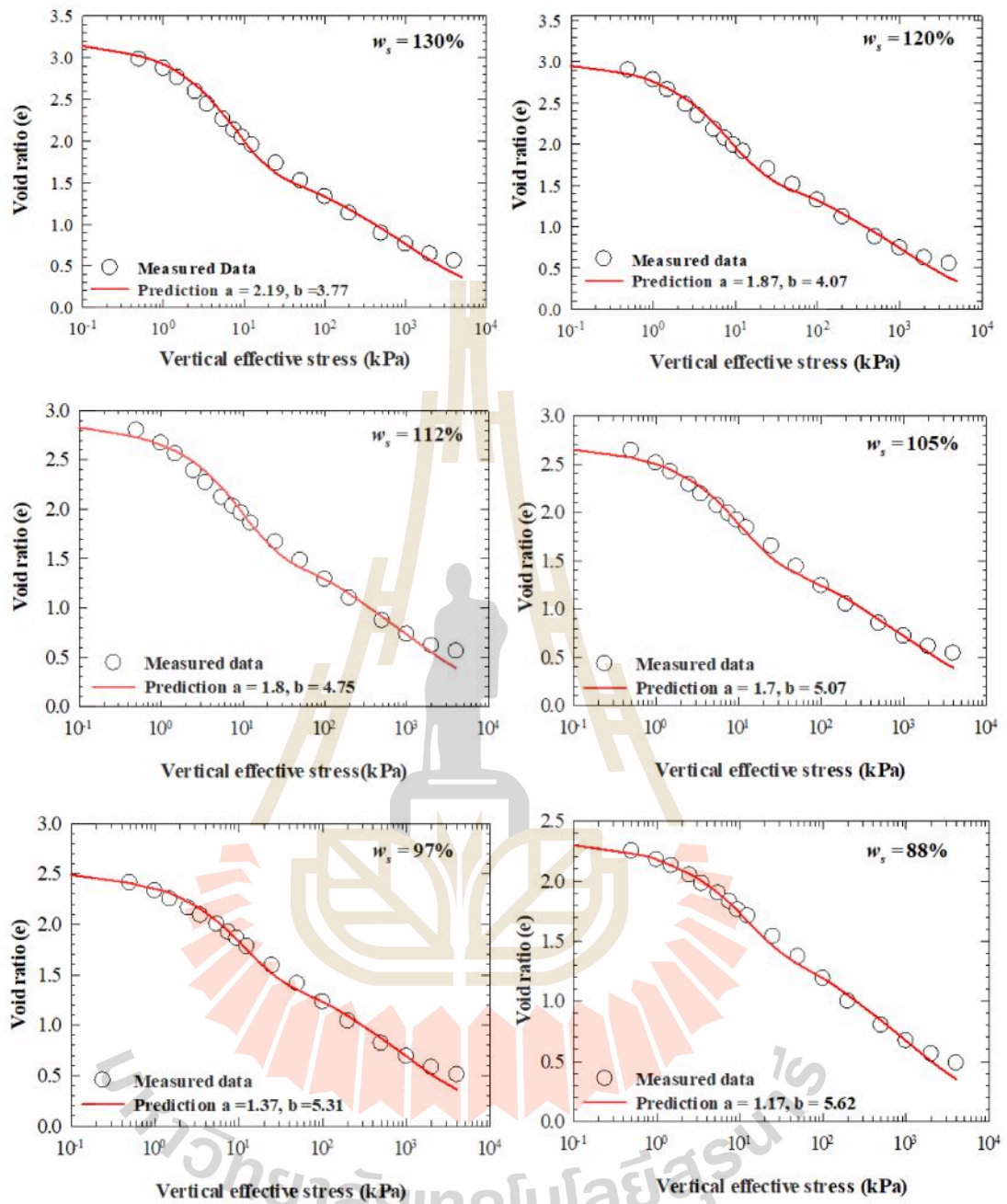


Figure 3.13 Prediction of consolidation curves of sediment soil using S-shaped equation.

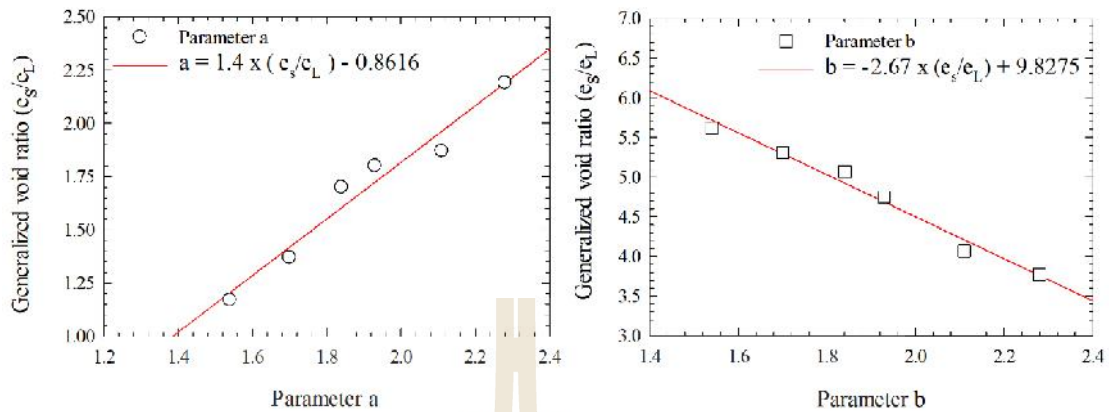


Figure 3.14 Relationship between parameters a and b versus e_s/e_L .

Since the liquid limit is the state parameter reflecting the soil structure (Mitchell, 1993 and Nagaraj et al. 1990), it is logical to relate the consolidation parameters a and b to generalized void ratio, e_s/e_L where e_s is the sedimentation void ratio and e_L is the liquid limit void ratio. **Figure 3.14** presents the relationship of parameters a and b versus e_s/e_L ratio of Mae Moh soil at different w_s . As a result, the generalized equation to describe compression behavior of the Mae Moh sedimentation soil can be proposed as:

$$e = \left\{ \frac{1.4(e_s/e_L) - 0.8618}{\exp\left[\frac{\dot{\tau}_v}{-2.67(e_s/e_L) + 9.8275}\right]^{0.5}} + \frac{0.31}{\dot{\tau}_v} \left[1 + \frac{10\dot{\tau}_v - 1}{\exp(0.0551\dot{\tau}_v^{0.425})} \right] - 2.1 \right\} \times C_c^* + e_{100} \quad (3.5)$$

The compression behavior of Mae Moh slurry soil was predicted using this generalized equation and presented in **Fig. 3.15**. It is evident that compression

behavior of the soil at different w_s can be captured successfully by proposed equation using the generalized void ratio.

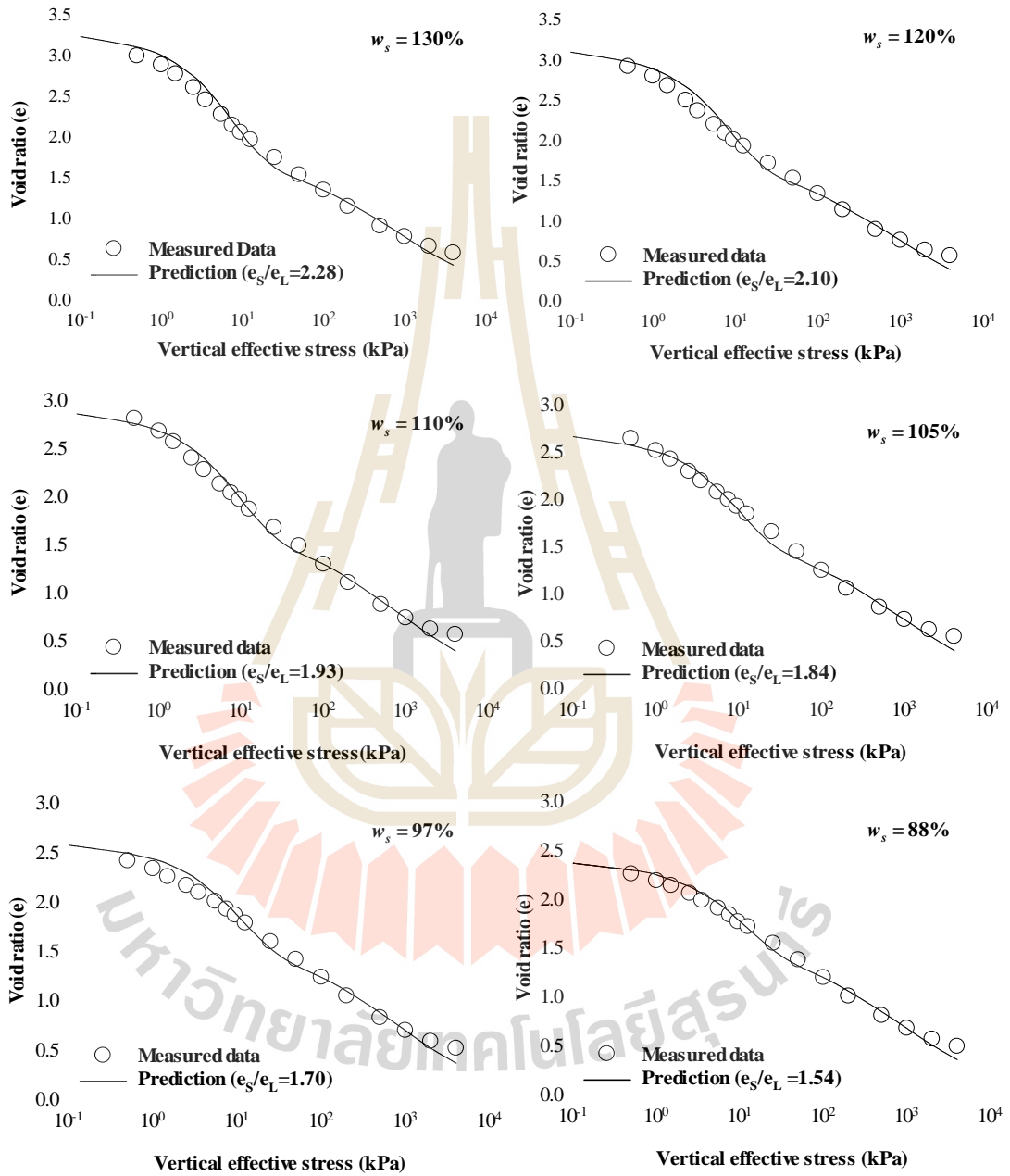


Figure 3.15 Prediction of consolidation curves of Mae Moh sediment soil using generalized S-shaped equation.

The compression behavior of remolded Kemen and Baimahu clay samples with different w_s reported by Hong et al. (2010) were taken to validate the modified equation by comparing the predicted results with measured data. The w_s was ranged from 99% to 116% and from 101% to 180% for Kemen clay and Baimahu clay, respectively. The soil parameters used for simulation are presented in **Table 3.3**.

Table 3.3: The soil parameters of Kemen and Baimahu clay used for simulation.

Soil	Water content W (%)	Liquid Limit LL (%)	e^*_{100}	e^*_{1000}
Kemen Clay	116	61	1.34	0.81
	110	61	1.31	0.76
	99	61	1.23	0.71
Baimahu Clay	180	91	1.78	0.95
	143	91	1.65	0.81
	101	91	1.47	0.70

Fig. 3.16 shows the prediction of consolidation curves of Kemen and Baimahu clays based on Eqs.5. For Kemen clay, the soil behavior can be well described by the generalized equation, except for loading at 0.5 kPa of the sample with the $w_s = 116\%$. For Baimahu clay, the predicted results and measured data are in very good agreement except for the first loading of sample with very high $w_s = 141\%$. This reinforces the applicability of the generalized equation. The generalized equation using e_s / e_L ratio can describe satisfactorily consolidation behavior for various soils (Mae Moh soil, Kemen clay and Baimahu clay) at very high and low stresses.

Even with limited available test data, the development of the generalized equation is based on sound principles. The variable parameters can be refined by more test data, which can be performed in future research.

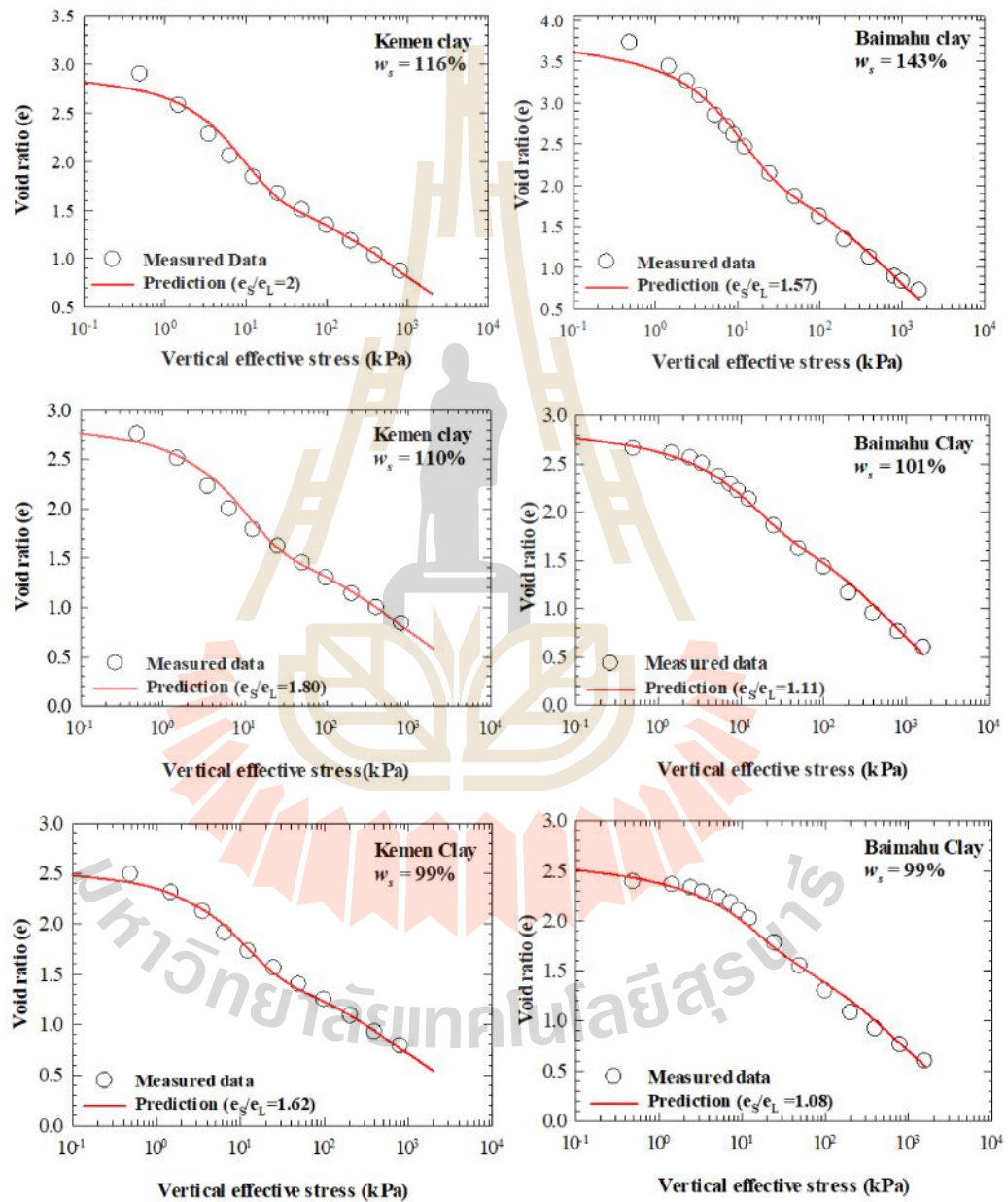


Figure 3.16: Prediction of consolidation curves of Kemen and Baimahu Clay using generalized S-Shaped equation.

3.4 Assessment of stress state of ultra-soft soil

Based on the sedimentation and consolidation test results, the e versus $\log \sigma'_v$ relationship of sedimentation soil is controlled by w_s . The w_s is approximately the same equal to w_{cr} and independent of w_i for large sedimentation soil. Consequently, the consolidation curve of large sedimentation soil is unique and defined as intrinsic state line (ISL). For the studied Mae Moh soil with $w_{cr} = 171\%$, the ISL can be represented by the following equation as presented in **Fig. 3.17**.

$$e = \left\{ \frac{3.31}{\exp\left[\frac{-\sigma'_v}{1.864}\right]^{0.5}} + \frac{0.31}{\sigma'_v} \times \left[1 + \frac{10\sigma'_v - 1}{\exp(0.0551\sigma'_v)^{0.425}} \right] - 2.1 \right\} \times 0.74 + 1.62 \quad (3.6)$$

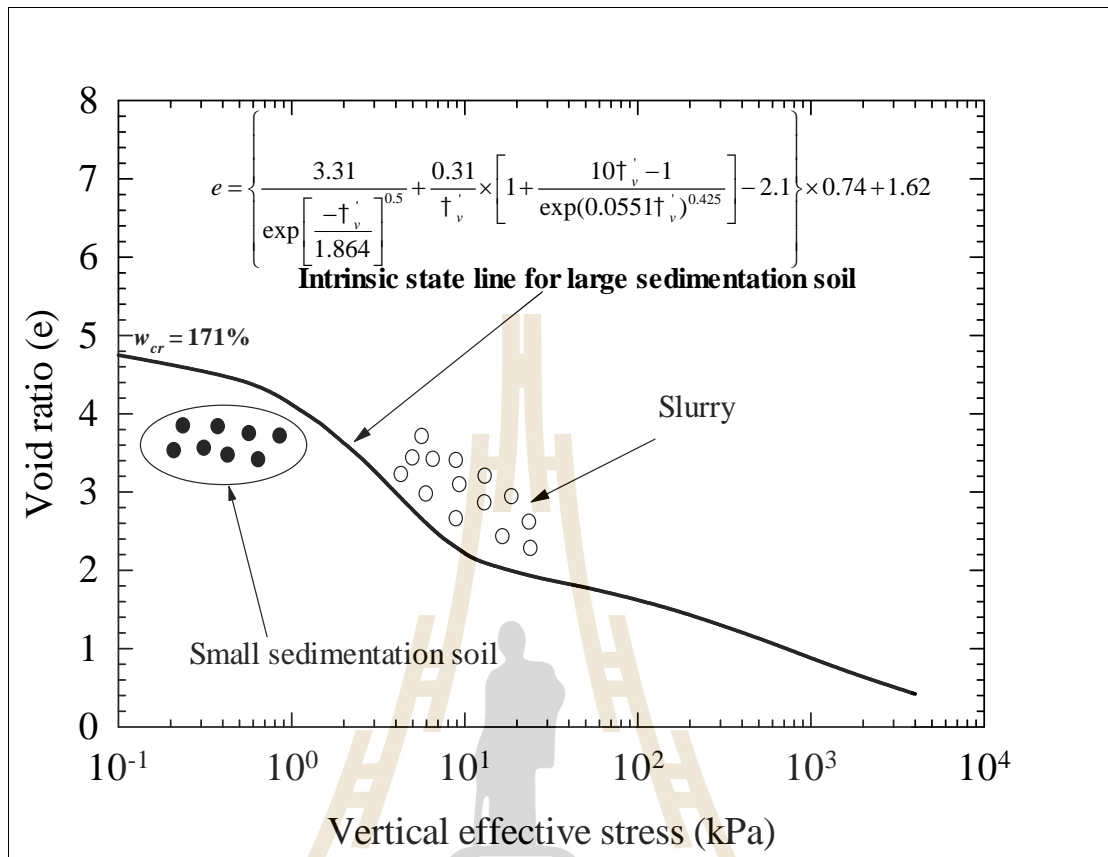


Figure 3.17 Intrinsic state line for large sedimentation soil.

It is long accepted that the compressibility of soil in both the slurry and sedimentation states is controlled by the stress state (e and σ_v). In this study, examination of the stress state using ISL is introduced. The ultra-soft soil is divided into high sedimentation soil, small sedimentation soil and slurry. The soil is classified as high sedimentation soil when the stress state is on the ISL, as low sedimentation soil when the stress state is below the ISL and as slurry when the stress state is above the ISL.

A suggested stepwise procedure for examining the stress state and compressibility of ultra-soft soil can be presented as follows:

1. Determine liquid limit and specific gravity of ultra-soft soil samples

2. Prepare the slurry at $w_i > 3$ times liquid limit
3. Perform the sedimentation test on the slurry to determine w_{cr}
4. From the known e_L , draw the ISL using Eq. (5)
5. Take the in-situ soil samples at various depths and determine e and corresponding τ'_v
6. Classify the stress state
 - 6.1 If the stress state is on the ISL, the ultra-soft soil is high sedimentation soil
 - 6.2 If the stress state is below the ISL, the ultra-soft soil is low sedimentation soil
 - 6.3 If the stress state is above the ISL, the ultra-soft soil is slurry and under sedimentation process
7. Approximate consolidation curves of either low or high sedimentation soil at various depths using Eq. (5)

The stress state assessment is important for predicting the settlement of ultra-soft soil. If the ultra-soft soil is in a slurry state, the settlement is due to both sedimentation of slurry and consolidation of the sedimentation soil. The sedimentation settlement is calculated from the difference between in-situ water content and w_s . The consolidation settlement can be calculated using Eq. (5) where e_s is equal to critical void ratio, e_{cr} for high sedimentation soil and approximately equal to initial void ratio, e_i for small sedimentation soil. From this study, the w_{cr} was found to be 171% while the in-situ water content was 98%, with an effective vertical stress of less than 6.2 kPa. This effective vertical stress is considered to be very low, considering that the

soil sample was collected at 1 m depth from the soil surface and had unit weight of approximately 16 kN/m^3 . Based on the proposed method, the Mae Moh soil can therefore be classified as a low sedimentation soil.

3.5 Conclusion

This research studied the compressibility and hydraulic conductivity characteristics of ultra-soft soil at the Mae Moh mine, Thailand. The study is useful for designing the land reclamation of ultra-soft soil using preloading technique with vertical drains. The following conclusions can be made from this study.

1. The sedimentation process of Mae Moh slurry was divided into two distinct stages: flocculation and settling. The flocculation occurred at the early stage of sedimentation process with very small change in soil-fluid interface. The settling stage then commenced, when the floc particles started to settle uniformly, causing the significant change in soil-fluid interface.

2. A critical water content (w_{cr}) separating the large sedimentation and small sedimentation slurry, was found to be 171% for studied Mae Moh soil. For large sedimentation slurry, the water content reduces significantly after sedimentation process. On the other hand, the water content of small sedimentation slurry slightly decreases during sedimentation process and thus w_s can be assumed to be w_i .

3. The consolidation curve of high sedimentation soil is unique and independent of w_i . On the other hand, the consolidation curve of small sedimentation soil is significantly dependent upon w_s . The consolidation curves of sedimentation soil can be represented by the inverse S-shape function from a very low (0.5 kPa) to very high vertical effective stresses.

4. The powerful S-shape equation proposed by Horpibulsuk et al. (2016) was extended to develop the generalized equation using generalized void ratio (e_s / e_L) as the prime parameter. The generalized equation can satisfactorily capture the compression behavior of various sedimentation soils at different w_s .

5. The intrinsic state line (ISL) for high sedimentation soil was proposed to assess the stress state of ultra-soft soil. The soil is classified as high sedimentation soil when the stress state is on the ISL, as low sedimentation soil when the stress state is below the ISL and as slurry when the stress state is above the ISL. The stepwise procedure for assessing stress state and compressibility of ultra-soft soil is suggested.

6. The stress state assessment is important to predict the settlement of the ultra-soft soil when subjected to ground improvement and land reclamation. For the ultra-soft soil in a slurry state, the settlement is due to both sedimentation of the slurry and consolidation of the sedimentation soil. The sedimentation settlement can be calculated from the difference between in-situ water content and w_s . The consolidation settlement can be calculated using the proposed S-shaped equation for both low and high sedimentation soils.

3.6 Reference

Been, K., Sills, G., 1981. **Self-weight consolidation of soft soils: an experimental and theoretical study**. *Geotechnique*, 31 (4), 519-535.

Blewett, J., McCarter, W., Chrisp, T., Starrs, G., 2001. **Monitoring sedimentation of a clay slurry**. *Geotechnique*, 51 (8), 723-728.

Burland, J., 1990. **On the compressibility and shear strength of natural clays**. *Geotechnique*, 40(3), 329-378.

- Chai, J.C., Miura, N., Zhu, H.H., Yudhbir., 2004. **Compression and consolidation characteristics of structured natural clay**. Canadian Geotechnical Journal, 41 (6), 1250-1258.
- Chai, J.C., Shen, J. S.L., Liu, M. D., Yuan, D.J., 2018. **Predicting the performance of embankments on PVD-improved subsoils**. Computers and Geotechnics, 93, 222-231.
- Chen, Q., Zhang, C., Yang, C., Ma, C., Pan, Z., Daemen, J., 2019. **Strength and deformation of tailings with fine-grained interlayers**. Engineering Geology, 256, 110-120.
- Desai, C.S., 2000. **Mechanics of materials and interfaces: The disturbed state concept**. CRC press.
- Fitch, B., 1957. **Sedimentation process fundamentals**. Biological treatment of sewage and industrial wastes. 2.
- Fitch, B., 1966. **Mechanism of sedimentation**. Industrial & Engineering Chemistry Fundamentals, 5 (1), 129-134.
- Fitch, B., 1979. **Sedimentation of flocculent suspensions: state of the art**. AICHE Journal, 25 (6), 913-930.
- Fukue, M., Mulligan, C. N., 2009. **Equations of state in soil compression based on statistical mechanics**. Soils and Foundations, 49(1), 99-114.
- Hong, Z., Yin, J., Cui, Y.J., 2010. **Compression behavior of reconstituted soils at high initial water contents**. Geotechnique, 60 (9), 691-700.
- Horpibulsuk, S., Liu, M.D., Zhuang, Z., Hong, Z.S., 2016. **Complete compression curves of reconstituted clays**. International Journal of Geomechanics, 16 (6), 06016005.

- Horpibulsuk, S., Shibuya, S., Fuenkajorn, K., Katkan, W., 2007. **Assessment of engineering properties of Bangkok clay**. Canadian Geotechnical Journal, 44(2), 173-187.
- Horpibulsuk, S., Yangsukkaseam, N., Chinkulkijniwat, A., Du, Y. J., 2011. **Compressibility and permeability of Bangkok clay compared with kaolinite and bentonite**. Applied Clay Science, 52(1-2), 150-159.
- Imai, G., 1980. **Settling behavior of clay suspension**. Soils and Foundations, 20 (2), 61-77.
- Imai, G., 1981. **Experimental studies on sedimentation mechanism and sediment formation of clay materials**. Soils and Foundations, 21 (1), 7-20.
- Kynch, G.J., 1952. **A theory of sedimentation**. Transactions of the Faraday society, 48, 166-176.
- Liu, M.D., Zhuang, Z., Horpibulsuk, S., 2013. **Estimation of the compression behaviour of reconstituted clays**. Engineering Geology, 167, 84-94.
- Liu, X. X., Shen, S. L., Xu, Y. S., Yin, Z. Y., 2018. **Analytical approach for time-dependent groundwater inflow into shield tunnel face in confined aquifer**. International Journal for Numerical and Analytical Methods in Geomechanics, 42(4), 655-673.
- Nagaraj, T., Pandian, N., Narashimha R. P., 1998. **Compressibility behaviour of soft cemented soils**. Geotechnique, 48(2).
- Özer, A.T., Bromwell, L.G., 2012. **Stability assessment of an earth dam on silt/clay tailings foundation: A case study**. Engineering Geology, 151, 89-99.

- Scott, J.D., Dusseault, M.B., Carrier, W.D., 1986. **Large-scale self-weight consolidation testing**. In Consolidation of Soils: Testing and Evaluation. ASTM International.
- Shipton, B., Coop, M. R., 2012. **On the compression behaviour of reconstituted soils**. Soils and Foundations, 52(4), 668-681.
- Sills, G., 1998. **Development of structure in sedimenting soils**. Philosophical Transactions-Royal Society of London Series A: Mathematical Physical and Engineering Sciences, 356 (1747), 2515-2534.
- Tan, T., 1995. **Sedimentation to consolidation: a geotechnical perspective**. Compression and Consolidation of Clayey Soils, 937-948.
- Tan, T., Yong, K., Leong, E., Lee, S., 1990. **Sedimentation of clayey slurry**. Journal of Geotechnical Engineering, 116(6), 885-898.
- Terzaghi, K., 1951. **Theoretical soil mechanics**: Chapman And Hall, Limited; London.
- Watabe, Y., Saitoh, K., 2015. **Importance of sedimentation process for formation of microfabric in clay deposit**. Soils and Foundations, 55(2), 276-283.
- Wu, Y.X., Lyu, H.M., Han, J., & Shen, S.L., 2019. **Dewatering-Induced Building Settlement around a Deep Excavation in Soft Deposit in Tianjin, China**. Journal of Geotechnical and Geoenvironmental Engineering, 145(5), 05019003.
- Xu, G.Z., Gao, Y.F., Hong, Z.S., Ding, J.W., 2012. **Sedimentation behavior of four dredged slurries in China**. Marine Georesources & Geotechnology, 30 (2), 143-156.

- Xu, Y.S., Yan, X.X., Shen, S.L., Zhou, A.N., 2019. **Experimental investigation on the blocking of groundwater seepage from a waterproof curtain during pumped dewatering in an excavation.** Hydrogeology Journal, 27(7), 2659-2672.
- Zeng, L.L., Hong, Z.S., & Cui, Y.J., 2015. **Determining the virgin compression lines of reconstituted clays at different initial water contents.** Canadian Geotechnical Journal, 52 (9), 1408-1415.
- Zhang, Q., Yin, G., Wei, Z., Fan, X., Wang, W., Nie, W., 2015. **An experimental study of the mechanical features of layered structures in dam tailings from macroscopic and microscopic points of view.** Engineering Geology, 195, 142-154.



CHAPTER IV

CONSOLIDATION BEHAVIOR OF ULTRA-SOFT SOIL IMPROVED WITH PREFABRICATED VERTICAL DRAIN AT THE MAE MOH MINE, THAILAND

4.1 Introduction

The Mae Moh mine is situated at Mae Moh district, Lampang province, located about 600 km north of Bangkok, Thailand. It is well-known as the largest open-pit lignite mine in Southeast Asia covering an area of 4 km in width and 7.5 km in length. Approximately 45,000 tons of coal/day, which represent 70% of the total coal production of Thailand, are processed to generate power at the Mae Moh power plants (Udomchai et al., 2017). This mine is operated by the Electricity Generating Authority of Thailand (EGAT). Sump1 C1 is a low-lying area, located in the north of the Mae Moh mine with the total area of 80,000 m². The soil erosion caused by the discharge of surface water along the mine slope was finally collected and formed up to approximately 38 m thickness of soil deposits under water in sump 1 C1 for over decades.

According to the mine planning and development of EGAT, the mine will be excavated to a depth of approximately 500 m from original surface in the next 40 years. As a result, this mine will become the deepest open-pit lignite mine in the world. The excavated soil from mining activity will be transferred to dump in the Sump 1 C1. It will be subjected approximately 300 m of overburden material in 2038.

However, the soil in the Sump 1 C1 is ultra-soft soil and possesses very low bearing capacity. Therefore, it is imperative to improve the existing ultra-soft dredged soil before commencing any construction activities in order to prevent any failure due to the mud flow.

Soil improvement techniques generally include soil replacement, preloading, stone column, and cement column, etc (Arulrajah et al., 2005; Cai et al., 2018; Cao et al., 2019; Horpibulsuk et al., 2013; Jiang & Liu, 2019; Morohoshi et al., 2010; Pham et al., 2019; Pham et al., 2019; Wang et al., 2020; Yonghui et al., 2019; Zhang et al., 2019). Among these methods, the preloading with prefabricated vertical drains (PVDs) is cost-effective and commonly used in land reclamation projects on ultra-soft soil deposits (Arulrajah et al., 2004; Bo et al., 2005; Chen et al., 2016; Geng et al., 2017; Mesri & Kane, 2019). PVDs are band-shaped, which can be inserted into the soft ground up to even 40m depth to reduce the drainage path and therefore shorten the consolidation time (Almeida et al., 2004; Bo et al., 2016; Chai et al., 2001; Fang & Yin, 2006; Saowapakpiboon et al., 2010). However, a few laboratory testing and field instrumentation have been conducted to study the performance of PVDs improved ultra-soft soil in dredged sump (Bo 2004; Choa et al., 2001; Chu et al., 2004; Chu et al., 2006). It was evident that the PVDs accelerate settlement, enhance shear strength, and reduce moisture content of the ultra-soft clay for a particular water content and PVD dimension. However, the PVD dimensions and water content, which play an important role in successful performance of PVD in the ultra-soft soil have not been well examined.

In this study, a series of large - scale model test was carried out to assess the effectiveness of PVD in the consolidation of the Mae Moh ultra-soft soil. The effects

of PVD dimension and water content of the ultra-soft soil on the settlement, excess pore pressure dissipation and undrained shear strength of PVD improved ground under various loading conditions were investigated. The large-scale consolidation test results were analyzed and compared with the simulation results by finite element method (FEM). The distinct consolidation behavior especially excess pore pressure dissipation of ultra-soft clay was presented and compared with the conventional soil mechanics theory. Also, the suitable numerical method for predicting settlement at various consolidation time was recommended. The research outputs will facilitate the selection of design parameters and numerical method for the future design of soil in Sump 1 C1 using preloading with PVD system. The knowledge gained can be applied to the ground improvement of ultra-soft soils in future dredging projects.

4.2 Large-scale consolidation test

To investigate the effectiveness of PVD for the ground improvement of ultra-soft soil, the large-scale consolidation tests were conducted at various initial water contents (case 1 and case 2) and dimensions of the PVDs (case 1 and case 3) as listed in **Table 4.1**. The details of the sample preparation and testing procedure of each testing case are being presented.

4.2.1 Soil sample

The ultra-soft soil samples were obtained from a slurry pond (Sump 1 C1). The disturbed bulk samples were collected from 1.5 m depth below the soil surface. It was then stored in plastic tanks and kept inside the laboratory at a room temperature of approximately 27°C.

The ultra-soft soil consists of 1% sand, 58% silt, and 41% clay. The 85% of soil particles by weight, D_{85} were smaller than 0.017 mm. The liquid limit and the plastic limit determined using Casagrande method were 57% and 26%, respectively. The specific gravity was 2.5. The activity of this soil is about 0.756 and it is therefore classified as a normal clay based on Skempton's classification (Skempton, 1953). The natural water content was in the range of 114% - 180%. The in-situ strength was extremely low.

Table 4.1 Cases tested

Case	Height of soil (mm)	Water content W_i (%)	PVD dimensions (mm)	Loading step (kPa)	Total loading time (hours)
Case 1	950	120	100 × 5	20, 40, 80	1362
Case 2	950	180	100 × 5	20, 40, 80	1362
Case 3	950	120	50 × 5	20, 40, 80	1362

4.2.2 Selection of PVD

During consolidation, very fine particles may infiltrate into the core of the PVD and consequently clog the drainage channels, and reduce the discharge capacity (Cao et al., 2019; Chu et al., 2004, 2006; Holtz, 1987). Therefore, the selection of PVD types plays a major role in the successful performance of PVD in ultra-soft clay (Chu et al., 2004, 2006). In this study, the filter of PVD was selected carefully based on the requirement of permeability and the apparent opening size of the filter. In general, the permeability of filter is required to be higher than that of soil. On the other hand, the apparent opening size should meet the requirement as follows:

$$O_{95} \leq (4 - 7.5) \frac{D_{85}}{K_a} \quad (4.1)$$

where O_{95} is the apparent opening size of the filter; and K_a is a reduction factor considering the effect of loading and partial clogging on the geotextiles. The value of K_a varies from 1.9 to 4.4 as recommended by Chu et al. (2006) and Palmeira and Gardoni (2002). Based on this criterion, two types of PVDs, namely Ali-drain type AD250 having 100 mm and 50 mm width but with the same thickness of 5 mm were selected. The apparent opening size of the filter was smaller than 0.08 mm, satisfied the requirement in **Equation 4.1**. The hydraulic conductivity of the PVD filter was 1.8×10^{-4} m/s, higher than the laboratory permeability of the ultra-soft soil (1.21×10^{-9} m/s). The core of the PVD had a discharge capacity of 150×10^{-6} m³/s in the straight condition and 110×10^{-6} m³/s in the kinked condition, under a confining pressure of 250 kPa. The characteristics of the PVDs are summarized in **Table 4.2**.

Table 4.2 PVDs characteristics

Thickness (mm)	Width (mm)	Permeability of the filter (m/s)	Discharge capacity of straight drain under 300 kPa pressure (m ³ /s)	Discharge capacity of kinked drain under 250 kPa pressure (m ³ /s)	Apparent opening size (mm)
100	5	1.8×10^{-4}	150×10^{-6}	110×10^{-6}	0.08
50	5	1.8×10^{-4}	150×10^{-6}	110×10^{-6}	0.08

4.2.3 Model test

Large-scale consolidation apparatus

A large-scale consolidation apparatus was developed at the Center of Excellence in Innovation for Sustainable Infrastructure Development of Suranaree University of Technology, Thailand for this research. **Fig. 4.1** shows the schematic and photo of the fully-instrumented large-scale consolidation tank. The consolidation tank was made of stainless steel with an inside diameter of 495 mm and a height of 1200 mm. Six saturated miniature pore pressure transducers (PPT) were installed to measure excess pore water pressures at different positions. Six pore pressure transducers (PPTs) were installed at 100 mm (PPT 2, PPT 4, and PPT 6) and 200 mm (PPT 1, PPT 3, and PPT5) away from the center of vertical drain, respectively. A total earth pressure cell was placed on the steel plate in order to control the pressure acting on the sample during the test. To reduce wall friction, the inner surface was polished and smeared with lubricating oil beforehand.

Sample preparation

For each test, the remolded sample was prepared by adding a sufficient amount of water to obtain the initial water content greater than its liquid limits and then thoroughly mixed by a mechanical mixer. The sedimentation process is special characteristic of ultra-soft soil at very high initial water content (Been & Sills, 1981; Blewett et al., 2001; Sills, 1998; Tan et al., 1990; Xu et al., 2012). The remolded soil was hence poured into the tank for about 1 month to negate the effect of sedimentation on the consolidation. The water on the top of slurry soil was taken out of the tank after the 1 month of sedimentation. The final height of the soil in the consolidation tank was approximately 95 cm while the water contents of the soil in

the 3 tested cases were respectively 120%, 180%, and 120% after sedimentation time. One geotextile layer with a rectangular hole of 120 mm × 15 mm at the center of the model ground for PVD installation using a mandrel was placed on the top of the model ground.

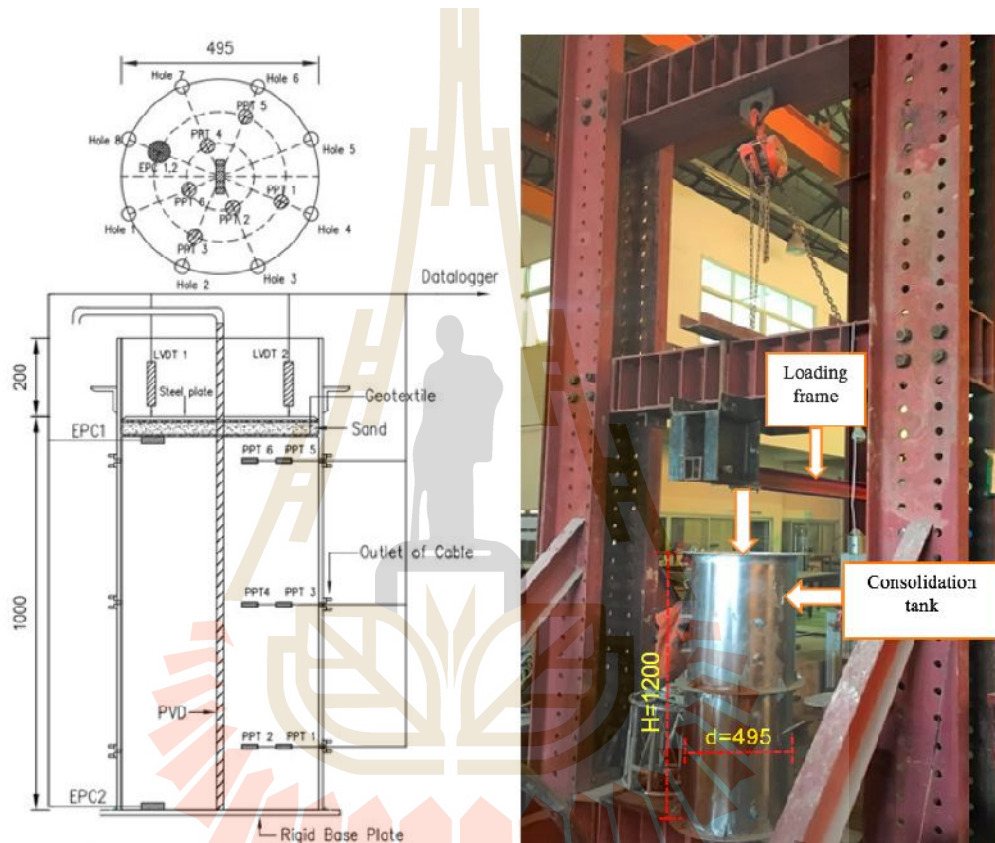


Figure 4.1 Large scale of consolidation tank (dimensions are in mm)

Installation of PVD

After the 1 month of sedimentation, two small aluminum mandrels with different rectangular sections of 120 mm × 10 mm and 60 mm × 10 mm connected with an aluminum tip shoe at the end were used to simulate field installation of PVDs with 10 cm width and 5 cm width, respectively. In each case, the mandrel with PVD inside was penetrated through the hole at the center of geotextile

and vertically into the ultra-soft soil. When the mandrel touched the bottom of the tank, it was slowly withdrawn from the soil. A 10 cm thick sand layer was then spread on the geotextile layer (on top of the ultra-soft clay) after PVD installation and covered with the other geotextile (*see Fig. 4.1*). A steel plate with one rectangular hole of 120 mm by 15 mm (for PVD to pass through) at the center was placed on the top of geotextile to impose the same displacement. It is noted that a hole of 50 mm diameter was manufactured in the steel plate to push the mini vane shear into the consolidated soil during the consolidation process to measure the undrained shear strength. The sand layer and geotextiles could prevent the ultra-soft clay from being squeezed out from the holes. During the consolidation stage, no squeezed soil was however observed from the holes.

Step loading

After assembling the tank, three incremental vertical pressures (20 kPa, 40 kPa, and 80 kPa) were applied at the top of the soil layer until the degree of consolidation in each loading stage was more than 90% for case 1. The degree of consolidation and the magnitude of final settlement were estimated based on the Asaoka's observational method (Asaoka, 1978). Chung et al. (2014) and Hiep & Chung (2018) also proposed an observational method, which is comparable to the Asaoka's method. The consolidation times of case 1 were also applied for case 2 and case 3 for comparison. The consolidation times were 620 hours, 410 hours and 333 hours for 20 kPa, 40 kPa and 80 kPa vertical stresses, respectively. The top surface was drainage boundary and the bottom of tank were closed drainage. The water flows towards to the PVDs and vertically drains to the top surface. In this study, the settlement was measured by two Linear Variable Displacement Transducers (LVDTs)

having the reading accuracy of 0.01 mm and 500 mm maximum deformation reading. The pore water pressure, earth pressure, and settlement were automatically recorded in real-time with a data logger. To investigate the effectiveness of PVDs on the strength improvement, the undrained shear strengths were measured by using a mini vane shear apparatus after the end of each loading. The vane blade was made of stainless steel with 30 mm in diameter and 60 mm in height. It was attached to a stainless steel rod with 5 mm in diameter, which can measure undrained shear strength at different depths in the consolidation tank.

4.2.4 Numerical simulation

In reality, the PVD improved soil can be represented by the unit-cell theory in the axisymmetric condition (three-dimensional, 3D), which is similar to the large consolidation model. However, the 3D finite element modeling of PVDs improved soil is very sophisticated and requires large computational effort. Consequently, the transformation of the unit cell condition to equivalent plane strain condition was introduced by Hird et al. (1992). In practice, the plane strain model satisfactorily simulates the settlement behavior of soil improved by PVD (Indraratna & Redana, 2000). The equations to determine an equivalent hydraulic conductivity of soil were proposed by several researchers to convert an axisymmetric model to an equivalent plane strain model (Indraratna et al., 2010). The equivalent hydraulic conductivity is determined in term of hydraulic conductivity of soil, PVD dimension and spacing, and smear effect. In this study, the settlement behavior of the ultra-soft soil of case 1 as an example was modeled by both the axisymmetric and plane strain models using the Plaxis modeling software. The suitable plane strain model, which can simulate the settlement of the model ground was suggested to predict the

settlement behavior of the ultra-soft soil in the field in the next phase of this research. In this study, four different approaches were adopted to simulate the consolidation behavior of ultra-soft soil using vertical drain as follows:

a) Axisymmetry model with drain element:

An axisymmetric unit cell model was considered to analyze the consolidation of ultra-soft soil in the large-scale test. At the center of the unit cell, the rectangular sized PVD was converted into an equivalent radius, r_w . The r_w was equal to one fourth of sum of width and thickness of PVDs (Chai et al., 1999; Rixner et al., 1986). The PVDs were modeled as 3 nodes drainage element (excess pore water pressure is always zero) with the equivalent radius (r_w) of 26.25 mm for PVDs 10 cm, as shown in **Fig. 4.2a**. The top boundary was set to drainage while outer vertical and bottom boundaries were assigned as closed drainage. The vertical stress of each loading stage was applied as uniform stress at the top of boundary. The horizontal hydraulic conductivity of the surrounding soil, k_h , was taken as 2.03 times of the vertical hydraulic conductivity, which was recommended by Arulrajah et al. (2005) for ultra-soft soil. The soil parameters using axisymmetric model are indicated in **Tables 4.3**. The modified compression index (λ^*), modified swelling index (λ^*), the vertical hydraulic conductivity were obtained from the oedometer test. The cohesion (c') and friction angle (ϕ') were based on the undrained triaxial compression test results.

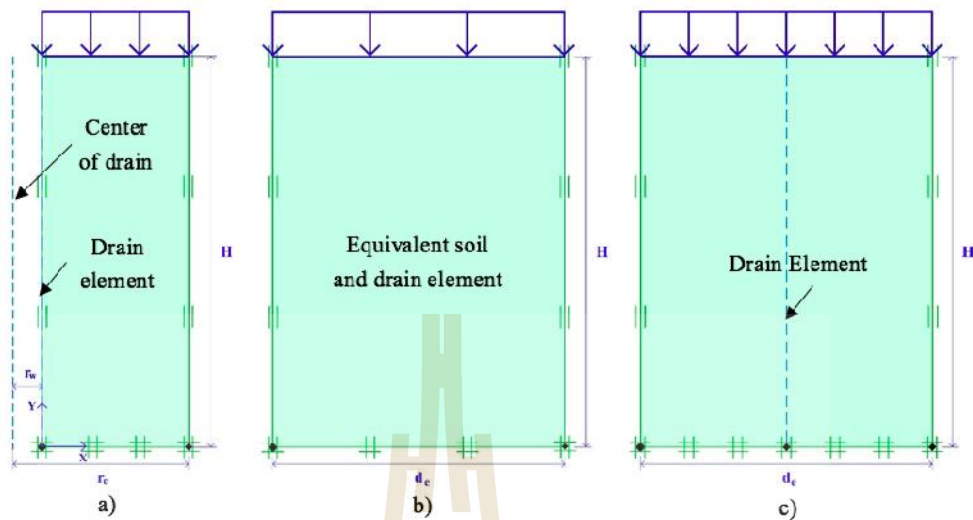


Figure 4.2 Geometry conditions using a) Axisymmetry model; b) Plane strain model using Chai et al.'s method; c) Plane strain model using Lin et al.'s method and Indraratna and Redana's method.

Table 4.3 Soil parameters for modeling case 1.

Model	Axisymetry (Soft soil model)	Plane strain (Chai et al.'s method)	Plane strain Lin et al.'s method	Plane strain (Indraratna and Redana's method)
Type	Undrained	Undrained	Undrained	Undrained
γ_{unsat} (kN/m ³)	16	16	16	16
γ_{sat} (kN/m ³)	18	18	18	18
k_h (m/hour)	8.85×10^{-6}	-	-	-
k_v (m/hour)	4.36×10^{-6}	-	-	-
k_{he} (m/hour)	-	5.89×10^{-5}	3.10×10^{-6}	3.48×10^{-6}
k_{ve} (m/hour)	-	5.89×10^{-5}	1.53×10^{-6}	1.72×10^{-6}
*	0.068	0.068	0.068	0.068
*	0.025	0.025	0.025	0.025
Void ratio (e_{int})	3.02	3.02	3.02	3.02
Cohesion (c')	1	1	1	1
Friction angle (ϕ')	29	29	29	29
$r_e - r_w$	0.2221	0.2475	0.2475	0.2475

b) Plane strain model using Chai et al.'s method (Chai et al., 2001)

In this approach, a plane strain model without the drain element was adopted, in which the PVD and surrounded soil were considered as a uniform layer with the equivalent value of vertical hydraulic conductivity (k_{ve}). The equivalent value of vertical hydraulic conductivity can be expressed as:

$$k_{ve} = \left(1 + \frac{2.5l^2 k_h}{\sim d_e^2 k_v} \right) k_v \quad (4.2)$$

The value of \sim can be taken as

$$\sim = \ln \frac{n}{s} + \frac{k_h}{k_s} \ln(s) - \frac{3}{4} + f \frac{2l^2 k_h}{3q_w} \quad (4.3)$$

where $n = d_e / d_w$; $s = d_s / d_w$; d_e is the diameter of unit cell; d_w is the diameter of drain; d_s is the diameter of smear zone; k_s is the horizontal hydraulic conductivity in smear zone, which can be assumed as the vertical hydraulic conductivity (k_v), l is the drainage path of PVD, which is the same as the PVD length for one-way drainage, q_w is the discharge capacity of PVD.

The geometry and loading conditions of this model are shown in **Fig. 4.2b**. The boundary on the top was set as drainage and the other boundaries were assigned as closed drainage.

c) Plane strain model using Lin et al.'s method (Lin et al., 2000)

To simulate the PVDs in plane strain model, Lin et al. (2000) proposed an equation to convert the radial flow of an axisymmetric model to that of a plane strain model. The horizontal hydraulic conductivity in an axisymmetric model (k_h) was converted to plane strain model with consideration of the smear effect as follows.

$$k_{he} = \frac{k_h \times f}{6[\ln(n/s) + (k_h/k_s)\ln(s) - 0.75]} \quad (4.4)$$

in which k_{he} is the horizontal hydraulic conductivity in the undisturbed zone in the plane strain model.

d) Plane strain model using Indraratna and Redana's method (Indraratna & Redana, 2000)

Indraratna and Redana (2000) proposed an equation to convert the horizontal hydraulic conductivity of axisymmetry model to that of plane strain model. With considering the smear effect, the equivalent plane strain hydraulic conductivity is calculated as follows:

$$k_{he} = \frac{k_h \left[r + s \frac{k_{h,pl}}{k_{s,pl}} \right]}{\ln\left(\frac{n}{s}\right) + \left(\frac{k_h}{k_h}\right)\ln(s) - 0.75 - r} \quad (4.5)$$

The terms r and s consider the geometric conversion of an axisymmetric unit cell into plane strain, and smear zone effects, respectively. The parameters r and s are given by:

$$r = \frac{2}{3} - \frac{2b_s}{B} \left(1 - \frac{b_s}{B} + \frac{b_s^2}{3B^2}\right) \quad (4.6)$$

$$s = \frac{1}{B^2} (b_s - b_w)^2 + \frac{b_s}{3B^3} (3b_w^2 - b_s^2) \quad (4.7)$$

in which $b_s = \frac{f r_s^2}{2S}$ and $b_w = \frac{f r_w^2}{2S}$

The geometry conditions of plane strain model using Lin et al.'s and Indraratna and Redana's methods to simulate the consolidation settlement of ultra-soft soil improved by PVD are illustrated in **Fig. 4.2c**.

The soil parameters in plane strain model used for FEM are indicated in **Table 4.3**. It is noted that the soil parameters used for the axisymmetric and plane strain models are the same, except the horizontal and vertical hydraulic conductivities. For Chai et al.'s method, 1-D consolidation settlement is assumed so only k_{ve} controls the rate of settlement. As such, k_{he} can be taken as k_{ve} . For Lin et al and Indraratna and Redana's methods, the k_{he}/k_{ve} ratio was taken as 2.03, which is the same as the axisymmetric condition. As such, the k_{ve} can be calculated after obtaining k_{he} from Eqs. (4) or (5).

4.3 Results and Discussion

4.3.1 Model test results

4.3.1.1 Settlement results

The relationship between the settlement versus time of the three tested cases is shown in **Fig. 4.3**. The settlement occurred in the first loading stage (20 kPa) was much higher than the settlement induced in the second loading (40 kPa) and the last loading (80 kPa), respectively for all studied cases. The value of settlement reduced as the consolidation stress increased due to non-linear compression behavior of the ultra-soft soil (Fang & Yin, 2006; Hong et al., 2010; Horpibulsuk et al., 2016; Liu et al., 2013).

The large settlements for all cases were observed, especially for case 2 with the initial water content of 180% that exhibited the highest value. The settlement of case 1 was in the order of 240 mm, which was about 27% of strain under the vertical consolidation stress of 80 kPa. The values of ultimate settlement (S_{ult}) and the degree of consolidation (S_f/S_{ult}) at the end of each loading are presented in **Fig. 4.3** and **4.4**, where S_f is the measured settlement at the end of each loading and S_{ult} is the ultimate settlement predicted by using the Asaoka's observational method (Asaoka, 1978). The time interval used for Asaoka's observational method, t , was 40 hours. The soil in case 1 achieved more than 90% the degree of consolidation in all stages of loading, which was about 90.65%, 96.80%, and 97.90% for consolidation stresses of 20 kPa, 40 kPa, and 80 kPa, respectively.

The measured settlement in case 2 was much higher than that in case 1, which was approximately 393.02 mm after 1362 hours of testing. A very large vertical strain of approximately 42% was developed at the end of consolidation test.

Large settlements induced by PVDs in both cases (case 1 and case 2) proved the effectiveness of PVDs in improving the ultra-soft soil at different initial water contents. The degree of consolidation in case 2 in each loading stage was smaller than that in case 1. This indicates that the higher initial water content leads to the higher final settlement and the lower rate of consolidation settlement.

The effect of PVD dimension on the consolidation behavior of the ultra-soft soil can be noticed by comparing case 1 with case 3. Under the same testing condition (the water content of the soil, and loading pressure), the measured settlement for 5 cm PVD was smaller than that for 10 cm PVD at the same consolidation time, especially at low vertical stress. For instance, the settlement at the end of loading stage 1 (20 kPa of vertical stress) was approximately 126.03 mm for case 1 while it was 111.53 mm for case 3 (**Fig. 4.3**). The degree of consolidation at the end of test in case 3 was 80.20%, 94.80%, and 96.20% at 20 kPa, 40 kPa, and 80 kPa, respectively, as presented in **Fig. 4.4**, which is lower than that in case 1. However, based on the Asaoka's observational method, the ultimate settlement at 100% degree of consolidation for case 1 and case 3 was approximately the same. It is evident that at low vertical stress where the viscosity is relatively high, the PVD dimension significantly affected the rate of consolidation settlement while at high vertical stress, the effect of PVD dimension was less. The larger PVD has the higher drainage area per soil volume, which can stimulate the flow rate of the PVD improved ground. It was observed during the test that the water volume squeezed out from the soil in case 1 (10 cm PVD) was higher than that in case 2 (5 cm PVD).

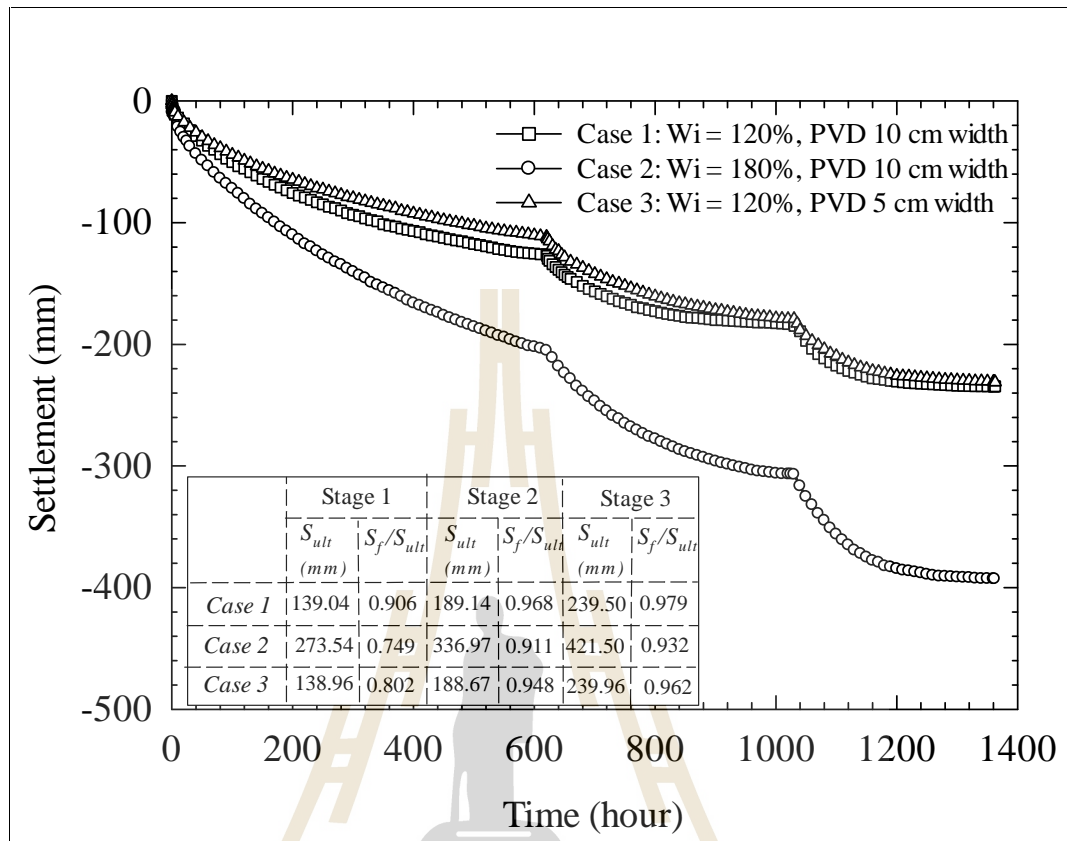


Figure 4.3 Measured settlement versus time curve of 3 cases under 3 loading stages

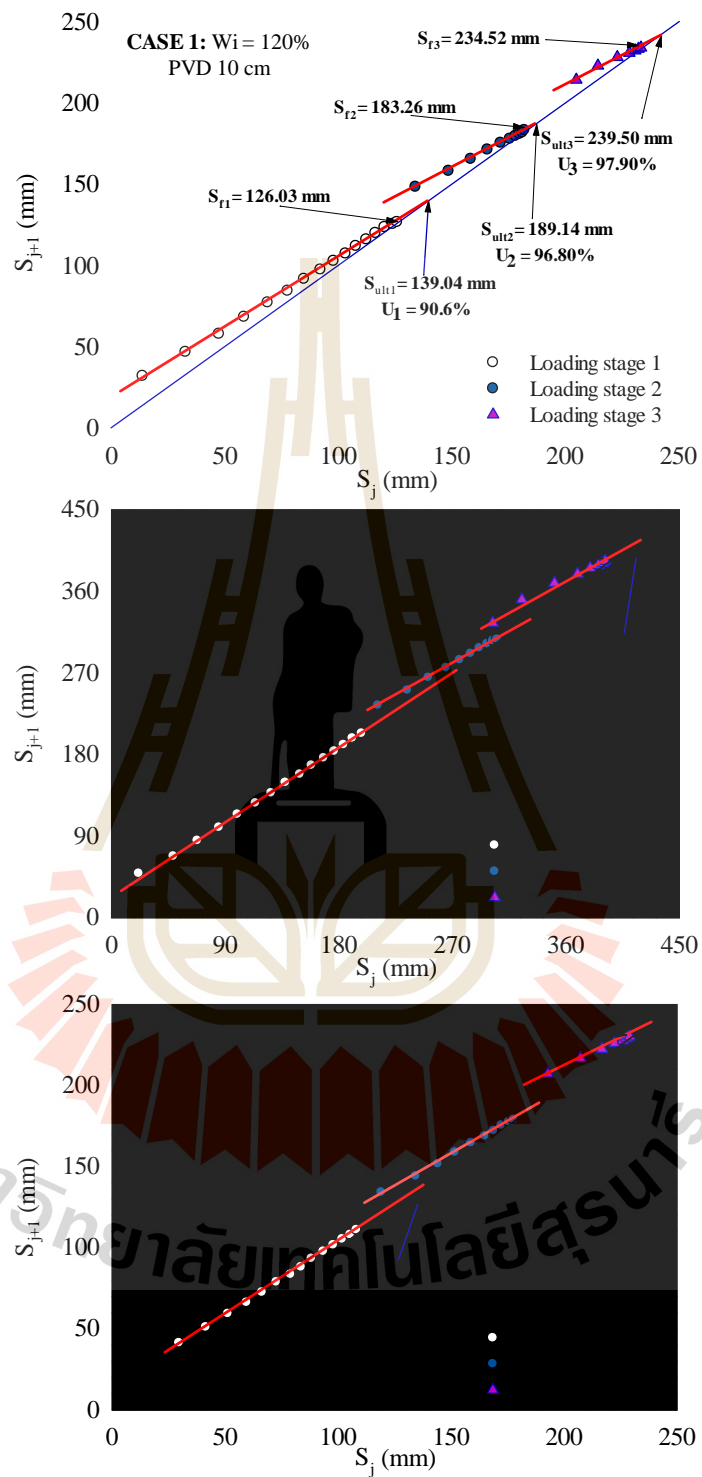


Figure 4.4 Ultimate settlements of each loading stage predicted by using Asaoka's observational method

The PVD of each test was extruded from the tank at the end of each test. The drain filter was cut open to check the soil particles entering into the PVD core. In all studied cases, the core was clean, which shows a good selection of PVDs filter for the consolidation of Mae Moh ultra-soft soil. For Mae Moh ultra-soft soil, the apparent opening size of the filter is therefore suggested to be:

$$O_{95} \leq 4.71 \times D_{85} \quad (4.8)$$

4.3.1.2 Excess pore water pressure

The dissipation of excess pore water pressures from six transducers of 3 tested cases is shown in **Figs. 4.5-4.7**. In all cases, the initial excess pore water pressures (at time $t = 0$) measured from 6 PPTs were slightly lower than the total vertical stress. It can be explained by the pore pressure coefficients A and B proposed by Skempton (1954). The change in pore water pressure under the change in the principle stresses $\Delta\sigma_1$ and $\Delta\sigma_3$ is given as $\Delta u = B[\Delta\sigma_3 + A(\Delta\sigma_1 - \Delta\sigma_3)]$. For saturated soils, the coefficient B is equal 1 while the value A varies with stresses and strains (Fang & Yin, 2006; Skempton, 1954). This behavior is similar to previous studies by Fang and Yin (2006) for Hong Kong marine clay. The excess pore water pressures recorded at the top (PPT 5, PPT 6) were different with those measured at the bottom of the tank (PPT 1, PPT 2), showing the different distribution of pressures on the soil along the depth possibly due to different drainage conditions. Only minimal pore pressure dissipation was recorded by the six transducers in the early of loading stages, although the majority of settlements took place during this time (**Figs. 4.5-4.7**). Bo (2008) explained that for ultra-soft soil, settlement is induced during the

initial time of loading due to reduction of water which will not lead to a subsequent reduction of pore water pressure in the soil. For instance, **Fig. 4.3** shows that the settlement in case 2 after 50 hours was 53.61 mm, which was 30.89% of degree of consolidation, with the delay of excess pore water pressure during the first loading stage. The delayed time is defined as the transitional point from small change to large change in excess pore pressure. The delay of excess pore water pressures was also observed in the second and the last loading stage. It is noted that the delayed time tended to reduce with the increase of vertical consolidation pressure, as shown in **Figs. 4.5-4.7**. The delayed time observed in PWP 5 and PWP6 was shorter than that in the other locations in the first loading stage and this difference was noted by 2 dotted line in **Figs. 4.5-4.7**.

The delay of excess pore water pressure of case 1 (**Fig. 4.5**) and case 2 (**Fig. 4.6**) was compared under the same total vertical stresses but different water contents. The higher initial water content resulted in the longer delay of excess pore pressure dissipation. The delayed time observed in PWP 5 and PW6 of case 2 ($W_i = 180\%$) was approximately 50 hours in the first loading, which was approximately 20 hours longer than that of case 1 ($W_i = 120\%$). Although there was little or no pore pressure dissipation, the water squeezed out from the soil was observed in the early of the loading stages.

The consolidation behavior of Mae Moh ultra-soft soil improved by PVD in case 1 was compared with that of soft Bangkok clay (Saowapakpiboon et al., 2011) in the relationship of S/S_{ult} and u/u_0 , as shown in **Fig. 4.8** where S is the settlement at any time, u is the excess pore water pressure at any

time and u_0 is the initial excess pore water pressure. It was evident that the u/u_0 ratio reduced remarkably with the increase of S/S_{ult} ratio for the soft Bangkok clay.

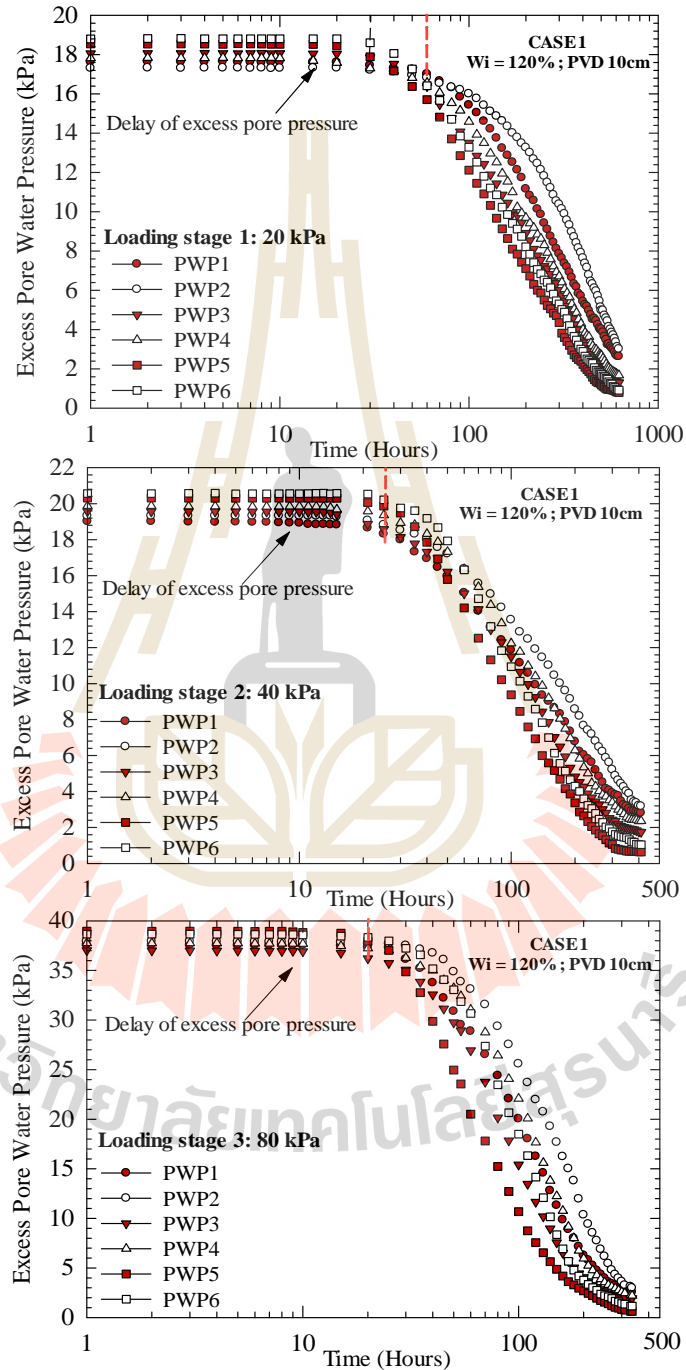


Figure 4.5 Measured excess pore water pressure versus time relationships for case 1

($W_i = 120\%$ and PVD 10 cm width)

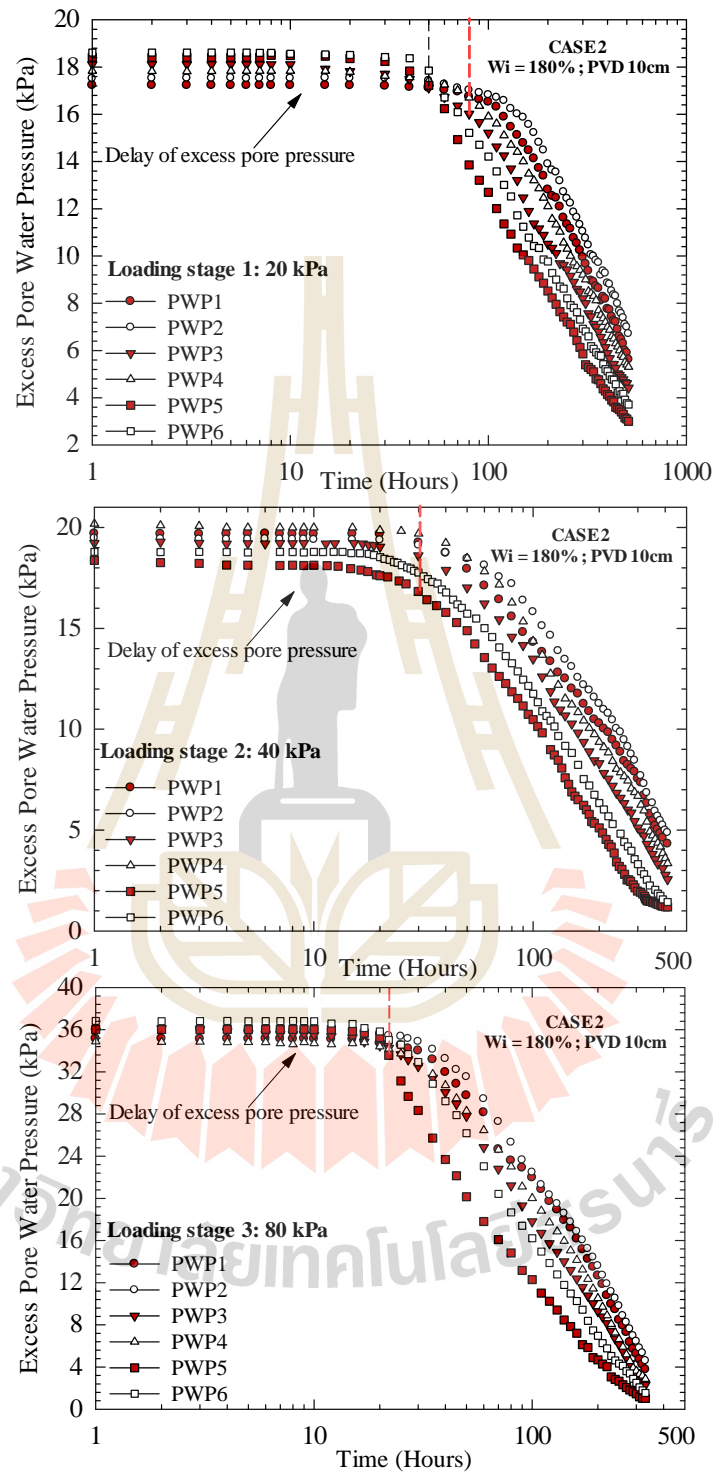


Figure 4.6 Measured excess pore water pressure versus time relationships for case 2

($W_i = 180\%$ and PVD 10 cm width)

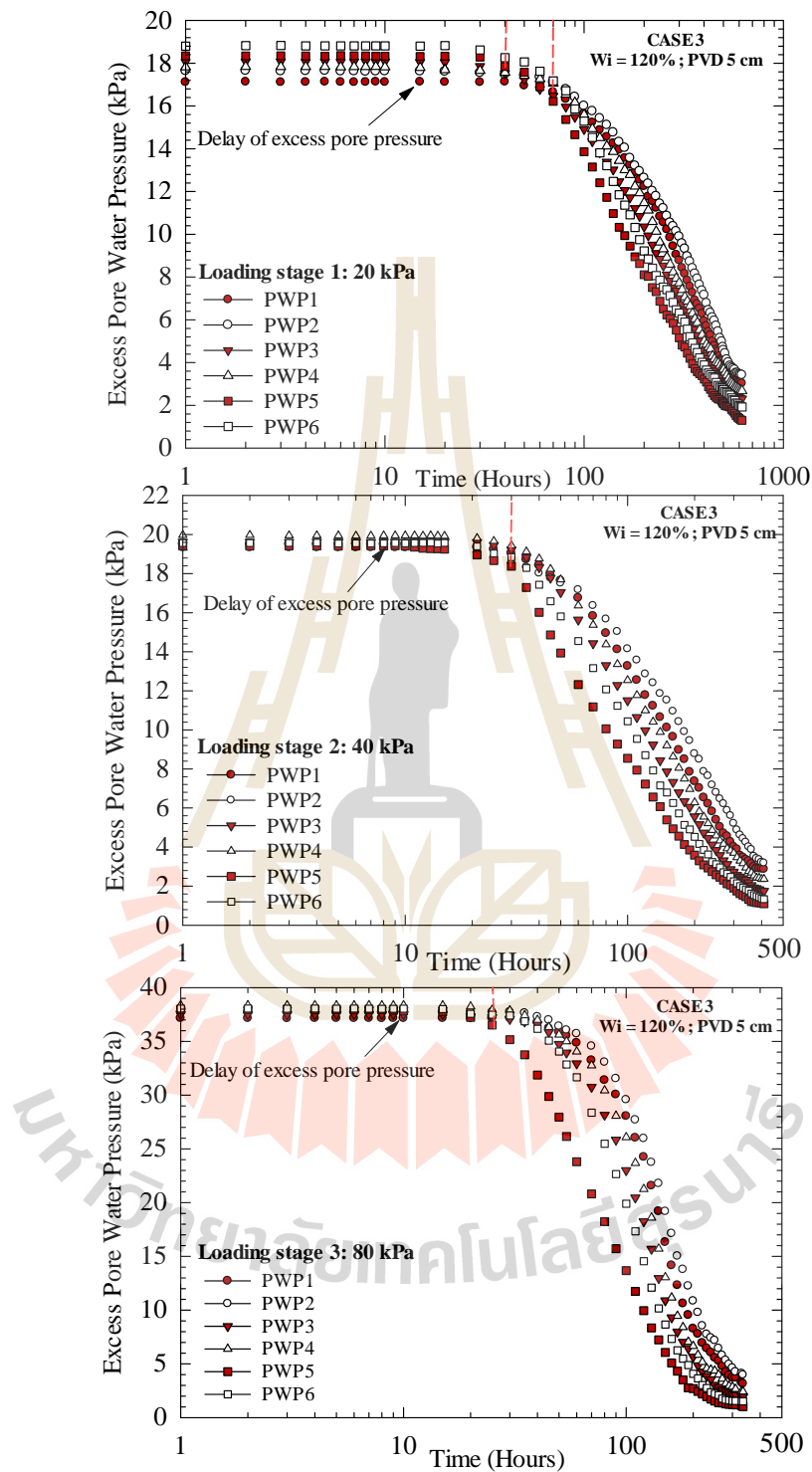


Figure 4.7 Measured excess pore water pressure versus time relationships for case 3

($W_i = 120\%$ and PVD 5 cm width)

The same trend was however not found for Mae Moh ultra-soft soil. The u/u_0 ratio was approximately constant and equal to 1 when the S/S_{ult} ratio < 0.28 . Beyond this S/S_{ult} ratio of 0.28, the u/u_0 ratio reduced significantly with increasing S/S_{ult} ratio. This delay in excess pore pressure dissipation with progressive settlement is a distinct behavior of ultra-soft clay which diverts from the behavior of natural soft clay. This similar behavior was also noticed in the previous research reported by Bo (2002), Chu et al. (2006), and Tanaka (1997).

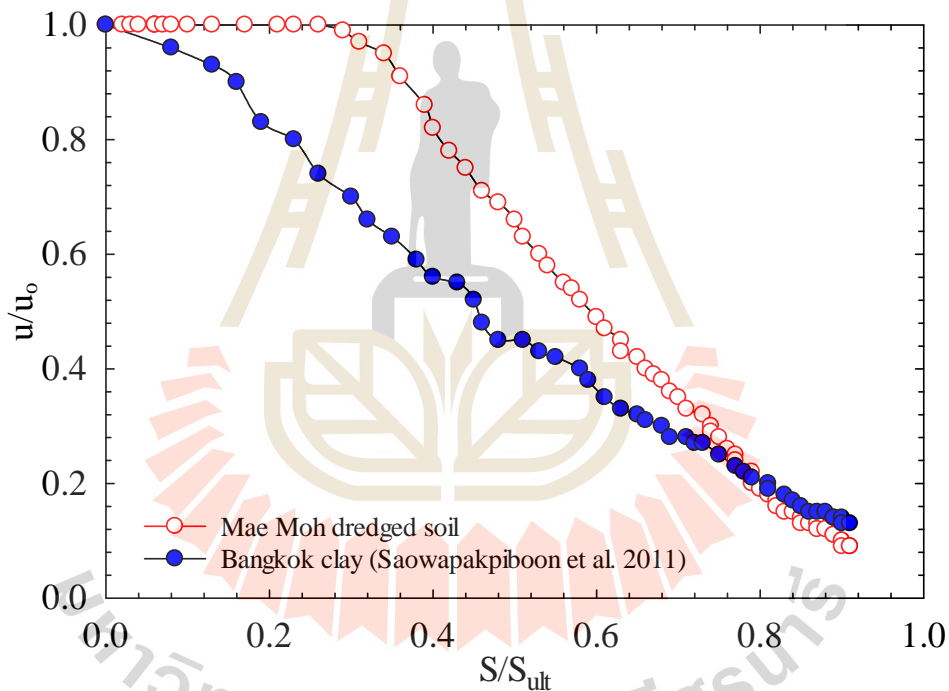


Figure 4.8 Relationships between S/S_{ult} versus u/u_0 of Mae Moh ultra-soft soil and soft Bangkok clay improved with PVD.

The effect of PVD dimension on the delay of excess pore water pressure dissipation was evident by comparing case 1 and case 3. The delayed time observed in

the top of the soil (PWP 5 and PWP6) was 30 hours for case 1, while it was 40 hours for case 3 at low vertical stress (20 kPa). At high vertical stress (80 kPa), the effect of PVD dimension on the delayed time was essentially the same (approximately the same delay times). Beyond the delayed time, the pore water pressure reduced significantly (**Figs. 4.5-4.7**). At the same depth, the excess pore water pressures close to the PVD (PPT 2, PPT 4, and PPT 6) indicated a faster rate of dissipation than the others. Because the drainage was only allowed at the top of surface of the model ground, the decrease of excess pore pressures observed from 2 PPTs at the bottom of tank (PPT 1 and PPT 2) were lower than those measured on the top of the tank.

4.3.1.3 Water content and undrained shear strength

The water contents of the ultra-soft soil, W , in all cases were measured at radial distances (r) from the center of PVD after the end of consolidation test at vertical stress of 80 kPa. The relationship between water content, W/W_i ratio, versus angle ratio, $r/360^\circ$, at different r/r_0 ratio (0.4 and 0.8), is shown in **Fig. 4.9** where W_i is the initial water content and r_0 is the radius of the tank). A significant reduction of the water content was noticed in all tested cases. The water content of the soil at the same radius (r) was found to be approximately the same. The lower water content was found for lower r/r_0 ratio of 0.4. For case 1 ($W_i = 120\%$), the final water contents varied from 42.01% to 52.66%. It was noted that the reduction of water content in case 2 ($W_i = 180\%$) was very large, which reduced by approximately 129% near the vertical drain. The effect of PVD dimension was noticed when compared the results of case 1 with case 3, the water contents in case 3 were found to be higher than those in case 1, which varied from 46.12% to 57.84%. The undrained shear strength (S_u) of the soil in the middle of the soil layer in the tank was measured by using the

mini vane shear equipment. For all total vertical stress, the undrained shear strengths in case 1 (larger PVD) were higher than those in case 3 (smaller PVD) because of higher degree of consolidation under the same vertical stress and consolidation time. The higher water contents and lower initial undrained shear strengths were observed in case 2 when compared with the results in case 1. **Fig. 4.10** shows the undrained shear strength, S_u , versus the vertical effective stress, τ'_v relationship for the three cases. The vertical effective stress (τ'_v) at the end of test of each vertical consolidation pressure was a product of the total vertical stress (τ_v) and the degree of consolidation (U) calculated using the Asaoka's observation method. It was evident that the undrained shear strength was directly related to vertical effective stress ($\Delta\tau'_v$). The S_u versus τ'_v relationship was therefore developed based on the SHANSEP equation proposed by Ladd and Foott (1974):

$$\frac{S_u}{\tau'_v} = 0.22 \quad (4.9)$$

This constant value of 0.22 was found to be similar with the proposed value for Bangkok clay by Shibuya and Hanh (2001). Although the reclamation and soil improvement processes for ultra-soft soil are more difficult and challenging than those of natural soft soils, the results from the large-consolidation test highlighted the successful performance of PVDs for improvement of ultra-soft soil. The PVDs can be used to accelerate the settlement, enhance the shear strength and decrease significantly the water content of the ultra-soft soil in pond Sump 1 C1, Mae Moh mine, Thailand.

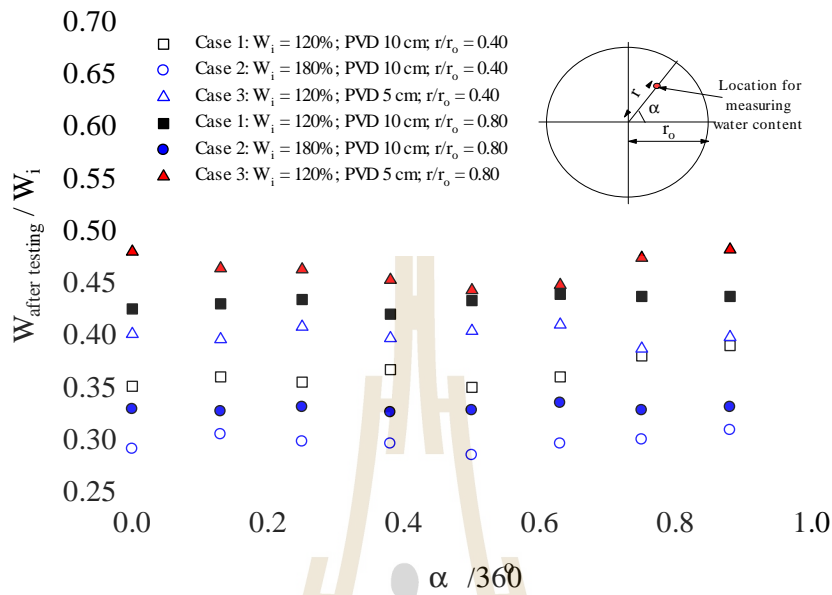


Figure 4.9 Change of water contents at various distances from PVDs in 3 cases.

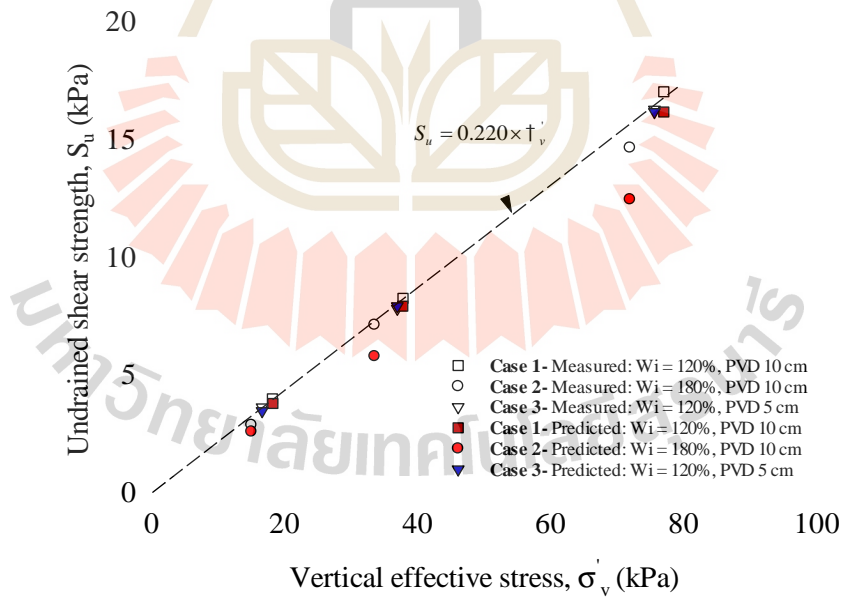


Figure 4.10 Measured and predicted undrained shear strength (in kPa) during the consolidation process

4.3.2 Numerical test results

4.3.2.1 Settlement and excess pore water pressure

Fig. 4.11 presents the comparison of measured settlement from the large consolidation tank and predicted settlement by FEM analysis using 4 different approaches for case 1. The axisymmetric analysis provided an excellent agreement with measured data in term of settlement. The measured settlement in case 1 after loading stage 3 (80 kPa) was 234.52 mm, which was only 2 mm higher than the predicted one from the axisymmetric model by means of conventional modeling method using $k_h = 2.03 \times k_v$, as shown in **Fig. 4.11**.

Fig. 4.12 shows a relationship between measured and simulated excess pore water pressures versus time in the first loading of case 1, which is similar to the other cases. The observed data from the two different pore pressure transducers (PPT 3, PPT4) were compared with the axisymmetric simulation results. The measured excess pore pressures diverted from the predicted ones due to the delay in excess pore water pressures at the early stages of loading. The prediction of excess pore water pressures by the Soft Soil model is based on the principle of effective stress (Terzaghi, 1943) in that for an incremental total stress, the reduction in excess pore water pressure is equal to the increase in effective stress, leading to the soil settlement. However, the settlement of Mae Moh ultra-soft soil occurred with minimal reduction of excess pore water pressure at the initial loading stage.

The predicted excess pore water pressure increased to reach the maximum value and then decreased rapidly in the early stages of loading while a little or no pore water pressure dissipation was observed from 2 pore pressure transducers. However, the predicted excess pore pressures agreed well with measured excess pore pressures at

the end of loading stages. To simply simulate the performance of PVD in plane-strain condition in 2D FEM analysis, 3 different approaches proposed by Chai et al. (2001), Lin et al. (2000), and Indraratna and Redana (2000) were adopted in this study. The smear effect was considered in the analysis in term of the ratio between the smear zone diameter and the equivalent drain diameter (d_s/d_w) to transform parameters from axisymmetric to plane strain conditions. The smear ratio (d_s/d_w) was taken as 1 for all cases in the plane strain model. The smear effect during the installation of PVDs was considered as small because the Mae Moh ultra-soft soil was extremely soft.

The predicted settlements obtained from the plane strain solutions were compared with measured data, as illustrated in **Fig. 4.11**. It can be seen that the predicted settlements using Chai et al.'s method were in good agreement with the measured data. The simulated settlements from Chai et al.'s method were slightly lower than the measured one in the first loading stage. The difference in predicted and measured settlements was very small in the second and last stages. Based on the comparison of plane strain model with the model test results, it is recommended that the plane strain models using Chai et al.'s method and Indraratna and Redana's method is proposed to predict the performance of PVD for reclamation of Mae Moh ultra-soft soil in the field.

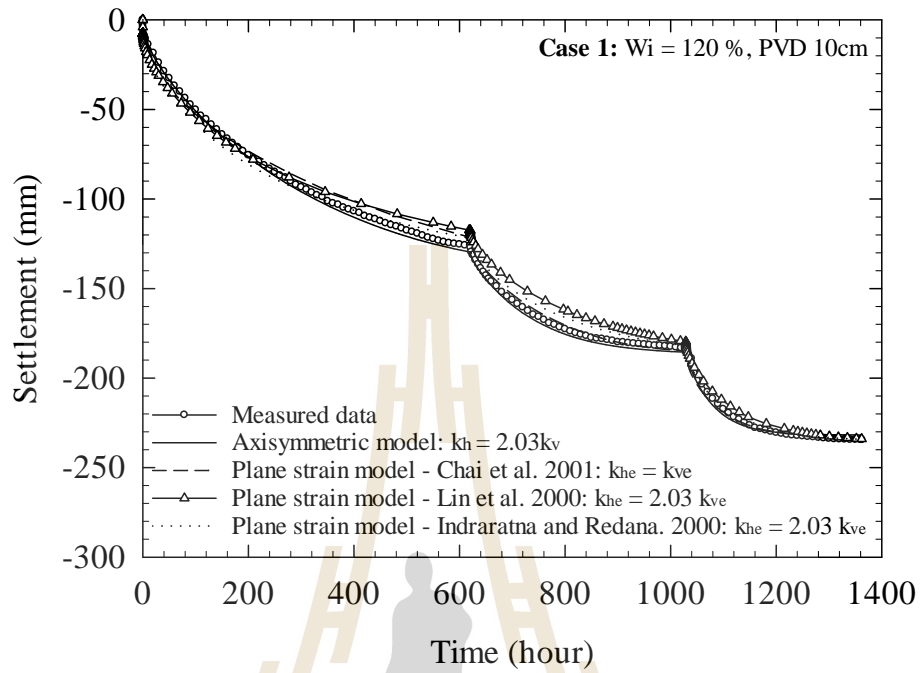


Figure 4.11 Measured and predicted settlement versus time curves in case 1

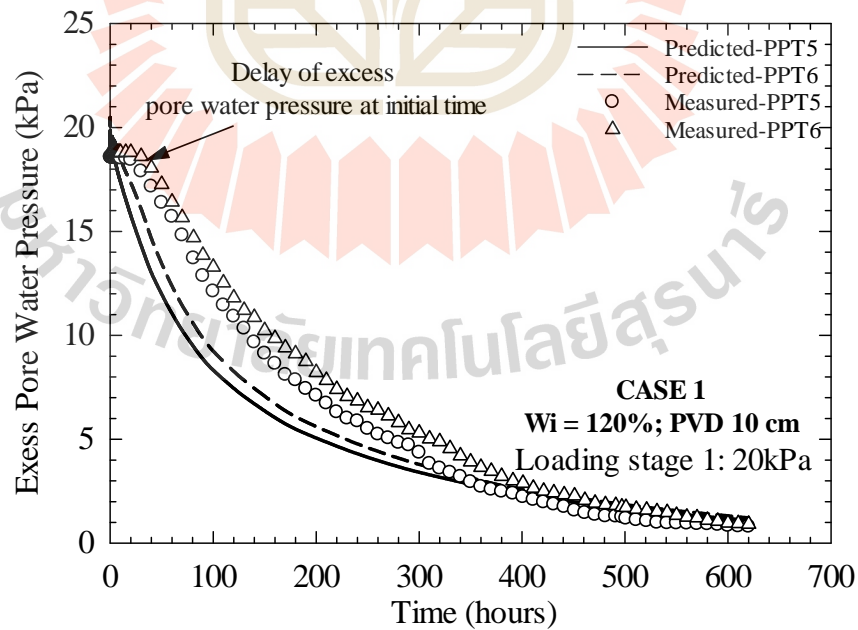


Figure 4.12 Measured and predicted excess pore water pressures in case 1

4.3.2.2 Undrained shear strength

The comparison between predicted and measured settlements of the ultra-soft soil in the consolidation apparatus provided an insight in the suitability of the soft soil model, as well as the appropriate model parameters to simulate the consolidation of the ultra-soft soil in FEM analysis. Considering a soil sample, which has been normally compressed at mean effective stress $p' = p'_o$, S_u can be predicted using the critical state soil mechanics as (Atkinson & Bransby, 1977; Wood, 1990):

$$S_u = \frac{M}{2} \exp \left[\frac{(\Gamma - v_\gamma)}{\lambda} + \ln p'_o \right] \quad (4.10)$$

$$\text{with } p'_o = \frac{1}{3} \lambda'_v (1 + 2K_0); \quad M = \frac{6 \sin \lambda'}{3 - \sin \lambda'}$$

in which M is the slope of critical state line; v_γ is the specific volume at the normal compression line with $p' = 1$; Γ is the specific volume of soil at critical state line with $p' = 1$, λ is the slope of normal compression line. K_0 varies from 0.5 to 1 as recommended by Shibuya and Hanh (2001) for Bangkok soft clay.

Eq. 10 was adopted to predict S_u of Mae Moh ultra-soft soil in the large consolidation apparatus after each loading stages. The parameters $M, v_\gamma, \Gamma, \lambda, K_0$ for the prediction of undrained shear strength of the soil in each case are presented in **Table 4.4**. The slope of the critical state line (M) and the slope of normal compression line (λ) were calculated from λ' and λ'^* . The v_γ and Γ were obtained from the undrained triaxial

compression test results. It is noted that the soil parameters for cases 1 and 3 were the same because they had the same initial water content of 120%.

Table 4.4 Soil parameter for predictions of undrained shear strength

Case No.	Water content (W_i)	Soil parameters				
		M	Γ	v_{λ}	λ	K_0
Case 1	120%	1.1565	4.111	4.279	0.2733	0.5
Case 2	180%	1.1565	5.394	5.898	0.629	0.5
Case 3	120%	1.1565	4.111	4.279	0.2733	0.5

$$* M = 6 \sin \left\{ \frac{\lambda}{3 - \sin \lambda} \right\} \times (1 + e_{int})$$

The predicted undrained shear strengths are comparable with the measured results presented in **Fig. 4.10**. It is evident that the undrained shear strength of the soil in 3 tested cases can be well predicted by using the constant soil parameter M , v_{λ} , Γ , λ . However, the simulated values were lower than the measured one, especially in case 2 with the initial water content of 180%.

4.4 Conclusion

This research studied the application of PVD for reclamation of ultra-soft soil in Mae Moh mine, Thailand. To assess the performance of PVD in the consolidation of slurry soil, a series of large-scale consolidation test was conducted at different water contents and PVD dimensions. The following conclusions can be drawn:

1. The large settlements for all cases were observed, especially for case 2 with the initial water content of 180% that exhibited the highest value after the consolidation stage of ultra-soft soil improved by PVDs. The test results indicated that the higher initial water content resulted in the higher settlement and the lower rate of

consolidation settlement. At low vertical stress where the viscosity is relatively high, the PVD dimension significantly affected the rate of consolidation settlement while at high vertical stress, the effect of PVD dimension was less.

2. The distinct behavior of Mae Moh ultra-soft soil was the delay of excess pore water pressure at the initial stage of consolidation although the settlements had taken place. The delay of excess pore water pressure reduced with the increase of consolidation pressure. The higher initial water content and the smaller of PVDs dimension resulted in the longer delay of excess pore pressure dissipation. Beyond the delayed time, the excess pore water pressures rapidly decreased with time.

3. A significant reduction of water content and increase of undrained shear strength after testing highlighted the successful performance of PVDs on the improvement of the Mae Moh ultra-soft soil. The equation for predicting undrained shear strengths at various vertical effective stress was developed based on SHANSEP's method.

4. The consolidation behavior of the PVD improved Mae Moh ultra-soft soil can be simulated by finite element method using Plaxis 2D software. The axisymmetric model produced an excellent match with measured data in term of settlement value. However, the excess pore water pressure was not well predicted using the axisymmetric model due to the delay of excess pore water pressure at the initial time of loading. The settlement of Mae Moh ultra-soft soil can be simulated satisfactorily by the plane strain models proposed by Chai et al. (2001) and Indraratna and Redana (2000). Therefore, both models are suggested for field reclamation in practice.

5. Based on the Cam Clay and Soft Soil models, the undrained shear strength (S_u) can be well predicted using the constant soil parameter $M, v_p, \Gamma, \}$. As such, the Soft Soil model together with the plane strain model by Chai et al. (2001) and Indraratna and Redana (2000) can be used to analyze both settlement and stability of reclamation of ultra-soft soil in Mae Moh mine.

4.5 References

- Almeida, M., Santa Maria, P., Martins, I., Spotti, A., Coelho, L., 2004. **Consolidation of a very soft clay with vertical drains**. In Ground and Soil Improvement Thomas Telford Publishing, 29-39.
- Arulrajah, A., Nikraz, H., Bo, M., 2004. **Factors affecting field instrumentation assessment of marine clay treated with prefabricated vertical drains**. Geotextiles and Geomembranes. 22(5), 415-437.
- Arulrajah, A., Nikraz, H., Bo, M., 2005. **Finite element modelling of marine clay deformation under reclamation fills**. Proceedings of the Institution of Civil Engineers-Ground Improvement, 9(3), 105-118.
- Asaoka, A., 1978. **Observational procedure of settlement prediction**. Soils and foundations, 18(4), 87-101.
- Atkinson, J., Bransby, P., 1977. **The mechanics of soils, an introduction to critical state soil mechanics**, 0042-3114.
- Been, K., Sills, G., 1981. **Self-weight consolidation of soft soils: an experimental and theoretical study**. Geotechnique, 31(4), 519-535.
- Blewett, J., McCarter, W., Chrisp, T., Starrs, G., 2001. **Monitoring sedimentation of a clay slurry**. Geotechnique, 51(8), 723-728.

- Bo, M., 2004. **Discharge capacity of prefabricated vertical drain and their field measurements.** *Geotextiles and Geomembranes*, 22(1-2), 37-48.
- Bo, M. 2008. **Compressibility of ultra-soft soil.** World Scientific Publishing Company.
- Bo, M., Choa, V., Wong, K., 2005. **Reclamation and soil improvement on ultra-soft soil.** *Proceedings of the Institution of Civil Engineers-Ground Improvement*, 9(1), 23-31.
- Bo, M.W., 2002. **Deformation of ultra-soft soil.** Nanyang Technological University, School of Civil & Environmental Engineering,
- Bo, M.W., Arulrajah, A., Horpibulsuk, S., Chinkulkijniwat, A., Leong, M., 2016. **Laboratory measurements of factors affecting discharge capacity of prefabricated vertical drain materials.** *Soils and foundations*, 56(1), 129-137.
- Cai, Y., Xie, Z., Wang, J., Wang, P., Geng, X., 2018. **New approach of vacuum preloading with booster prefabricated vertical drains (PVDs) to improve deep marine clay strata.** *Canadian Geotechnical Journal*, 55(10), 1359-1371.
- Cao, Y., Xu, J., Bian, X., Xu, G., 2019. **Effect of Clogging on Large Strain Consolidation with Prefabricated Vertical Drains by Vacuum Pressure.** *KSCE Journal of Civil Engineering*, 23(10), 4190-4200.
- Chai, J.C., Shen, S.L., Miura, N., Bergado, D.T., 2001. **Simple method of modeling PVD-improved subsoil.** *Journal of Geotechnical and Geoenvironmental Engineering*, 127(11), 965-972.

- Chai, J., Miura, N., Sakajo, S., 1999. **A theoretical study on smear effect around vertical drain.** International Conference on Soil Mechanics and Foundation Engineering.
- Chen, J., Shen, S.L., Yin, Z.Y., Xu, Y.S., Horpibulsuk, S., 2016. **Evaluation of effective depth of PVD improvement in soft clay deposit: a field case study.** Marine Georesources & Geotechnology, 34(5), 420-430.
- Choa, V., Bo, M., Chu, J., 2001. **Soil improvement works for Changi East reclamation project.** Proceedings of the Institution of Civil Engineers-Ground Improvement, 5(4), 141-153.
- Chu, J., Bo, M., Choa, V., 2004. **Practical considerations for using vertical drains in soil improvement projects.** Geotextiles and Geomembranes, 22(1-2), 101-117.
- Chu, J., Bo, M., Choa, V., 2006. **Improvement of ultra-soft soil using prefabricated vertical drains.** Geotextiles and Geomembranes, 24(6), 339-348.
- Chung, S., Kweon, H., Jang, W., 2014. **Observational method for field performance of prefabricated vertical drains.** Geotextiles and Geomembranes, 42(4), 405-416.
- Fang, Z., Yin, J.H., 2006. **Physical modelling of consolidation of Hong Kong marine clay with prefabricated vertical drains.** Canadian Geotechnical Journal, 43(6), 638-652.
- Geng, C., Yonghui, C., Jiangwei, S., Long, C., 2017. **Newly developed technique and analysis solution to accelerate consolidation of ultra-soft soil.** Marine Georesources & Geotechnology, 35(2), 292-299.

- Hiep, H., Chung, S., 2018. **Back-analysis of geotechnical parameters on PVD-improved ground in the Mekong Delta**. *Geotextiles and Geomembranes*, 46(4), 402-413.
- Hird, C., Pyrah, I., Russel, D., 1992. **Finite element modelling of vertical drains beneath embankments on soft ground**. *Geotechnique*, 42(3), 499-511.
- Holtz, R., 1987. **Preloading with prefabricated vertical strip drains**. *Geotextiles and Geomembranes*, 6(1-3), 109-131.
- Hong, Z., Yin, J., Cui, Y.J., 2010. **Compression behavior of reconstituted soils at high initial water contents**. *Geotechnique*, 60(9), 691-700.
- Horpibulsuk, S., Liu, M. D., Zhuang, Z., Hong, Z.S., 2016. **Complete compression curves of reconstituted clays**. *International Journal of Geomechanics*, 16(6), 06016005.
- Horpibulsuk, S., Phetchuay, C., Chinkulkijniwat, A., Cholphatsorn, A., 2013. **Strength development in silty clay stabilized with calcium carbide residue and fly ash**. *Soils and foundations*, 53(4), 477-486.
- Indraratna, B., Geng, X., Rujikiatkamjorn, C., 2010. **Review of methods of analysis for the use of vacuum preloading and vertical drains for soft clay improvement**. *Geomechanics and Geoengineering*, 5(4), 223-236.
- Indraratna, B., Redana, I., 2000. **Numerical modeling of vertical drains with smear and well resistance installed in soft clay**. *Canadian Geotechnical Journal*, 37(1), 132-145.
- Jiang, J., Liu, R., 2019. **Effect of Improvement and Application of Composite Prefabricated Vertical Drain Method in Marine Soft Ground: A Case Study**. *Advances in Civil Engineering*.

- Ladd, C. C., Foott, R., 1974. **New design procedure for stability of soft clays.** Journal of Geotechnical and Geoenvironmental Engineering, 100.
- Lin, D., Kim, H., Balasubrammaniam, A., 2000. **Numerical modeling of prefabricated vertical drain.** Geotechnical Engineering, 31(2).
- Liu, M. D., Zhuang, Z., Horpibulsuk, S., 2013. **Estimation of the compression behaviour of reconstituted clays.** Engineering Geology, 167, 84-94.
- Mesri, G., Kane, T., 2019. **Discussion of new approach of vacuum preloading with booster prefabricated vertical drains (PVDs) to improve deep marine clay strata.** Canadian Geotechnical Journal, 56(12), 2015-2016.
- Morohoshi, K., Yoshinaga, K., Miyata, M., Sasaki, I., Saitoh, H., Tokoro, M., Shikawa, M., 2010. **Design and long-term monitoring of Tokyo International Airport extension project constructed on super-soft ground.** Geotechnical and Geological Engineering, 28(3), 223-232.
- Palmeira, E. M., Gardoni, M. G., 2002. **Drainage and filtration properties of non-woven geotextiles under confinement using different experimental techniques.** Geotextiles and Geomembranes, 20(2), 97-115.
- Pham, H. T., Rühaak, W., Ngo, D. H., Nguyen, O. C., Sass, I., 2019. **Fully coupled analysis of consolidation by prefabricated vertical drains with applications of constant strain rate tests: Case studies and an open-source program.** Geotextiles and Geomembranes.
- Pham, H. T., Rühaak, W., Schulte, D., Sass, I., 2019. **Application of the Vimore–Taylor concept for fully coupled models of consolidation by prefabricated vertical drains.** Computers and Geotechnics, 116, 103201.

- Rixner, J., Kraemer, S., Smith, A., 1986. **Prefabricated vertical drains**, vol. I: engineering guidelines. Turner-Fairbank Highway Research Center.
- Saowapakpiboon, J., Bergado, D., Voottipruex, P., Lam, L., Nakakuma, K., 2011. **PVD improvement combined with surcharge and vacuum preloading including simulations**. *Geotextiles and Geomembranes*, 29(1), 74-82.
- Saowapakpiboon, J., Bergado, D., Youwai, S., Chai, J., Wanthong, P., Voottipruex, P., 2010. **Measured and predicted performance of prefabricated vertical drains (PVDs) with and without vacuum preloading**. *Geotextiles and Geomembranes*, 28(1), 1-11.
- Shibuya, S., Hanh, L., 2001. **Estimating undrained shear strength of soft clay ground improved by pre-loading with PVD: Case history in Bangkok**. *Soils and foundations*, 41(4), 95-101.
- Sills, G., 1998. **Development of structure in sedimenting soils**. *Philosophical transaction-royal society of London series a mathematical physical and engineering sciences*, 2515-2534.
- Skempton, A.W. 1953. **The colloidal activity of clays**. *Proceedings of 3rd International Conference on Soil Mechanics and Foundation Engineering*, 1, 57-61.
- Skempton, A., 1954. **The pore-pressure coefficients A and B**. *Geotechnique*, 4(4), 143-147.
- Tan, T., Yong, K., Leong, E., Lee, S., 1990. **Sedimentation of clayey slurry**. *Journal of geotechnical engineering*, 116(6), 885-898.
- Tanaka, Y., 1997. **Non-uniformly consolidated ground around a vertical drain**. Paper presented at the Proc. 30th Anniversary Symposium of Southeast Asian Geotechnical Society.

- Udomchai, A., Horpibulsuk, S., Suksiripattanapong, C., Mavong, N., Rachan, R., Arulrajah, A., 2017. **Performance of the bearing reinforcement earth wall as a retaining structure in the Mae Moh mine, Thailand.** *Geotextiles and Geomembranes*, 45(4), 350-360.
- Wood, D. M., 1990. **Soil behaviour and critical state soil mechanics:** Cambridge university press.
- Xu, G.Z., Gao, Y.F., Hong, Z.S., Ding, J.W., 2012. **Sedimentation behavior of four dredged slurries in China.** *Marine Georesources & Geotechnology*, 30(2), 143-156.
- Yonghui, C., Geng, C., Cheng, X., Qi, C., 2019. **Simple consolidation method for dredger fill treatment using plastic vertical drains with vacuum.** *Marine Georesources & Geotechnology*, 37(8), 915-923.
- Zhang, Z., Ye, G., Cai, Y., Zhang, Z., 2019. **Centrifugal and numerical modeling of stiffened deep mixed column-supported embankment with slab over soft clay.** *Canadian Geotechnical Journal*, 56(10), 1418-1432.

CHAPTER V

FULL SCALE CONSOLIDATION TEST ON ULTRA- SOFT SOIL IMPROVED BY PREFABRICATED VERTICAL DRAINS IN MAE MOH MINE, THAILAND

5.1 Introduction

Mae Moh Mine is the largest open-pit lignite mine in Southeast Asia, located in the Mae Moh district, Lampang province, Thailand. The total mining area and external dumping area of the Mae Moh mine are in the order of 38 km² and 42 km², respectively. This mine produces and supplies approximately 16 million tons of lignite annually to generate electricity in the Mae Moh power plant, which is operated by the Electricity Generating Authority of Thailand (EGAT) (Udomchai et al., 2017). The Mae Moh power plant has a production capacity of 24000 Megawatt, and currently supplies 50% of the electricity to the northern area, 30% to the central area, and 20% to the north-eastern area of Thailand. Sump1 C1, a slurry pond with a total area of 80000 m² located in the north of the Mae Moh mine, is the main water source for mining activities, e.g., mineral processing and dust suppression. According to the Mae Moh mine planning and development of EGAT, this mine will become the deepest open pit lignite mine in the world with an excavation depth of approximately 500 m from original surface in the next 40 years (Ngo et al., 2020a, b). Sump1 C1 will be dumped with a very high overburden material of approximately 300 m transferred from the mining areas within 2038. However, Sump1 C1 contains

approximately 40 m thickness of an ultra-soft soil deposit, which has very high water content of greater than liquid limit. The in-situ strength of ultra-soft soil are extremely low. The dumping activity in Sump1 C1 which is planned for the future is becoming a challenging issue for EGAT. Therefore, it is absolutely crucial to improve the ultra-soft soil deposit before dumping activity in order to prevent any failure, which might causes detrimental effects on the mining activities.

The prefabricated vertical drains (PVDs) with preloading technique, was recommended by the Geotechnical Engineering Department, Mae Moh mine for the improvement of the ultra-soft soil deposit in Sump1 C1, particularly for its effectiveness from economical and environmental perspectives. PVDs are increasingly being used to accelerate the consolidation process of soft soil deposits such as marine clay (Bergado et al., 2003; Bo et al., 2014; Chu et al., 2004) and ultra-soft soil (Arulrajah et a., 2004; Bo, 2004; Chen et al., 2016; Chu et al., 2006; Geng et al., 2017) in various land reclamation project. The consolidation of ultra-soft soil improved with PVDs has been studied in laboratory by several researchers (Arulrajah et al., 2004; Bo et al., 2016; Chu et al., 2004; Fang & Yin, 2006; Ngo et al., 2020a). The performance of PVDs in ultra-soft soil was affected by several factors, e.g., selected filter, and discharge capacity and deformation of PVDs under the loading condition (Bo et al., 2016; Chu et al., 2006; Ngo et al., 2020a). Ngo et al. 2020a conducted a series of large-scale model tests to investigate the effectiveness of using PVD for the improvement of Mae Moh ultra-soft soil at different water contents and PVD dimensions. The laboratory test results indicated that PVDs accelerated settlement, enhanced shear strength, and reduced water content of the ultra-soft soil tested for all various conditions (water contents and PVD dimensions) tested. Ngo et

al. 2020a also reported that the distinct behavior of Mae Moh ultra-soft soil was the delay of excess pore water pressure dissipation at the initial stage of consolidation although the large settlement had taken place. This finding is similar to that previously reported by Chu et al. (2006) for ultra-soft soil in Changi East reclamation project, Singapore. Besides the laboratory test, the field performance of PVD improved ultra-soft soil was also studied (Arulrajah et al., 2004; Bo, 2008; Chu et al., 2006). The reclamation and soil improvement processes on ultra-soft soil are more difficult and challenging than those on natural soft soil due to very low bearing capacity of ultra-soft soil foundation (Bo, 2008; Chu et al., 2006). A special sand-spreading method was used to construct a platform on a slurry pond in Changi East reclamation project, Singapore (Chu et al., 2006). The sand with a high water content was pumped through the pipelines and deposited on the slurry (Chu et al., 2006). However, a failure was occurred in the first phase of spreading sand due to the non-uniform thickness of sand layer and hence differential settlements (Bo, 2008; Chu et al., 2006). The PVDs were installed in two rounds to minimize the folding effect of PVD on drainage capacity. The field monitoring data indicated that large deformation was occurred with a little pore pressure dissipation in the initial stage of loading (Chu et al., 2006).

The Center of Excellence in Innovation for Sustainable Infrastructure Development of Suranaree University of Technology, Thailand was engaged by the Mae Moh mine of EGAT to undertake a full-scale test on PVD improved ultra-soft soil at a trial slurry pond prior to the PVD construction in Sump1 C1. This full-scale study is a continuation of previous laboratory model study (Ngo et al., 2020a) on the consolidation of PVD improved ultra-soft soil. The successful construction with field

measurement will be a lesson learned for a real construction project on the improvement of ultra-soft soil in Sump1 C1. The outcome of this field study will result in an effective design method for the reclamation of Sump1 C1 in Mae Moh mine and other similar reclamation works.

5.2 Site condition and material used

5.2.1 Full-scale test site

To investigate the effectiveness of PVD on the improvement of ultra-soft soil, a full trial was conducted at a trial slurry pond, which is located near Sump1 C1 in the north of Mae Moh mine, Thailand. The location of the trial slurry pond is shown in **Fig. 5.1**. The trial slurry pond with dimensions of 30 x 30 m at the top and 22 x 22 m at the bottom was prepared by excavating and blasting the claystone layer up to a depth of 8 m from the existing ground. The thickness of the claystone layer was between 60 to 200 m. The unconfined compressive strength of claystone was very high of approximately 4.2 MPa. The unit weight and the water content of claystone were 22.5 kN/m³ and 21.5%, respectively. The properties of claystone is summarized in **Table 5.1**. The preparation of the trial pond commenced in May, 2018 and was completed in June, 2018.



Figure 5.1: Location of full-scale test site in the field

5.2.2 Ultra-soft soil

After preparation of the trial slurry pond, the ultra-soft soil was transferred from Sump1 C1 to the trial slurry pond through a 400-mm diameter pipeline using a high-pressure pump, as shown in **Fig. 5.1**, which commenced on 16 August 2018. The initial water content of the slurry was higher than 200%. The transfer of slurry from Sump1 C1 to the trial pond took two weeks. After that, the slurry was allowed to settle. The compressibility of Mae Moh ultra-soft soil without PVDs is composed of the sedimentation and consolidation phases, which was discussed previously by Ngo et al. (2020b). Ngo et al. (2020b) revealed that the sedimentation process of ultra-soft soil was divided into the flocculation and settling stages. The flocculation occurred at the early stage of sedimentation process with a small change in soil-fluid interface, while the settling stage caused the significant change in soil-fluid interface, leading to the reduction of water content. In late April 2019, the water above the ultra-soft soil deposit was pumped out of the pond by using a small pump every day prior to the construction of sand platform. The thickness and

water content of ultra-soft soil deposit in the pond was approximately 4.5 m and 163%, respectively. The ultra-soft soil in the pond contained 1% sand, 58% silt and 41% clay. The liquid limit and the plastic limit were 57% and 26%, respectively. The specific gravity was 2.5. The undrained shear strength, S_u was extremely low of < 1.0 kPa. The effective strength parameters obtained from the triaxial drained test was $c' = 0$ and $w' = 29$ degrees and the compression index, C_c , was 1.10. The properties of the ultra-soft soil are summarized in **Table 5.1**.

Table 5.1 Properties of ultra-soft soil and clay stone

	Unit	Water	Liquid	Plastic	Cohesion	Friction	C_c	S_u
Soil layer	weight (kN/m ³)	content (%)	limit, LL, (%)	limit PL, (%)		angle		(kPa)
Ultra-soft soil	16	163	57	26	$c' = 0$	$w' = 29$	1.1	< 1
Claystone	22.5	21.5	50.6	27.5	NA	NA	NA	2100

5.2.3 Selection of prefabricated vertical drains

During the consolidation process, very fine particles of the ultra-soft soil might enter into the core and filter of PVDs and hence reducing the discharge capacity. Therefore, the selection of PVDs play a significant role on the consolidation process of ultra-soft soil. The selection of PVDs for Mae Moh ultra-soft soil was discussed previously (Ngo et al., 2020a) by considering apparent opening size of filter, O_{95} , and permittivity of PVD's filter. To prevent the clogging effect, the apparent opening size of the filter was recommended to be (Ngo et al. 2020a):

$$O_{95} = 4.71 \times D_{85} \quad (5.1)$$

in which D_{85} refers to the size for 85% of passing of soil particles by weight. In this study, the PVD AD250 type from Tecate Geosynthetics (Thailand), Co. Ltd. with 100 mm in width and 5 mm thick was chosen. It consisted of a permeable drainage core surrounded by a robust filter jacket. The O_{95} was smaller than 0.08 mm. The permeability of the PVD filter was 1.8×10^{-4} m/s. The discharge capacity of the PVD core was 150×10^{-6} m³/s and 110×10^{-6} m³/s in the straight condition and kinked condition under a confining pressure of 250 kPa, respectively. The characteristics of PVD are summarized in **Table 5.2**.

Table 5.2 Characteristics of PVD

Thickness (cm)	Width (cm)	Permeability of the filter (m/s)	Discharge capacity (m ³ /s)		Apparent opening size, O_{95} (mm)
			Straight condition	Kinked condition	
10	0.5	1.8×10^{-4}	150×10^{-6}	110×10^{-6}	0.08

5.3 Factor of safety analysis for construction process

Finite element (FE) modelling using PLAXIS 2D program was carried out to evaluate the stability of full-scale test site during construction of sand platform, sand blanket, and three loading stages. The geometry condition of full-scale test is shown in **Fig. 5.2**. The material parameters of the soil are summarized in **Table 5.3**. To consider the critical condition during the construction stage, the Moh-Coulomb model

with the undrained shear strength of the ultra-soft soil of 1.4 kPa was used to simulate in this study.

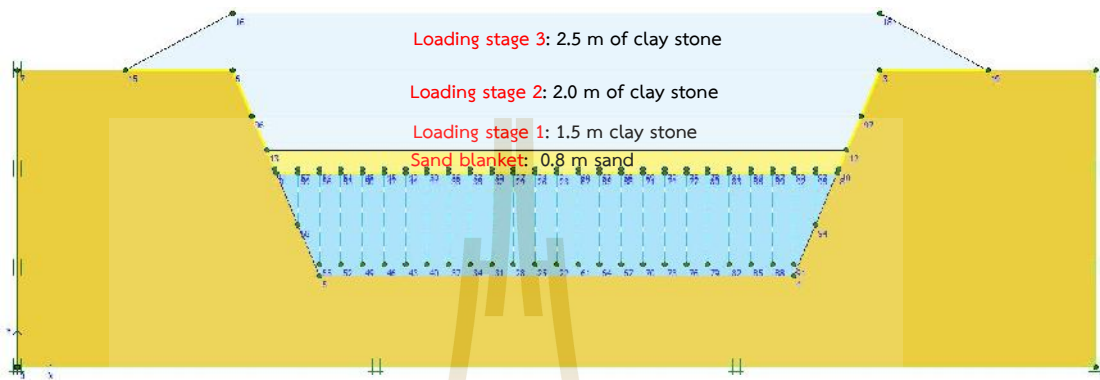


Figure 5.2 Geometry model

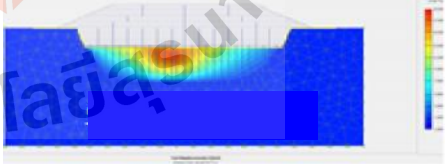
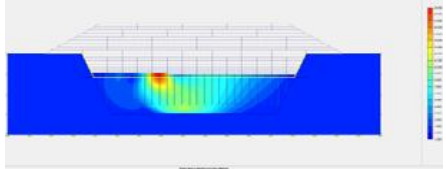
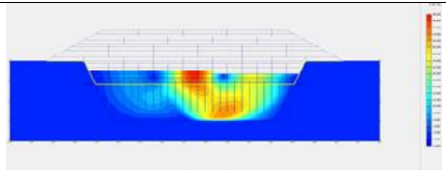
Table 5.3 Soil material properties for finite element analysis.

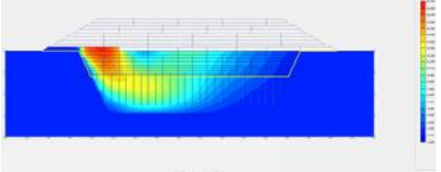
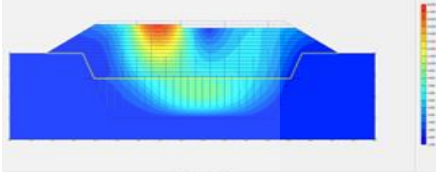
Parameter	Soft soil	Sand fill	Claystone (Existing ground)	Claystone (excavated soil)
Material model	Mohr- coulomb	Mohr- coulomb	Mohr- coulomb	Mohr- coulomb
Type of behavior	Undrained	Drained	Undrained	Undrained
γ_{unsat} (kN/m ³)	16	20	17	17
γ_{sat} (kN/m ³)	18	20	19	19
Young's modulus	500	4000	2.5×10^6	50 000
Poisson's ratio	0.35	0.33	0.25	0.33
Cohesion, c (kPa)	$S_u = 1.4$	3	500	50
Friction Angle,	-	30	33.5	30

Parameter	Soft soil	Sand fill	Claystone	Claystone
			(Existing ground)	(excavated soil)
K_x (m/day)	-	1	-	-
K_y (m/day)	-	1	-	-

The minimum factor of safety for construction of sand platform, sand blanket and the three loading stages is summarized in Table 5.4. The FEM results show that the minimum factor of safety (FS) of each construction stage (sand platform, sand blanket, loading stage 1, loading stage 2, loading stage 3) are greater than the required design FS = 1.5, commonly used by the geotechnical engineers and researchers. This demonstrates that the construction of full-scale test has a high stability.

Table 5.4. Minimum factor of safety during construction process.

Construction stages	Minimum Factor of Safety	Total displacement
Sand Platform	1.985	
Sand Blanket	1.610	
Loading stage 1	1.533	

Construction stages	Minimum Factor of Safety	Total displacement
Loading stage 2	2.07	
Loading stage 3	1.55	

5.4 Construction of field trial

5.4.1 Construction of platform

Since the S_u of the ultra-soft soil was extremely low, the construction of the platform in the trial pond was impossible without ground improvement. The non-uniform thickness of spreading sand may cause the shear failure on the ultra-soft soil foundation even with low overburden sand fill (Bo, 2008; Chu et al., 2006). The sand layer might then progressively sink into the underlying ultra-soft soil. In this research, the geotextile was applied to enhance the bearing capacity of ultra-soft soil prior to the construction of sand platform. The role of geotextile on improving the short-term bearing capacity of soft clay foundation was successfully reported by Rashid et al. (2019). It was designed to place a seamed geotextile on the ultra-soft soil surface and the surrounding areas with a dimension of 40 x 40 m. The stitch between geotextiles was done by sewing them with high strength threads. The geotextiles type polyfelt TS 70 were selected and the construction was performed during 3 to 10 May 2019. The geotextiles were bonded continuous-filament nonwovens manufactured

from UV-stabilized polypropylene. Each sheet of geotextile was 4 m wide and 40 m long per roll. The opening size, O_{90} , and the mass per unit area of the geotextile were 0.09 mm and 325g/m^2 , respectively. The geotextile properties are summarized in **Table 5.5**. Three sheets of geotextile were sewn together using a portable sewing machine. The overlapping between two geotextile sheets was 2 m as shown in **Fig. 5.3**. The total width and weight of a single seamed sheet (composed of 3 geotextile sheets) were about 6 m and 156 kg, respectively. The first seamed geotextile sheet was laid slowly to the trial pond by 10 labors in 2 sides of the pond, as presented **Fig. 5.3**.

Table 5.5 Characteristic of geotextile.

Type	Mass / Unit area of filter (g/m^2)	Thickness (mm)	Opening size of filter, O_{90} (mm)	Tensile strength (kN/m)	Elongation (%)
Polyfelt	325	2.9	0.09	25	46

The other seamed geotextile sheets were subsequently installed in the trial pond in the same manner as the previous one. In total, eight seamed geotextile sheets (6 m in width/seamed sheet) were sewn together in the pond, with the overlapping width between 2 seamed geotextile sheets of 1.5 m. It took seven days to complete the sewing and the placement of the eight-seamed geotextile sheets in the trial pond. To enhance the bearing capacity, 12 rubber balloons were sewn with the geotextile sheets (**Fig. 5.3**). Both sides of the geotextiles were embedded in a 0.2 m thick sand on the

ground surface (top of the pond) to prevent slippage of geotextile during the sand filling.

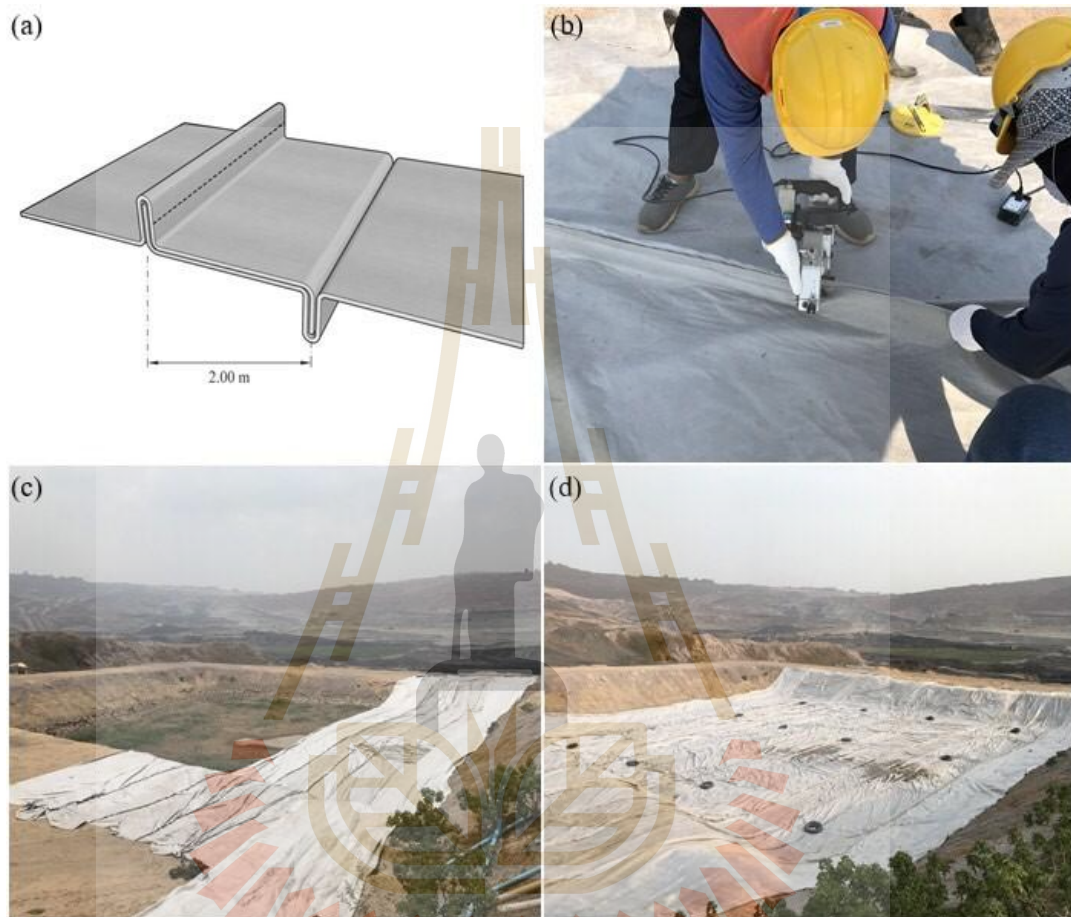


Figure 5.3 Stitches of the geotextile sheets (a) Concept of sewing geotextile; (b) Sewing geotextile at the site; (c) Installing a connected geotextile in the pond; (d) Completion of connected geotextile installation in the pond.

After completion of the geotextile installation, the construction of platform commenced on 11 May 2019. The thickness of sand platform was 0.2 m. The sand platform was constructed using a crane transferring the sand to the pond. Then, labors standing on the geotextile spread the transferred sand from one side to other side of

the pond. The detail construction procedure of sand platform is presented in **Fig. 5.4**.

The construction of platform was completed on 13 May 2019.



Figure 5.4 Construction procedure for platform

The sand on both sides of geotextile sheets and the rubber balloons were removed after completion of platform without any track of failure. Due to heavy rain and typhoon, the PVD installation was postponed to 15 July 2019. During the rainy season, the rain water above the sand platform was pumped out of the trial pond regularly by using a hydraulic pump machine.

5.4.2 Installation of PVD

The PVDs installation commenced from 16 July 2019. A 15-mm diameter steel rod connected with a steel tip shoe at the toe was made and used to install the PVDs, instead of using a conventional mandrel. Because S_u of ultra-soft soil was very low, the steel rod with PVDs could be penetrated easily through the predetermined holes in the geotextiles. When the steel rod reached the desired length, it was slowly withdrawn from the soil. The PVDs were installed to a depth of 4 m in a square pattern with 1 m center to center spacing, which was commonly designed in land reclamation project (Arulrajah et al., 2004; Bo, 2008; Chu et al., 2006). It was observed that a small amount of ultra-soft soil was squeezed out from the hole during the installation of PVDs. This indicated that the excess pore water pressures due to the loading of the sand platform were not fully dissipated during two months of consolidation. **Fig. 5.5** shows a photo of the trial pond after the completion of installation of PVDs on 3 August 2019.



Figure 5.5: Completion of PVDs installation on 3 August 2019

5.4.3 Installation of drainage system and sand blanket

After two months of consolidation with PVDs and preloading under the vertical load of approximately 4 kPa (0.2 m thick sand platform), the first 0.2 m sand blanket was constructed and a drainage system was then built. 65-mm diameter Neodrain pipes made from a high density polyethylene and reinforced with hollow strand ribs were used to collect water from the sand layer. The Neodrain pipes can resist an axial load of 150 kPa with a strain < 8%. The pipes were wrapped with geotextiles to prevent the sand clogging into the drainage channel, as shown in **Fig. 5.6.**



Figure 5.6 Installation of Neodrain pipes on 30 September 2019: (a) Step 1: Installing Neodrain pipes; (b) Step 2: Preparing geotextile to wrap the pipes; (c) Step 3: Wrapping the pipes by using geotextile; (d) Step 4: Connecting the pipes with the tanks

The Neodrain pipes were connected with two tanks at the center of the pond. The tanks had diameter of 0.6 m and were made of steel with all-round reinforced steel bars to prevent buckling due to the backfill loading. The installation of drainage system was started on 28 September 2019 and completed on 30 September 2019. The collected water was pumped out of the pond during the consolidation of the ultra-soft soil regularly (**Fig. 5.6**). Additional sand blanket of 0.6 m was filled to have a total thickness of sand platform and sand blanket of 1.0 m.

5.4.4 Loading stages

The step loading after the completion of sand blanket was divided into 3 stages: loading stage 1 (1.5 m height), loading stage 2 (2.0 m height) and loading stage 3 (2.5 m height). The total height of fill was 6 m. Abundant claystone in the Mae Moh mine was used as a fill for the three loading stages. A loading period for each loading was allowed until the degree of consolidation was more than 90%. The degree of consolidation and the final settlement were determined based on the Asaoka's observational method (Asaoka, 1978). The consolidation times were 73 days, 53 days, 36 days, and 30 days for sand blanket, loading stage 1, stage 2, and stage 3, respectively. The loading stage versus time is presented in **Fig. 5.7**. A 10-ton bulldozer was used for loading stage 2 and stage 3 without bearing failure as S_u was gained enough after the loading stage 1. During the consolidation in all loading stages, the water from the ultra-soft soil through the water tanks was pumped out regularly. Photos of the trial pond after construction of each loading stage is shown in **Fig. 5.8**.

In total, 9 settlement plates (SP01 to SP09) and 3 piezometers were installed in the trial pond to monitor the consolidation behavior of ultra-soft soil. A settlement plate (SP05) was installed at the center of the pond and the others were at the edges to measure differential surface settlements. The piezometers (PZ01, PZ02, PZ03) were installed at different depths of 1 m, 2.5 m, and 4 m at the center of the pond, respectively. To investigate the effectiveness of PVDs on the shear strength improvement, the undrained shear strengths were measured with a field vane shear apparatus for each loading stage. The plan and section views of the trial pond with full instrumentations are presented in **Fig. 5.9**.

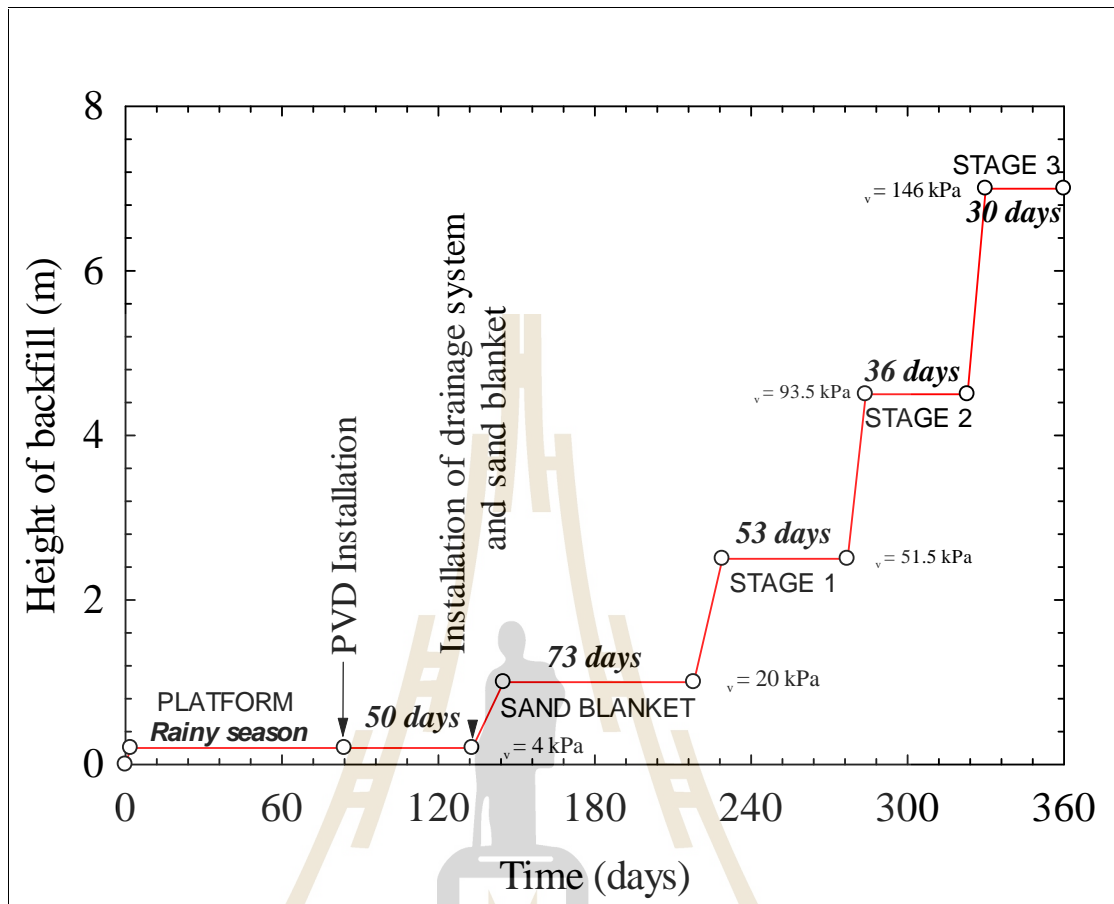


Figure 5.7 Loading stage with time



Figure 5.8 Photos of trial pond after finishing construction of each loading stage: (a) Sand blanket; (b) Loading stage 1: 1.0 m clay stone; (c) Loading stage 2: 1.5m clay stone; (d) Loading stage 3: 2.5 m claystone.

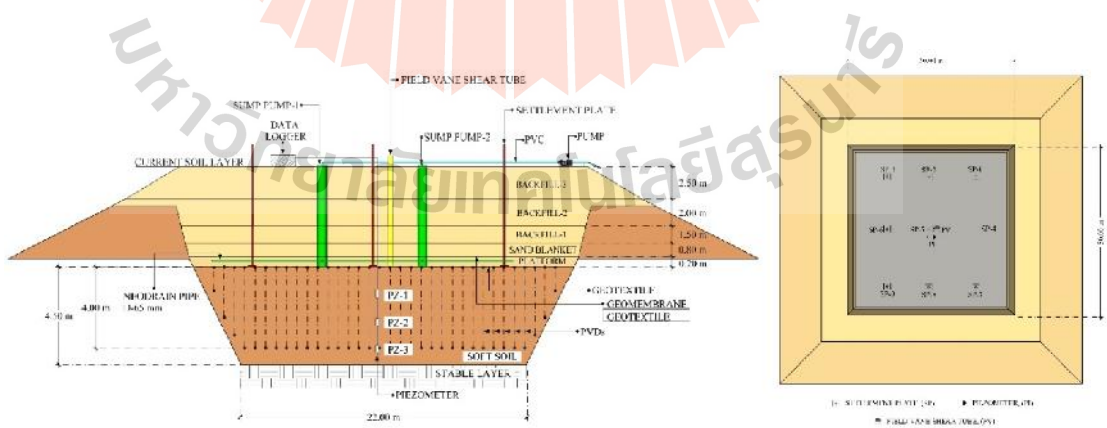


Figure 5.9 Plan and top views of full-scale test pond

5.5 Field test results and discussion

5.5.1 Settlement

The relationship between the settlement versus consolidation time at three selected settlement plates, which were located at the center (SP5) and the edges (SP2 and SP8) of the pond, is shown in **Fig. 5.10**. The record from settlement plates was started after the PVDs installation because the settlement plates could not be installed after finishing construction of platform due to a very heavy rain and typhoon in the rainy season. The settlement before installation of settlement plates was measured using a survey levelling and was approximately 30 mm. With PVDs, the ultra-soft soil underwent rapid settlement and reached 89.93% degree of consolidation (based on the observational Asaoka's method) after 50 days of PVD installation (**Fig. 5.10** and **Fig. 5.11**). The settlement at SP5 was 87 mm, which was higher than that without PVD. **Fig. 5.10** indicates that the final settlement due to the 0.8 m sand blanket (16 kPa) was the highest, followed by the final settlements due to loading stage 1 (1.5 m claystone), stage 2 (2.0 m claystone) and stage 3 (2.5 m claystone). The decrease in settlement even with the increase in consolidation stress is due to non-linear compression behavior of the ultra-soft soil (Fang & Yin, 2006; Hong et al., 2010; Horpibulsuk et al., 2016; Ngo et al., 2020a,b).

The measured settlement at the center of the pond (SP5) was slightly higher than that at the edges of the pond (SP2 and SP8) at the end of the sand blanket installation and loading stage 1. For instance, the settlement at SP5 was 0.37 m, while the settlement at SP2 was 0.35 m at the end of sand blanket installation. However, the measured settlement at SP5, was significantly higher than that at SP2 and SP8 in the loading stages 2 and 3. The measured settlement at SP5, SP2, and SP8 after 360 days

of testing were approximately 1.10 m, 1.01 m, and 1.07 m, respectively. This indicated that the large differential settlements happened at high consolidation stresses. A large vertical strain of approximately 24.44 % was recorded after loading stage 3. The predicted final settlement (S_f) and the degree of consolidation (U_s %) using the Asaoka's observational method (Asaoka, 1978) at the end of each loading stage for SP5 are shown in **Fig. 5.11**. The time interval, t , used for the calculation was four days. **Fig. 5.11** shows that the settlements achieved $U_s > 90\%$ for all loading stages, being 96.57%, 95.70%, 91.19%, and 96.50% for the sand blanket installation and loading stage 1, stage 2, stage 3, respectively.

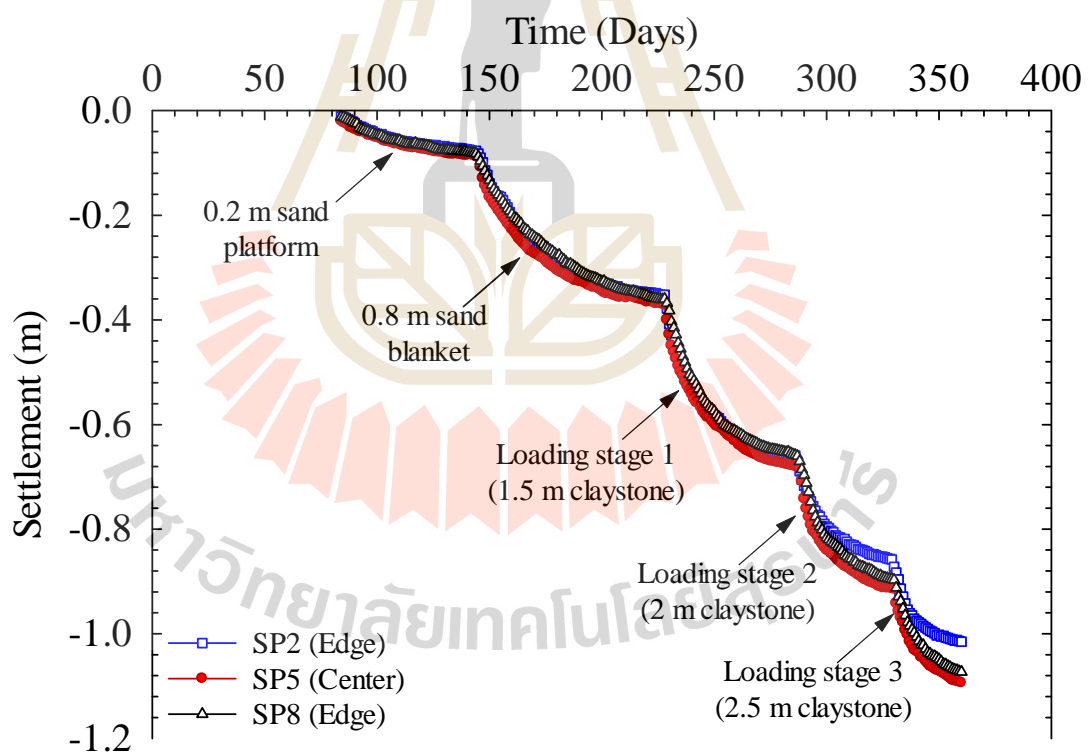


Figure 5.10 Settlement versus time curves obtained from 3 settlement plates

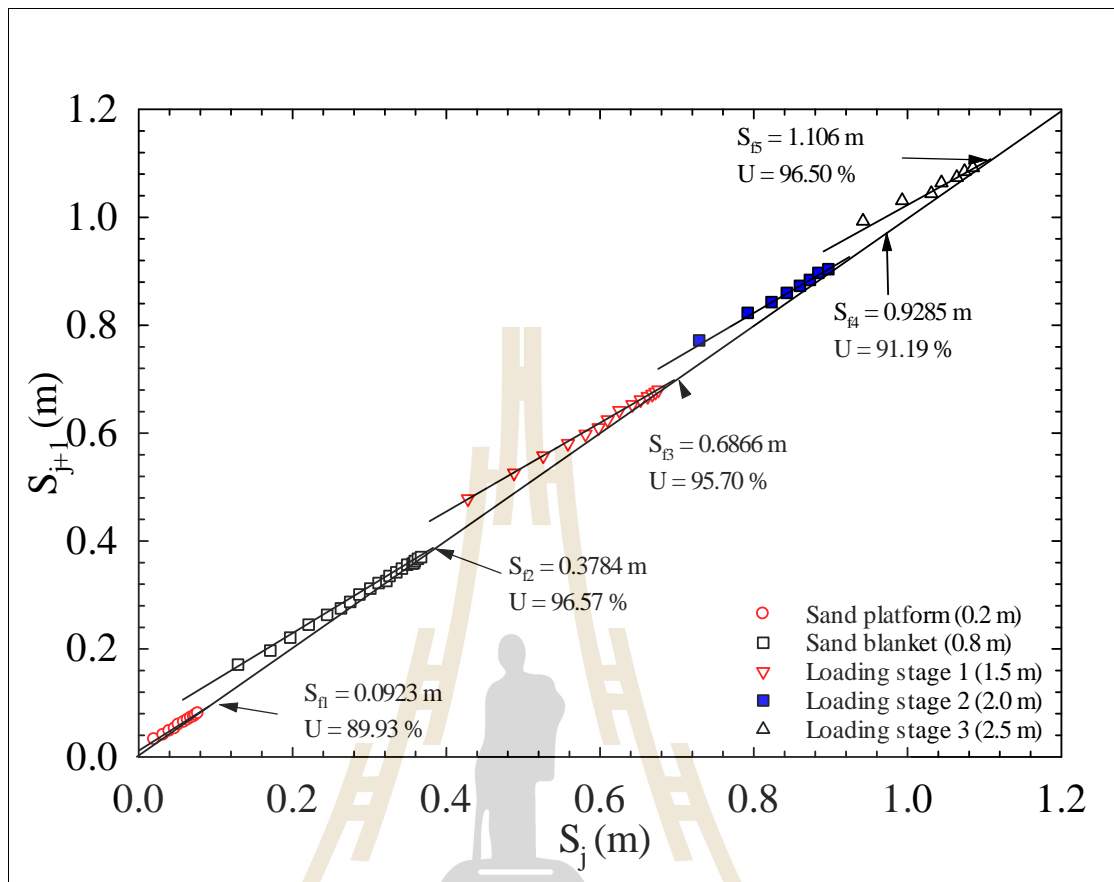


Figure 5.11 Final settlements of each loading stage predicted by using Asaoka's observational method.

5.5.2 Excess pore water pressure

The measured excess pore water pressure versus consolidation time curves at the center of trial pond and at three different depths of 1 m, 2.5 m, and 4 m (PZ01, PZ02, and PZ03) are shown in **Fig. 5.12**. Since the piezometers were installed after the installation of PVDs, the pore water pressure during the first 83 days was not recorded. A quick increase in excess pore water pressure was observed immediately after filling for all loadings. However, the increase of excess pore water pressure in each loading stage was slightly lower than the increased total vertical stress, which

was equal to the product of the thickness of backfill and its unit weight. The difference between the excess pore water pressure and the increased total vertical stress can be explained by using Equation (Skempton, 1954) as follows:

$$\Delta u = B[\Delta \sigma_3 + A(\Delta \sigma_1 - \Delta \sigma_3)] \quad (5.2)$$

in which $\Delta \sigma_1$ and $\Delta \sigma_3$ are the principal stresses; A and B are pore pressure coefficients. The B value can be taken as 1 for saturated soil and the A value varies with stresses and strains (Fang & Yin, 2006; Ngo et al., 2020a; Skempton, 1954). This similar behavior was also reported in laboratory model tests by Ngo et al. (2020a) for Mae Moh ultra-soft soil, and Fang and Yin (2006) for Hong Kong marine clay.

Similar to the laboratory model test results reported by Ngo et al. (2020a), the delay in excess pore water pressure dissipation (PZ01, PZ02, PZ03) was observed in the early loading stages, despite the ultra-soft soil underwent large settlements. For instance, the settlement after 14 days of 0.8-m sand blanket installation was 0.2270 m (**Fig. 5.10**), resulting in $U_s = 59.73\%$, while $u/u_0 = 97.32\%$, 98.4%, 98.53% at depths of 1 m, 2.5 m, and 4 m where u is the excess pore pressure at any depth and time and u_0 is the initial excess pore pressure (**Fig. 5.12**). These high u/u_0 values indicated the very slow dissipation of excess pore water pressure. The delay of excess pore water pressure dissipation was observed in all the loading stages and the delayed time, defined as the transitional time separating slow and fast excess pore water pressure dissipation, decreased with increasing vertical consolidation stress, which is also reported by Ngo et al. (2020a) in laboratory model test. The delayed time observed in PZ02 was 14 days, 12 days, 8 days, and 6 days for the sand blanket installation and

loading stage 1, stage 2, and stage 3, respectively (**Fig. 5.12**). The excess pore water pressure recorded at PZ02 and PZ03 (2.5 m and 4 m) was slightly higher than that at PZ01 (1 m) due to different drainage conditions. The PZ01 was closer to the sand blanket.

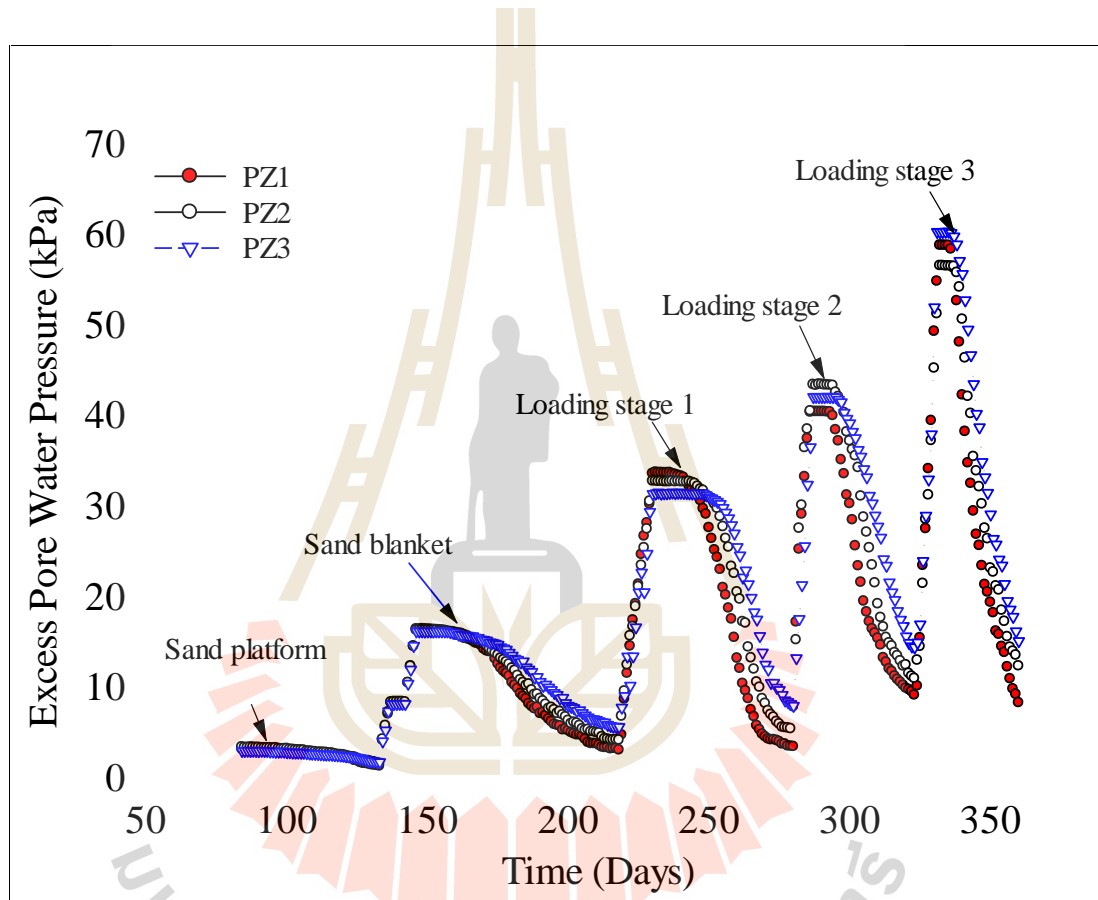


Figure 5.12 Measured excess pore water pressure versus time relationships

The dissipation of excess pore water pressure of PVD improved Mae Moh ultra-soft soil from both field (present work) and laboratory (Ngo et al. 2020a) studies was compared with that of PVD improved Bangkok soft clay from laboratory study (Saowapakpiboon et al., 2010). **Fig. 5.13** shows the relationship between $U_s (S/S_f)$ and

u/u_0 , where S is the settlement at any time. The data of excess pore water pressure at the middle of the soil layer were taken for the calculation of u/u_0 for both Mae Moh ultra-soft soil and soft Bangkok clay. For soft Bangkok clay, the u/u_0 ratios reduced significantly with the increase of S/S_f ratio, which is different from Mae Moh ultra-soft soil. The u/u_0 ratios were remained constant at 1.0 when the S/S_f ratios < 0.28 and 0.32 for the laboratory and field test results, respectively. When the S/S_f ratios > 0.28 and 0.32 , the u/u_0 ratios decreased significantly with the increase of S/S_f . The delay of excess pore water pressure dissipation with the occurrence of settlement is a distinct behavior of ultra-soft soils, which differs from that of natural soft clays. It is also noted that the delay of excess pore water pressure dissipation in the field study was longer than that in the laboratory study even at the same consolidation stress of 20 kPa, possibly due to the field water content being higher.

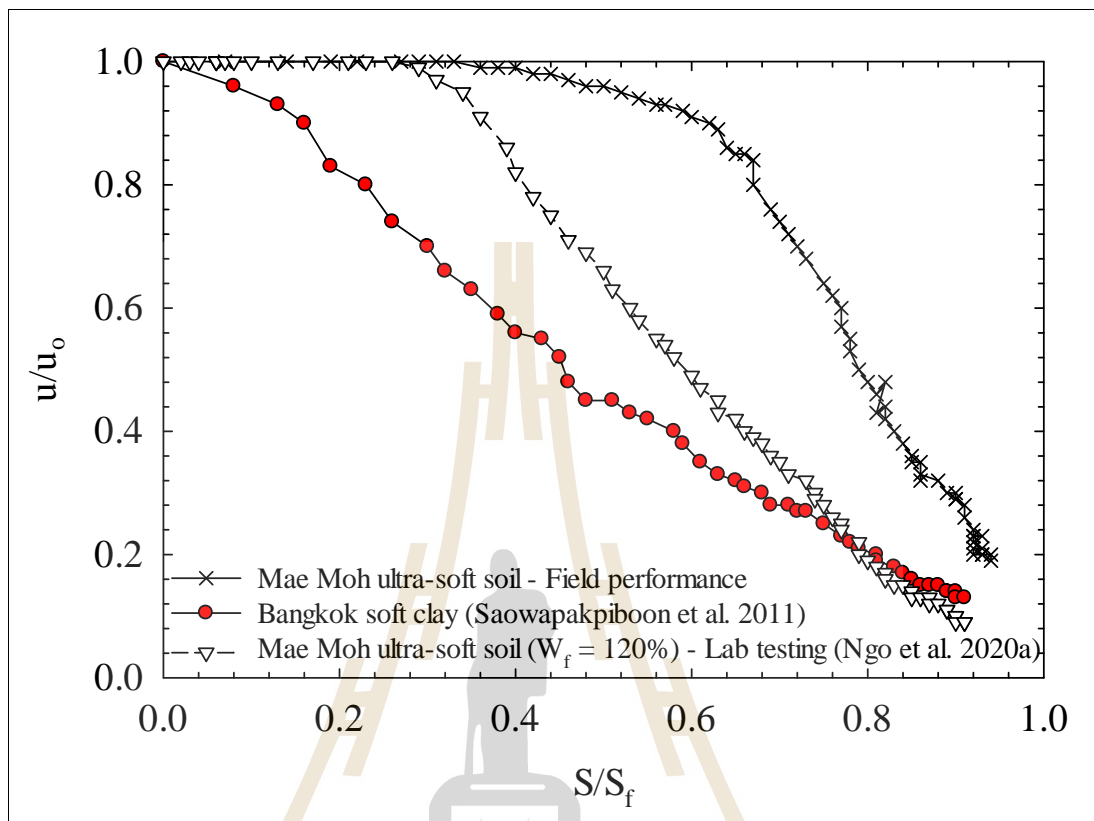


Figure 5.13 Relationship between S/S_f versus u/u_o of Mae Moh ultra-soft soil compared with soft Bangkok clay.

5.5.3 Degree of consolidation

Two means of determining degree of consolidation was calculated: one was based on the measured excess pore water pressure, U_e %, and the other is based on the measured settlement, U_s % to illustrate the role of delay in excess pore water pressure in the Terzaghi's effective stress concept. The data of excess pore water pressure and the settlement due to the sand blanket installation were selected to determine U_e and U_s as an example. To determine U_e , the relationships between u at

any time against depth were plotted, as shown in **Fig. 5.14**. The U_e was then approximated using the following equation (Terzaghi, 1943):

$$U_e(\%) = 1 - \frac{\int u_t(z) dz}{\int u_o(z) dz} \quad (5.3)$$

in which $u_o(z)$ is the initial excess pore water pressure at depth z under the surcharge loading; $u_t(z)$ is the excess pore water pressure at depth z at time t .

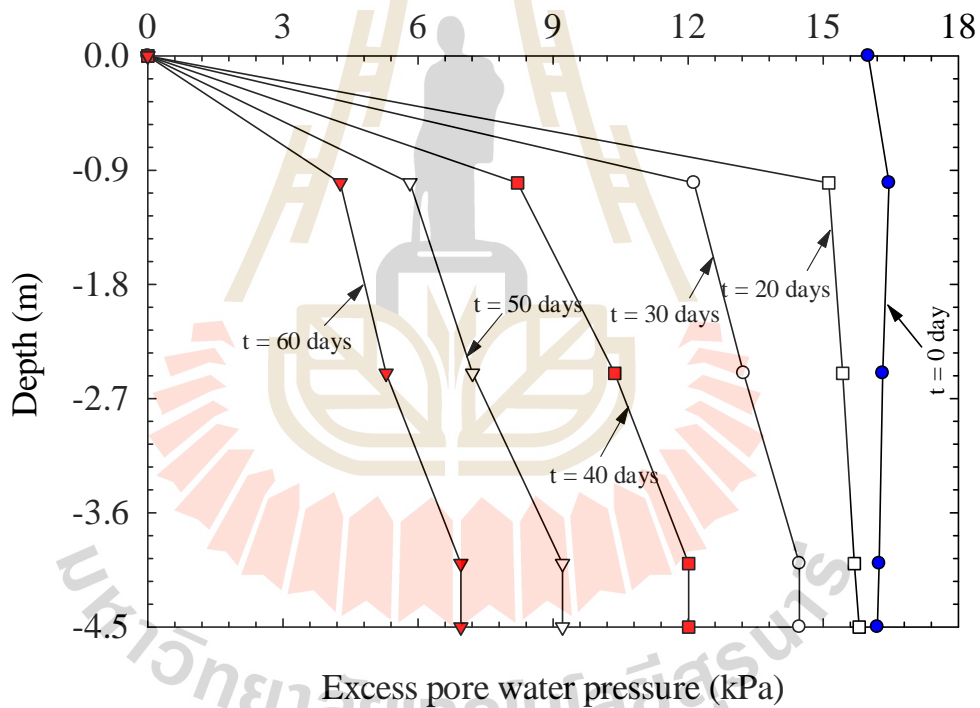


Figure 5.14 Excess pore water pressure versus depth relationships at any time during sand blanket installation

The relationship between U_s and U_e for Mae Moh ultra-soft soil was plotted and compared to that of PVD improved Bangkok clay (Bergado et al. 2002), as

presented in **Fig. 5.15**. It is seen that at different consolidation times, U_s was slightly higher than U_e for Bangkok soft clay, while U_s was remarkably higher than U_e for the Mae Moh ultra-soft soil due to the delay in excess pore water pressure. The U_e for Mae Moh ultra-soft soil would approach the U-Line ($U_s = U_e$) at the end of loading stage.

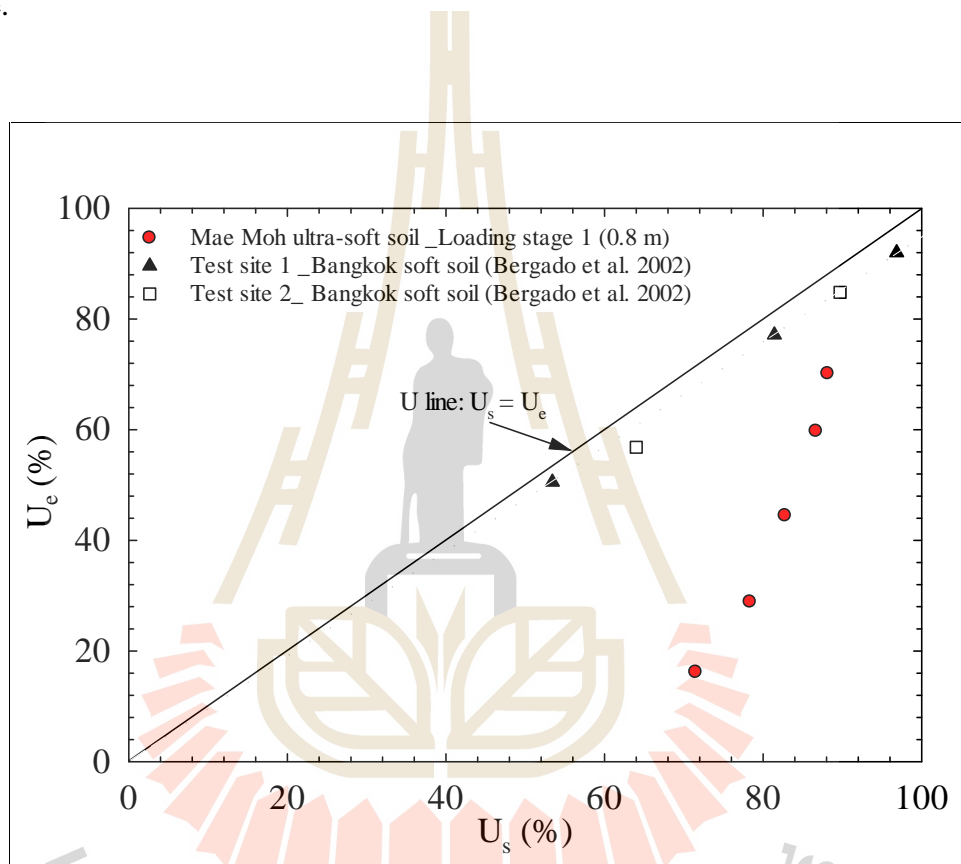


Figure 5.15 Comparison of degrees of consolidation based on measured settlement (U_s %) and excess pore water pressure (U_e %) for Mae Moh ultra-soft soil and Bangkok soft clay.

5.5.4 Undrained shear strength

The relationships between measured S , u , and S_u versus time for loading stage 3 are presented in **Fig. 5.16** to investigate the influence of delay in

excess pore water pressure dissipation on S_u development. There was a very little gain in S_u within the delayed time while the large settlement was recorded. For instance, the settlement during the first 6 days were increased from 0.915 m to 1.1015 m while there was almost no change of u and S_u . After the reduction of u , the S_u development over time was being started, as shown in **Fig. 5.16**. This implied that the S_u development is dependent upon the dissipation of excess pore water pressure, not settlement. Since U_s is simpler to calculated than U_e and almost equal to U_s when $U_s > 90\%$ (**Fig. 5.15**), the S_u when $U_s > 90\%$ is suggested to be calculated based U_s . The relationships between S_u versus depth and average S_u versus the increased vertical effective stress (σ'_v) at each loading stage are plotted in **Fig. 5.17** where $\sigma'_v = U_s \times \sigma_v$ and σ_v is the increased vertical total stress. The S_u value were significantly increased as σ'_v increased. Similar to laboratory model test results (Ngo et al., 2020), the S_u development with σ'_v can be described based on the SHANSEP equation proposed by Ladd and Foott (1974):

$$\frac{S_u}{\Delta \sigma'_v} = 0.213 \quad (5.4)$$

The constant value of 0.213 was slightly lower with that of 0.22 obtained from laboratory test result (Ngo et al., 2020a).

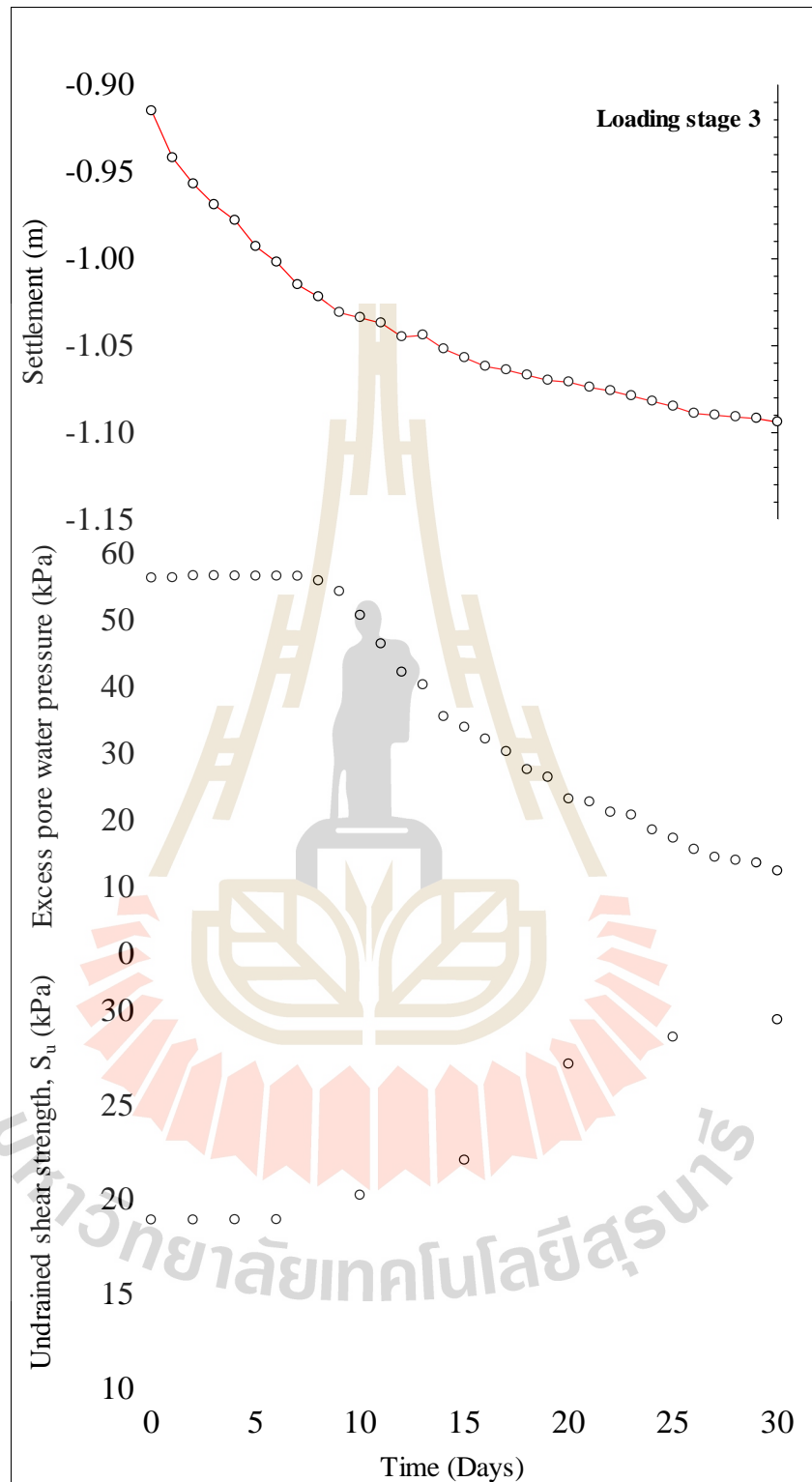


Figure 5.16 Settlement, excess pore water pressure and the undrained shear strength versus time relationships in loading stage 3

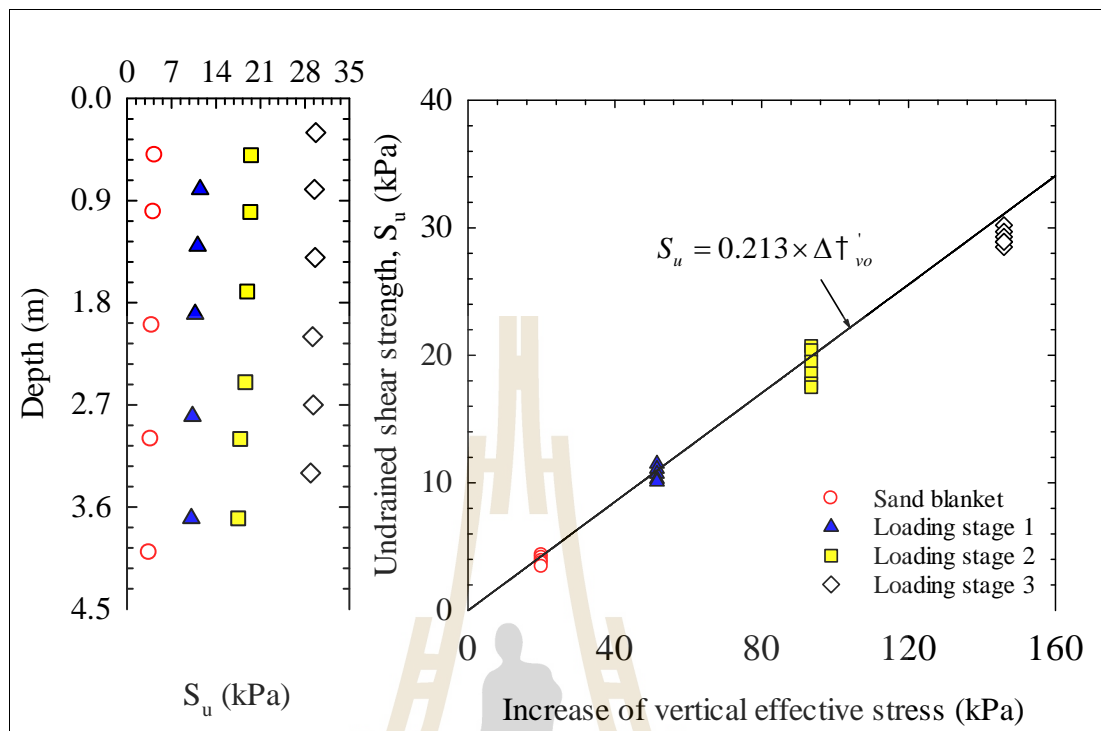


Figure 5.17 Undrained shear strength at different depths under different increased of vertical effective stresses (kPa)

5.6 Conclusion

This research studied the consolidation behavior of PVD improved ultra-soft soil in Mae Moh mine, Thailand on a full-scale trial. The conclusions of this research can be drawn as follows:

- Since S_u of the ultra-soft soil was extremely low, geotextile reinforcement was used to strengthen the bearing capacity of ultra-soft soil foundation prior to the sand platform installation. The differential surface settlements due to step loading increased with the increase in vertical stress. The Asoaka's method was used to determine the final settlements for each loading stage and to confirm that U_s at the end of each loading stage was greater than 90%; $U_s = 96.57\%$, 95.70% , 91.19% , and

96.50 % for sand blanket installation, loading stage 1, stage 2, and stage 3, respectively.

- The delay of excess pore water pressure dissipation at the initial stage of loading despite the occurrence of large settlements is the distinct behavior of Mae Moh ultra-soft soil, which is different from the behavior of natural soft clay. Beyond the delayed time, the excess pore water pressure reduced significantly with time. The delayed time of excess pore water pressure dissipation was reduced with the increase of vertical stress.

- Within the delayed time, U_s value increased as the settlement increased while U_e and S_u retained almost unchanged. Beyond the delayed time, both U_e and S_u increased; moreover, U_e and U_s was essentially the same when $U_s > 90\%$. Since U_s is simply obtained from Asaoka's method, it was suggested to use U_s for approximation of S_u when $U_s > 90\%$ based on the SHANSEP's method. The increase of S_u at the end of each loading demonstrated the efficiency of PVDs in the improvement of the Mae Moh ultra-soft soil.

- The successful installation and application of PVD to improve ultra-soft soil in this research would be a lesson learned for a real construction project on the reclamation of Sump1 C1. The outcome of this study will also result in an effective design method of preloading technique with PVDs on ultra-soft soils.

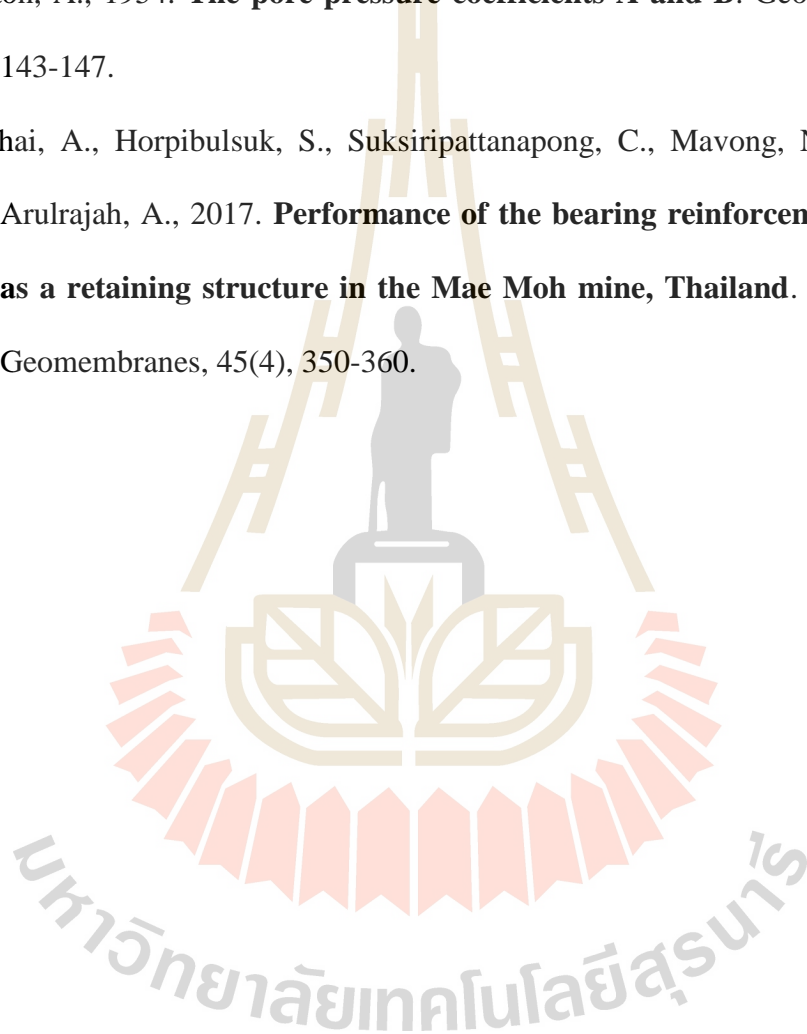
5.7 References

- Arulrajah, A., Nikraz, H., Bo, M., 2004. **Factors affecting field instrumentation assessment of marine clay treated with prefabricated vertical drains.** *Geotextiles and Geomembranes*, 22(5), 415-437.

- Asaoka, A., 1978. **Observational procedure of settlement prediction**. Soils and Foundations, 18(4), 87-101.
- Bergado, D. T., Sasanakul, I., Horpibulsuk, S., 2003. **Electro-osmotic consolidation of soft Bangkok clay using copper and carbon electrodes with PVD**. Geotechnical testing journal, 26(3), 277-288.
- Bo, M., 2004. **Discharge capacity of prefabricated vertical drain and their field measurements**. Geotextiles and Geomembranes, 22(1-2), 37-48.
- Bo, M., 2008. **Compressibility of ultra-soft soil**: World Scientific Publishing Company.
- Bo, M., Arulrajah, A., Leong, M., Horpibulsuk, S., Disfani, M., 2014. **Evaluating the in-situ hydraulic conductivity of soft soil under land reclamation fills with the BAT permeameter**. Engineering Geology, 168, 98-103.
- Bo, M. W., Arulrajah, A., Horpibulsuk, S., Chinkulkijniwat, A., Leong, M., 2016. **Laboratory measurements of factors affecting discharge capacity of prefabricated vertical drain materials**. Soils and Foundations, 56(1), 129-137.
- Chen, J., Shen, S. L., Yin, Z.-Y., Xu, Y.S., Horpibulsuk, S., 2016. **Evaluation of effective depth of PVD improvement in soft clay deposit: a field case study**. Marine Georesources & Geotechnology, 34(5), 420-430.
- Chu, J., Bo, M., Choa, V., 2004. **Practical considerations for using vertical drains in soil improvement projects**. Geotextiles and Geomembranes, 22(1-2), 101-117.
- Chu, J., Bo, M., Choa, V., 2006. **Improvement of ultra-soft soil using prefabricated vertical drains**. Geotextiles and Geomembranes, 24(6), 339-348.

- Fang, Z., Yin, J. H., 2006. **Physical modelling of consolidation of Hong Kong marine clay with prefabricated vertical drains**. Canadian Geotechnical Journal, 43(6), 638-652.
- Geng, C., Yonghui, C., Jiangwei, S., Long, C., 2017. **Newly developed technique and analysis solution to accelerate consolidation of ultrasoft soil**. Marine Georesources & Geotechnology, 35(2), 292-299.
- Hong, Z., Yin, J., Cui, Y. J., 2010. **Compression behaviour of reconstituted soils at high initial water contents**. Geotechnique, 60(9), 691-700.
- Horpibulsuk, S., Liu, M. D., Zhuang, Z., Hong, Z. S., 2016. **Complete compression curves of reconstituted clays**. International Journal of Geomechanics, 16(6), 06016005.
- Ladd, C. C., Foott, R., 1974. **New design procedure for stability of soft clays**. Journal of Geotechnical and Geoenvironmental Engineering, 100(Proc Paper 10064).
- Ngo, D. H., Horpibulsuk, S., Suddeepong, A., Hoy, M., Udomchai, A., Doncommul, P., Arulrajah, A., 2020a. **Consolidation behavior of dredged ultra-soft soil improved with prefabricated vertical drain at the Mae Moh mine, Thailand**. Geotextiles and Geomembranes.
- Ngo, D. H., Horpibulsuk, S., Suddeepong, A., Hoy, M., Chinkulkijniwat, A., Arulrajah, A., Chaiwan, A., 2020b. **Compressibility of ultra-soft soil in the Mae Moh Mine, Thailand**. Engineering Geology, 105594.
- Rashid, A. S. A., Shirazi, M. G., Nazir, R., Mohamad, H., Sahdi, F., Horpibulsuk, S., 2019. **Bearing capacity performance of soft cohesive soil treated by kenaf limited life geotextile**. Marine Georesources & Geotechnology, 1-6.

- Saowapakpiboon, J., Bergado, D., Youwai, S., Chai, J., Wanthong, P., Voottipruex, P., 2010. **Measured and predicted performance of prefabricated vertical drains (PVDs) with and without vacuum preloading.** *Geotextiles and Geomembranes*, 28(1), 1-11.
- Skempton, A., 1954. **The pore-pressure coefficients A and B.** *Geotechnique*, 4(4), 143-147.
- Udomchai, A., Horpibulsuk, S., Suksiripattanapong, C., Mavong, N., Rachan, R., Arulrajah, A., 2017. **Performance of the bearing reinforcement earth wall as a retaining structure in the Mae Moh mine, Thailand.** *Geotextiles and Geomembranes*, 45(4), 350-360.



CHAPTER VI

CONCLUSIONS AND RECOMMENDATIONS

6.1 General summary

The primary objective of this study was to investigate the performance of PVD improved ultra-soft soil in Mae Moh mine, Thailand. A detailed discussion on the problem statement in Mae Moh mine was provided in Chapter 1. Chapter 2 provided a literature review of the prefabricated vertical drains and the factor affecting on the performance of PVD on the consolidation of soft soil. Chapter 3 presented the compressibility characteristic of Mae Moh ultra-soft soil without PVDs, which is composed of the sedimentation and consolidation phases. Chapter 4 presented the performance of PVDs in the consolidation of ultra-soft soil with various soil water contents in Mae Moh mine, Thailand via a series of large-scale model tests and numerical analysis. Chapter 5 presented a full-scale test on PVD improved ultra-soft at a trial slurry pond for future the PVD construction in Sump1 C1. The following conclusions can be drawn from this study:

6.1.1 Compressibility of Mae Moh ultra-soft soil without PVDs

The compressibility characteristics of Mae Moh ultra-soft soil is composed of the sedimentation and consolidation phases. The sedimentation process of Mae Moh ultra-soft soil was divided into two distinct stages: flocculation and settling. The flocculation occurred at the early stage in which soil particles were dispersed in the mixture and very small change in soil-fluid interface was observed in

this stage. The settling stage then commenced, when the floc particles started to settle uniformly, causing the significant change in soil-fluid interface. A critical water content (w_{cr}) separating the large sedimentation and small sedimentation slurry, was found to be 171% for Mae Moh ultra-soft soil. For large sedimentation slurry, the water content reduces significantly after sedimentation process. On the other hand, the water content of small sedimentation slurry slightly decreases during sedimentation process. The consolidation curve of Mae Moh sedimentation soil can be represented by the inverse S-shape function from very low to very high vertical effective stress and it can be simulated by generalized equation using generalized void ratio (e_v/e_L). The intrinsic state line for high sedimentation soil was proposed for examining the stress state and predicting the consolidation curve of ultra-soft soil.

6.1.2 Consolidation behavior of Mae Moh ultra-soft soil improved with PVDs via laboratory testing.

A series of large-scale consolidation test was conducted to assess the performance of PVD in the consolidation of Mae Moh ultra-soft soil. The higher water content of the soil, the higher settlement and the lower rate of consolidation settlement. Large settlement with the delay of excess pore pressure at the initial stage of loading is a distinct behavior of Mae Moh ultra-soft soil. The higher initial water content, the lower consolidation pressure and the smaller of PVDs dimension resulted in the longer delay of excess pore pressure dissipation. Beyond the delayed time, the excess pore water pressures rapidly decreased with time. The reduction of water content and the increase of undrained shear strength of the soil after testing highlighted the successful performance of PVDs on the improvement of Mae Moh ultra-soft soil. The undrained shear strength of the soil could be approximated by the

vertical effective stress based on SHANSEP's method. The finite element analysis with axisymmetric and plain strains model indicated that the axisymmetric model produced an excellent match with measured data in term of settlement value. However, the excess pore water pressure was not well predicted using the axisymmetric model due to the delay of excess pore water pressure at the initial time of loading. The settlement of Mae Moh dredged soil can be simulated satisfactorily by the plane strain models proposed by Chai et al. (2001) and Indraratna and Redana (2000).

6.1.3 Consolidation behavior of Mae Moh ultra-soft soil improved with PVDs via full-scale test

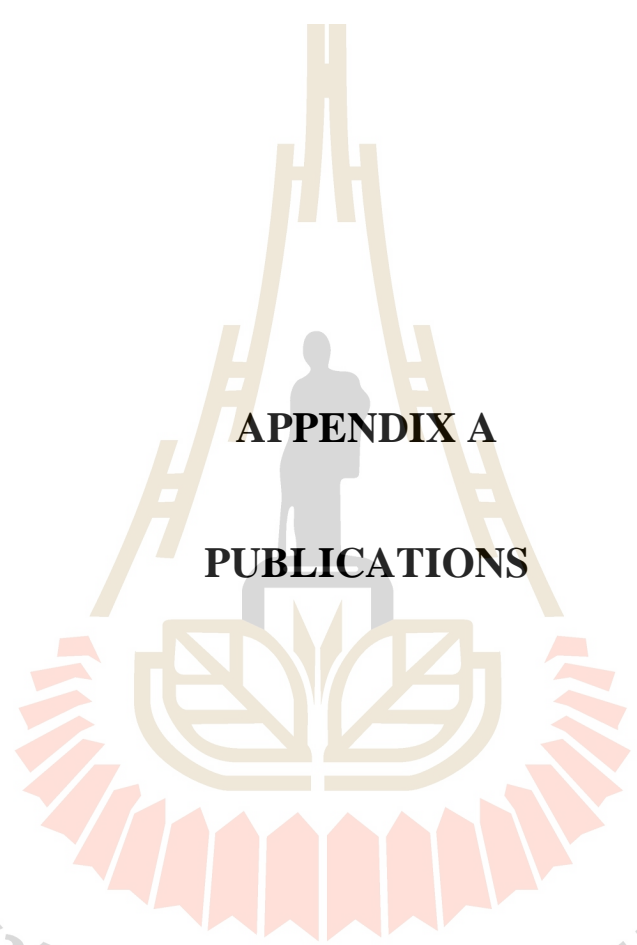
A full-scale trial was conducted to study the consolidation behavior of PVD improved ultra-soft soil in Mae Moh mine, Thailand. Geotextile reinforcement was used to strengthen the bearing capacity of ultra-soft soil foundation prior to the sand platform installation. The field study indicated that the delay of excess pore water pressure dissipation at the initial stage of loading despite the occurrence of large settlements is the distinct behavior of Mae Moh ultra-soft soil, which is different from the behavior of natural soft clay. Beyond the delayed time, the excess pore water pressure reduced significantly with time. The delayed time of excess pore water pressure dissipation was reduced with the increase of vertical stress. Within the delayed time, the calculated degree of consolidation based on the measured settlement increased while the calculated degree of consolidation based on the measured excess pore water pressure and the undrained shear strength remained constant. Beyond the delayed time, both U_e and S_u increased significantly with time and the U_e value was essentially similar with U_s when $U_s > 90\%$. Since U_s is simply obtained from

Asaoka's method, it was suggested to determine the undrained shear strength when $U_s > 90\%$ based on the SHANSEP's method. The increase of undrained shear strength at the end of each loading stage demonstrated the efficiency of PVDs in the improvement of the Mae Moh ultra-soft soil.

6.2 Recommendations for future work

Some plausible avenues of future work that could extend the work in this thesis are stated as follows:

1. The development of generalized equation to estimate the consolidation curve of sedimentation soil at very high and low vertical stresses was based on sound principles. It would be interesting to confirm the applicability of this method by more test data.
2. The three dimensional analysis (3D) should be performed to predict the consolidation behavior of Mae Moh ultra-soft soil conducted in the large-scale model test and compared with 2D analysis and measured data.
3. The two dimensional and three dimensional finite element analysis of full-scale test should be performed for the full-scale test and compared with the measured data.



APPENDIX A
PUBLICATIONS

มหาวิทยาลัยเทคโนโลยีสุรนารี

List of Publications

INTERNATIONAL JOURNAL PAPERS

- Ngo, D. H., Horpibulsuk, S., Suddeepong, A., Hoy, M., Chinkulkijniwat, A., Arulrajah, A., & Chaiwan, A. (2020). **Compressibility of ultra-soft soil in the Mae Moh Mine, Thailand.** Engineering Geology Journal, 271, 105594.
- Ngo, D. H., Horpibulsuk, S., Suddeepong, A., Hoy, M., Udomchai, A., Doncommul, P., Arulrajah, A. (2020). **Consolidation behavior of dredged ultra-soft soil improved with prefabricated vertical drain at the Mae Moh mine, Thailand.** Geotextiles and Geomembranes Journal, 48, 561-574.
- Pham, H. T., Rühaak, W., Ngo, D. H., Ngo, O. C., & Sass, I. (2019). **Fully coupled analysis of consolidation by prefabricated vertical drains with applications of constant strain rate tests: Case studies and an open - source program.** Geotextiles and Geomembranes Journal, 48, 380-391.



Contents lists available at ScienceDirect

Geotextiles and Geomembranes

journal homepage: www.elsevier.com/locate/geotextmem

Consolidation behavior of dredged ultra-soft soil improved with prefabricated vertical drain at the Mae Moh mine, Thailand

Dong Huy Ngo^a, Suksun Horpibulsuk^{b,*}, Apichat Suddeepong^c, Menglim Hoy^b, Artit Udomchai^c, Prajueb Doncommul^d, Runglawan Rachan^e, Arul Arulrajah^f

^a School of Civil Engineering, Suranaree Univ. of Technology, 111 University Ave., Muang District, Nakhon Ratchasima, 30000, Thailand

^b School of Civil Engineering, Center of Excellence in Innovation for Sustainable Infrastructure Development, Suranaree Univ. of Technology, Thailand

^c Center of Excellence in Innovation for Sustainable Infrastructure Development, Suranaree Univ. of Technology, Thailand

^d Mae Moh Mine Planning and Management Division, Electricity Generating Authority of Thailand, Thailand

^e Department of Civil Engineering, Maharakorn Univ. of Technology, Thailand

^f Department of Civil and Construction Engineering, Swinburne University of Technology, Hawthorn, Victoria 3122, Australia



ARTICLE INFO

Keywords:

Ultra-soft soil
Large-scale model test
Prefabricated vertical drains
Consolidation
Ground improvement

ABSTRACT

The effectiveness of the prefabricated vertical drains (PVDs) in the consolidation of ultra-soft dredged soil with various soil water contents (W) in Mae Moh mine, Lampang, Thailand was researched via a series of large-scale model tests and numerical analysis. Large settlements with the delay of excess pore pressures is a distinct behavior of ultra-soft soil. The PVD dimensions were found to have a significant effect on the rate of consolidation and the delay of excess pore pressure at low total vertical stress (σ_v). The smaller PVD dimension resulted in the smaller rate of consolidation and longer delay of excess pore pressure. The undrained shear strength (S_u) of ultra-soft clay at various degrees of consolidation could be approximated by the vertical effective stress (σ'_v) based on the SHANSEP where the σ'_v was determined from the Asaoka's observational method. The finite element analysis with axisymmetric and plane strain models showed that the axisymmetric model produced an excellent settlement prediction. However, the excess pore pressures were not well predicted by the axisymmetric model, due to the delay of excess pore pressures at the early stages of consolidation. In practice, the plane strain models proposed by Chai et al. and Indraratna and Redana's methods are suggested to predict the consolidation settlement of the Mae Moh dredged soil improved with PVD. The outcome of this research will facilitate the geotechnical design of reclamation of ultra-soft dredged soil in Mae Moh mine and other similar soils.

1. Introduction

The Mae Moh mine is situated at Mae Moh district, Lampang province, located about 600 km north of Bangkok, Thailand. It is well-known as the largest open-pit lignite mine in Southeast Asia covering an area of 4 km in width and 7.5 km in length. Approximately 45,000 tons of coal/day, which represent 70% of the total coal production of Thailand, are processed to generate power at the Mae Moh power plants (Udomchai et al., 2017). This mine is operated by the Electricity Generating Authority of Thailand (EGAT). Sump 1 C1 is a low-lying area, located in the north of the Mae Moh mine with the total area of 80,000 m². The soil erosion caused by the discharge of surface water along the mine slope was finally collected and formed up to

approximately 38 m thickness of dredged soil deposits under water in sump 1 C1 for over decades.

According to the mine planning and development of EGAT, the mine will be excavated to a depth of approximately 500 m from original surface in the next 40 years. As a result, this mine will become the deepest open-pit lignite mine in the world. The excavated soil from mining activity will be transferred to dump in the Sump 1 C1. It will be subjected approximately 300 m of overburden material in the next 40 years. However, the dredged soil in the Sump 1 C1 is ultra-soft soil and possesses very low bearing capacity. Therefore, it is imperative to improve the existing ultra-soft dredged soil before commencing any construction activities in order to prevent any failure due to the mud flow. Soil improvement techniques generally include soil replacement,

* Corresponding author. School of Civil Engineering, Suranaree University of Technology, 111 University Avenue, Muang District, Nakhon Ratchasima, 30000, Thailand.

E-mail addresses: d6040147@g.sut.ac.th (D.H. Ngo), suksun@g.sut.ac.th (S. Horpibulsuk), suddeepong8@hotmail.com (A. Suddeepong), menglim@g.sut.ac.th (M. Hoy), artit.u@g.sut.ac.th (A. Udomchai), prajueb.d@egat.co.th (P. Doncommul), runglawan@mut.ac.th (R. Rachan), arulrajah@swin.edu.au (A. Arulrajah).

<https://doi.org/10.1016/j.geotextmem.2020.03.002>

Received 3 September 2019; Received in revised form 1 March 2020; Accepted 2 March 2020

Available online 20 March 2020

0266-1144/ © 2020 Elsevier Ltd. All rights reserved.

preloading, stone column, and cement column, etc (Arulrajah et al., 2005; Cai et al., 2018; Cao et al., 2019; Horpibulsuk et al., 2013; Jiang and Liu, 2019; Morohoshi et al., 2010; Pham et al., 2019a,b; Yonghui et al., 2019; Zhang et al., 2019). Among these methods, the preloading with prefabricated vertical drains (PVDs) is cost-effective and commonly used in land reclamation projects on ultra-soft soil deposits (Arulrajah et al., 2004; Bo et al., 2005; Chen et al., 2016; Geng et al., 2017; Mesri and Kane, 2019). PVDs are band-shaped, which can be inserted into the soft ground up to even 40m depth to reduce the drainage path and therefore shorten the consolidation time (Almeida et al., 2004; Bo et al., 2016; Chai et al., 2001; Fang and Yin, 2006; Saowapakpiboon et al., 2010). However, a few laboratory testing and field instrumentation have been conducted to study the performance of PVDs improved ultra-soft soil in dredged sump (Bo, 2004; Choa et al., 2001; Chu et al., 2004, 2006). It was evident that the PVDs accelerate settlement, enhance shear strength, and reduce moisture content of the ultra-soft clay for a particular water content and PVD dimension. However, the PVD dimensions and water content, which play an important role in successful performance of PVD in the ultra-soft soil have not been well examined.

In this study, a series of large – scale model test was carried out to assess the effectiveness of PVD in the consolidation of the Mae Moh ultra-soft soil. The effects of PVD dimension and water content of the ultra-soft soil on the settlement, excess pore pressure dissipation and undrained shear strength of PVD improved ground under various loading conditions were investigated. The large-scale consolidation test results were analyzed and compared with the simulation results by finite element method (FEM). The distinct consolidation behavior especially excess pore pressure dissipation of ultra-soft clay was presented and compared with the conventional soil mechanics theory. Also, the suitable numerical method for predicting settlement at various consolidation time was recommended. The research outputs will facilitate the selection of design parameters and numerical method for the future design of dredged soil in Sump 1 C1 using preloading with PVD system. The knowledge gained can be applied to the ground improvement of ultra-soft soils in future dredging projects.

2. Large-scale consolidation test

To investigate the effectiveness of PVD for the ground improvement of dredged soil, the large-scale consolidation tests were conducted at various initial water contents (case 1 and case 2) and dimensions of the PVDs (case 1 and case 3) as listed in Table 1. The details of the sample preparation and testing procedure of each testing case are being presented.

2.1. Soil sample

The ultra-soft soil samples were obtained from a dredged soil pond (Sump 1 C1). The disturbed bulk samples were collected from 1.5 m depth below the dredged soil surface. It was then stored in plastic tanks and kept inside the laboratory at a room temperature of approximately 27 °C.

The dredged soil consists of 1% sand, 58% silt, and 41% clay. The 85% of soil particles by weight, D_{85} were smaller than 0.017 mm. The liquid limit and the plastic limit determined using Casagrande method were 57% and 26%, respectively. The specific gravity was 2.5. The

activity of this soil is about 0.756 and it is therefore classified as a normal clay based on Skempton's classification (Skempton, 1953). The natural water content was in the range of 114%–180%. The in-situ strength was extremely low.

2.2. Selection of PVD

During consolidation, very fine particles may infiltrate into the core of the PVD and consequently clog the drainage channels, and reduce the discharge capacity (Cao et al., 2019; Chu et al., 2004, 2006; Holtz, 1987). Therefore, the selection of PVD types plays a major role in the successful performance of PVD in ultra-soft clay (Chu et al., 2004, 2006).

In this study, the filter of PVD was selected carefully based on the requirement of permeability and the apparent opening size of the filter. In general, the permeability of filter is required to be higher than that of soil. On the other hand, the apparent opening size should meet the requirement as follows:

$$O_{95} \leq (4 - 7.5) \frac{D_{85}}{K_a} \quad (1)$$

where O_{95} is the apparent opening size of the filter; and K_a is a reduction factor considering the effect of loading and partial clogging on the geotextiles. The value of K_a varies from 1.9 to 4.4 as recommended by Chu et al. (2006) and Palmeira and Gardoni (2002).

Based on this criterion, two types of PVDs, namely Ali-drain type AD250 having 100 mm and 50 mm width but with the same thickness of 5 mm were selected. The apparent opening size of the filter was smaller than 0.08 mm, satisfied the requirement in Equation (1). The hydraulic conductivity of the PVD filter was 1.8×10^{-4} m/s, higher than the laboratory permeability of the dredged soil (1.21×10^{-9} m/s). The core of the PVD had a discharge capacity of 150×10^{-6} m³/s in the straight condition and 110×10^{-6} m³/s in the kinked condition, under a confining pressure of 250 kPa. The characteristics of the PVDs are summarized in Table 2.

2.3. Model test

2.3.1. Large-scale consolidation apparatus

A large-scale consolidation apparatus was developed at the Center of Excellence in Innovation for Sustainable Infrastructure Development of Suranaree University of Technology, Thailand for this research. Fig. 1 shows the schematic and photo of the fully-instrumented large-scale consolidation tank. The consolidation tank was made of stainless steel with an inside diameter of 495 mm and a height of 1200 mm. Six saturated miniature pore pressure transducers (PPT) were installed to measure excess pore water pressures at different positions. Six pore pressure transducers (PPTs) were installed at 100 mm (PPT 2, PPT 4, and PPT 6) and 200 mm (PPT 1, PPT 3, and PPT 5) away from the center of vertical drain, respectively. A total earth pressure cell was placed on the steel plate in order to control the pressure acting on the sample during the test. To reduce wall friction, the inner surface was polished and smeared with lubricating oil beforehand.

2.3.2. Sample preparation

For each test, the remolded sample was prepared by adding a sufficient amount of water to obtain the initial water content greater than

Table 1
Cases tested.

Case	Height of soil (mm)	Water content W _i (%)	PVD dimensions (mm)	Loading step (kPa)	Total loading time (hours)
Case 1	950	120	100 × 5	20, 40, 80	1362
Case 2	950	180	100 × 5	20, 40, 80	1362
Case 3	950	120	50 × 5	20, 40, 80	1362

Table 2
PVDs characteristics.

Thickness (mm)	Width (mm)	Permeability of the filter (m/s)	Discharge capacity of straight drain under 300 kPa pressure (m ³ /s)	Discharge capacity of kinked drain under 250 kPa pressure (m ³ /s)	Apparent opening size (mm)
100	5	1.8×10^{-4}	$\geq 150 \times 10^{-6}$	110×10^{-6}	≤ 0.08
50	5	1.8×10^{-4}	$\geq 150 \times 10^{-6}$	110×10^{-6}	≤ 0.08

its liquid limits and then thoroughly mixed by a mechanical mixer. The sedimentation process is special characteristic of dredged soil at very high initial water content (Been and Sills, 1981; Biewett et al., 2001; Sills, 1998; Tan et al., 1990; Xu et al., 2012). The remolded soil was hence poured into the tank for about 1 month to negate the effect of sedimentation on the consolidation. The water on the top of slurry soil was taken out of the tank after the 1 month of sedimentation. The final height of the soil in the consolidation tank was approximately 95 cm while the water contents of the soil in the 3 tested cases were respectively 120%, 180%, and 120% after sedimentation time. One geotextile layer with a rectangular hole of 120 mm × 15 mm at the center of the model ground for PVD installation using a mandrel was placed on the top of the model ground.

2.3.3. Installation of PVD

After the 1 month of sedimentation, two small aluminum mandrels with different rectangular sections of 120 mm × 10 mm and 60 mm × 10 mm connected with an aluminum tip shoe at the end were used to simulate field installation of PVDs with 10 cm width and 5 cm width, respectively. In each case, the mandrel with PVD inside was penetrated through the hole at the center of geotextile and vertically into the ultra-soft soil. When the mandrel touched the bottom of the tank, it was slowly withdrawn from the soil. A 10 cm thick sand layer was then spread on the geotextile layer (on top of the ultra-soft clay)

after PVD installation and covered with the other geotextile (see Fig. 1). A steel plate with one rectangular hole of 120 mm by 15 mm (for PVD to pass through) at the center was placed on the top of geotextile to impose the same displacement. It is noted that a hole of 50 mm diameter was manufactured in the steel plate to push the mini vane shear into the consolidated soil during the consolidation process to measure the undrained shear strength. The sand layer and geotextiles could prevent the ultra-soft clay from being squeezed out from the holes. During the consolidation stage, no squeezed soil was however observed from the holes.

2.3.4. Step loading

After assembling the tank, three incremental vertical pressures (20 kPa, 40 kPa, and 80 kPa) were applied at the top of the soil layer until the degree of consolidation in each loading stage was more than 90% for case 1. The degree of consolidation and the magnitude of final settlement were estimated based on the Asaoka's observational method (Asaoka, 1978). Chung et al. (2014) and Hiep and Chung (2018) also proposed an observational method, which is comparable to the Asaoka's method. The consolidation times of case 1 were also applied for case 2 and case 3 for comparison. The consolidation times were 620 h, 410 h and 333 h for 20 kPa, 40 kPa and 80 kPa vertical stresses, respectively. The top surface was drainage boundary and the bottom of tank were closed drainage. The water flows towards to the PVDs and vertically



Fig. 1. Large scale of consolidation tank (dimensions are in mm).

drains to the top surface. In this study, the settlement was measured by two Linear Variable Displacement Transducers (LVDTs) having the reading accuracy of 0.01 mm and 500 mm maximum deformation reading. The pore water pressure, earth pressure, and settlement were automatically recorded in real-time with a data logger. To investigate the effectiveness of PVDs on the strength improvement, the undrained shear strengths were measured by using a mini vane shear apparatus after the end of each loading. The vane blade was made of stainless steel with 30 mm in diameter and 60 mm in height. It was attached to a stainless steel rod with 5 mm in diameter, which can measure undrained shear strength at different depths in the consolidation tank.

2.4. Numerical simulation

In reality, the PVD improved soil can be represented by the unit-cell theory in the axisymmetric condition (three-dimensional, 3D), which is similar to the large consolidation model. However, the 3D finite element modeling of PVDs improved soil is very sophisticated and requires large computational effort. Consequently, the transformation of the unit cell condition to equivalent plane strain condition was introduced by Hird et al. (1992). In practice, the plane strain model satisfactorily simulates the settlement behavior of soil improved by PVD (Indraratna and Redana, 2000). The equations to determine an equivalent hydraulic conductivity of soil were proposed by several researchers to convert an axisymmetric model to an equivalent plane strain model (Indraratna et al., 2010). The equivalent hydraulic conductivity is determined in term of hydraulic conductivity of soil, PVD dimension and spacing, and smear effect. In this study, the settlement behavior of the dredged soil of case 1 as an example was modeled by both the axisymmetric and plane strain models using the Plaxis modeling software (Plaxis v. 8). The suitable plane strain model, which can simulate the settlement of the dredged soil in the field in the next phase of this research. In this study, four different approaches were adopted to simulate the consolidation behavior of dredged soil using vertical drain as follows:

2.4.1. Axisymmetry model with drain element

An axisymmetric unit cell model was considered to analyze the consolidation of dredged soil in the large-scale test. At the center of the unit cell, the rectangular sized PVD was converted into an equivalent radius, r_w . The r_w was equal to one fourth of sum of width and thickness of PVDs (Chai et al., 1999; Rixner et al., 1986). The PVDs were modeled as 3 nodes drainage element (excess pore water pressure is always zero)

with the equivalent radius (r_w) of 26.25 mm for PVDs 10 cm, as shown in Fig. 2a. The top boundary was set to drainage while outer vertical and bottom boundaries were assigned as closed drainage. The vertical stress of each loading stage was applied as uniform stress at the top of boundary. The horizontal hydraulic conductivity of the surrounding soil, k_h , was taken as 2.03 times of the vertical hydraulic conductivity, which was recommended by Arulrajah et al. (2005) for ultra-soft soil. The soil parameters using axisymmetric model are indicated in Table 3. The modified compression index (λ^*), modified swelling index (κ^*), the vertical hydraulic conductivity were obtained from the oedometer test. The cohesion (c') and friction angle (ϕ') were based on the undrained triaxial compression test results.

2.4.2. Plane strain model using Chai et al.'s method (Chai et al., 2001)

In this approach, a plane strain model without the drain element was adopted, in which the PVD and surrounded soil were considered as a uniform layer with the equivalent value of vertical hydraulic conductivity (k_{ve}). The equivalent value of vertical hydraulic conductivity can be expressed as:

$$k_{ve} = \left(1 + \frac{2.5l^2 k_h}{\mu d_c^2 k_v} \right) k_v \quad (2)$$

The value of μ can be taken as

$$\mu = \ln \frac{n}{s} + \frac{k_h}{k_v} \ln(s) - \frac{3}{4} + \pi \frac{2l^2 k_h}{3q_w} \quad (3)$$

where $n = d_u/d_w$; $s = d_s/d_w$; d_u is the diameter of unit cell; d_w is the diameter of drain; d_s is the diameter of smear zone; k_h is the horizontal hydraulic conductivity in smear zone, which can be assumed as the vertical hydraulic conductivity (k_v), l is the drainage path of PVD, which is the same as the PVD length for one-way drainage, q_w is the discharge capacity of PVD.

The geometry and loading conditions of this model are shown in Fig. 2b. The boundary on the top was set as drainage and the other boundaries were assigned as closed drainage.

2.4.3. Plane strain model using Lin et al.'s method (Lin et al., 2000)

To simulate the PVDs in plane strain model, Lin et al. (2000) proposed an equation to convert the radial flow of an axisymmetric model to that of a plane strain model. The horizontal hydraulic conductivity in an axisymmetric model (k_h) was converted to plane strain model with consideration of the smear effect as follows.

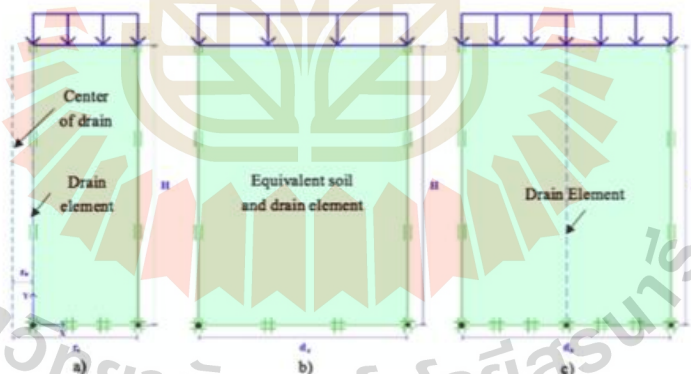


Fig. 2. Geometry conditions using a) Axisymmetry model; b) Plane strain model using Chai et al.'s method; c) Plane strain model using Lin et al.'s method and Indraratna and Redana's method.

Table 3
Soil parameters for modeling case 1.

Model	Axisymmetry (Soft soil model)	Plane strain (Chai et al.'s method)	Plane strain Lin et al.'s method	Plane strain (Indraratna and Redana's method)
Type	Undrained	Undrained	Undrained	Undrained
γ_{unsat} (kN/m ³)	16	16	16	16
γ_{sat} (kN/m ³)	18	18	18	18
k_h (m/hour)	8.85×10^{-8}	–	–	–
k_v (m/hour)	4.36×10^{-6}	–	–	–
k_{hs} (m/hour)	–	5.89×10^{-5}	3.10×10^{-6}	3.48×10^{-6}
k_{vs} (m/hour)	–	5.89×10^{-5}	1.53×10^{-8}	1.72×10^{-8}
λ^*	0.068	0.068	0.068	0.068
κ^*	0.025	0.025	0.025	0.025
Void ratio (e_{sat})	3.02	3.02	3.02	3.02
Cohesion (c')	1	1	1	1
Friction angle (ϕ')	29	29	29	29
τ_c/τ_w	0.2221	0.2475	0.2475	0.2475

$$k_{hs} = \frac{k_h \times \pi}{6[\ln(n/s) + (k_h/k_v)\ln(s) - 0.75]} \quad (4)$$

in which k_{hs} is the horizontal hydraulic conductivity in the undisturbed zone in the plane strain model.

2.4.4. Plane strain model using Indraratna and Redana's method (Indraratna and Redana, 2000)

Indraratna and Redana (2000) proposed an equation to convert the horizontal hydraulic conductivity of axisymmetry model to that of plane strain model. With considering the smear effect, the equivalent plane strain hydraulic conductivity is calculated as follows:

$$k_{hs} = \frac{k_h \left[\alpha + \beta \frac{b_h a_1}{b_v a_1} \right]}{\ln\left(\frac{a}{r}\right) + \left(\frac{b_h}{b_v}\right)\ln(s) - 0.75 - \alpha} \quad (5)$$

The terms α and β consider the geometric conversion of an axisymmetric unit cell into plane strain, and smear zone effects, respectively. The parameters α and β are given by:

$$\alpha = \frac{2}{3} - \frac{2b_h}{B} \left(1 - \frac{b_h}{B} + \frac{b_h^2}{3B^2} \right) \quad (6)$$

$$\beta = \frac{1}{B^2} (b_h - b_w)^2 + \frac{b_h}{3B^2} (3b_w^2 - b_h^2) \quad (7)$$

in which $b_w = \frac{a_1^2}{25}$ and $b_v = \frac{a_1^2}{25}$.

The geometry conditions of plane strain model using Lin et al.'s and Indraratna and Redana's methods to simulate the consolidation settlement of dredged soil improved by PVD are illustrated in Fig. 2c.

The soil parameters in plane strain model used for FEM are indicated in Table 3. It is noted that the soil parameters used for the axisymmetric and plane strain models are the same, except the horizontal and vertical hydraulic conductivities. For Chai et al.'s method, 1-D consolidation settlement is assumed so only k_{ve} controls the rate of settlement. As such, k_{hs} can be taken as k_{ve} . For Lin et al. and Indraratna and Redana's methods, the k_{hs}/k_{ve} ratio was taken as 2.03, which is the same as the axisymmetric condition. As such, the k_{hs} can be calculated after obtaining k_{ve} from Eq. (4) or (5).

3. Results and discussion

3.1. Model test results

3.1.1. Settlement results

The relationship between the settlement versus time of the three tested cases is shown in Fig. 3. The settlement occurred in the first loading stage (20 kPa) was much higher than the settlement induced in

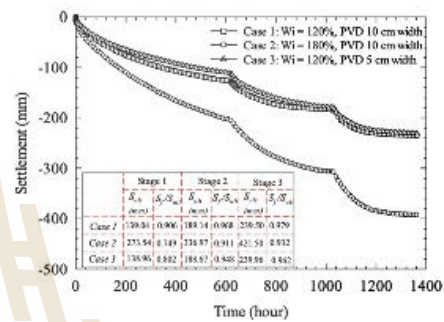


Fig. 3. Measured settlement versus time curve of 3 cases under 3 loading stages.

the second loading (40 kPa) and the last loading (80 kPa), respectively for all studied cases. The value of settlement reduced as the consolidation stress increased due to non-linear compression behavior of the dredged soil (Fang and Yin, 2006; Hong et al., 2010; Horpibulsuk et al., 2016; Liu et al., 2013).

The large settlements for all cases were observed, especially for case 2 with the initial water content of 180% that exhibited the highest value. The settlement of case 1 was in the order of 240 mm, which was about 27% of strain under the vertical consolidation stress of 80 kPa. The values of ultimate settlement (S_{ult}) and the degree of consolidation (S_r/S_{ult}) at the end of each loading are presented in Figs. 3 and 4, where S_r is the measured settlement at the end of each loading and S_{ult} is the ultimate settlement predicted by using the Asaoka's observational method (Asaoka, 1978). The time interval used for Asaoka's observational method, Δt , was 40 h. The soil in case 1 achieved more than 90% the degree of consolidation in all stages of loading, which was about 90.65%, 96.80%, and 97.90% for consolidation stresses of 20 kPa, 40 kPa, and 80 kPa, respectively.

The measured settlement in case 2 was much higher than that in case 1, which was approximately 393.02 mm after 1362 h of testing. A very large vertical strain of approximately 42% was developed at the end of consolidation test. Large settlements induced by PVDs in both cases (case 1 and case 2) proved the effectiveness of PVDs in improving the ultra-soft soil at different initial water contents. The degree of consolidation in case 2 in each loading stage was smaller than that in case 1. This indicates that the higher initial water content leads to the higher final settlement and the lower rate of consolidation settlement.

The effect of PVD dimension on the consolidation behavior of the ultra-soft dredged soil can be noticed by comparing case 1 with case 3.

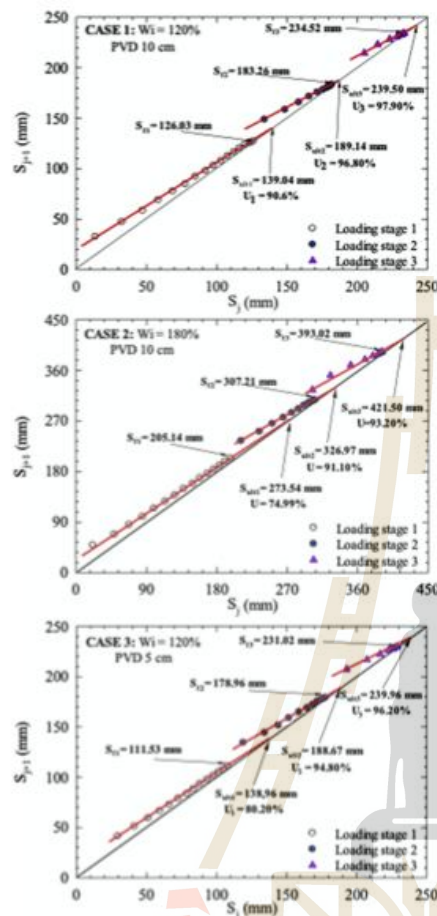


Fig. 4. Ultimate settlements of each loading stage predicted by using Asaoka's observational method.

Under the same testing condition (the water content of the soil, and loading pressure), the measured settlement for 5 cm PVD was smaller than that for 10 cm PVD at the same consolidation time, especially at low vertical stress. For instance, the settlement at the end of loading stage 1 (20 kPa of vertical stress) was approximately 126.03 mm for case 1 while it was 111.53 mm for case 3 (Fig. 3). The degree of consolidation at the end of test in case 3 was 80.20%, 94.80%, and 96.20% at 20 kPa, 40 kPa, and 80 kPa, respectively, as presented in Fig. 4, which is lower than that in case 1. However, based on the Asaoka's observational method, the ultimate settlement at 100% degree of consolidation for case 1 and case 3 was approximately the same. It is evident that at low vertical stress where the viscosity is relatively high, the PVD dimension significantly affected the rate of consolidation settlement while at high vertical stress, the effect of PVD dimension was less. The larger PVD has the higher drainage area per soil volume, which can

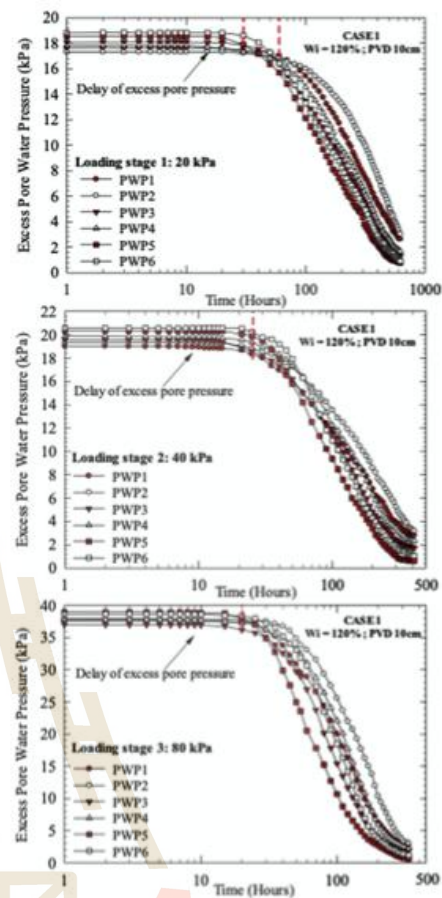


Fig. 5. Measured excess pore water pressure versus time relationships for case 1 ($W_i = 120\%$ and PVD 10 cm width).

stimulate the flow rate of the PVD improved ground. It was observed during the test that the water volume squeezed out from the soil in case 1 (10 cm PVD) was higher than that in case 2 (5 cm PVD).

The PVD of each test was extruded from the tank at the end of each test. The drain filter was cut open to check the soil particles entering into the PVD core. In all studied cases, the core was clean, which shows a good selection of PVDs filter for the consolidation of Mae Moh dredged soil. For Mae Moh dredged soil, the apparent opening size of the filter is therefore suggested to be:

$$O_{95} \leq 4.71 \times D_{45} \quad (8)$$

3.1.2. Excess pore water pressure

The dissipation of excess pore water pressures from six transducers of 3 tested cases is shown in Figs. 5–7. In all cases, the initial excess pore water pressures (at time $t = 0$) measured from 6 PPTs were slightly lower than the total vertical stress. It can be explained by the

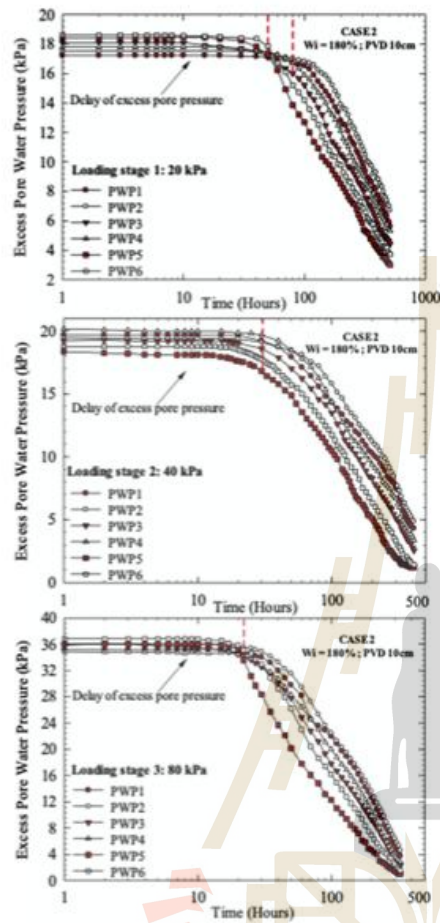


Fig. 6. Measured excess pore water pressure versus time relationships for case 2 ($W_i = 180\%$ and PVD 10 cm width).

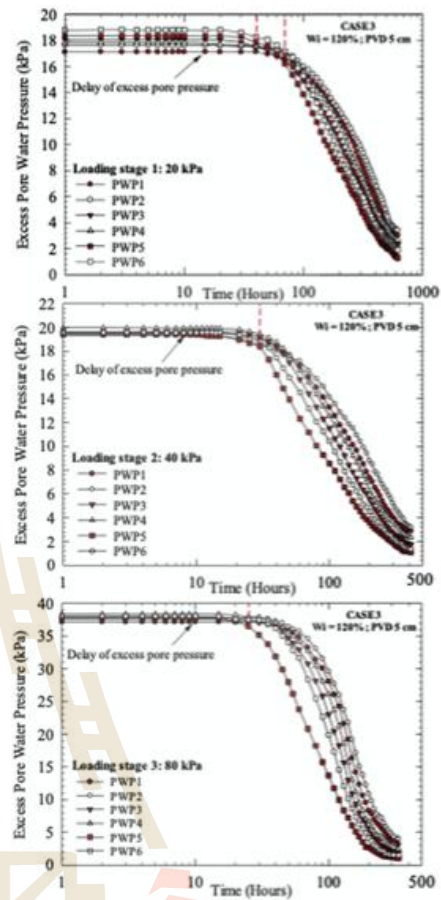


Fig. 7. Measured excess pore water pressure versus time relationships for case 3 ($W_i = 120\%$ and PVD 5 cm width).

pore pressure coefficients A and B proposed by Skempton (1954). The change in pore water pressure under the change in the principle stresses $\Delta\sigma_1$ and $\Delta\sigma_3$ is given as $\Delta u = B[\Delta\sigma_1 + A(\Delta\sigma_1 - \Delta\sigma_3)]$. For saturated soils, the coefficient B is equal 1 while the value A varies with stresses and strains (Fang and Yin, 2006; Skempton, 1954). This behavior is similar to previous studies by Fang and Yin (2006) for Hong Kong marine clay. The excess pore water pressures recorded at the top (PPT 5, PPT 6) were different with those measured at the bottom of the tank (PPT 1, PPT 2), showing the different distribution of pressures on the soil along the depth possibly due to different drainage conditions.

Only minimal pore pressure dissipation was recorded by the six transducers in the early of loading stages, although the majority of settlements took place during this time (Figs. 5–7). B_0 (2008) explained that for dredged soil, settlement is induced during the initial time of loading due to reduction of water which will not lead to a subsequent

reduction of pore water pressure in the soil. For instance, Fig. 3 shows that the settlement in case 2 after 50 h was 53.61 mm, which was 30.89% of degree of consolidation, with the delay of excess pore water pressure during the first loading stage. The delayed time is defined as the transitional point from small change to large change in excess pore pressure. The delay of excess pore water pressures was also observed in the second and the last loading stage. It is noted that the delayed time tended to reduce with the increase of vertical consolidation pressure, as shown in Figs. 5–7. The delayed time observed in PWP 5 and PWP6 was shorter than that in the other locations in the first loading stage and this difference was noted by 2 dotted line in Figs. 5–7.

The delay of excess pore water pressure of case 1 (Fig. 5) and case 2 (Fig. 6) was compared under the same total vertical stresses but different water contents. The higher initial water content resulted in the longer delay of excess pore pressure dissipation. The delayed time observed in PWP 5 and PWP6 of case 2 ($W_i = 180\%$) was approximately

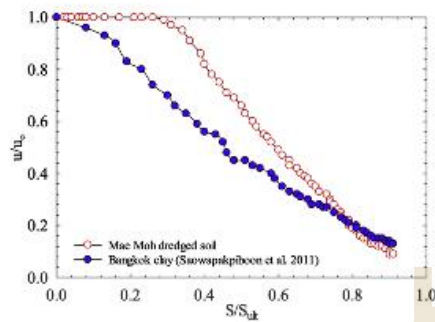


Fig. 8. Relationships between S/S_{ult} versus u/u_0 of Mae Moh ultra-soft dredged soil and soft Bangkok clay improved with PVD.

50 h in the first loading, which was approximately 20 h longer than that of case 1 ($W_i = 120\%$). Although there was little or no pore pressure dissipation, the water squeezed out from the soil was observed in the early of the loading stages. The consolidation behavior of Mae Moh ultra-soft dredged soil improved by PVD in case 1 was compared with that of soft Bangkok clay (Saowapakpiroon et al., 2011) in the relationship of S/S_{ult} and u/u_0 , as shown in Fig. 8 where S is the settlement at any time, u is the excess pore water pressure at any time and u_0 is the initial excess pore water pressure. It was evident that the u/u_0 ratio reduced remarkably with the increase of S/S_{ult} ratio for the soft Bangkok clay. The same trend was however not found for Mae Moh ultra-soft soil. The u/u_0 ratio was approximately constant and equal to 1 when the S/S_{ult} ratio < 0.28 . Beyond this S/S_{ult} ratio of 0.28, the u/u_0 ratio reduced significantly with increasing S/S_{ult} ratio. This delay in excess pore pressure dissipation with progressive settlement is a distinct behavior of ultra-soft clay which deviates from the behavior of natural soft clay. This similar behavior was also noticed in the previous research reported by Bo (2002), Chu et al. (2006), and Tanaka (1997).

The effect of PVD dimension on the delay of excess pore water pressure dissipation was evident by comparing case 1 and case 3. The delayed time observed in the top of the soil (PWP 5 and PWP6) was 30 h for case 1, while it was 40 h for case 3 at low vertical stress (20 kPa). At high vertical stress (80 kPa), the effect of PVD dimension on the delayed time was essentially the same (approximately the same delay times).

Beyond the delayed time, the pore water pressure reduced significantly (Figs. 5–7). At the same depth, the excess pore water pressures close to the PVD (PPT 2, PPT 4, and PPT 6) indicated a faster rate of dissipation than the others. Because the drainage was only allowed at the top of surface of the model ground, the decrease of excess pore pressures observed from 2 PPTs at the bottom of tank (PPT 1 and PPT 2) were lower than those measured on the top of the tank.

3.1.3. Water content and undrained shear strength

The water contents of the ultra-soft soil, W , in all cases were measured at radial distances (r) from the center of PVD after the end of consolidation test at vertical stress of 80 kPa. The relationship between water content, W/W_i ratio, versus angle ratio $\alpha/360^\circ$, at different r/r_0 ratio (0.4 and 0.8), is shown in Fig. 9 where W_i is the initial water content and r_0 is the radius of the tank). A significant reduction of the water content was noticed in all tested cases. The water content of the soil at the same radius (r) was found to be approximately the same. The lower water content was found for lower r/r_0 ratio of 0.4. For case 1 ($W_i = 120\%$), the final water contents varied from 42.01% to 52.66%. It was noted that the reduction of water content in case 2 ($W_i = 180\%$) was very large, which reduced by approximately 129% near the vertical

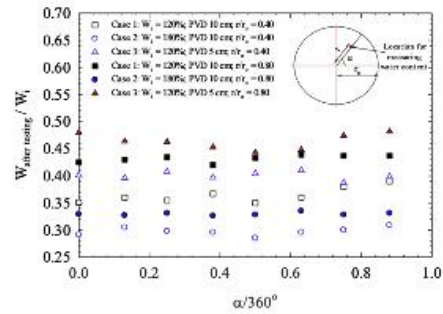


Fig. 9. Change of water contents at various distances from PVDs in 3 cases.

drain. The effect of PVD dimension was noticed when compared the results of case 1 with case 3, the water contents in case 3 were found to be higher than those in case 1, which varied from 46.12% to 57.84%.

The undrained shear strength (S_u) of the soil in the middle of the soil layer in the tank was measured by using the mini vane shear equipment. For all total vertical stress, the undrained shear strengths in case 1 (larger PVD) were higher than those in case 3 (smaller PVD) because of higher degree of consolidation under the same vertical stress and consolidation time. The higher water contents and lower initial undrained shear strengths were observed in case 2 when compared with the results in case 1. Fig. 10 shows the undrained shear strength, S_u , versus the vertical effective stress, σ'_v relationship for the three cases. The vertical effective stress (σ'_v) at the end of test of each vertical consolidation pressure was a product of the total vertical stress (σ_v) and the degree of consolidation (U) calculated using the Asaoka's observation method. It was evident that the undrained shear strength was directly related to vertical effective stress ($\Delta\sigma'_v$). The S_u versus σ'_v relationship was therefore developed based on the SHANSEP equation proposed by Ladd and Foott (1974):

$$\frac{S_u}{\sigma'_v} = 0.22 \tag{9}$$

This constant value of 0.22 was found to be similar with the proposed value for Bangkok clay by Shibuya and Hanh (2001).

Although the reclamation and soil improvement processes for ultra-soft dredged soil are more difficult and challenging than those of natural soft soils, the results from the large-consolidation test highlighted

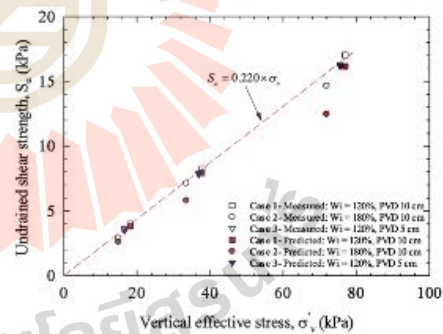


Fig. 10. Measured and predicted undrained shear strength (in kPa) during the consolidation process.

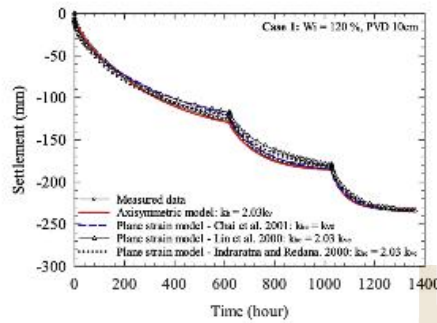


Fig. 11. Measured and predicted settlement versus time curves in case 1.

the successful performance of PVDs for improvement of dredged soil. The PVDs can be used to accelerate the settlement, enhance the shear strength and decrease significantly the water content of the dredged soil in pond Sump 1 C1, Mae Moh mine, Thailand.

3.2. Numerical test results

3.2.1. Settlement and excess pore water pressure

Fig. 11 presents the comparison of measured settlement from the large consolidation tank and predicted settlement by FEM analysis using 4 different approaches for case 1. The axisymmetric analysis provided an excellent agreement with measured data in term of settlement. The measured settlement in case 1 after loading stage 3 (80 kPa) was 234.52 mm, which was only 2 mm higher than the predicted one from the axisymmetric model by means of conventional modeling method using $k_h = 2.03 \times k_v$, as shown in Fig. 11.

Fig. 12 shows a relationship between measured and simulated excess pore water pressures versus time in the first loading of case 1, which is similar to the other cases. The observed data from the two different pore pressure transducers (PPT 3, PPT4) were compared with the axisymmetric simulation results. The measured excess pore pressures diverted from the predicted ones due to the delay in excess pore water pressures at the early stages of loading. The prediction of excess pore water pressures by the Soft Soil model is based on the principle of effective stress (Terzaghi, 1943) in that for an incremental total stress, the reduction in excess pore water pressure is equal to the increase in effective stress, leading to the soil settlement. However, the settlement of Mae Moh ultra-soft soil occurred with minimal reduction of excess

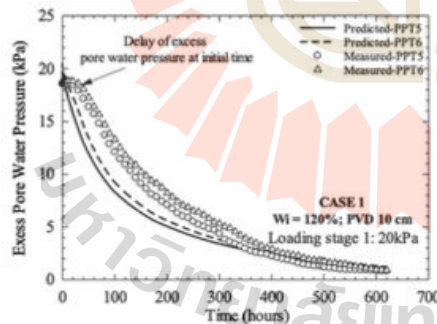


Fig. 12. Measured and predicted excess pore water pressures in case 1.

pore water pressure at the initial loading stage.

The predicted excess pore water pressure increased to reach the maximum value and then decreased rapidly in the early stages of loading while a little or no pore water pressure dissipation was observed from 2 pore pressure transducers. However, the predicted excess pore pressures agreed well with measured excess pore pressures at the end of loading stages.

To simply simulate the performance of PVD in plane-strain condition in 2D FEM analysis, 3 different approaches proposed by Chai et al. (2001), Lin et al. (2000), and Indraratna and Redana (2000) were adopted in this study. The smear effect was considered in the analysis in term of the ratio between the smear zone diameter and the equivalent drain diameter (d_s/d_w) to transform parameters from axisymmetric to plane strain conditions. The smear ratio (d_s/d_w) was taken as 1 for all cases in the plane strain model. The smear effect during the installation of PVDs was considered as small because the Mae Moh dredged soil was extremely soft.

The predicted settlements obtained from the plane strain solutions were compared with measured data, as illustrated in Fig. 11. It can be seen that the predicted settlements using Chai et al.'s method were in good agreement with the measured data. The simulated settlements from Chai et al.'s method were slightly lower than the measured one in the first loading stage. The difference in predicted and measured settlements was very small in the second and last stages.

Based on the comparison of plane strain model with the model test results, it is recommended that the plane strain models using Chai et al.'s method and Indraratna and Redana's method is proposed to predict the performance of PVD for reclamation of Mae Moh dredged soil in the field.

3.2.2. Undrained shear strength

The comparison between predicted and measured settlements of the dredged soil in the consolidation apparatus provided an insight in the suitability of the soft soil model, as well as the appropriate model parameters to simulate the consolidation of the dredged soil in FEM analysis. Considering a soil sample, which has been normally compressed at mean effective stress $p' = p'_v$, S_u can be predicted using the critical state soil mechanics as (Atkinson and Bransby, 1977; Wood, 1990):

$$S_u = \frac{M}{2} \exp \left[\frac{(\Gamma - v_v)}{\lambda} + \ln p'_v \right] \tag{10}$$

with $p'_v = \frac{1}{3} \sigma'_v (1 + 2K_0)$; $M = \frac{6 \sin \phi'}{3 - \sin \phi'}$

in which M is the slope of critical state line; v_v is the specific volume at the normal compression line with $p' = 1$; Γ is the specific volume of soil at critical state line with $p' = 1$, λ is the slope of normal compression line. K_0 varies from 0.5 to 1 as recommended by Shibuya and Hanh (2001) for Bangkok soft clay.

Eq. (10) was adopted to predict S_u of Mae Moh dredged soil in the large consolidation apparatus after each loading stages. The parameters M , v_v , Γ , λ , K_0 for the prediction of undrained shear strength of the soil in each case are presented in Table 4. The slope of the critical state line (M) and the slope of normal compression line (λ) were calculated from ϕ' and λ^* . The v_v and Γ were obtained from the undrained triaxial

Table 4
Soil parameter for predictions of undrained shear strength.

Case No.	Water content (W)	Soil parameters			
		M	Γ	v_v	λ
Case 1	120%	4.1565	4.111	4.279	0.2733
Case 2	180%	1.1565	5.394	5.898	0.629
Case 3	120%	1.1565	4.111	4.279	0.2733

* $M = 6 \sin \phi' / (3 - \sin \phi')$; $\lambda = \lambda^* \times (1 + \epsilon_{H1})$

compression test results. It is noted that the soil parameters for cases 1 and 3 were the same because they had the same initial water content of 120%.

The predicted undrained shear strengths are comparable with the measured results presented in Fig. 10. It is evident that the undrained shear strength of the soil in 3 tested cases can be well predicted by using the constant soil parameter M , v_s , Γ , λ . However, the simulated values were lower than the measured one, especially in case 2 with the initial water content of 180%.

4. Conclusion

This research studied the application of PVD for reclamation of dredged soil in Mae Moh mine, Thailand. To assess the performance of PVD in the consolidation of slurry soil, a series of large-scale consolidation test was conducted at different water contents and PVD dimensions. The following conclusions can be drawn:

1. The large settlements for all cases were observed, especially for case 2 with the initial water content of 180% that exhibited the highest value after the consolidation stage of dredged soil improved by PVDs. The test results indicated that the higher initial water content resulted in the higher settlement and the lower rate of consolidation settlement. At low vertical stress where the viscosity is relatively high, the PVD dimension significantly affected the rate of consolidation settlement while at high vertical stress, the effect of PVD dimension was less.
2. The distinct behavior of Mae Moh ultra-soft dredged soil was the delay of excess pore water pressure at the initial stage of consolidation although the settlements had taken place. The delay of excess pore water pressure reduced with the increase of consolidation pressure. The higher initial water content and the smaller of PVDs dimension resulted in the longer delay of excess pore pressure dissipation. Beyond the delayed time, the excess pore water pressures rapidly decreased with time.
3. A significant reduction of water content and increase of undrained shear strength after testing highlighted the successful performance of PVDs on the improvement of the Mae Moh dredged soil. The equation for predicting undrained shear strengths at various vertical effective stress was developed based on SHANSEP's method.
4. The consolidation behavior of the PVD improved dredged soil can be simulated by finite element method using Plaxis 2D software. The axisymmetric model produced an excellent match with measured data in term of settlement value. However, the excess pore water pressure was not well predicted using the axisymmetric model due to the delay of excess pore water pressure at the initial time of loading. The settlement of Mae Moh dredged soil can be simulated satisfactorily by the plane strain models proposed by Chai et al. (2001) and Indraratna and Redana (2000). Therefore, both models are suggested for field reclamation in practice.
5. Based on the Cam Clay and Soft Soil models, the undrained shear strength (S_u) can be well predicted using the constant soil parameter M , v_s , Γ , λ . As such, the Soft Soil model together with the plane strain model by Chai et al. (2001) and Indraratna and Redana (2000) can be used to analyze both settlement and stability of reclamation of dredged soil in Mae Moh mine.

Acknowledgements

This work was financially supported by Electricity Generating Authority of Thailand grant no61-G201000-11-IO.SS03G3008344.

References

Almeida, M., Santa Maria, P., Martins, I., Spotti, A., Guelbs, L., 2004. Consolidation of a very soft clay with vertical drains. In: *Ground and Soil Improvement*. Thomas Telford Publishing, pp. 29–39.

Arulrajah, A., Nikraz, H., Bo, M., 2004. Factors affecting field instrumentation assessment of marine clay treated with prefabricated vertical drains. *Geotext. Geomembranes* 22 (5), 415–437.

Arulrajah, A., Nikraz, H., Bo, M., 2005. Finite element modelling of marine clay deformation under reclamation fills. *Proc. Inst. Civil. Eng. Ground Improv.* 9 (3), 105–118.

Asakha, A., 1978. Observational procedure of settlement prediction. *Soils Found.* 18 (4), 87–101.

Atkinson, J., Bransby, P., 1977. *The Mechanics of Soils, an Introduction to Critical State Soil Mechanics*. 0042-3114.

Been, K., Sills, G., 1981. Self-weight consolidation of soft soils: an experimental and theoretical study. *Geotechnique* 31 (4), 519–535.

Blewett, J., McCarter, W., Chrisp, T., Starrs, G., 2001. Monitoring sedimentation of a clay slurry. *Geotechnique* 51 (8), 723–728.

Bo, M., 2004. Discharge capacity of prefabricated vertical drain and their field measurements. *Geotext. Geomembranes* 22 (1–2), 37–48.

Bo, M., 2008. *Compressibility of Ultra-soft Soil*. World Scientific Publishing Company.

Bo, M., Choa, V., Wong, K., 2005. Reclamation and soil improvement on ultra-soft soil. *Proc. Inst. Civil. Eng. Ground Improv.* 9 (1), 23–31.

Bo, M.W., 2002. *Deformation of Ultra-soft Soil*. Nanyang Technological University, School of Civil & Environmental Engineering.

Bo, M.W., Arulrajah, A., Horpibulsuk, S., Chinkulkijniwat, A., Leong, M., 2016. Laboratory measurements of factors affecting discharge capacity of prefabricated vertical drain materials. *Soils Found.* 56 (1), 129–137.

Cal, Y., Xie, Z., Wang, J., Wang, P., Geng, X., 2018. New approach of vacuum preloading with booster prefabricated vertical drains (PVDs) to improve deep marine clay strata. *Can. Geotech. J.* 55 (10), 1359–1371.

Cao, Y., Xu, J., Bian, X., Xu, G., 2019. Effect of clogging on large strain consolidation with prefabricated vertical drains by vacuum pressure. *KSCE J. Civil. Eng.* 23 (10), 4190–4200.

Chai, J.C., Shen, S.L., Miura, N., Bergado, D.T., 2001. Simple method of modeling PVD-improved subsoil. *J. Geotech. Geoenviron. Eng.* 127 (11), 965–972.

Chai, J., Miura, N., Sakajo, S., 1999. A theoretical study on smear effect around vertical drain. In: *International Conference on Soil Mechanics and Foundation Engineering*.

Chen, J., Shen, S.L., Yin, Z.Y., Xu, Y.S., Horpibulsuk, S., 2016. Evaluation of effective depth of PVD improvement in soft clay deposit: a field case study. *Mar. Georesour. Geotechnol.* 34 (5), 420–430.

Choa, V., Bo, M., Chu, J., 2001. Soil improvement works for Changi East reclamation project. *Proc. Inst. Civil. Eng. Ground Improv.* 5 (4), 141–153.

Chu, J., Bo, M., Choa, V., 2004. Practical considerations for using vertical drains in soil improvement projects. *Geotext. Geomembranes* 22 (1–2), 101–117.

Chu, J., Bo, M., Choa, V., 2006. Improvement of ultra-soft soil using prefabricated vertical drains. *Geotext. Geomembranes* 24 (6), 339–348.

Chung, S., Kweon, H., Jang, W., 2014. Observational method for field performance of prefabricated vertical drains. *Geotext. Geomembranes* 42 (4), 405–416.

Fang, Z., Yin, J.H., 2006. Physical modelling of consolidation of Hong Kong marine clay with prefabricated vertical drains. *Can. Geotech. J.* 43 (6), 638–652.

Geng, C., Yonghui, C., Jiangwei, S., Long, C., 2017. Newly developed technique and analysis solution to accelerate consolidation of ultra-soft soil. *Mar. Georesour. Geotechnol.* 35 (2), 292–299.

Hiep, H., Chung, S., 2018. Back-analysis of geotechnical parameters on PVD-improved ground in the Mekong Delta. *Geotext. Geomembranes* 46 (4), 402–413.

Hird, C., Pyrah, I., Russel, D., 1992. Finite element modelling of vertical drains beneath embankments on soft ground. *Geotechnique* 42 (3), 499–511.

Holtz, R., 1987. Preloading with prefabricated vertical strip drains. *Geotext. Geomembranes* 6 (1–3), 109–131.

Hong, Z., Yin, J., Cui, Y.J., 2010. Compression behavior of reconstituted soils at high initial water contents. *Geotechnique* 60 (9), 691–700.

Horpibulsuk, S., Liu, M.D., Zhuang, Z., Hong, Z.S., 2016. Complete compression curves of reconstituted clays. *Int. J. Geomech.* 16 (6), 06016005.

Horpibulsuk, S., Phetchuay, C., Chinkulkijniwat, A., Cholaphatsoorn, A., 2013. Strength development in silty clay stabilized with calcium carbide residue and fly ash. *Soils Found.* 53 (4), 477–486.

Indraratna, B., Geng, X., Rujikiatkarnjorn, C., 2010. Review of methods of analysis for the use of vacuum preloading and vertical drains for soft clay improvement. *Geomechanics Geoenviron. Eng.* 5 (4), 223–236.

Indraratna, B., Redana, I., 2000. Numerical modeling of vertical drains with smear and well resistance installed in soft clay. *Can. Geotech. J.* 37 (1), 132–145.

Jiang, J., Liu, R., 2019. Effect of improvement and application of composite prefabricated vertical drain method in marine soft ground: a case study. *Adv. Civ. Eng.*

Ladd, C.C., Foott, R., 1974. New design procedure for stability of soft clays. *J. Geotech. Geoenviron. Eng.* 100.

Lin, D., Kim, H., Balasubramanian, A., 2000. Numerical modeling of prefabricated vertical drain. *Geotech. Eng.* 31 (2).

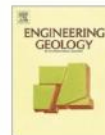
Liu, M.D., Zhuang, Z., Horpibulsuk, S., 2013. Estimation of the compression behaviour of reconstituted clays. *Eng. Geol.* 167, 84–94.

Mesri, G., Kane, T., 2019. Discussion of "New approach of vacuum preloading with booster prefabricated vertical drains (PVDs) to improve deep marine clay strata". *Can. Geotech. J.* 56 (12), 2015–2016.

Morohoshi, K., Yoshinaga, K., Miyata, M., Sasaki, I., Saitoh, H., Tokoro, M., Shikawa, M., 2010. Design and long term monitoring of Tokyo International Airport extension project constructed on super-soft ground. *Geotech. Geol. Eng.* 28 (3), 223–232.

Palmeira, E.M., Caronni, M.G., 2002. Drainage and filtration properties of non-woven geotextiles under confinement using different experimental techniques. *Geotext. Geomembranes* 20 (2), 97–115.

- Pham, H.T., Rühaak, W., Ngo, D.H., Nguyen, O.C., Sass, I., 2019a. Fully coupled analysis of consolidation by prefabricated vertical drains with applications of constant strain rate tests: case studies and an open-source program. *Geotext. Geomembranes*.
- Pham, H.T., Rühaak, W., Schulte, D., Sass, I., 2019b. Application of the Vimeke–Taylor concept for fully coupled models of consolidation by prefabricated vertical drains. *Comput. Geotech.* 116, 103201.
- Rixner, J., Kraemer, S., Smith, A., 1986. *Prefabricated Vertical Drains*, Vol. I: Engineering Guidelines. Turner-Fairbank Highway Research Center.
- Saowapakpiroon, J., Bergado, D., Vootipruex, P., Lam, L., Nakakuma, K., 2011. PVD improvement combined with surcharge and vacuum preloading including simulations. *Geotext. Geomembranes* 29 (1), 74–82.
- Saowapakpiroon, J., Bergado, D., Youwai, S., Chai, J., Wanthong, P., Vootipruex, P., 2010. Measured and predicted performance of prefabricated vertical drains (PVDs) with and without vacuum preloading. *Geotext. Geomembranes* 28 (1), 1–11.
- Shibuya, S., Hanh, L., 2001. Estimating undrained shear strength of soft clay ground improved by pre-loading with PVD: case history in Bangkok. *Soils Found.* 41 (4), 95–101.
- Sills, G., 1998. Development of structure in sedimenting soils. *Philosophical transactions-royal society of London series a mathematical physical and engineering sciences*, pp. 2515–2534.
- Skempton, A.W., 1953. The colloidal activity of clays. In: *Proceedings of 3rd International Conference on Soil Mechanics and Foundation Engineering*, vol. 1, pp. 57–61.
- Skempton, A., 1954. The pore-pressure coefficients A and B. *Geotechnique* 4 (4), 143–147.
- Tan, T., Yong, K., Leong, E., Lee, S., 1990. Sedimentation of clayey slurry. *J. Geotech. Eng.* 116 (6), 885–898.
- Tanaka, Y., 1997. Non-uniformly consolidated ground around a vertical drain. In: *Paper Presented at the Proc. 30th Anniversary Symposium of Southeast Asian Geotechnical Society*.
- Udomchai, A., Horpibulsuk, S., Sukstripattanapong, C., Mavong, N., Rachan, R., Arulrajah, A., 2017. Performance of the bearing reinforcement earth wall as a retaining structure in the Mae Moh mine, Thailand. *Geotext. Geomembranes* 45 (4), 350–360.
- Wood, D.M., 1990. *Soil Behaviour and Critical State Soil Mechanics*. Cambridge university press.
- Xu, G.Z., Gao, Y.F., Hong, Z.S., Ding, J.W., 2012. Sedimentation behavior of four dredged slurries in China. *Mar. Georesour. Geotechnol.* 30 (2), 143–156.
- Yonghui, C., Geng, C., Cheng, X., Qi, C., 2019. Simple consolidation method for dredger fill treatment using plastic vertical drains with vacuum. *Mar. Georesour. Geotechnol.* 37 (8), 915–923.
- Zhang, Z., Ye, G., Cai, Y., Zhang, Z., 2019. Centrifugal and numerical modeling of stiffened deep mixed column-supported embankment with slab over soft clay. *Can. Geotech. J.* 56 (10), 1418–1432.



Compressibility of ultra-soft soil in the Mae Moh Mine, Thailand

Dong Huy Ngo^a, Suksun Horpibulsuk^{b,*}, Apichat Suddeepong^c, Menglim Hoy^b, Avirut Chinkulkijniwat^{b,*}, Arul Arulrajah^d, Apipat Chaiwan^e^a School of Civil Engineering, Suranaree University of Technology, Nakhon Ratchasima 30000, Thailand^b School of Civil Engineering, and Center of Excellence in Innovation for Sustainable Infrastructure Development, Suranaree University of Technology, Nakhon Ratchasima 30000, Thailand^c Center of Excellence in Innovation for Sustainable Infrastructure Development, Suranaree University of Technology, Nakhon Ratchasima 30000, Thailand^d Department of Civil and Construction Engineering, Swinburne University of Technology, Hawthorn, Victoria 3122, Australia^e Geotechnical Engineering Department, Mae Moh Mine, Electricity Generating Authority of Thailand, Lampang, Thailand

ARTICLE INFO

Keywords:

Mae Moh ultra-soft soil
Compressibility
Large sedimentation soil
Small sedimentation soil
Critical water content
Intrinsic state line

ABSTRACT

The compressibility characteristics of ultra-soft soils are an important issue for the deformation analysis of reclaimed land. This research study investigated the compressibility characteristics of ultra-soft soil present in a slurry pond, which is composed of the sedimentation and consolidation phases. The ultra-soft soil under the sedimentation process is termed as a slurry while the ultra-soft soil after completion of sedimentation is termed as a sedimentation soil. The samples were obtained from a slurry pond in the Mae Moh mine, Lampang province, Thailand. A series of sedimentation tests were performed on slurry at various initial water contents, w_0 , ranging from 116% to 437%. It was found that the sedimentation curve of the Mae Moh slurry was divided into two distinct different stages, being flocculation and settling. A novel parameter, being the critical water content (w_{cr}), was proposed to separate the large sedimentation slurry and small sedimentation slurry. The w_{cr} for Mae Moh slurry was found to be 171%. The sedimentation water content, w_s , was found to be equal to w_{cr} for the slurry undergoing large sedimentation and lower for the slurry undergoing low sedimentation. The consolidation curve of the large sedimentation soil was assumed to be unique for different w_0 . The w_0 of small sedimentation soil is governed by w_0 and thus the consolidation curves are different for different w_0 . The consolidation curves of the ultra-soft soil at different w_0 can be assessed by a proposed generalized S-shaped equation. The intrinsic state line for high sedimentation soil was proposed for examining the stress state and predicting the consolidation curve of the ultra-soft soil, which is significant for reclamation projects.

1. Introduction

The Mae Moh Mine is the largest open-pit lignite mine in Thailand, as well as in Southeast Asia, with a total mining area of approximately 37.5 km² and external dumping area of approximately 41.4 km². It is situated at the Mae Moh district, Lampang province in the north of Thailand, located 630 km away from Bangkok. The lignite material at the Mae Moh basin is the main raw feed material used to generate power at the Mae Moh power plants, operated by the Electricity Generating Authority of Thailand (EGAT). Approximately 16 million tons of coal are produced annually and transferred to the 10 units of the Mae Moh power plants in order to generate the total power supply of 2400 Megawatt. Several water ponds were constructed as the main

source for mining activities such as mineral processing and dust suppression. The discharge of surface water and groundwater flow has caused soil erosion along the mine slope, which has resulted in ultra-soft soil deposits located underwater in the slurry ponds over the years. The thickness of the ultra-soft soil in some ponds is even up to 40 m.

According to the mine planning and development of EGAT, this mine will be excavated to a depth of approximately 500 m from the original surface over the next four decades, resulting in this becoming the deepest open pit lignite mine in the world. The excavated soil from mining activities will be dumped in the slurry ponds for land reclamation. Fig. 1 shows a schematic of a slurry pond, which will be subjected to a very high overburden material of approximately 300 m in the next 40 years. However, the soil in the ponds is in the ultra-soft

* Corresponding authors at: School of Civil Engineering, Suranaree University of Technology, 111 University Avenue, Muang District, Nakhon Ratchasima 30000, Thailand.

E-mail addresses: dho40147@eng.sut.ac.th (D.H. Ngo), suksun@g.sut.ac.th (S. Horpibulsuk), suddeepong@g.sut.ac.th (A. Suddeepong), menglim@g.sut.ac.th (M. Hoy), avirut@g.sut.ac.th (A. Chinkulkijniwat), arulrajah@swin.edu.au (A. Arulrajah), apipat.c@egat.co.th (A. Chaiwan).

<https://doi.org/10.1016/j.enggeo.2020.105594>

Received 29 May 2019; Received in revised form 6 March 2020; Accepted 18 March 2020

Available online 20 March 2020

0013-7952/ © 2020 Elsevier B.V. All rights reserved.

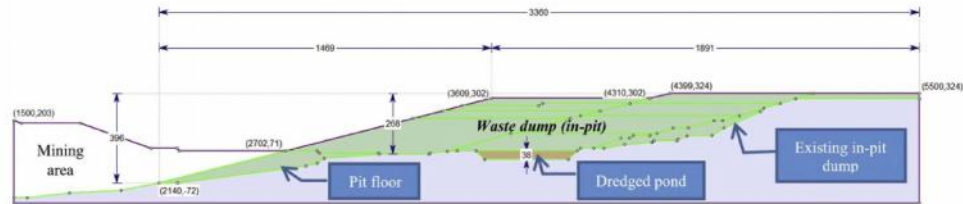


Fig. 1. Typical cross-section of In-pit dump in the Mae Moh mine (dimension in meter).

state, with very low undrained shear strength and high water content of greater than liquid limit. In-pit dumping without mechanical property improvement of this ultra-soft soil is almost impossible. Due to very low undrained shear strength, the mud flood of the ultra-soft soil could occur immediately after the in-pit dump and causes detrimental effects on the mining activities.

A suitable ground improvement method for the ultra-soft soil in the Mae Moh mine is the preloading with vertical drains technique. It is effective in term of economic and environmental perspectives as compared to other techniques, such as deep soil mixing and soil replacement. The preloading can be performed using a 1-m thickness of clean sand as a drainage layer and the usage of abandoned clayey stone as a backfill material. A sufficient understanding of the mechanical behavior, especially compressibility and hydraulic conductivity of the ultra-soft soil is therefore required for calculating the settlement and rate of consolidation settlement (Chai et al., 2004; Chai et al., 2018; Horpibulsuk et al., 2007; Horpibulsuk et al., 2011; Liu et al., 2013; Liu et al., 2018; Xu et al., 2019). The compressibility of the ultra-soft soil includes the sedimentation and consolidation stages. The ultra-soft soil under the sedimentation process is termed as a slurry while the ultra-soft soil after completion of sedimentation is termed as a sedimentation soil.

The sedimentation process is a special characteristic of slurry at high water content (Been and Sills, 1981; Blewett et al., 2001; Chen et al., 2019; Özer and Bromwell, 2012; Sills, 1998; Tan et al., 1990; Zhang et al., 2015). The evaluation of consecutive process from sedimentation to consolidation is a major challenge on the geological and geotechnical practical design of land-filling and disposal work. The void ratio of the sedimentation soil is a required parameter for the calculation of the consolidation settlement (Imai, 1980, 1981; Watabe and Saitoh, 2015). The first well-known theory of sedimentation was proposed by Kynch (1952) and was later modified by Fitch (1957, 1966, and 1979). The sedimentation of slurry has been studied by using a traditional method of slowly injecting slurry into a column or cylinder. Based on the observation of the sedimentation tests, three stages can be distinguished: flocculation, settling, and self-weight consolidation stages (Imai, 1980, 1981; Fan, 1995; Tan et al., 1990; Xu et al., 2012). Scott et al. (1986) reported that the sedimentation and consolidation stages are different from each other. The sedimentation process includes the flocculation and settling stages. The self-weight consolidation occurs at the bottom of the settling column after the sedimentation process. During the sedimentation process, it is postulated that there is no effective stress in the slurry and the slurry acts as fluid (Xu et al., 2012). When soil particles come close to each other to develop the soil structure, the slurry turns into soil and the effective stress can be determined.

After the sedimentation process, the sedimentation soil has sufficient strength to carry an external load. The understanding of compression behavior of sedimentation soil in term of compressibility and hydraulic conductivity characteristics has played a key role in geological and geotechnical engineering practice for many decades (Chai et al., 2004; Desai, 2000; Horpibulsuk et al., 2007; Horpibulsuk et al.,

2011; Wu et al., 2019; Xu et al., 2019). Forty-eight reconstituted clay samples at different water contents (ranging from 0.7 to 2.0 times their liquid limit) were tested using a modified oedometer test with a light loading cap (Hong et al., 2010). Most of these tests were applied at low effective stress of 0.5 kPa and gradually increased to reach high effective stress (1600 kPa). Based on the test results, it has been well documented that the completed virgin compression curve of reconstituted clay is represented by S-shape function (Horpibulsuk et al., 2016; Liu et al., 2013; Zeng et al., 2015). Horpibulsuk et al. (2016) proposed an S-shaped equation to predict the consolidation curve of reconstituted clays over the wide range of stresses and initial water contents.

Even though there are available research on sedimentation of slurries and consolidation behavior of sedimentation soils, they have been previously studied in isolation. As such, the role of water content on the overall compressibility characteristics of the ultra-soft soil is still uncertain. The compressibility characteristics of the ultra-soft soil are thus a challenge for geological and geotechnical designers in land reclamation projects.

The aim of this paper is to assess the compressibility characteristics, which include sedimentation and consolidation at different initial water contents, w_i . A series of sedimentation tests were conducted which analyzed the change of soil interface, void ratio, and water content over time. The consolidation behavior of the sedimentation soil at a wide range of effective stresses and water contents was also investigated. Finally, a practical method for assessing the stress state of slurry and consolidation curve of sedimentation soil is proposed, based on the complete S-shaped function (Horpibulsuk et al., 2016). The outcomes of this research will enable geological and geotechnical engineers to assess the compressibility of ultra-soft soils in land reclamation and ground improvement projects, such as in the Mae Moh slurry pond.

2. Material and methods

2.1. Soil sample

The soil samples were taken from a slurry pond in a low lying area of the Mae Moh mine, Lampang province in Thailand. Disturbed samples were collected at a depth of approximately 1 m below soil surface of the pond with a backhoe and placed in a plastic tank. The studied site is shown in Fig. 2.

The grain size distribution curve of the soil sample is shown in Fig. 3. The soil sample contained 41% clay and 58% silt with 1% sand. The liquid limit and the plastic limit were measured in accordance with Casagrande method (BS 1377 – Part 2: 4.3 and BS1377 – Part 2: 5.3), and were 57% and 26%, respectively. The specific gravity was 2.57. The soil had a very high in-situ water content of 98%, greater than 1.7 times the liquid limit. The in-situ strength was 1.5 kPa, which is considered to be extremely low. As this research mainly focuses on the compressibility and hydraulic conductivity characteristics of the ultra-soft soil, the chemical properties of the ultra-soft soil was not examined. The comparison of the physical and chemical properties between the



Fig. 2. Sampling site.

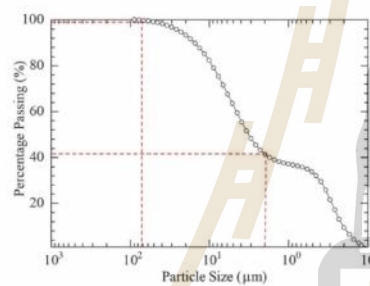


Fig. 3. Grain size distribution curve.

ultra-soft soil and its parent rocks is however useful for soil science technology and is recommended for further research.

2.2. Sedimentation test

To study the sedimentation behavior of slurry under various water contents, the water content of the samples was adjusted to be greater than that of the liquid limit. The slurry sample at the target w_t was thoroughly mixed using a mechanical mixer for 15 min and then slowly injected into a unified transparent glass cylinder, using a funnel with a small tube down to the bottom of the cylinder. The injection process was stopped upon reaching 36 cm height of the slurry (Imai, 1980, 1981; Tan, 1995; Tan et al., 1990; Xu et al., 2012). The cylinder was then covered with a plastic sheet to prevent water evaporation during testing and kept in the laboratory at a controlled temperature of $20 \pm 1^\circ$. Eight different initial water contents ($w_i = 116\%$, 137% , 193% , 219% , 230% , 325% , 400% , and 437%) were prepared as shown in Fig. 4. The w_i values were selected to cover the in-situ water content and far higher than liquid limit of up to approximately 7.7 times so as to understand the role of w_i on the sedimentation behavior. During 42 days of the sedimentation process, the height of slurry was recorded at different times (minutes). A schematic diagram of the sedimentation

process is shown in Fig. 5.

According to the theory of soil mechanics (Terzaghi, 1951), a fully saturated soil consists of two phases: solid soil particles and pore water. Consequently, the water content of the sedimentation layer is the ratio of the mass of water to the mass of solid, except for the mass of water above the soil surface. The water content (w_t) of the slurry at time t can be calculated from the change of soil interface (the surface between slurry and water):

$$w_t = \left[e_0 - \frac{\Delta h \times (1 + e_0)}{h_0} \right] \times \frac{S_r}{G_s} \quad (1)$$

where h_0 and e_0 are the initial height and initial void ratio of the slurry, respectively; Δh is the change of soil interface at time t using calibration scale in cylinder wall; G_s is specific gravity of the soil.

The calculated water contents were validated by comparing with the measured water content at the end of the test (w_f). After completion of the sedimentation test, the water above the soil mass was slowly taken out of each cylinder by using a small syringe. The soil mass was then oven-dried to determine the w_f of the slurry.

2.3. Consolidation test

The consolidation behavior of the sedimentation soil upon application of the additional load due to the effect of the sedimentation water content, w_t (water content at the end of sedimentation), as well as under the same loading sequence were studied. Six samples were prepared by mixing the slurry thoroughly with a quantity of distilled water to reach the target initial water contents. Once the target initial water contents were obtained, at 1.45, 1.79, 1.84, 1.97, 2.10, and 2.28 times the liquid limit, the slurry was carefully poured into the consolidation ring by controlling the mass of specimen, which was calculated by considering the slurry in fully saturated condition. A metal rod of 5 mm in diameter was used to remove air bubbles inside the oedometer ring (Hong et al., 2010; Zeng et al., 2015). The consolidation sample was 105 mm in diameter and 20 mm in nominal height. After preparing the sample in O-ring, the slurry was kept in the consolidation cell and covered by plastic sheet under room temperature for 42 days to ensure that the sedimentation process was completed. This rest period of 42 days was obtained from the sedimentation test. After that the

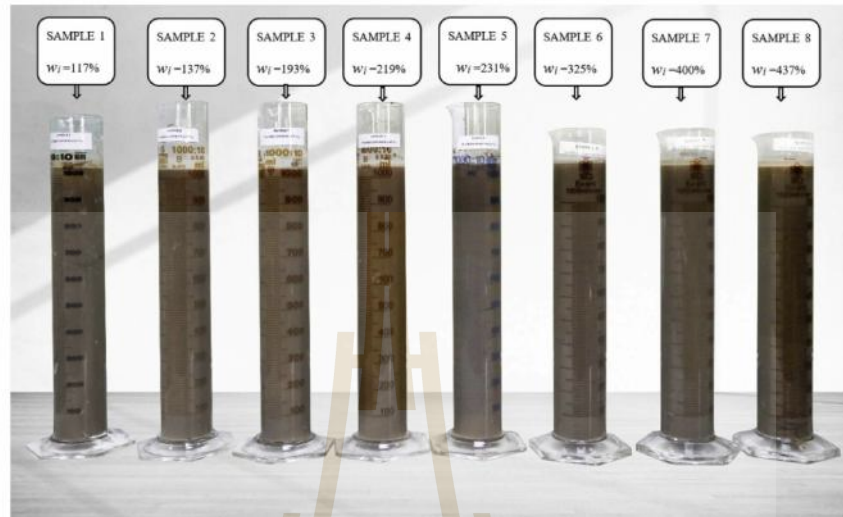


Fig. 4. 8 cylinders containing slurry at different initial water contents.

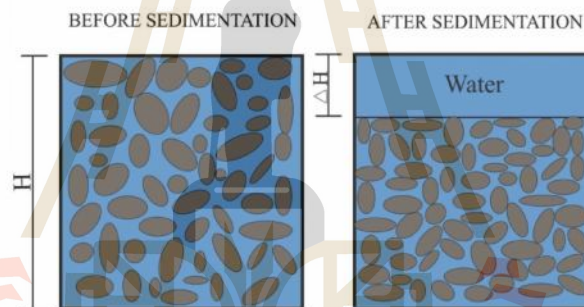


Fig. 5. Illustration of changing interface location before and after sedimentation process.

samples were then subjected to both low and high loads. A very low effective vertical stress of 0.5 kPa was first applied and gradually increased with following vertical stresses of 1 kPa, 1.5 kPa, 2.5 kPa, 3.5 kPa, 5.5 kPa, 7.5 kPa, 9.5 kPa, 12.5 kPa, 25 kPa, 50 kPa, 100 kPa, 200 kPa, 500 kPa, 1000 kPa, 2000 kPa, 4000 kPa. The duration of each loading step was fixed at 24 h. For each loading increment, the hydraulic conductivity, k , was calculated by the following equation.

$$k = c_v m_v \gamma_w \quad (2)$$

where c_v is the coefficient of consolidation determined using the root time method proposed by Taylor (1942), m_v is the coefficient of volume change, and γ_w is the density of water.

3. Results and discussion

3.1. Sedimentation of slurry

Fig. 6 presents the change of interface location of the slurry samples

at different initial water contents and their measured water contents (w_f) at the end of the test. The measured water contents were compared with the calculated ones using Eq. (1) at the end of the test as summarized in Table 1. The results indicated that the measured water contents are in excellent agreement with the calculated ones. On the other hand, the soil-fluid interface location decreases significantly after 42 days of sedimentation (comparing Fig. 6 with Fig. 4). The sedimentation curves of the slurry at various w_i are shown in Fig. 7, which can be divided into two stages: flocculation and settling. The flocculation occurs at an early stage in which the soil particles were dispersed in the mixture and no interface between soil mass and water was observed in this stage. When the flocculation stage finishes, the settling begins whereby the flocs start to settle uniformly with a clearly observed interface change. During this stage, the interface location moves downward with a constant rate and the sedimentation curve shows a linear behavior in arithmetic time scale. After the settling stage, the flocs in the slurry deposit onto bottom and voids are consolidated under self-weight in the self-weight consolidation stage (Scott et al., 1986).

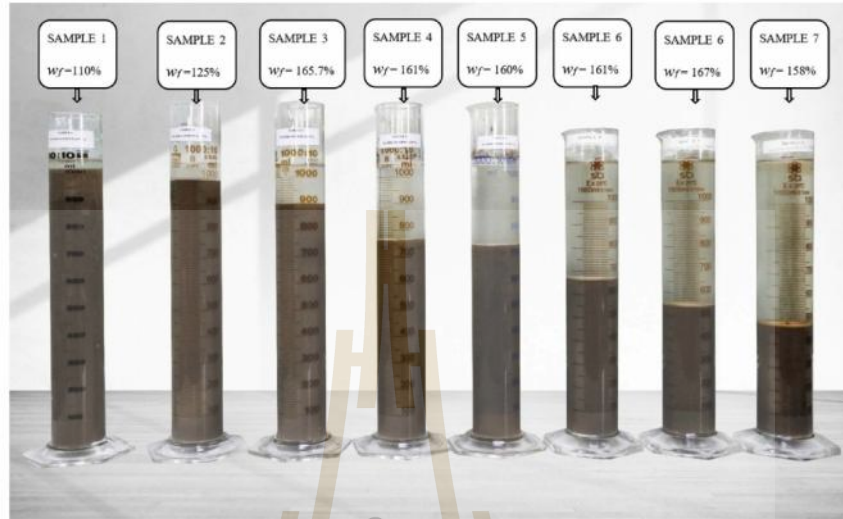


Fig. 6. Interface location of 8 samples the end of test.

Table 1
The comparison of calculated and measured water content at the end of the test.

Cylinder no.	Initial water content, w_i (%)	Measured water content, $w_{f, \text{measured}}$ (%)	Calculated water content, $w_{f, \text{calculated}}$ (%)
1	117	110	111.02
2	137	125	124.75
3	193	165.7	165.78
4	219	161	159.67
5	231	160	161.70
6	325	161	162.49
7	400	167	166.03
8	437	158	160.15

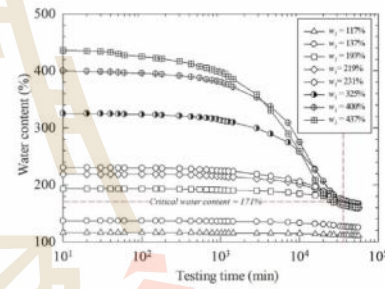


Fig. 8. Water content versus with time (log scale) relationship.

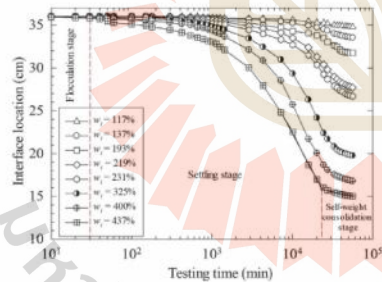


Fig. 7. Sedimentation curves at different initial water contents in logarithmic time scale.

Similar to Fig. 7, the water content versus time was plotted and is presented in Fig. 8. The sedimentation water content, w_s , defined as the water content at the end of sedimentation, was determined from the interception of the two straight lines extended from settling and self-

weight consolidation stages. The w_s can be considered as the transition point between the sedimentation process and the self-weight consolidation stage. It is worth noting that the w_s value was essentially the same, at 171% for the slurry with very high w_i while it deviates for slurry with low w_i . The constant w_s of the slurry at various w_i is defined herewith as critical water content, w_{cr} . The w_{cr} for the studied ultra-soft soil is therefore 171%. It is noted that w_{cr} was approximately 3 times liquid limit.

Based on the sedimentation test result (Fig. 3), the slurry is divided into large and small sedimentation slurry separated using w_{cr} as the reference. The slurry with $w_i > w_{cr}$ is defined as large sedimentation slurry while the slurry with $w_i < w_{cr}$ is defined as small sedimentation slurry. Two stages (flocculation and settling) of the sedimentation process were clearly observed for the large sedimentation slurry. The soil particles are far apart from each other, hence the water content reduces significantly with high velocity in the settling stage. On the other hand, for the small sedimentation slurry, the change in water content with time during the first 1000 min is little and then the water content slightly decreases with time. This slight change in water

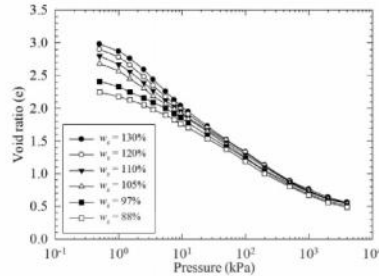


Fig. 9. Consolidation curve of sediment soil at different sedimentation water contents.

content is consistent with change in soil interface in that very little compression takes place during the first 1000 min, and then the soil interface decreases with low velocity. As such, the w_r of small sedimentation slurry is dependent upon the w_i and practically its value can be assumed to be the w_i value.

3.2. Consolidation behavior of sedimentation soil

3.2.1. Consolidation curve

The w_r is assumed to be the same for high sedimentation slurry. As such, the consolidation curve of high sedimentation soil is unique, irrespective of w_i . On the other hand, the consolidation curve of small sedimentation soil varies and is dependent upon w_r , which will be examined in this section. The consolidation curves in term of void ratio versus effective vertical stress in a semi-logarithmic (e vs $\log \sigma'_v$) for six samples at different w_r are shown in Fig. 9. The consolidation behavior of sedimentation soil is an inverse S-shape curve, which is similar to previous studies reported by Hong et al. (2010) for Lianyungang, Baimahu clay and Liu et al. (2013) for Kemen clay. The transitional stress separating small and large change in void ratio is defined as yield stress or suction pressure, which is similar to the pre-consolidation pressure for natural soils (Hong et al., 2010). Hong et al. (2010) explained that at pre-yield state, the load is carried by the suction pressure. At post-yield stage, the soil undergoes large compression strain due to the destructuring of soil structure.

The yield stress of the soil samples can be determined by the interception of two straight lines (pre-yield and post-yield state line) in bilogarithmic graph $\ln(1 + e) - \log \sigma'_v$ as plotted in Fig. 10 (Hong et al., 2010). These two straight lines are assumed for $\sigma'_v < 100$ kPa. The calculated yield stresses of six samples at different w_r are presented in

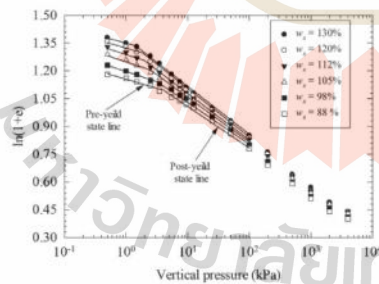


Fig. 10. Bilogarithmic consolidation curves of sediment soil at different sedimentation water contents.

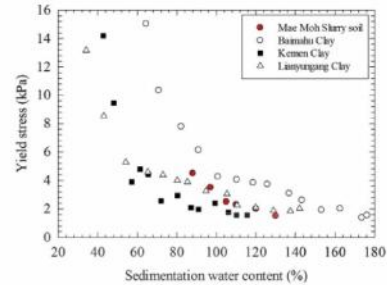


Fig. 11. Yield stress versus sedimentation water content.

Fig. 11 and also compared with that of Lianyungang, Baimahu, and Kemen clays studied by Hong et al. (2010). It is evident that the yield stresses of all soils reduce with an increase of w_r . The reduction in yield stress is due to the fact that the higher w_r results in resistance to vertical consolidation pressure and the shear strength (Horpiulsuk et al., 2007; Horpiulsuk et al., 2011; Nagaraj et al., 1998).

3.2.2. Hydraulic conductivity

Fig. 12 shows the relationship between the hydraulic conductivity and void ratio of sedimentation soil at various water contents. Even though the hydraulic conductivity of six samples at various σ'_v is different, the hydraulic conductivity is however the same at the same void ratio. The hydraulic conductivity significantly reduces with the reduction of void ratio. The non-linear relationship between e and $\log k$ for the Mae Moh sedimentation soil samples can be represented by the following equation.

$$e = 141.84 \times k^{0.239} \tag{3}$$

where k is expressed in cm/s.

With Eq. (3), the k value of Mae Moh sedimentation soil at any e can be approximated.

3.2.3. Estimation of the consolidation curve of Mae Moh sedimentation soil

Based on the collected compression data of 24 reconstituted clays, Horpiulsuk et al. (2016) proposed a robust S-shaped equation to predict the complete compression behavior of reconstituted clays with effective vertical stress $\sigma'_v \geq 0.01$ kPa. The consolidation equation in term of void ratio and mean effective stress is given as (Horpiulsuk et al., 2016):

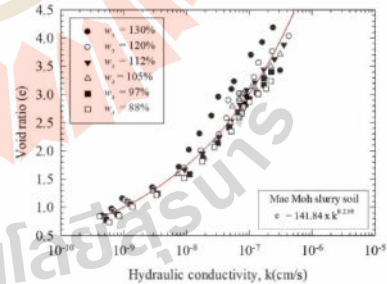


Fig. 12. $e - \log(k)$ relationship of sediment soil at different sedimentation water contents.

Table 2
Values of equation parameter for Mae Moh slurry soil.

Water content of the soil	$e^{*}_{v,100}$	$e^{*}_{v,1000}$	a	b
W = 130%	1.33	0.76	2.19	3.77
W = 120%	1.32	0.74	1.87	4.07
W = 112%	1.29	0.73	1.8	4.75
W = 105%	1.24	0.72	1.7	5.07
W = 97%	1.23	0.69	1.37	5.31
W = 88%	1.19	0.67	1.17	5.62

$$e = \left\{ \frac{a}{\exp\left(\frac{\sigma'_v}{b}\right)^{0.5}} + \frac{0.31}{\sigma'_v} \left[1 + \frac{10\sigma'_v - 1}{\exp(0.0551\sigma'_v)^{0.425}} \right] - 2.1 \right\} \times C_c^* + e_{100} \quad \text{for } \sigma'_v \geq 0.01 \text{ kPa} \quad (4)$$

with $C_c^* = e_{100} - e_{1000}$ where e is the void ratio corresponding to a vertical effective stress σ'_v ; e_{100} and e_{1000} are the void ratio at $\sigma'_v = 100$ kPa and 1000 kPa, respectively. Two parameters a and b are used to predict the compression behavior at a low range of stresses.

The applicability of the equation was illustrated by the excellent simulation of compression curves of various soils such as kaolin (Shipton and Coop, 2012), marine soil (Fukue and Mulligan, 2009), Weiner Tegel clay (Burland, 1990), and Huaian clay (Zeng et al., 2015). Therefore, Eq. (4) was adopted to predict the compression behavior of Mae Moh sedimentation soil. Two parameters a and b were obtained by a trial and error method. The trial and error process started from selecting the parameter a as a fixed value between 1 and 4 (recommended by Horpibulsak et al., 2016), and then varies b value until fitting the experiment curve. The a and b values for Mae Moh sedimentation soil with w_s in a range of 88% to 130% are shown in Table 2. It is noted that the a value decreases with decreasing w_s . On the other hand, the b value increases with the decrease of w_s . The simulation results are comparable with the measured results as seen in Fig. 13.

Since the liquid limit is the state parameter reflecting the soil structure (Mitchell, 1993 and Nagaraj et al., 1998), it is logical to relate the consolidation parameters a and b to generalized void ratio, e_s/e_L where e_s is the sedimentation void ratio and e_L is the liquid limit void ratio. Fig. 14 presents the relationship of parameters a and b versus e_s/e_L ratio of Mae Moh soil at different w_s . As a result, the generalized equation to describe compression behavior of the Mae Moh sedimentation soil can be proposed as:

$$e = \left\{ \frac{1.4(e_s/e_L) - 0.8618}{\exp\left[\frac{\sigma'_v}{-2.67(e_s/e_L) + 9.8275}\right]^{0.5}} + \frac{0.31}{\sigma'_v} \left[1 + \frac{10\sigma'_v - 1}{\exp(0.0551\sigma'_v)^{0.425}} \right] - 2.1 \right\} \times C_c^* + e_{100} \quad (5)$$

The compression behavior of Mae Moh slurry soil was predicted using this generalized equation and presented in Fig. 15. It is evident that the compression behavior of the soil at different w_s can be obtained successfully with the proposed equation when using the generalized void ratio.

The compression behavior of remolded Kemen and Baimahu clay samples with different w_s reported by Hong et al. (2010) were taken to validate the modified equation by comparing the predicted results with measured data. The w_s was ranged from 99% to 116% and from 101% to 180% for Kemen clay and Baimahu clay, respectively. The soil parameters used for simulation are presented in Table 3.

Fig. 16 shows the prediction of consolidation curves for Kemen and Baimahu clays based on Eqs. (5). For Kemen clay, the soil behavior can be described well when using the generalized equation, except for

loading at 0.5 kPa of the sample with the $w_s = 116\%$. For Baimahu clay, the predicted results and measured data are in very good agreement except for the first loading of sample with very high $w_s = 141\%$. This reinforces the applicability of the generalized equation. The generalized equation using e_s/e_L ratio can satisfactorily describe the consolidation behavior for various soils (Mae Moh soil, Kemen clay and Baimahu clay) at very high and low stresses.

Even with limited available test data, the development of the generalized equation is based on sound principles. The variable parameters can be refined by more test data, which can be performed in future research.

4. Assessment of stress state of ultra-soft soil

Based on the sedimentation and consolidation test results, the e versus $\log \sigma'_v$ relationship of sedimentation soil is controlled by w_s . The w_s is approximately equal to w_{cr} and independent of w_i for large sedimentation soil. Consequently, the consolidation curve of large sedimentation soil is unique and defined as intrinsic state line (ISL). For the studied Mae Moh soil with $w_{cr} = 171\%$, the ISL can be represented by the following equation as presented in Fig. 17.

$$e = \left\{ \frac{3.31}{\exp\left[\frac{-\sigma'_v}{1.864}\right]^{0.5}} + \frac{0.31}{\sigma'_v} \left[1 + \frac{10\sigma'_v - 1}{\exp(0.0551\sigma'_v)^{0.425}} \right] - 2.1 \right\} \times 0.74 + 1.62 \quad (6)$$

It is long accepted that the compressibility of soil in both the slurry and sedimentation states is controlled by the stress state (e and σ'_v). In this study, examination of the stress state using ISL is introduced. The ultra-soft soil is divided into high sedimentation soil, small sedimentation soil and slurry. The soil is classified as high sedimentation soil when the stress state is on the ISL, as low sedimentation soil when the stress state is below the ISL and as slurry when the stress state is above the ISL.

A suggested stepwise procedure for examining the stress state and compressibility of ultra-soft soil can be presented as follows:

1. Determine liquid limit and specific gravity of ultra-soft soil samples
2. Prepare the slurry at $w_i > 3$ times liquid limit
3. Perform the sedimentation test on the slurry to determine w_{cr}
4. From the known e_L , draw the ISL using Eq. (5)
5. Take the in-situ soil samples at various depths and determine e and corresponding σ'_v
6. Classify the stress state
 - 6.1 If the stress state is on the ISL, the ultra-soft soil is high sedimentation soil.
 - 6.2 If the stress state is below the ISL, the ultra-soft soil is low sedimentation soil.
 - 6.3 If the stress state is above the ISL, the ultra-soft soil is slurry and under sedimentation process
7. Approximate consolidation curves of either low or high sedimentation soil at various depths using Eq. (5)

The stress state assessment is important for predicting the settlement of ultra-soft soil. If the ultra-soft soil is in a slurry state, the settlement is due to both sedimentation of slurry and consolidation of the sedimentation soil. The sedimentation settlement is calculated from the difference between in-situ water content and w_s . The consolidation settlement can be calculated using Eq. (5) where e_s is equal to critical void ratio, e_{cr} for high sedimentation soil and approximately equal to initial void ratio, e_i for small sedimentation soil. From this study, the w_{cr} was found to be 171% while the in-situ water content was 98%, with an effective vertical stress of less than 6.2 kPa. This effective vertical stress is considered to be very low, considering that the soil sample was

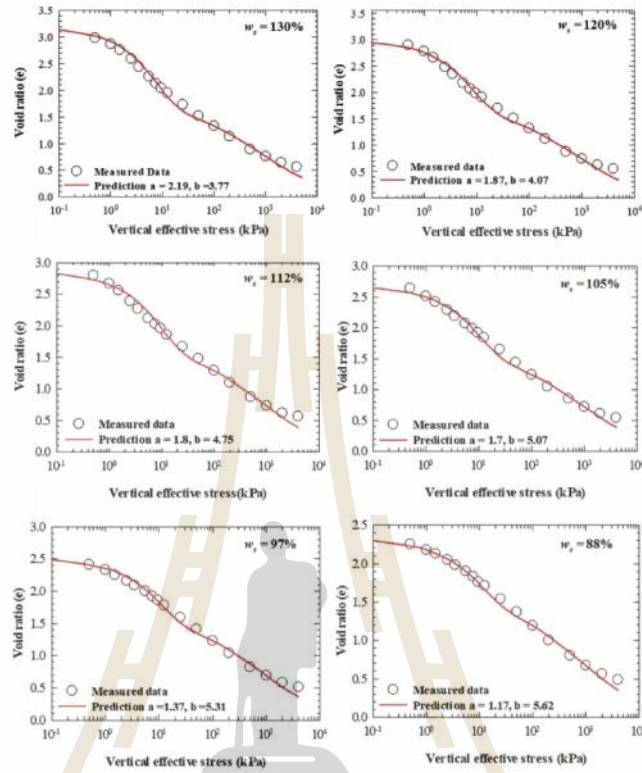


Fig. 13. Prediction of consolidation curves of sediment soil using S-shaped equation.

collected at 1 m depth from the soil surface and had unit weight of approximately 16 kN/m³. Based on the proposed method, the Mae Moh soil can therefore be classified as a low sedimentation soil.

conductivity characteristics of ultra-soft soil at the Mae Moh mine, Thailand. The study is useful for designing the land reclamation of ultra-soft soil using preloading technique with vertical drains. The following conclusions can be made from this study.

5. Conclusions

This research studied the compressibility and hydraulic

1. The sedimentation process of Mae Moh slurry was divided into two distinct stages: flocculation and settling. The flocculation occurred

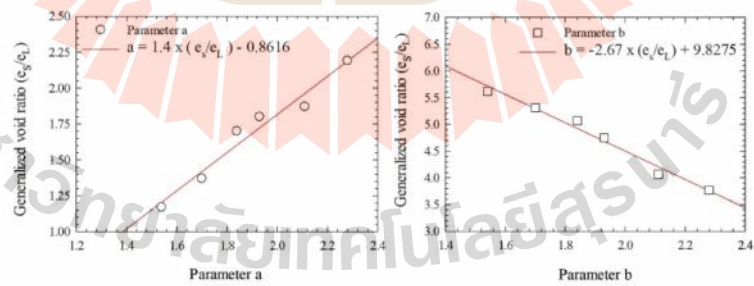


Fig. 14. Relationship between parameters a and b versus e_s/e_l .

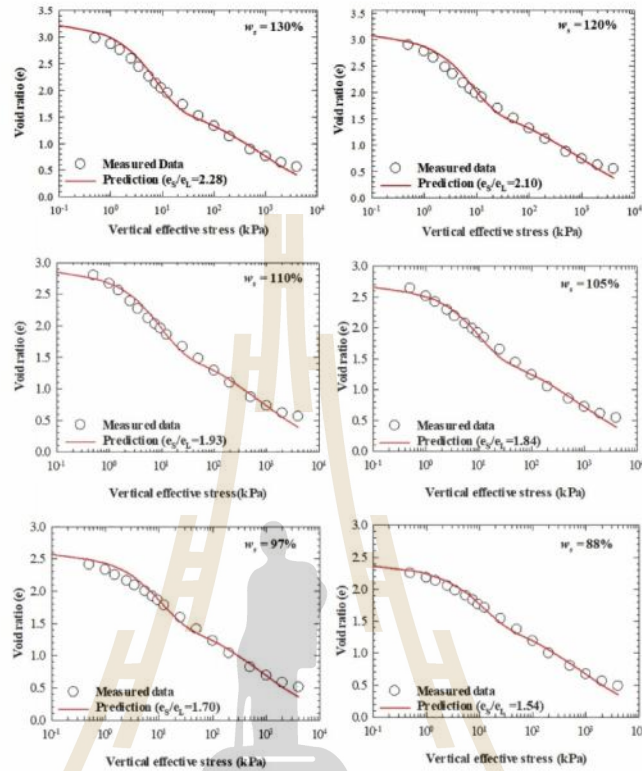


Fig. 15. Prediction of consolidation curves of Mae Moh sediment soil using generalized S-shaped equation.

Table 3
The soil parameters of kemen and baimahu clay used for simulation.

Soil	Water content W (%)	Liquid Limit LL (%)	e ₁₀₀	e ₁₀₀₀
Kemen clay	116	61	1.34	0.81
	110	61	1.31	0.76
	99	61	1.23	0.71
Baimahu clay	180	91	1.78	0.95
	143	91	1.65	0.81
	101	91	1.47	0.70

at the early stage of sedimentation process with very small change in soil-fluid interface. The settling stage then commenced, when the floe particles started to settle uniformly, causing the significant change in soil-fluid interface.

2. A critical water content (w_c) separating the large sedimentation and small sedimentation slurry, was found to be 171% for studied Mae Moh soil. For large sedimentation slurry, the water content reduces significantly after sedimentation process. On the other hand, the water content of small sedimentation slurry slightly decreases during sedimentation process and thus w_c can be assumed to be w_r .
3. The consolidation curve of high sedimentation soil is unique and independent of w_r . On the other hand, the consolidation curve of small sedimentation soil is significantly dependent upon w_r . The

consolidation curves of sedimentation soil can be represented by the inverse S-shape function from a very low (0.5 kPa) to very high vertical effective stresses.

4. The powerful S-shape equation proposed by Horpibulsuk et al. (2016) was extended to develop the generalized equation using generalized void ratio (e_c/e_r) as the prime parameter. The generalized equation can satisfactorily capture the compression behavior of various sedimentation soils at different w_r .
5. The intrinsic state line (ISL) for high sedimentation soil was proposed to assess the stress state of ultra-soft soil. The soil is classified as high sedimentation soil when the stress state is below the ISL, as low sedimentation soil when the stress state is above the ISL, and as slurry when the stress state is above the ISL. The stepwise procedure for assessing stress state and compressibility of ultra-soft soil is suggested.
6. The stress state assessment is important to predict the settlement of the ultra-soft soil when subjected to ground improvement and land reclamation. For the ultra-soft soil in a slurry state, the settlement is due to both sedimentation of the slurry and consolidation of the sedimentation soil. The sedimentation settlement can be calculated from the difference between in-situ water content and w_r . The consolidation settlement can be calculated using the proposed S-shaped equation for both low and high sedimentation soils.

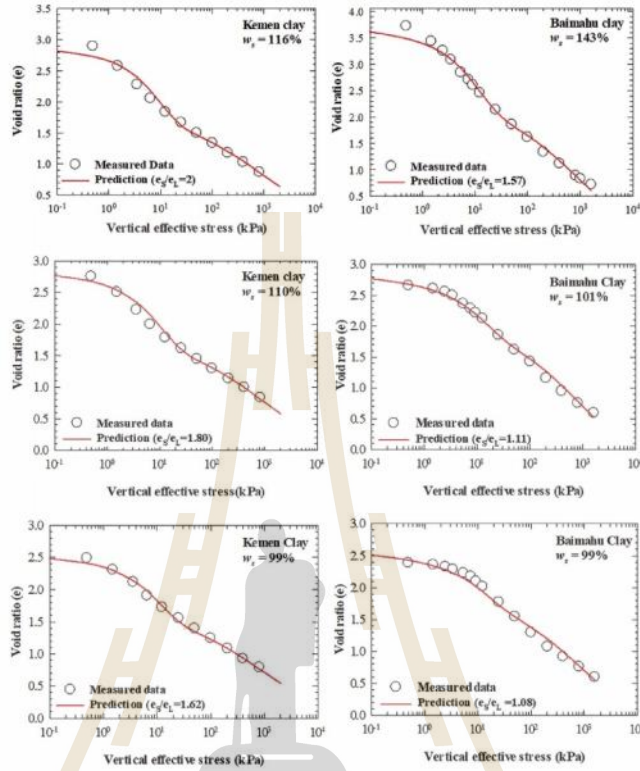


Fig. 16. Prediction of consolidation curves of Kemen and Baimahu sediment clay using generalized S-shaped equation.

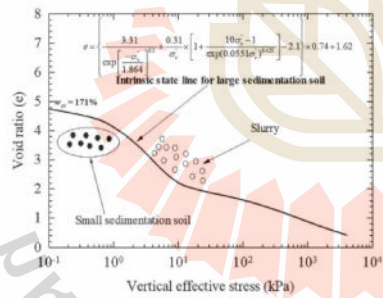


Fig. 17. Intrinsic state line for large sedimentation soil.

Declaration of Competing Interest

None.

Acknowledgements

This work was financially supported by Electricity Generating Authority of Thailand grant no. 61-G201000-11-IO.SS03G3008344, Suranaree University of Technology, and the Higher Education Research Promotion and National Research University Project of Thailand, Office of Higher Education Commission.

References

Been, K., Sills, G., 1981. Self-weight consolidation of soft soils: an experimental and theoretical study. *Geotechnique* 31 (4), 519–535.
 Blewett, J., McCarter, W., Chrisp, T., Stars, G., 2001. Monitoring sedimentation of a clay slurry. *Geotechnique* 51 (8), 723–728.
 Burland, J., 1990. On the compressibility and shear strength of natural clays. *Geotechnique* 40 (FB), 329–378.
 Chai, J.C., Miura, N., Zhu, H.H., Yadavir, 2004. Compression and consolidation characteristics of structured natural clay. *Can. Geotech. J.* 41 (6), 1250–1258.
 Chai, J.C., Shen, J.S.L., Liu, M.D., Yuan, D.J., 2018. Predicting the performance of embankments on PVD-improved subsoils. *Comput. Geotech.* 93, 222–231.
 Chen, Q., Zhang, C., Yang, C., Ma, C., Pan, Z., Daemen, J., 2019. Strength and deformation of tailings with fine-grained interlayers. *Eng. Geol.* 256, 110–120.

- Dessi, C.S., 2000. *Mechanics of Materials and Interfaces: The Disturbed State Concept*. CRC press.
- Fitch, B., 1957. Sedimentation process fundamentals. *Biol. Treat. Sew. Ind. Wastes*. 2.
- Fitch, B., 1966. Mechanism of sedimentation. *Ind. Eng. Chem. Fundam.* 5 (1), 129–134.
- Fitch, B., 1979. Sedimentation of flocculent suspensions: state of the art. *AIChE J.* 25 (6), 913–930.
- Fukur, M., Malligan, C.N., 2009. Equations of state in soil compression based on statistical mechanics. *Soils Found.* 49 (1), 99–114.
- Hong, Z., Yin, J., Cai, Y.J., 2010. Compression behavior of reconstituted soils at high initial water contents. *Geotechnique* 60 (9), 691–700.
- Horpibulsuk, S., Shibuya, S., Fuenkajorn, K., Katkan, W., 2007. Assessment of engineering properties of Bangkok clay. *Can. Geotech. J.* 44 (2), 173–187.
- Horpibulsuk, S., Yangsukdeeam, N., Chinkulkijniwat, A., Da, Y.J., 2011. Compressibility and permeability of Bangkok clay compared with kaolinite and bentonite. *Appl. Clay Sci.* 52 (1–2), 150–159.
- Horpibulsuk, S., Liu, M.D., Zhuang, Z., Hong, Z.S., 2016. Complete compression curves of reconstituted clays. *Int. J. Geomech.* 16 (6), 06016005.
- Imai, G., 1980. Settling behavior of clay suspension. *Soils Found.* 20 (2), 61–77.
- Imai, G., 1981. Experimental studies on sedimentation mechanism and sediment formation of clay materials. *Soils Found.* 21 (1), 7–20.
- Kynch, G.J., 1952. A theory of sedimentation. *Trans. Faraday Soc.* 48, 166–176.
- Liu, M.D., Zhuang, Z., Horpibulsuk, S., 2013. Estimation of the compression behaviour of reconstituted clays. *Eng. Geol.* 167, 84–94.
- Liu, X.X., Shen, S.L., Xu, Y.S., Yin, Z.Y., 2018. Analytical approach for time-dependent groundwater inflow into shield tunnel face in confined aquifer. *Int. J. Numer. Anal. Methods Geomech.* 42 (4), 655–673.
- Mitchell, J.K., 1993. *Fundamentals of Soil Behaviour*. John Wiley & Sons Inc, New York (437p).
- Nagaraj, T., Pandian, N., Narashimha, R.P., 1998. Compressibility behaviour of soft cemented soils. *Geotechnique* 48 (2).
- Özer, A.T., Bromwell, L.G., 2012. Stability assessment of an earth dam on silt/clay tailings foundation: a case study. *Eng. Geol.* 151, 89–99.
- Scott, J.D., Dusseault, M.B., Carrier, W.D., 1986. Large-scale self-weight consolidation testing. In: *Consolidation of Soils: Testing and Evaluation*. ASTM International.
- Shipton, B., Coop, M.R., 2012. On the compression behaviour of reconstituted soils. *Soils Found.* 52 (4), 668–681.
- Sills, G., 1998. Development of structure in sedimenting soils. *Philos. Trans. Royal Soc. Lond. Series A* 356 (1747), 2515–2534.
- Tan, T., 1995. Sedimentation to consolidation: a geotechnical perspective. In: *Compression Consolidation of Clayey Soils*, pp. 937–948.
- Tan, T., Yong, K., Leong, E., Lee, S., 1990. Sedimentation of clayey slurry. *J. Geotech. Eng.* 116 (6), 885–898.
- Taylor, D.W., 1942. *Research on consolidation of clays*, Massachusetts Institute of Technology.
- Terzaghi, K., 1951. *Theoretical Soil Mechanics*. Chapman And Hall, Limited, London.
- Watabe, Y., Saitoh, K., 2015. Importance of sedimentation process for formation of microfabric in clay deposit. *Soils Found.* 55 (2), 276–283.
- Wu, Y.X., Lyu, H.M., Han, J., Shen, S.L., 2019. Dewatering-Induced Building Settlement around a Deep Excavation in Soft Deposit in Tianjin, China. *J. Geotech. Geoenviron.* 145 (5), 05019003.
- Xu, G.Z., Gao, Y.F., Hong, Z.S., Ding, J.W., 2012. Sedimentation behavior of four dredged slurries in China. *Mar. Georesour. Geotechnol.* 30 (2), 143–156.
- Xu, Y.S., Yan, X.X., Shen, S.L., Zhou, A.M., 2019. Experimental investigation on the blocking of groundwater seepage from a waterproof curtain during pumped dewatering in an excavation. *Hydrogeol. J.* 27 (7), 2659–2672.
- Zeng, L.L., Hong, Z.S., Cai, Y.J., 2015. Determining the virgin compression lines of reconstituted clays at different initial water contents. *Can. Geotech. J.* 52 (9), 1408–1415.
- Zhang, Q., Yin, G., Wei, Z., Fan, X., Wang, W., Nie, W., 2015. An experimental study of the mechanical features of layered structures in dam tailings from macroscopic and microscopic points of view. *Eng. Geol.* 195, 142–154.

BIOGRAPHY

Mr. Huy Dong Ngo was born on October 30, 1993 in Nghe An province, Vietnam. He obtained a Bachelor's degree in Civil Engineering – Advanced training program from University of Transport and Communication, Hanoi, Vietnam. Soon after graduated, he worked for Vietnam Expressway Consultant Company (VECC) as a civil engineer. In 2017, he has been awarded a SUT-Ph.D. scholarship (5-years) in academic year 2017-2022, studies in the School of Civil Engineering, Suranaree University of Technology, Thailand. During his Ph.D. study, he conducted his research under the supervision of Prof. Dr. Suksun Horpibulsuk. He has published 2 leading international journal papers as the first author and 1 co-authored international journal paper.

